



Terms and Conditions of Use of Digitised Theses from Trinity College Library Dublin

Copyright statement

All material supplied by Trinity College Library is protected by copyright (under the Copyright and Related Rights Act, 2000 as amended) and other relevant Intellectual Property Rights. By accessing and using a Digitised Thesis from Trinity College Library you acknowledge that all Intellectual Property Rights in any Works supplied are the sole and exclusive property of the copyright and/or other IPR holder. Specific copyright holders may not be explicitly identified. Use of materials from other sources within a thesis should not be construed as a claim over them.

A non-exclusive, non-transferable licence is hereby granted to those using or reproducing, in whole or in part, the material for valid purposes, providing the copyright owners are acknowledged using the normal conventions. Where specific permission to use material is required, this is identified and such permission must be sought from the copyright holder or agency cited.

Liability statement

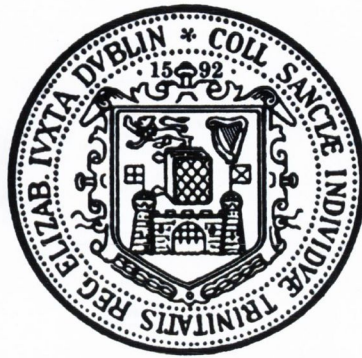
By using a Digitised Thesis, I accept that Trinity College Dublin bears no legal responsibility for the accuracy, legality or comprehensiveness of materials contained within the thesis, and that Trinity College Dublin accepts no liability for indirect, consequential, or incidental, damages or losses arising from use of the thesis for whatever reason. Information located in a thesis may be subject to specific use constraints, details of which may not be explicitly described. It is the responsibility of potential and actual users to be aware of such constraints and to abide by them. By making use of material from a digitised thesis, you accept these copyright and disclaimer provisions. Where it is brought to the attention of Trinity College Library that there may be a breach of copyright or other restraint, it is the policy to withdraw or take down access to a thesis while the issue is being resolved.

Access Agreement

By using a Digitised Thesis from Trinity College Library you are bound by the following Terms & Conditions. Please read them carefully.

I have read and I understand the following statement: All material supplied via a Digitised Thesis from Trinity College Library is protected by copyright and other intellectual property rights, and duplication or sale of all or part of any of a thesis is not permitted, except that material may be duplicated by you for your research use or for educational purposes in electronic or print form providing the copyright owners are acknowledged using the normal conventions. You must obtain permission for any other use. Electronic or print copies may not be offered, whether for sale or otherwise to anyone. This copy has been supplied on the understanding that it is copyright material and that no quotation from the thesis may be published without proper acknowledgement.

THE ROLE OF PARKIN-PICK1 IN MITOCHONDRIAL DYSFUNCTION



**A thesis submitted to the University of Dublin
for the Degree of Doctor of Philosophy**

February 2012

By
Debadutta Deb

Under the supervision of Prof. Kumlesh K Dev
Molecular Neuropharmacology Group
School of Medicine, Institute of Neuroscience
Trinity College Dublin
Ireland

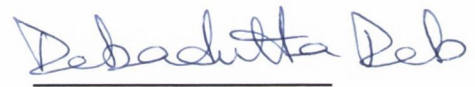


Thesis 9749

A. Declaration

I declare that this thesis has not been submitted as an exercise for a degree at this or any other university and it is entirely my own work.

I agree to deposit this thesis in the University's open access institutional repository or allow the library to do so on my behalf, subject to Irish Copyright Legislation and Trinity College Library conditions of use and acknowledgement.

A handwritten signature in blue ink that reads "Debadutta Deb". The signature is written in a cursive style and is positioned above a horizontal line.

Debadutta Deb

B. Acknowledgements

I would like to take the privilege to acknowledge all those persons who helped me completing this work. First of all, I want to thank all the lab members of KKD lab; Priyanka, Luke, Gill, Marika, Graham, Fiona, Adam and Ola for the support they showed me and for all those lab fun/jokes they kept on making to keep a taste of life in rigorous lab hours. I must acknowledge Priyanka for helping me with the yeast two hybrid assay and Gill for sharing her precious neuronal cultures without any bragging. Gill, those little chat about life, etc are one of my most cherishable moment here. I also want to thank Yvonne for her advices during her tenure in the lab. In biochemistry department, I would like to thank Stephen for all his helps and not getting annoyed in my stupidest questions. The small family which I found here, far from home was something I never expected. Many thanks to my friends and housemates Ani, Arnab and Aurab; and people like Shibuda, Swagata, Kapil and Soumya for all their support and giving me a taste of home in this foreign land. You guys rock! I also want to mention Gablu, with whom I started chasing the dream of doing true research 10 years ago as a undergrad student. I wish you all the luck for successful completion of your PhD thesis. I thank Sany for joining me here in Dublin and reviving the old days of Bangalore and New Delhi. I would like to thank the woman behind this successful completion of PhD, Raheleh, for all the motivation and support she has given me, time to time. Last but not the least, I thank my Ma, Baba and Dalia for providing me with the wonderful family which made me what I am today. I would like to dedicate this work to Baba. In this occasion, I also wish a happy and peaceful married life to Dalia.

A huge thanks to Prof. Kumlesh K. Dev for his immense support, guidance, patience, motivation and assistance which helped to think, execute, analyse and compose scientifically. I also want to extend my thanks to Dr Gavin Davey for his guidance for all the mitochondrial work. I thank Science Foundation Ireland for funding the work and Institute of Neuroscience, Trinity College Dublin for providing adequate space, facility and ambience for scientific research.

C. Abbreviations

The following abbreviations have been used

°C	: Degree Celsius	kDa	: Kilodalton
μF	: Microfarad	IBR	: In between RING fingers
μg	: Microgram	K ⁺	: Potassium ion
μl	: Microliter	kan	: Kanamycin
ABP	: AMPA receptor binding protein	kV	: Kilovolt
AD	: Alzheimer's disease	LRRK2	: Leucine-rich repeat kinase 2
ALS	: Amyotrophic lateral sclerosis	lt	: Liter
amp	: Ampicillin	M	: Molar
AMPA	: α-amino-3-hydroxyl-5-methyl-4-isoxazole-propionate	mA	: Milliampere
ARJP	: Autosomal recessive juvenile Parkinsonism	MBP	: Maltose binding protein
ASIC2a	: Acid-sensing ion channel subunit 2a	MCS	: Multiple cloning site
BAR	: Bin-Amphiphysin-Rvs	mg	: Milligram
Bax	: Bcl-2 associated X protein	min	: Minute(s)
Bcl-2	: B-cell CLL/lymphoma 2	ml	: Milliliter
bp	: Basepair(s)	mM	: Millimolar
CASK	: Calcium/calmodulin-dependent serine protein kinase	Na ⁺	: Sodium ion
Ca ²⁺	: Calcium ion	ng	: Nanogram
CNS	: Central nervous system	OD	: Optical density
CPD	: Cdc4α phosphodegron	PAGE	: Poly acrylamide gel electrophoresis
CREB	: cAMP response element-binding	PARK1	: α-synuclein
ct	: Carboxyl terminal end	PCI	: Phenol-chloroform-isoamyl alcohol
Cul1	: Cullin 1	PCR	: Polymerase chain reaction
DEG	: Degenerin/epithelial Na ⁺ channel	PD	: Parkinson's disease
DMD	: Duchenne muscular dystrophy	PDZ	: PSD95/DlgA/ZO-1
DMSO	: Di-methyl sulfoxide	pg	: Picogram
dNTP	: de-oxyribonucleotide tri-phosphate	PGC-1α	: Peroxisome proliferator-activated
E1	: Ubiquitin activating enzyme	PICK1	: Protein interacting C kinase
E2	: Ubiquitin conjugating enzyme	PINK1	: PTEN-induced kinase piperazineethanesulfonic acid
E3	: Ubiquitin ligase enzyme	PKCα	: Protein kinase C α
EDTA	: Ethylene diamine tetraacetic acid	Rbx1	: RING-box protein 1 receptor- γ coactivator
EGTA	: Ethylene glycol tetraacetic acid	rpm	: Revolution per minute
ER	: Endoplasmic reticulum	RRM	: RNA recognition motif
ETC	: Electron transport chain	SCF	: Skp1-Cullin-F-box protein
g	: Gram	SDS	: Sodium dodecyl sulphate
GluR2	: Glutamate receptor subunit 2	sec	: Second
GRIP	: Glutamate receptor interacting protein	Skp1	: S-phase kinase-associated protein1
GSK3β	: Glycogen Synthase Kinase	SOD	: Superoxide dismutase
GST	: Glutathione S-transferase	U	: Enzyme units
HD	: Huntington's disease	UBL	: Ubiquitin like domain
HECT	: Homology to E6-AP carboxy terminus	UCH-L1	: Ub carboxyl-terminal hydrolase
HEK 293	: Human Embryonic Kidney 293	UPS	: Ubiquitin proteasomal system
HEPES	: 4-(2-hydroxyethyl)-1	V	: Volt
h	: Hour(s)	WD40	: Beta-transducin repeat
		xg	: Relative centrifugal force
		YPAD	: Peptone adenine D-glucose
		Ω	: Ohm

D. Table of content

A. Declaration	1
B. Acknowledgements	2
C. Abbreviations	3
D. Table of content	4
E. Abstract	12
1. Introduction	14
1. Central Nervous System	15
2. Synaptic transmission	16
2.1 Glutamate release	16
2.2 Glutamate receptors	19
2.2.1 Ionotropic glutamate receptors	19
AMPA receptor	20
KA receptor	20
NMDA receptor	20
2.2.2 Metabotropic glutamate receptors	21
Group I	21
Group II and III	21
2.2.3 Glutamate receptor interacting proteins	21
2.3 Glutamate excitotoxicity	22
3. Introduction to mitochondria	22
3.1 Basics of Electron Transport Chain (ETC)	23
3.2 Mitochondrial calcium sequestration	26
3.3 Mitochondrial dysfunction	27
4. Synaptosomes	28
4.1 Cytosolic and vesicular glutamate release by synaptosomes	30
4.2 Depolarization of synaptosomes	31
5. Parkinson's Disease	32
5.1 Introduction	32
5.2 Genetic forms of PD	32
5.3 GWAS and Linkage studies in PD	33
5.4 Current treatments for PD	35
6. Neurodegeneration & protein aggregation	37
6.1 Lewy bodies: Hallmark of PD	37
6.2 Ubiquitination	38
6.3 Sumoylation	40
7. Parkin as an E3 Ligase	41
8. Parkin interacting proteins	42
8.1 E2 conjugating enzymes: Ubch7 and Ubch8	46
8.2 Parkin ubiquitinated proteins	46
8.2.1 α -synuclein	46

8.2.2 Synphilin-1	46
8.2.3 Synaptotagmin XI	47
8.2.4 CDCrel-1	47
8.2.5 PAEL-R	48
8.2.6 PARIS (ZNF746)	48
8.2.7 p38 subunit of aminoacyl-tRNA synthase (ARS) complex	48
8.2.8 Proteasomal subunit S5a	49
8.2.9 Endocytic protein Eps15	50
8.2.10 Non-receptor tyrosine kinase c-Abl	50
8.3 E3 ligase partners of parkin	51
8.3.1 Cdc4 α	51
8.3.2 Heat shock protein 70 (HSP70) and CHIP	51
8.4 Parkin scaffolding proteins	52
8.4.1 PDZ domains (CASK and PICK1)	52
8.4.2 Actin	52
9. Post-translational modification in parkin	53
10. PICK1 as a PDZ domain protein	55
10.1 Introduction to PICK1	55
11. PICK1 interacting proteins	57
11.1 Protein kinase C α (PKC α)	57
11.2 Monoamine Transporters	60
11.2.1 Dopamine transporter	60
11.2.2 Norepinephrine transporter	60
11.2.3 Serotonin transporter	61
11.3 Glutamate receptors	61
11.3.1 GluR2 (AMPA receptor subunit)	61
11.3.2 GluR5 (KA receptor subunit)	62
11.3.3 mGluR7 (Metabotropic receptor subtype)	62
12. Parkin-PICK1 interaction	63
12.1 The PDZ motif of parkin	63
12.2 Role of parkin-PICK1 interaction	64
13. Parkin and Mitochondria	64
14. Use of blocking peptides and compounds	66
15. Aim of the thesis	70
16. Hypothesis	70
2. Materials and Methods	72
Materials and equipment used	73
Animals used in this thesis	74
1. Molecular biology methods	74
1.1 General molecular cloning strategies	74
1.2 Bacterial competent cell preparation	74
1.3 Heat shock transformation and plasmid DNA extraction from bacteria	76
1.4 Polymerase Chain Reaction and restriction digestion	76
1.5 Phenol/Chloroform/Isoamyl alcohol (PCI) purification	76

1.6	DNA gel extraction	78
1.7	Dephosphorylation and ligation	78
2.	Yeast two hybrid methods	79
2.1	Competent yeast preparation	79
2.2	Yeast transformation	79
2.3	Interaction plate assay	81
3.	Cellular protein expression methods	81
3.1	Protein expression in bacterial cell	81
3.2	Purification of protein expressed in bacterial cell	82
3.3	Mammalian cell culture and cell transfection	83
4.	Biochemical methods	83
4.1	Preparation of cell lysate	83
4.2	Preparation of rat brain lysate	83
4.3	GST/MBP pull-down assay	85
4.4	SDS-Poly Acrylamide Gel Electrophoresis and western blotting	85
5.	Mitochondrial assays	87
5.1	Isolation of synaptosomes using Ficoll gradients	87
5.2	Determination of protein concentration by Bradford assay	89
5.3	Measurement of ROS production	89
5.4	Mitochondrial membrane potential measurement	92
5.5	Glutamate release assay	93
5.6	Respiratory chain complex assay	94
6.	Primary Cell Culture	96
6.1	Set-up and preparation before primary cell culture	96
6.2	Brain dissection for primary cultures	96
6.3	Neuronal Culture	97
6.4	Immunocytochemistry	97
3.	Results: 1 Validation of parkin-PICK1 interaction and of the MNP201 parkin peptide	99
	Abstract	100
	Introduction	101
	Results	103
3.1	Design of MNP201	103
3.2	Pull-down of PICK1 with GST-GluR2-ct	103
3.3	Pull-down of endogenous parkin by MBP-PICK1	106
3.4	Co-IP experiments using HA-parkin and Flag-PICK1 co-transfected in HEK293 cells	106
3.5	Identification of non-specific bands expressed by Flag beads and MBP-beads	109
3.6	Identification of non-specific bands expressed by anti-PRK8 and anti-PICK1 antibody	109
3.7	Pull-down of HA-parkin Δ Ub by MBP-PICK1	111
3.8	Production of lentiviral constructs of HA-parkin and HA-parkin Δ pdz	113
3.9	Binding of MNP201 in PDZ domain of MBP-PICK1 in fluorescence polarisation assay	113

Discussion	118
4. Results: 2 Effect of MNP201 on mitochondrial function	121
Abstract	122
Introduction	123
Results	126
4.1 Design and use of MNP202	126
4.2 The ct of Cdc4 α does not interact with PICK1	126
4.3 Synaptosomes contain both parkin and PICK1	129
4.4 Effect of MNP201 on complex I assay	129
4.5 Effect of MNP201 on complex IV assay	132
4.6 Effect of MNP201 on peroxide production	134
4.7 Effect of MNP201 on mitochondrial membrane potential	134
4.8 Standardisation of glutamate release assay	137
4.9 Effect of MNP201 on KCl-induced glutamate release without CaCl ₂	140
4.10 Effect of MNP201 on KCl-induced glutamate release with CaCl ₂	140
4.11 Effect of MNP201 on 4-AP-induced glutamate release	143
Discussion	146
1. Summary of results	146
2. Design of MNP201 parkin peptide	146
3. Effects of MNP201 in mitochondrial function	148
4. Effects of MNP201 on glutamate release assay	148
5. Permeability of MNP201	149
6. Effect of MNP201 in condition of cell stress	150
7. Moving to the next chapter	150
5. Results: 3 Effect of Tat-MNP201 on mitochondrial function	152
Abstract	153
Introduction	154
Results	157
5.1 Concentration-dependent internalisation of FITC-Tat-MNP201 into neuronal cells	157
5.2 Concentration-dependent internalisation of FITC-Tat-MNP201 into astrocytes	160
5.3 Effect of Tat-MNP201 on peroxide production	160
5.4 Effect of Tat-MNP201 on mitochondrial membrane potential	164
5.5 Dose-dependent increase in mitochondrial membrane depolarization with FCCP	166
5.6 Tat-MNP201 depolarizes mitochondrial membrane potential in partial stress condition	166
5.7 Effect of Tat-MNP201 on 4-AP-induced glutamate release without CaCl ₂	169
5.8 Effect of Tat-MNP201 on 4-AP-induced glutamate release with CaCl ₂	171
Discussion	173
1. Summary of results	173
2. Tat-MNP201 reduces mitochondrial membrane potential	173

3.	Effect of Tat-MNP201 in glutamate release	175
4.	Parkin-PICK1 role in mitochondrial membrane potential	175
5.	Alternative mechanisms for MNP201 effects on mitochondrial membrane potential	176
7.	Moving to the next chapter	177
6. Results: 4 Effect of FSC231 on mitochondrial function		178
	Abstract	179
	Introduction	180
	Results	183
6.1	Computational data shows docking of FSC231 in PICK1 PDZ domain	183
6.2	Effect of FSC231 in complex I assay	183
6.3	Effect of FSC231 in complex IV assay	185
6.4	Effect of FSC231 on peroxide production	188
6.5	Effect of FSC231 on mitochondrial membrane potential	188
6.6	FSC231 depolarizes mitochondrial membrane potential in partial stress condition	191
6.7	Effect of FSC231 in KCl-stimulated glutamate release assay in the absence of CaCl ₂	193
6.8	Effect of FSC231 in KCl-stimulated glutamate release assay in the presence of CaCl ₂	195
6.9	Effect of FSC231 in 4-AP-stimulated glutamate release	195
	Discussion	200
1.	Inhibition of PICK1 by FSC231 induces mitochondrial depolarization	200
2.	PICK1 plays no role in glutamate release	200
3.	The role of parkin-PICK1 and PKC α -PICK1 in mitochondria	202
7. Final discussion		204
7.1	Summary of findings	205
7.2	The parkin-PICK1 interaction	205
7.3	Oligopeptides need assistance to internalise through bi-lipid membrane	206
7.4	Possible effect of Tat portion of Tat-MNP201	206
7.5	Proposed model of FSC231 on mitochondrial dysfunction	207
7.6	Caveat of this study	208
7.7	Future direction	210
7.8	Closing comments	211
8. References		212

List of Figures

Introduction

Figure 1.1:	Glutamate release and mitochondria	18
Figure 1.2:	ETC cycle of mitochondria	24
Figure 1.3:	Pathways of mitochondrial dysfunction	29
Figure 1.4:	Ubiquitin Proteasome System	39
Figure 1.5:	Structure and protein sequence of parkin	43
Figure 1.6:	Parkin interacting partners	44
Figure 1.7:	Phosphorylation sites of parkin and responsible kinases.	54
Figure 1.8:	Structure and protein sequence of PICK1	56
Figure 1.9:	The PICK1 interacting partners	58
Figure 1.10:	Mechanism of blocking agents to disrupt parkin-PICK1	67
Figure 1.11:	Working hypothesis of the project	71

Materials and Methods

Figure 2.1:	Cloning strategy	75
Figure 2.2:	Yeast plasmid vectors	80
Figure 2.3:	Mammalian plasmid vectors	84
Figure 2.4:	Bacterial plasmid vectors	86
Figure 2.5:	Isolation of synaptosomes using Ficoll gradient	90

Results 1: Validation of parkin-PICK1 interaction and of the MNP201 parkin peptide

Figure 3.1:	Blocking peptides based on the ct of parkin	104
Figure 3.2:	GST pull-down experiment showing PICK1-GluR2 interaction	105
Figure 3.3:	MBP pull-down experiment with bacterial expressed MBP-PICK1 and endogenous parkin	107
Figure 3.4:	Co-IP experiment with transiently transfected HEK293 cells with HA-parkin and Flag-PICK1	108
Figure 3.5:	Identification of non-specific bands expressed by Flag beads	110
Figure 3.6:	Identification of non-specific bands expressed by anti-PRK8 and anti-PICK1 antibodies	112
Figure 3.7:	MBP pull-down experiment with bacterial expressed MBP-PICK1 and transiently transfected HEK293 cells with HA-parkin Δ Ub	114
Figure 3.8:	Cloning of Lenti-HA-parkin and Lenti-HA-parkin Δ pdz	115
Figure 3.9:	Binding of MNP201 in PDZ domain of PICK1	116

Results 2: Effect of MNP201 on mitochondrial function

Figure 4.1:	List of peptides based on ct of Cdc4 α	127
Figure 4.2:	Yeast two hybrid assay shows no interaction between Cdc4 α and PICK1	128
Figure 4.3:	Presence of parkin and PICK1 in synaptic and non-synaptic fraction	130
Figure 4.4:	Effect of MNP201 in complex I of ETC cycle	131
Figure 4.5:	Effect of MNP201 in complex IV of ETC cycle	133
Figure 4.6:	Effect of MNP201 on ROS production	135
Figure 4.7:	Effect of MNP201 on mitochondrial membrane potential	136

Figure 4.8:	KCl and 4-AP-stimulated glutamate release	138
Figure 4.9:	Standard curve of glutamate release	139
Figure 4.10:	Effect of MNP201 on KCl-induced glutamate release in the absence of CaCl ₂	141
Figure 4.11:	Effect of MNP201 on KCl-induced glutamate release in the presence of CaCl ₂	142
Figure 4.12:	Effect of MNP201 on 4-AP-induced glutamate release in the absence of CaCl ₂	144
Figure 4.13:	Effect of MNP201 on 4-AP-induced glutamate release in the presence of CaCl ₂	145
Results 3:	Effect of Tat-MNP201 on mitochondrial function	
Figure 5.1:	List of Tat-tagged MNP201 peptides	158
Figure 5.2:	Dose-dependent uptake of FITC-Tat-MNP201 into neuronal cells	159
Figure 5.3:	Dose-dependent uptake of FITC-Tat-MNP201 into astrocytes	161
Figure 5.4:	Dose-dependent uptake of FITC-Tat-MNP201 into the processes of astrocytes	162
Figure 5.5:	Effect of Tat-MNP201 on ROS production	163
Figure 5.6:	Effect of Tat-MNP201 on mitochondrial membrane potential	165
Figure 5.7:	FCCP standard curve	167
Figure 5.8:	Effect of Tat-MNP201 on mitochondrial membrane potential under FCCP-induced partial stress condition	168
Figure 5.9:	Effect of Tat-MNP201 on 4-AP-induced glutamate release without CaCl ₂	170
Figure 5.10:	Effect of Tat-MNP201 on 4-AP-induced glutamate release with CaCl ₂	172
6. Results: 4	Effect of FSC231 in mitochondrial function	
Figure 6.1:	FSC231, the blocking compound of PICK1 PDZ domain	184
Figure 6.2:	Effect of FSC231 on complex I of ETC cycle	186
Figure 6.3:	Effect of FSC231 on complex IV of ETC cycle	187
Figure 6.4:	Effect of FSC231 on ROS production	189
Figure 6.5:	Effect of FSC231 on mitochondrial membrane potential	190
Figure 6.6:	Effect of FSC231 on mitochondrial membrane potential under FCCP-induced partial stress condition	192
Figure 6.7:	Effect of FSC231 on KCl-induced glutamate release in the absence of CaCl ₂	194
Figure 6.8:	Effect of FSC231 on KCl-induced glutamate release in the presence of CaCl ₂	196
Figure 6.9:	Effect of FSC231 on 4-AP-induced glutamate release in the absence of CaCl ₂	197
Figure 6.10:	Effect of FSC231 on 4-AP-induced glutamate release in the presence of CaCl ₂	199
7. Final discussion		
Summary figure:	Probable Involvement of parkin-PICK1 to regulate mitochondrial function and apoptosis	209

List of Tables

1. Introduction

Table 1.1:	List of gene associated with PD	34
Table 1.2:	Novel loci associated with PD	36
Table 1.3:	List of proteins associated with parkin	45
Table 1.4:	List of PICK1 interacting proteins	59

2. Materials and methods

Table 2.1:	List of primers	77
Table 2.2:	List of antibodies used	88
Table 2.3:	A) Method of Bradford assay	91
	B) List of peptides	91

4. Results 2: Effect of MNP201 on mitochondrial function

Table 4.1:	Summary of data obtained using MNP201	147
------------	---------------------------------------	-----

5. Results: 3 Effect of Tat-MNP201 on mitochondrial function

Table 5.1:	Summary of data obtained by using Tat-MNP201	174
------------	--	-----

6. Results: 4 Effect of FSC231 in mitochondrial function

Table 6.1:	Summary of data obtained by using FSC231	201
------------	--	-----

E. Abstract

Autosomal Recessive Juvenile Parkinsonism (ARJP) is the most common motor-related neurodegenerative disease, which occurs in young adults between 20-40 years of age. Mutations in the *parkin* (PARK2) gene are associated ARJP, which result in the loss of dopaminergic neurons of substantia nigra pars compacta in the mid brain. Parkin, an E3 ligase, is an enzyme responsible for ubiquitination of several proteins leading to their degradation in Ubiquitin Proteasomal System (UPS) and promoting autophagy of depolarized mitochondria. Mutations in the *parkin* gene are thought to result in protein aggregation of parkin substrates resulting in neuronal toxicity. Among these parkin interacting proteins and substrates, several play important roles in mitochondrial function, oxidative stress, cellular toxicity and apoptosis. This project focused on investigating the role of one particular protein that interacts with parkin, namely, PICK1. Specifically, the studies herein investigated the role of a parkin-PICK1 interaction in mitochondrial function and oxidative stress. PICK1 (Protein Interacting C Kinase) is a scaffolding protein, which is thought to recruit PKC α and likely parkin to the outer membrane of mitochondria to regulate cellular apoptosis. To decipher the importance of the parkin-PICK1 protein complex, a 'molecular neuro peptide' MNP201 (VCMGDHWFDV) was engineered to block this interaction. The MNP201 peptide was based on the amino acid sequence of the C-terminus (ct) of parkin, which contains a PDZ motif that interacts with PDZ domain of PICK1. Here, the biological activities of wildtype and mutated versions of MNP201 are reported on mitochondrial function and glutamate release. Firstly, to demonstrate the binding of MNP201 to PICK1, various affinity purification studies and fluorescence polarisation assays were performed. The results suggested that the MNP201 parkin peptide binds to PICK1 in a concentration-dependent manner. Secondly, the effect of MNP201 was tested on reactive oxygen species production, mitochondrial membrane potential and the activity of complex I and complex IV as well as rate of glutamate release. The results suggested that MNP201 had little or no effect on these mitochondrial properties or on the rate of glutamate release. Thirdly, to ensure the entry of MNP201 into synaptosomes, a tat tagged version of MNP201 (Tat-MNP201) was synthesised and its effect on mitochondrial properties and rate of glutamate release was examined. Similar to the non-tagged version of MNP201, no change was observed in the presence of Tat-MNP201 on reactive oxygen species production, the activity of complex I and complex IV or the rate of glutamate release. Importantly, however, the results suggested that Tat-MNP201 increased the rate of mitochondrial depolarization in comparison to control values. Finally, to support the findings that the Tat-MNP201 parkin peptide increases the rate of mitochondrial membrane depolarization, the compound FSC231, which binds the PDZ domain of PICK1, was tested on similar mitochondrial and

glutamate release assays. In agreement with results obtained using Tat-MNP201, the FSC231 compound also increased the rate of depolarization in mitochondrial membrane potential under FCCP-induced stress conditions. Taken together, the data suggested that PICK1 plays a role in the maintenance of mitochondrial membrane potential likely via its PDZ domain interacting proteins such as parkin and PKC α .

1. Introduction

1. Central Nervous System

The central nervous system (CNS) is composed four major cell types, namely, neurons and the three glial cells oligodendrocytes, microglia and astrocytes. The neuron is the structural and functional unit of the CNS responsible for communicating information in both chemical and electrical forms. Functionally, neurons can be divided into sensory (or afferent) and motor (or efferent) neurons. Structurally, a neuron can be divided into three parts, namely, the soma (cell body), dendrites and the axon. The soma or the cell body of a neuron contains its cellular organelles, including the nucleus, rough endoplasmic reticulum (RER), smooth endoplasmic reticulum (SER), the Golgi apparatus and mitochondria in a potassium rich cytosol. Axons originate at the axon hillock of the soma and end in pre-synaptic terminals forming synapses with post-synaptic terminals of neuronal dendrites. Dendrites are cellular extensions emerging from the soma that can appear highly reticulated, thus are often also referred to as dendritic trees. The membrane, in particular the post-synaptic density (PSD), of dendrites contains a high number of cellular receptors, which respond to an array of molecules, including neurotransmitters, neurohormones and growth factors.

Glial cells, unlike neurons, are capable of mitotic cell division and, in general terms, function to provide nutrition, physical support, and immuno-protection. Broadly, glial cells are divided into two groups, macroglia and microglia. The group of macroglial cells include astrocytes, oligodendrocytes and ependymal cells. Astrocytes are the most abundant glial cells in the CNS and are responsible for regulating the fluid-content of the extracellular space in the CNS by active removal of excess ions, including K^+ . These cells also uptake excess neurotransmitters released, such as glutamate, thus can limit excitotoxicity. Astrocytes also release a number of growth factors and cytokines allowing them to communicate with and regulate the function of neuronal, glial and immune cells. In addition, astrocytes, via their end feet can 'synapse' onto endothelial cells to control the permeability of the blood-brain-barrier. During insult, for example in spinal cord injury, astrogliosis can result, forming scar tissue that acts as a barrier to neuronal regeneration. Oligodendrocytes, on the other hand, are cells that form a myelin sheath that insulates axons and consequently promotes the speed of action potentials and nerve conductance. The loss of oligodendrocyte function, cell numbers and/or myelin integrity is particularly important in the study of demyelinating disorders such as multiple sclerosis. Although, often forgotten as glial, ependymal cells are members of this cell-type and are involved in cerebrospinal fluid (CSF) production and circulation. These cells form the epithelial lining inside the ventricular cavities of CNS. The cilia present on the apical surface of these cells are responsible for the circulation of CSF. Lastly, microglia cells are known as the fixed macrophages of the brain, providing a well described immune function in

the nervous system (Kettenmann et al., 2011). The aberrant function of microglia has been associated with a number of neurodegenerative disorders including Alzheimer's disease. These cells release a range of chemokines and cytokines and also play a role in a number of neuroinflammatory disorders. Thus, taken together, neurons and glial cells function in a synchronised manner to maintain synaptic transmission and CNS function.

2. Synaptic transmission

Synaptic transmission, in simple terms, is the conductance of an electric and chemical signal from one neuron to another through the pre-synaptic release of a neurotransmitter, triggered by an action potential, into the synaptic cleft and subsequent binding of the neurotransmitter to post-synaptic receptors and/or ion channels. A wide range of neurotransmitters exist, including amino acids (such as glutamate, glycine, aspartate, D-serine and γ -aminobutyric acid or GABA); amines (for example dopamine, norepinephrine, epinephrine, histamine and serotonin); peptides (such as β -endorphin) or others (including acetylcholine, adenosine, anandamide and nitric oxide). Generally, these neurotransmitters are synthesised pre-synaptically and packaged into secretory vesicles. Upon receiving a stimulus, these vesicles fuse to the membrane of pre-synaptic terminal to release the neurotransmitter. The released neurotransmitter then activates the post-synaptic region by binding with their cognate receptors. The synthesis, mechanism of release and function of glutamate are described below, the most common excitatory neurotransmitter present in the CNS.

2.1 Glutamate release

Glutamate is the major excitatory neurotransmitter in the mammalian CNS and was identified by a German chemist Karl Heinrich Leopold Ritthausen in the year 1866 as an amino acid. Glutamate is one of the two excitatory amino acid neurotransmitters (the other being aspartate) that plays a key role in physiological processes of the CNS, such as cognition and learning and memory (Bliss and Collingridge, 1993). In addition, glutamate plays roles in brain development, cellular survival and synaptic plasticity, i.e., formation and elimination of synaptic strength. The mammalian brain is enriched with glutamate, on average 5-15 mmol glutamate per kg brain tissue depending on the region of the brain. However, release of excessive amounts of glutamate causes excitotoxic death of neurons (Bergman et al., 1994; Obeso et al., 2004).

The reserve of glutamate is maintained in neuronal cells by two processes. First, glucose is metabolised to α -oxoglutarate via the Krebs cycle, which is further transaminated to

glutamate by α -oxoglutarate transaminase. Secondly, uptake of released glutamate takes place from the synaptic cleft by the pre-synaptic terminal. Glial cells also take up glutamate with the help of cell membrane expressing glutamate transporters through a high affinity, sodium (Na^+)-dependent uptake mechanism. In glial cells, glutamate is converted to glutamine by glutamine synthetase enzyme.

The steps involved in glutamate release are outlined below (**Figure 1.1**)

1. Glutamate is produced from α -oxoglutarate, a byproduct of Krebs cycle. Recycled glutamine is then converted to glutamate by glutaminase in mitochondria present in the neuronal terminal.
2. Glutamate is packaged by active transport into secretory vesicles to form a neurotransmitter filled vesicle. This step occurs through a vesicular transporter present on the surface of vesicles through which glutamate is taken into synaptic vesicles.
3. Upon receiving a stimulus, glutamate filled vesicles travel to the pre-synaptic terminal to fuse with the pre-synaptic membrane. Fusion of the vesicle and the pre-synaptic terminal membranes is mediated by two groups of soluble N-ethylmaleimide-sensitive factor attachment protein receptors (SNARE) proteins, namely, vesicular SNARE (V-SNARE) and target SNARE (T-SNARE). V-SNARE proteins such as syntaxin and SNAP-25 (soluble NSF attachment protein) are present on the pre-synaptic plasma membrane, while T-SNARE such as synaptobrevin is present on the surface of vesicles (Söllner et al., 1993). These three proteins form a trimeric SNARE complex binding site for proteins, such as NSF (N-ethylmaleimide sensitive factor) and SNAP (soluble NSF attachment protein), which help in the fusion process between the membranes of vesicle and pre-synaptic terminal (Block et al., 1988; Clary et al., 1990). The action potential also triggers influx of calcium ions (Ca^{2+}) to bind synaptotagmin, a Ca^{2+} sensor protein present on the vesicle membranes. The activated synaptotagmin binds with SNAP-25 to initiate fusion of the synaptic vesicle with the pre-synaptic membrane (Schiavo et al., 1997). In particular, synaptotagmin binds to syntaxin and VAMP, causing docking and fusion of vesicle and pre-synaptic membranes (Rothman, 1994; Söllner, 1995).
4. Fusion of these two membranes then leads to the exocytosis of glutamate, i.e., release of glutamate into synaptic cleft to activate the receptors at the post-synaptic region and/or auto-receptors at the pre-synaptic site.

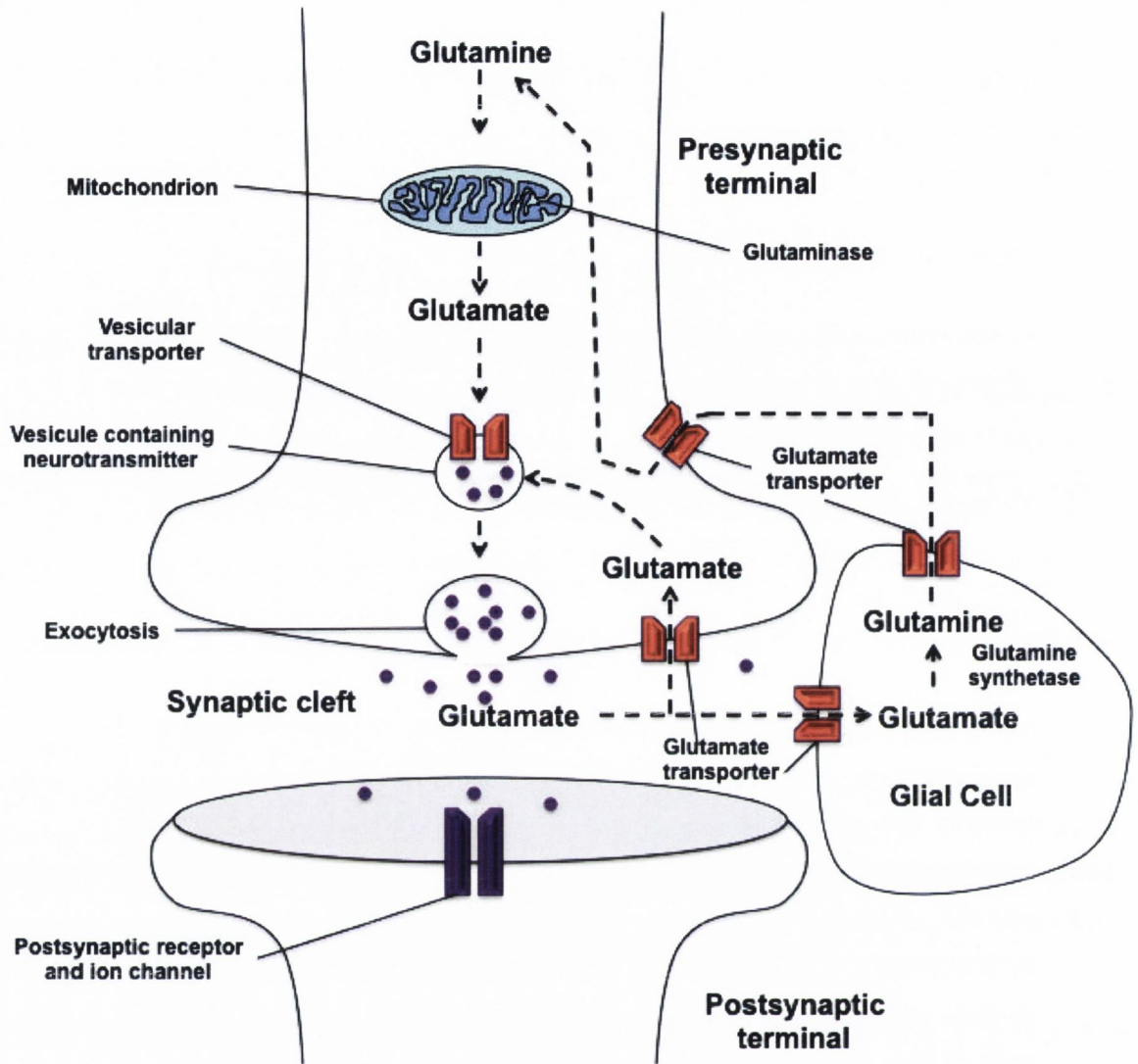


Figure 1.1: Glutamate release and mitochondria

Glutamate is a major excitatory neurotransmitter present in the mammalian brain. Glutamate is produced from glutamine by a mitochondrial enzyme glutaminase and packaged into vesicles through vesicular transporters. Action potentials mediate glutamate-filled vesicles to fuse with the pre-synaptic membrane and glutamate is released into the synaptic cleft by exocytosis to bind post- and/or pre-synaptic receptors. Excess glutamate is taken up from the synaptic cleft by glutamate transporters present on pre-synaptic terminals and glial cells. In glial cells, glutamate is converted to glutamine and transported to the pre-synaptic nerve terminals through glutamate transporters. In the pre-synaptic terminal, glutamine is converted to glutamate and included into the packaging vesicles.

5. Glutamate transporters, present on pre-synaptic nerve terminals and adjacent glial cells, uptake glutamate from the synaptic cleft through a high affinity, Na⁺-dependent mechanism and repack glutamate into synaptic vesicles for reuse.
6. On the other hand, the glutamate that is taken up by glial cells is converted to glutamine by glutamine synthetase. This glutamine is then transported to the nerve terminals through glutamine transporters present on the surface of glia and nerve terminals.
7. In the pre-synaptic terminal, glutamine is again converted to glutamate by mitochondrial enzyme glutaminase. The recycled glutamate is then repackaged by active transport into the synaptic vesicles to form a neurotransmitter filled vesicles, ready for release.

2.2 Glutamate receptors

Glutamate receptors are divided into two groups, ionotropic and metabotropic glutamate receptors. These receptors are grouped based on sequence homology, pharmacological and electrophysiological properties (Scannevin and Huganir, 2000).

2.2.1 Ionotropic glutamate receptors

There are three subtypes of ionotropic glutamate receptors present on pre- and/or post-synaptic regions of the synapses namely, the 2-amino-3-hydroxy-5-methyl-4-isoxazole propionate (AMPA) receptor subtype (Nakanishi et al., 1990; Colquhoun, 1992), the N-methyl D-aspartate (NMDA) receptor subtype (Moriyoshi et al., 1991; Kumar et al., 1991; Barnard, 1992) and kainate (KA) receptor subtype (Egebjerg et al., 1991). These receptors have a homologous structure and a common evolutionary origin. Typically, they contain three transmembrane domains (M1, M3 and M4) and one cytoplasmic re-entrant loop (M2) and an intracellular carboxy terminal (ct). The ligand-binding domain is formed by two globular domains S1 (N-terminal end of M1 domain) and S2 (between M3 and M4) (Bleakman and Lodge, 1998; Chen and Wyllie, 2006). These receptors are permeable to cations (Ca²⁺, Na⁺, K⁺), where Ca²⁺ is responsible for triggering a number of intracellular signalling cascades (Dingledine et al., 1999). Short descriptions of these receptors are presented below.

AMPA receptor

AMPA receptors, responsible for the fast excitatory neurotransmission, are found ubiquitously expressed in the CNS. Certain areas, including the hippocampus have a high density of AMPA receptors, where their role in excitatory transmission and synaptic plasticity events such as long term potentiation (LTP) and depression (LTD) have been best described (Ozawa et al., 1998). The AMPA receptor is made up of four subunits, including GluR1-GluR4, which share 65-75% homology in structure. AMPA receptor undergo splicing and RNA editing, allowing for further diversity. These subunits are believed to form a tetrameric structure by homomeric and heteromeric combination (Chen and Wyllie, 2006). AMPA receptors control the influx of Na^+ and Ca^{2+} ; and the presence of the GluR2 subunit determines AMPA receptor-associated Ca^{2+} permeability.

KA receptor

KA receptors are also responsible for the fast excitatory neurotransmission in CNS. KA receptors are distributed in the spinal cord, cerebellum, pyramidal neurons of neocortex and hippocampus (Bleakman and Lodge, 1998). The KA receptors subunit family is composed five subunits KA1, KA2, GluR5, GluR6 and GluR7. Similar to AMPA receptor subunits, KA receptor subunits, are approximately 900 amino acids in length, undergo alternative splicing and RNA editing to give rise to a number of receptor isoforms (Chittajallu et al., 1999). Of interest, pre-synaptic KA receptors regulate the release of GABA and glutamate (Darstein et al., 2003; Jaskolski et al., 2004). At post-synaptic terminals, KA receptors are believed to play a role in temporal integration of excitatory signals and regulate neuronal excitability by modulating a low excitatory post-synaptic current (EPSC) (Jaskolski et al., 2004).

NMDA receptor

NMDA receptors are heterotetrameric complexes, responsible for slow phase neurotransmission (Scannevin and Huganir, 2000; Doucet et al., 2012). In general, four subunits assemble to form a functional NMDA receptor ion channel, including two NR1 and two NR2 (A-D) subunits (Doucet et al., 2012). Activation of NMDA receptors takes place by the binding of both glutamate on NR1 and glycine on NR2 (Dingledine et al., 1999). Some NMDA receptors are also reported to contain NR3 (A-B) subunits, which may influence single channel conductance (Dingledine et al., 1999). At a resting membrane potential, NMDA receptors remain blocked by

extracellular Mg^{2+} , which is removed by AMPA receptor-mediated depolarization, making the NMDA receptor functional (Doucet et al., 2012). Activated NMDA receptors allow the influx of high amounts of Ca^{2+} and low amounts of Na^{+} and K^{+} (Doucet et al., 2012). The influx of Ca^{2+} triggers a number of intracellular signalling cascades, including a Ca^{2+} /calmodulin complex (Doucet et al., 2012). Overactivation of NMDA receptors, however, can lead to excitotoxicity via pathways that stimulate neuronal nitric oxide synthases (nNOS) and nitric oxide (Aarts and Tymianski, 2003).

2.2.2 Metabotropic glutamate receptors

In addition to the ionotropic glutamate receptors indicated above, several G-protein coupled metabotropic glutamate receptors (mGluR1-8) have been identified, which may be present either pre or post-synaptically (Sladeczek et al., 1985; Sugiyama et al., 1987; Schoepp et al., 1990). These receptors are distributed throughout the CNS with specific localisation in synaptic and extra-synaptic areas in neurons and in glial cells (Niswender and Conn, 2010). These receptors (mGluR1-8) have an extracellular N-terminal glutamate binding domain, seven transmembrane domains and an intracellular ct (Doucet et al., 2012). In general, mGluRs can be positively coupled to inositol phosphate or negatively to adenylyl cyclase. Metabotropic glutamate receptors are divided into three subtypes, group I-III.

Group I

Group I mGluRs comprise two receptor subtypes, mGluR1 and mGluR5, which are coupled to phospholipase C, responsible for excitatory glutamate release (Doucet et al., 2012). These receptors also activate Ca^{2+} channels but inhibit K^{+} channels. In addition, these receptors are also known to induce phosphorylation of ion channels and transcription factors (Doucet et al., 2012).

Group II and III

The group II (mGluR2 and mGluR3) and group III (mGluR4, 6, 7 and 8) mGluRs are coupled to adenylyl cyclase (Doucet et al., 2012). These receptors, such as mGluR7, can be predominantly located on pre-synaptic terminals and inhibit glutamate and GABA release (Hashimoto, 2009).

2.2.3 Glutamate receptor interacting proteins

Notably, the ct for all glutamate receptor subunits and subtypes are located intracellularly allowing these regions to interact with a number of trafficking and

scaffolding proteins. In particular, the ct of nearly all glutamate receptor subunits and subtype contain PDZ motifs, which allow them to interact with a wide range of PDZ domain containing proteins, such as PICK1. These interactions are vital for the correct temporal (activity-dependent) and spatial (synaptic and extrasynaptic) placement of glutamate receptors at the synaptic membrane of neurons.

2.3 Glutamate excitotoxicity

Excitotoxicity, elicited by glutamate is responsible for many neurodegenerative diseases, including Parkinson's disease (PD), Alzheimer's disease (AD), Huntington's disease (HD) and amyotrophic lateral sclerosis (ALS) (Beal, 1992; Mattson, 2003). Involvement of mitochondrial dysfunction is also implicated in these above mentioned diseases (Beal, 1992; Doble, 1999; Lin and Beal, 2006). Analysis of the substantia nigra pars compacta (SNPC) region of the mid brain, where selective elimination of dopaminergic neurons occurs in the case of PD, reveals that this area receives abundant glutamatergic excitation from the medial prefrontal cortex, subthalamic nucleus and pedunculopontine tegmental nucleus (Bezard et al., 1997). Reports also suggest that PD induced by the neurotoxin MPTP (1-methyl-4-phenyl-1, 2, 3, 6-tetrahydropyridine) stimulates excitotoxic levels of glutamate release in the SNPC area (Bezard et al., 1997). Upon administration of MPTP, the rate of firing increases significantly in glutamatergic nerve terminals, likely contributing to the excitotoxic cell death of dopaminergic neurons (Bergman et al., 1994; Obeso et al., 2004). MPTP is an inhibitor of complex I, the first respiratory complex of the electron transport chain (ETC) in mitochondria, and impairment of complex I in the SNPC, as well as the frontal cortex, is widely reported in PD patients (Schapira et al., 1989; 1990; Keeney et al., 2006; Parker et al., 2008). In addition, mitochondrial DNA mutation is also reported to be associated with idiopathic PD (Parker and Parks, 2005). All these studies suggest possible links between glutamate excitotoxicity and complex I mitochondrial dysfunction leading to PD (Greenamyre et al., 2001; Dawson and Dawson, 2003; Trepper et al., 2004).

3. Introduction to mitochondria

Mitochondria produce ATP via the electron transport chain (ETC) and oxidative phosphorylation in the eukaryotic cells. In addition, mitochondria are involved in haem and iron-sulphur biogenesis and the regulation of Ca^{2+} levels in the cell. Mitochondria are the primary source of energy for cells, including neurons, where at least 70% of nerve terminal ATP is reported to be produced by mitochondria (Kauppinen and Nicholls, 1986a). Nerve terminal integrity and neuronal function *per se* is reliant on mitochondrial aerobic metabolism

(Gunter et al., 1994) and failure to maintain adequate oxygen supply quickly leads to cell death (Navarro and Boveris, 2004). The mammalian CNS consists of only 2% of the body weight, although the metabolic rate is extraordinarily high, consuming 20% of the oxygen inspired at resting condition (Silver and Erecinska, 1998). Most of this energy is used to maintain ionic gradients across the cell membranes of neurons. Clusters of mitochondria are found to be present in specialised areas of neurons, including the synaptic terminals, nodes of Ranvier and active growth cones; where a high amount of energy and Ca^{2+} homeostasis are required (Hollenbeck and Saxton, 2005).

Mitochondria produce energy by various mechanisms, including Krebs cycle and oxidative phosphorylation. Among all the energy producing mechanisms present in the cell, oxidative phosphorylation produces the highest amount of energy. The process of oxidative phosphorylation takes place in the mitochondrial matrix, in particular where energy producing complexes, known as the ETC, are found present in the inner mitochondrial membrane.

3.1 Basics of Electron Transport Chain (ETC)

The ETC consists of four prosthetic groups of integral proteins that transfer electrons in series. These are described below (**Figure 1.2**).

A. Complex I: The first component of the ETC, complex I (NADH:ubiquinone oxidoreductase, EC 1.6.5.3), catalyses the oxidation of nicotinamide adenine dinucleotide (NADH) to NAD^+ at a redox potential of -300 mV, pumping four protons out of the mitochondrial matrix to the intermembrane space. Coenzyme Q (CoQ) is reduced to ubiquinol during the oxidation of NADH by complex I. Complex I is composed of 45 different polypeptide subunits (Carroll et al., 2006), including 6 iron-sulphur centres (Hinchliffe and Sazanov, 2005) and a flavoprotein (Hatefi, 1985). The 'L-shaped' form of complex I includes a long hydrophobic arm embedded in the mitochondrial inner membrane and a short hydrophilic arm extended into the mitochondrial matrix. The short arm contains the flavin mononucleotide (FMN) and nicotinamide adenine dinucleotide (NADH) active site (Hatefi, 1985). These arms assemble independently due to their separate genetic origin (Hofhaus et al., 1991). A neurotoxin, MPTP produces a toxic metabolite, MPP^+ inhibiting complex I to induce PD (Dauer and Przedborski, 2003). After the discovery of MPTP-induced PD, several studies have been conducted using complex I inhibitors. Rotenone, generally used as an insecticide and piscicide (fish toxin), was also found to be a specific and stoichiometric inhibitor of complex I activity in isolated mitochondria (Chance and

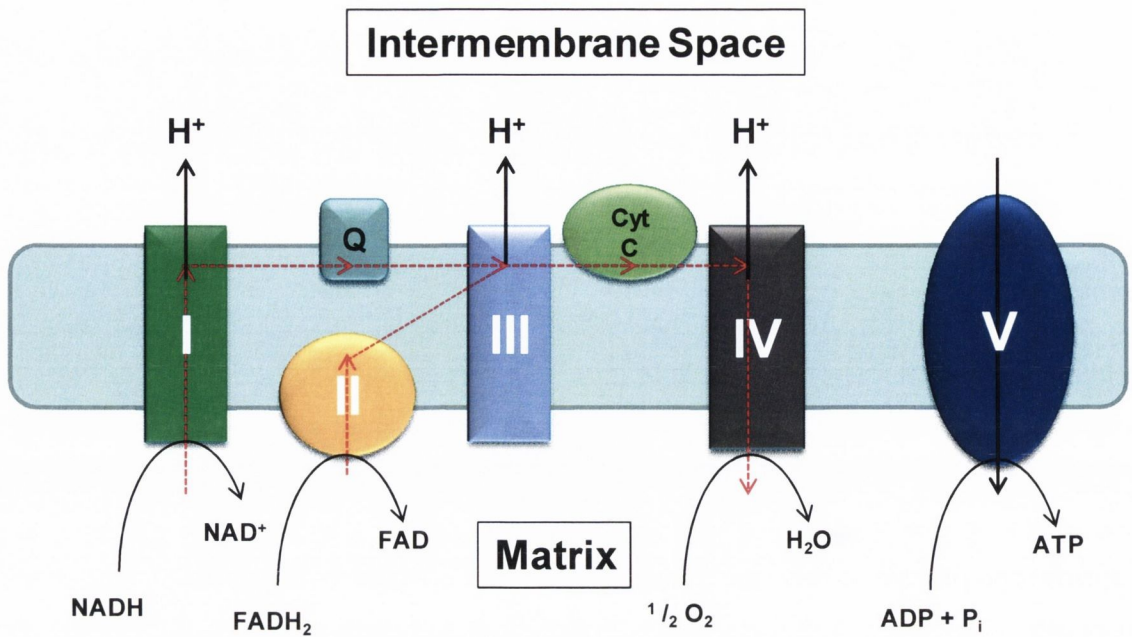


Figure 1.2: ETC cycle of mitochondria

The inner membrane of mitochondria contains all the molecular components for oxidative phosphorylation or ETC to take place. ETC has 5 components, complex I, II, III, IV and ATP synthase (V). Complex I and II use NADH and FAD, respectively, as a proton source (H^+). These complexes pump protons (dark arrows) into the intermembrane space, which are eventually used by ATP synthase to produce ATP. In this process the electrons can also flow through the complexes (I-III) to complex IV where water is also produced (Red arrows).

15. Aim of the thesis

PICK1 is monoubiquitinated by parkin, but does not promote PICK1 ubiquitination or degradation (Joch et al., 2007). The primary goal of this study was to decipher the role of the parkin-PICK1 interaction in mitochondrial maintenance. To decipher the role of parkin-PICK1, two types of blocking peptides based on the PDZ motif sequence of parkin (MNP201 and Tat-MNP201) (**Figure 1.11**) and the PICK1 PDZ domain binding compound, FSC231, (Thorsen et al., 2010) were used. In this thesis, the effect these three types of blocking agents was tested in different mitochondrial properties including the activity of mitochondrial respiratory chains (complex I and IV), ROS production and mitochondrial membrane potential. In addition, the effect of these blocking agents on glutamate release assay was also investigated.

The aims of the thesis were as follows and are presented in the results chapters 1-4:

- demonstrate that parkin blocking peptides (MNP201) interact with PICK1 using biochemical and spectrophotometric approaches (Result 1)
- determine the effects of the parkin blocking peptide, MNP201, in mitochondrial properties and glutamate release (Result 2).
- evaluate the effects of Tat-tagged MNP201 in mitochondrial properties and glutamate release (Result 3).
- examine the effects of FSC231 in mitochondrial properties and glutamate release (Result 4).

16. Hypothesis

The working hypothesis of this project was that parkin-PICK1 plays a role in mitochondrial function and that disruption of this interaction would result in aberrant mitochondrial function.

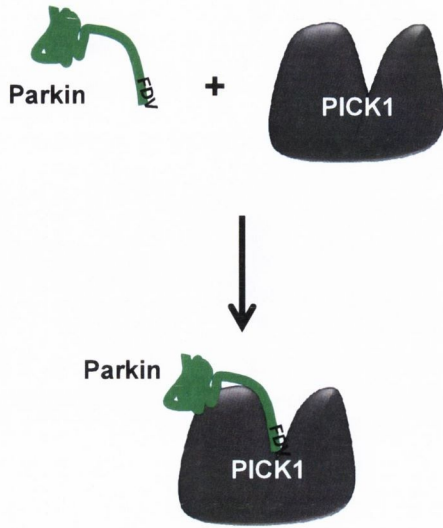
In addition to blocking peptides, small molecular weight compounds can also be used to block PDZ-based protein interactions (Blazer et al., 2009). A recent discovery of a small molecule inhibitor (E)-ethyl 2-cyano-3 (3, 4-dichlorophenyl) acryloyl carbamate (FSC231), specific for PICK1 PDZ domain, has been reported. FSC231 is a small compound of molecular weight 319 g/mol with a K_i value of 10 μM for the PDZ domain of PICK1 (Thorsen et al., 2010). Studies show that 50 μM FSC231 blocks the interaction between PICK1 and GluR2 (Thorsen et al 2010). When tested in hippocampal neurons, FSC231 blocks the interaction between GluR2 and PICK1 (Thorsen et al., 2010). Furthermore, FSC231 increased the rate of GluR2 recycling to the cell surface by blocking the PICK1 interaction (Thorsen et al., 2010). FSC231 is also reported to influence synaptic plasticity by inhibiting LTD and LTP in CA1 hippocampal neurons (Thorsen et al., 2010).

Here, the effects of PDZ-motif parkin peptides (MNP201) and of the PICK1 binding compound (FSC231) were determined in mitochondrial pathways to elucidate the role of PICK1 and its interacting proteins in mitochondrial maintenance.

example, a blocking peptide has been used to block the interaction between GluR2 and PICK1 (Daw et al., 2000). It has been shown that introduction of this peptide increases basal synaptic transmission and blocks long term depression (LTD) in CA1 pyramidal neurons of the hippocampus (Daw et al., 2000). In another similar study, employing a peptide with the last ten amino acid of GluR2 (NVYGIKSVKI), the interaction between GluR2 and GRIP was blocked (Li et al., 1999). This blocking peptide has been used to show that the interaction of GRIP with PDZ motif of GluR2 is necessary for activation of silent synapses (Li et al., 1999).

Delivery of polypeptides, compounds and peptidyl mimetics into a cell *in vivo* is possible with molecules of very small size (less than 600 Da) (Scheld et al., 1989). Highly lipophilic, bio-active peptides of a size up to 6 amino acids can be delivered into cells and also cross the blood-brain barrier unassisted (Scheld et al., 1989). To transport bigger peptides into the cell, peptides can be fused with cell penetrating peptides, such as Tat (trans-activation of transcription). Tat, Antennapedia and arginine-rich peptides are also called Trojan peptides. Several studies have been carried out with such trojan peptides, some of which are described below (Lindsay, 2002). A Tat sequence is an 11 amino acid (YGRKKRRQRRR) long stretch of polypeptide derived from the transduction domain (PTD) of human immunodeficiency virus (HIV) (Nagahara et al., 1998). This peptide enters the cell by a mechanism involving adsorptive endocytosis (Mann and Frankel, 1991). Using this technology, large sized proteins (up to 120kDa) have been delivered into a variety of human and murine cell types *in vitro* (Ezhevshy et al., 1997; Nagahara et al., 1998). For example, a study has showed delivery and expression of Tat tagged β -galactosidase protein (120 kDa) *in vivo* into mouse tissues, including the brain (Schwarze et al., 1999). In another study, a Tat-fused PDZ motif peptide (of 10 residues), which blocks the PDZ-based interaction between NMDA receptors and PSD-95 has been delivered *in vivo* in mice and shown to be protective in ischemic brain damaged (Aarts et al., 2002). Antennapedia (RQIKIWFQNRRMKWKK) or penetratin is another well established Trojan delivery peptide that has been used to internalise large molecules including hydrophilic oligonucleotides of 55 bases to cytoplasm and nucleus (Derossi et al., 1996; Prochiantz A, 1996). Antennapedia is derived from the homeodomain of the *Drosophila* transcription factor *Antennapedia* and is of 16 residues length (Derossi et al., 1998; Pooga et al., 1998; Astriab-Fisher et al., 2000). The mechanism of Antennapedia internalisation is still unknown, however reports suggest that the process of internalisation of Antennapedia is through a membrane lipid interaction based non-endocytotic and receptor/transporter independent pathway (Derossi et al., 1996; Fisher et al., 2000).

A) Interaction of Parkin and PICK1



B) No interaction of Parkin and PICK1 in the presence of blocking peptide

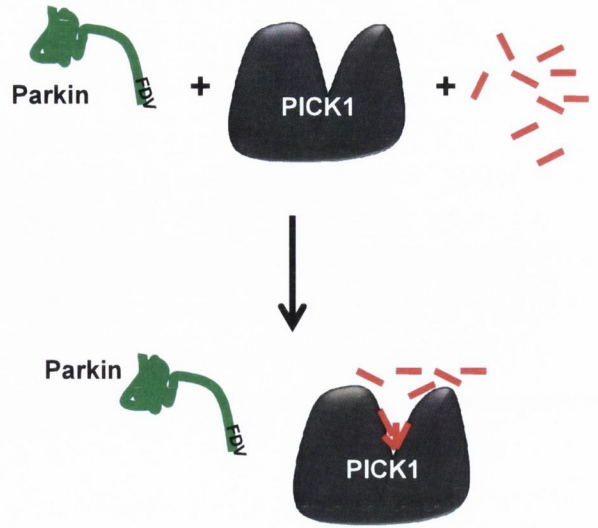


Figure 1.10: Mechanism of blocking agents to disrupt parkin-PICK1

A) Parkin and PICK1 interact with each other through a PDZ domain-motif discrete binding site. B) The parkin peptide (MNP201) (shown in red) binds the PDZ domain of PICK1 and competitively inhibit parkin from interacting. The parkin peptide (MNP201) is modelled on and contains the PDZ motif of parkin (-FDV).

GTPase family members including Drp1, OPA1 and Mfn2, which regulate mitochondrial fission and fusion (Poole et.al. 2008). Mitochondrial fragmentation induced by Drp1, a protein responsible for division of the outer mitochondrial membrane, is successfully suppressed by over-expression of parkin and PINK1 (Lutz et al., 2009). Moreover, parkin/PINK1 knockdown in Drp mutant cells did not show any of the mitochondrial alterations observed in the parkin/PINK1 knockout phenotype of wild type cells (Lutz et al., 2009). On the other hand, the phenotypes of parkin/PINK1 mutants can be partially recovered by overexpressing Drp1, or by suppressing the gene dosage of the mitochondrial Opa1 or Mfn2 (Poole et.al. 2008; Deng et al., 2008; Yang et al., 2008; Park et al., 2009). Taken together, this indicates that the PINK1/parkin pathway acts to promote mitochondrial fission or to inhibit mitochondrial fusion.

Lastly, it has been shown that parkin plays a role in promoting the removal of depolarised mitochondria through mitophagy, i.e., autophagy of mitochondria by recruitment of autophagosomes (Elmore et al., 2001; Tolkovsky et al., 2002; Twig et al., 2008; Narendra et al., 2008). It has been suggested that parkin interacts with PINK1 by translocating to the outer membrane of depolarized mitochondria in order to poly-ubiquitinate the voltage-dependent anion channel 1 (VDAC1) and the mitofusin protein-2 (Mfn2) (Geisler et al., 2010; Poole et al., 2010; Ziviani et al., 2010). Upon poly-ubiquitination, autophagosomes are recruited to depolarized mitochondria to perform mitophagy (Geisler et al., 2010). Studies identified a protein called Nix (a BH3-only Bcl-2 family protein) that promotes parkin translocation to depolarized mitochondria under CCCP-induced stress generating ROS species (Ding et al., 2010). Taken together these studies infer a role of parkin and PINK1 in regulating the removal of damaged mitochondria. However, the exact mechanism of interaction between parkin/PINK1 and GTPases as well as the trafficking mechanism of parkin to mitochondria is still unknown. It is interesting to speculate that PICK1 plays an important role in targeting parkin to mitochondria and in regulating parkin-mediated mitophagy and clearance of aberrant mitochondria.

14. Use of blocking peptides and compounds

Since PDZ motifs consist 3-4 critical amino acids (Sheng, 2001) it has been possible to engineer blocking peptides composed small stretches of amino acids that carry the PDZ motif sequence and bind the PDZ domain. These peptides thus competitively inhibit cognate PDZ motif containing proteins from interacting with their PDZ domains (**Figure 1.10**). As an

oxidative stress (Jenner and Olanow, 1996; Zhang et al., 2000) are considered as two main contributors in the aetiology of PD. Analysis of brain samples obtained from PD patients have suggested impairment of complex I activity of the mitochondrial ETC system in the SNPC (Schapira et al., 1990), frontal cortex (Parker et al., 2008), skeletal muscle and platelets (Bindoff et al., 1989; Parker et al., 1989), along with increased production of ROS and mitochondrial dysfunction (Keeney et al., 2006). Parkin-KO mice have showed hampered activity of complex I and IV of the ETC and reduced striatal mitochondrial respiratory capacity (Palacino et al., 2004). Moreover, PD patients with homozygous mutation in *parkin* show reduced activity of complex I and IV in the mitochondria of leucocytes (Muftuoglu et al., 2004). In addition, elongated mitochondria are reported in human fibroblasts containing parkin mutations (Mortiboys et al., 2008), which can trigger Bax-induced apoptosis. Many PD-associated *PARK* proteins are also reported to influence mitochondrial dynamic tubular organization e.g., PARK1, PARK2, PARK6, PARK8, and PARK13. Particularly, in addition to its localisation in the cytosol and ER, parkin is observed around small and fragmented mitochondria in conditions of cell stress (Shimura et al., 1999; Darios et al., 2003; Kuroda et al., 2006; Narendra et al., 2008). Furthermore, parkin is believed to influence the maintenance of the structure and function of mitochondria (Abou-Sleiman et al., 2006), although the mechanism of regulation is still unknown. A *Drosophila* parkin mutant has also showed malformed mitochondria in dopaminergic neurons (Greene et al., 2003; Whitworth et al., 2005), which can be rescued by over-expressing the fission promoting protein dynamin-related Protein (Drp1) and inhibiting the fusion-promoting protein optic atrophy protein 1 (Opa1) or mitofusin 2 (Mfn2) (Greene et al., 2003; Pesah et al. 2004; Poole et al., 2008).

PINK1, a mitochondrial serine/threonine kinase, is found as one of the important regulator of mitochondrial integrity along with parkin. The PINK1 protein resides on the outer membrane of mitochondria and has a cytosolic kinase domain and a mitochondrial targeting sequence (MTS) (Zhou et al., 2008). PINK1 mutation in *Drosophila* is reported to cause the phenotypes and mitochondrial morphology similar to parkin mutants flies. Interestingly, parkin is reported to rescue the PINK1 loss-of-function phenotypes, but not vice-versa, leading to the conclusion that PINK1 and parkin both function in a common genetic pathway for mitochondrial maintenance with parkin acting downstream of PINK1 (Clark et al., 2006; Park et al., 2006; Yang et al., 2006). PINK1 over-expression, in association with parkin, regulates mitochondrial morphology (Poole et al., 2008), biogenesis, and enhances replication and transcription of the mitochondrial genome (Kuroda et al., 2006). A link has been established between parkin/PINK1 proteins and mitochondrial fission/fusion (Bleazard et al., 1999; Chan, 2006). Specifically, parkin and PINK1 are found to closely associate with

when cortical neurons were treated with the protein synthesis inhibitor cycloheximide, the basal levels of both parkin and PICK1 were undisturbed for 24 h (Joch et al., 2007). A similar result is obtained when neurons are incubated with the proteasome inhibitor lactacystin. Together, this evidence suggests that monoubiquitination of PICK1 by parkin does not involve its proteasomal degradation (Joch et al., 2007). Furthermore, monoubiquitination of PICK1 by parkin does not regulate PICK1 expression levels, but instead, modulates its function.

12.2 Role of parkin-PICK1 interaction

The PICK1-parkin interaction has been reported as important in regulating the function of the acid-sensing ion channel subunit 2a (ASIC2a) (Baron et al., 2002). ASICs are a mammalian degenerin/epithelial Na⁺ channels (DEG/ENaC) that are activated by low extracellular pH (Duggan et al., 2002; Hruska-Hageman et al., 2002). Four genes (ASIC1-4) encode six subunits of transmembrane channels (ASIC1a, ASIC1b, ASIC2a, ASIC2b, ASIC3 and ASIC4) (Krishtal, 2003; Xiong et al., 2006). PICK1 interacts with ASIC1 and ASIC2 in a PDZ domain-motif manner and potentiates ASIC2a current by recruiting PKC α (Baron et al., 2002; Duggan et al., 2002; Hruska-Hageman et al., 2002). In agreement, studies on cortical neurons derived from PICK1 knockout (PICK1-KO) mice have demonstrated a reduction of ASIC current as well as decreased expression of ASIC1 and ASIC2 (Hu et al., 2009). Elimination of PICK1/PKC α -dependent ASIC2a currents was observed upon up-regulation of parkin in COS-7 cells suggesting that parkin inhibits PICK1/PKC α -dependent potentiation of ASIC currents (Joch et al., 2007). Studies also show that a loss of parkin increases a PKC-induced potentiation of ASIC2a currents in neurons, although in the absence of PICK1, these ASIC currents remain unaffected when parkin is over-expressed. Taken together, it appears that parkin prevents PICK1/PKC α -dependent potentiation of ASIC channel function, likely via a mechanism that involves PICK1 monoubiquitination and inhibition of interaction with ASIC and/or PKC α (Joch et al., 2007). It is also interesting to speculate that dysfunction of ASIC2a due to a mutation in parkin or PICK1 may be a possible mechanism underlying PD symptoms, as ASIC channels are associated with mechanosensation and pain (Joch et al., 2007).

13. Parkin and Mitochondria

While a number of reports have demonstrated a role for parkin in regulating mitochondrial function, as yet there is no report available indicating a role for a parkin-PICK1 interaction in mitochondria. Mitochondrial dysfunction (Kosel et al., 1999; Beal and Shults, 2003) and

(Stowell et al., 1999). The absence of this targeting sequence impairs the trafficking of mGluR7 to axons, but not to dendrites (Stowell et al., 1999). The distal region of ct-mGluR7 contains a PDZ binding motif (-LVI) that interacts with PDZ domain of PICK1 (Boudin et al., 2000; El Far et al., 2000; Dev et al., 2000). The PDZ binding motif of mGluR7 is essential for mGluR7 clustering at synapses (Boudin et al., 2000).

12. Parkin-PICK1 interaction

12.1 The PDZ motif of parkin

The ct-parkin contains a class II PDZ binding motif (-FDV), which interacts with the PDZ domain of CASK (Ca²⁺/calmodulin-dependent serine protein kinase) (Fallon et al., 2002). It has been reported that truncation of last 3 amino acids (W453*) makes parkin insoluble (Joch et al., 2007), supporting the hypothesis the ct-parkin is important for folding, trafficking, and/or degradation (Winklhofer et al., 2003). As described earlier, PICK1 can interact with class I and class II PDZ motifs (Staudinger et al., 1997; Dev et al., 1999; Williams et al., 2003; Madsen et al., 2005) and a parkin-PICK1 interaction has been demonstrated by pull down and immunoprecipitation studies (Joch et al. 2007). In pull down studies, endogenous PICK1 from mouse brain synaptosomes associated with bacterial expressed GST-tagged parkin via its PDZ motif (-FDV). In addition, transiently expressed constructs of parkin was found to immunoprecipitate with transiently expressed PICK1 (Joch et al. 2007). In contrast, PDZ motif deleted parkin constructs (D464*) failed to interact with PICK1, indicating involvement of the PDZ motif of parkin with PICK1. Moreover, PICK1 mutant with point mutations {lysine-27 and aspartic acid-28 (KD/AA)} in the carboxylate binding loop of PDZ domain failed to with parkin (Joch et al., 2007). The KD residues form the carboxylate binding loop of PICK1's PDZ domain (Doyle et al., 1996; Songyang et al., 1997) and are crucial for PICK1 to interact with its ligands (Staudinger et al., 1997; Xia et al., 1999). Taken together, these data suggest parkin and PICK1 interact in a PDZ-dependent manner (Joch et al. 2007).

Parkin functionally effects PICK1 activity. Unlike CASK, parkin induces the monoubiquitination of PICK1 (Joch et al. 2007). In contrast, a parkin mutant associated with PD and lacking the PDZ binding motif is not able to ubiquitinate PICK1. Monoubiquitination alters the protein-protein interactions and protein trafficking of PICK1, but not its degradation (Hicke and Dunn, 2003; Mukhopadhyay and Riezman, 2007). In support that parkin does not alter PICK1 protein levels, the basal expression of PICK1 in whole brain lysates and synaptic fractions obtained from normal and parkin-KO mice were found to be similar. In addition,

(ABP) (Srivastava et al., 1998; Dev et al., 1999; Xia et al., 1999). In this project, the interaction between PICK1 and GluR2 was used as a control.

11.3.2 GluR5 (KA receptor subunit)

GluR5 is one of the 5 subunits of KA receptors. KA receptors are found in pre and post-synaptic sites and at pre-synaptic sites can inhibit glutamate release (Chittajallu et al., 1999). Similar to GluR2, the ct-GluR5 subunit also interacts with several PDZ domain containing proteins including syntenin, GRIP, PSD95 and PICK1 through its PDZ motif (-TVA) present in the extreme ct (Hirbec et al., 2003). According to electrophysiological studies, infusion of blocking peptides, designed to block the interaction of PICK1-GluR5, causes a substantial reduction in EPSCs (Hirbec et al., 2003). In the same experimental setup, when AMPA receptor was activated, strong reduction in the EPSCs of KA receptors was observed (Hirbec et al., 2003). These data indicate a role of the PICK1-GluR5 interaction in regulation of synaptic KA receptor function (Hirbec et al., 2003). GluR5 also interacts with PKC α , where PKC α selectively phosphorylates two serine residues (S880 and S886) residues in GluR5 (Hirbec et al., 2003).

11.3.3 mGluR7 (Metabotropic receptor subtype)

The mGluR7 receptor belongs to the Group III of metabotropic glutamate receptors (Nakanishi, 1994; Pin et al., 1995). Like other Group III members, mGluR7 negatively regulates cAMP. The mGluR7 is found on the pre-synaptic membrane (Shigemoto et al., 1996) and inhibits glutamate release (Forsythe et al., 1990; Gereau et al., 1995; Herrero et al., 1996). The ct-mGluR7 stretch of 65 amino acids plays an important role in protein-protein interactions. There are several proteins including PICK1, Ca²⁺/Calmodulin (CaM) and PKC reported to interact with ct-mGluR7 to regulate its function and intracellular trafficking (O'Conner et al., 1999; Nakajima et al., 1999; Boudin et al., 2000; El Far et al., 2000; Dev et al., 2000). On the basis of these interacting partners, the ct-mGluR7 can be divided into three parts, i.e., the proximal region, the central region and the distal region. The proximal region interacts with the $\beta\gamma$ -subunit of G-protein and CaM (O'Connor et al., 1999; Nakajima et al., 1999). Upon phosphorylation (by PKC) of the CaM binding site of mGluR7, the interaction between CaM and mGluR7 is lost, although CaM itself is not phosphorylated by PKC (Minakami et al., 1997; Ishikawa et al., 1999; O'Connor et al., 1999; Nakajima et al., 1999). Previous reports suggest that CaM has an active role in the dissociation of the $\beta\gamma$ -subunit of G-protein from mGluR7 that results in G $\beta\gamma$ -induced inhibition of Ca²⁺ gated channels (Dev et al., 2001). The central region of ct-mGluR7 contains an axonal targeting sequence (amino acid 883-912), which is responsible for trafficking of mGluR7 receptors

to the DAT-PICK1 interaction (Torres et al., 2001). Yeast two hybrid assay showed that deletion of these last three amino acids completely abolished the interaction with PICK1 (Torres et al., 2001). The association between PICK1 and NET was confirmed in co-IP and co-localisation studies using transfected HEK293 cells (Torres et al., 2001). Endogenous PICK1 and NET were also found co-localised in cultured neurons obtained from the norepinephric locus coeruleus, where both PICK1 and NET were found clustered along neuronal processes (Torres et al., 2001).

11.2.3 Serotonin transporter

Serotonin transporter (SERT) is a monoamine transporter responsible for the uptake of serotonin from the extra-cellular synaptic environment (Jones et al., 1998). SERT are predominantly found on serotonergic neurons. Immunocytochemical data suggests an abundance of SERT proteins in the axolemma, outside the synaptic clefts of serotonergic neurons (Zhou et al., 1998; Tao-Cheng and Zhou 1999). SERTs are also found to be associated with DAT in the membrane of intracellular compartments, mainly in tubulovascular membranes (Torres et al., 2001). Similar to DAT and NET, SERT also binds the PDZ domain of PICK1 through the last three ct amino acids (-NAV) (Torres et al., 2001). However, the PDZ motif present in SERT is not a typical class II motif and thus the interaction with PICK1 is weaker than DAT or NET (Torres et al., 2001).

11.3 Glutamate receptors

11.3.1 GluR2 (AMPA receptor subunit)

One of the best studied PICK1 interacting protein is GluR2. The PDZ domain of PICK1 interacts with last ct-GluR2 (-LVI) (Dev et al., 1999; Xia et al., 1999). As indicated above, GluR2 is an AMPA receptor subunit that controls Ca^{2+} permeability of the AMPA receptor. Typically, the GluR2 polypeptide is made up of four hydrophobic membrane associated domains in which 1, 3 and 4 are transmembrane and the second domain is a re-entrant loop (Wo and Oswald, 1995). The N-terminal and the ct of GluR2 contain many glycosylation and phosphorylation sites, respectively (Roche et al., 1994; Taverna et al., 1994; Moss et al., 1993). AMPA receptors are regulated by phosphorylation, where interaction with PICK1 plays an important role. Briefly, interaction with PICK1 regulates the surface expression of GluR2 and controls synaptic plasticity such as LTD (Xia et al., 1999). In addition to PICK1, GluR2 also interacts with other PDZ domain containing proteins, including glutamate receptor interacting protein (GRIP) (Dong et al., 1997) and AMPA receptor binding protein

apoptotic Bax protein in human leukemia REH cells (Wang et al., 2007). Thus, PICK1 along with PKC α appear to be crucial in mitochondrial maintenance and cellular survival. The disruption of a PICK1-PKC α interaction is thus likely to result in mitochondrial dysfunction.

11.2 Monoamine Transporters

11.2.1 Dopamine transporter

Dopamine transporters (DAT) are biogenic monoamine plasma membrane proteins responsible for high affinity uptake of released dopamine through pre-synaptic sites of dopaminergic neurons (Jones et al., 1998). Monoamine transporters including DAT are reported to be involved in many neuro-psychiatric disorders including depression and obsessive-compulsive disorder (Giros and Caron, 1993; Amara and Kuhar, 1993). The importance of DAT has been elucidated using knockout mice, which show hyperlocomotion and differential cocaine and amphetamine sensitivity (Giros et al., 1996; Jones et al., 1998). DAT is primarily found near the site of pre-synaptic release in nigrostriatal dopaminergic neurons and uptake of released dopamine (Nirenberg et al., 1996; Hersch et al., 1997; Pickel and Chan 1999). The ct-DAT contains a class II PDZ motif (-LKV) and interacts with the PDZ domain of PICK1, as shown by yeast two hybrid, co-IP and co-localisation studies (Torres et al., 2001). When both DAT and PICK1 are co-expressed in HEK293 cells, both proteins cluster in the plasma membrane (Torres et al., 2001). Upon co-expression with PICK1, the uptake activity rate of DAT was found to be enhanced (Torres et al., 2001). DAT also co-localises with other proteins including the vesicular monoamine transporter-2 (a synaptic vesicle protein expressed in monoaminergic neurons) and synaptin (a pre-synaptic protein) in the axons of mid brain neurons (Torres et al., 2001). When DAT and PICK1 protein were co-expressed in immortalized dopaminergic neurons (1RB3AN27) (Clarkson et al., 1999), 50% enhancement of DAT uptake was found when compared with single transfected DAT cells suggesting that PICK1 helps trafficking of DAT (Torres et al., 2001).

11.2.2 Norepinephrine transporter

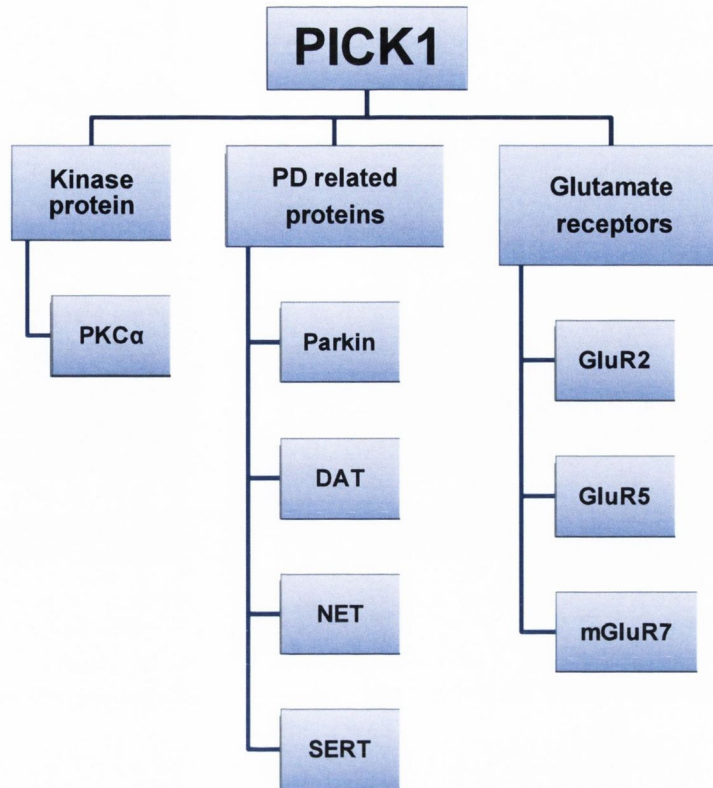
Norepinephrine transporter (NET) is a monoamine transporter responsible for the uptake of released norepinephrine from the synaptic cleft of norepinephrinergic neurons. The importance of this transporter was revealed when NET knockout mice showed increased sensitivity in D2/D3 receptors and sensitization to cocaine and amphetamine (Xu et al., 2000). NET shares approximately 78% amino acid sequence similarity with DAT (Pacholczyk et al., 1991; Giros et al., 1991; Kilty et al., 1991; Vandenberg et al., 1992). The ct-NET contains a Class II PDZ motif (-LAI) that also binds the PDZ domain of PICK1, similar

Name of protein	Sequence of interaction	PDZ motif	Reference
Protein kinase C	NPQFVHPILQSAV	I	Staudinger et al., 1995
Ephrin receptor A7	AQMLHLHGTTGIQV	II	Torres et al., 1998
Ephrin B1	MPPQSPANIYYKV	II	Torres et al., 1998
Ephrin receptor B2	MRAMQNQIQSVEV	II	Torres et al., 1998
Muscle-specific kinase	ERMCEAEGTVSV	II	Torres et al., 1998
GluR2 (AMPA)	EGYNVYGIKSVKI	II	Xia et al., 1999, Dev et al., 1999
GluR3/4 (AMPA)	EGYNVYGTESVKI	II	Dev et al., 1999
GluR4C (AMPA)	EGYNVYGTESI KI	II	Xia et al., 1999
GluR52b (KAR)	CHQRRTQRKETVA	I	Hirbec et al., 2003
GluR6 (KAR)	FNDRRLLPGKETMA	I	Hirbec et al., 2003
mGluR7A	AKKKYVSYNLVI	II	El Faret et al., 2000, Hirbec et al., 2002
mGluR7B	QKSVTWYTIPTTV	?	Hirbec et al., 2002
Anionic exchanger 1	EGRDEYDEVAMPV	?	Cowan et al., 2002
Anionic exchanger 2	EGVDEYNEMPMPV	?	Cowan et al., 2002
Aquaporin 1	ADDINSRVEMKPK	?	Cowan et al., 2002
Aquaporin 2	LHSPQSLPRGSKA	I	Cowan et al., 2002
Aquaporin 9	ENNLEKHEL SVIM	?	Cowan et al., 2002
ARF1 GTPase	GLDWLSNQLRNQK	?	Takeya et al., 2000
ARF3 GTPase	GLDWLANQLKNKK	?	Takeya et al., 2000
Dopamine transporter	EVRQFTLRHWLKV	II	Torres et al., 2001
Norepinephrine transporter	DIRQFQLQHWLAI	II	Torres et al., 2001
Serotonin transporter	TEIPCGDIRLNAV	?	Torres et al., 2001
ERBB2/HER2 RTK	AENPEYLGLDVPV	II	Lin et al., 2001
ERBB4/HER4 RTK	LPPPPYRHRNTVV	I	Jaulin-Bastard et al., 2001
PrPR GPCR	APHGQNMTVSVVI	II	Lin et al., 2001
BNaC1/ASIC2a	LQTALGTLEEIAC	?	Hruska-Hageman et al., 2002
BNaC2/ASIC1a	HHPARGTFEDFTC	?	Hruska-Hageman et al., 2002
Netrin receptor UNC5H1	5PDAGLFTVSEAEC	?	Williams et al., 2003
CAR cell adhesion	VMIPAQSKDGSIV	I	Ashbourne et al., 2004

Table 1.4: List of PICK1 interacting proteins

Various proteins interacting with PICK1's PDZ domain are depicted in the table (Madsen et al., 2005).

A)



B)

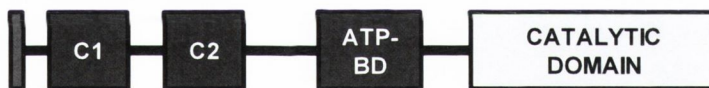


Figure 1.9: The PICK1 interacting partners

A) PICK1 acts as scaffolding and adapter protein to its interacting partners (parkin, GluR2, GluR5, mGluR7, PKC α) and transporter proteins (dopamine, norepinephrine and serotonin). B) PKC α comprises N-terminal diacylglycerol binding C1 domain (C1), a Ca²⁺-binding C2 domain (C2), an ATP binding domain (ATP-BD) and a ct catalytic domain. The ct last 3 amino acids (-SAV) of PKC α interacts with the PDZ domain of PICK1.

1997; Sheng, 2001). The PDZ domain of PICK1 can interact with a range of different PDZ motif containing proteins including Class I, Class II and atypical PDZ motifs (Staudinger et al., 1997; Dev et al., 1999; Madsen et al., 2005).

11. PICK1 interacting proteins

More than 60 proteins interact with PICK1. Some important PDZ motif containing proteins are explained below (**Figure 1.9A**). A summary of interacting partners of PICK1 are depicted in **Table 1.4**.

11.1 Protein kinase C α (PKC α)

There are 11 members of the PKC family, which play roles in a variety of cellular responses and signalling cascades (Nishizuka, 1992; Newton et al., 1995). These isoenzymes are translocated to different cellular compartments including the plasma membrane, the cytoskeleton and cellular organelles (Mochly-Rosen et al., 1995; Goodnight et al., 1995). Different stimuli result in translocation of PKC to different cellular compartments (Hocevar et al., 1991; Yedovitzky et al., 1997). Commonly, isoforms of PKC have similar structural organization, i.e., an amino terminal regulatory domain, a carboxyl-terminal catalytic domain and a linking central hinge region (**Figure 1.9B**). The last ct amino acids (-SAV) of PKC α specifically interact with the carboxylate-binding domain present in the PDZ domain of PICK1 (Staudinger et al., 1995). Sequence analysis of PKC α reveals absence of any mitochondrial targeting signal peptide. However, reports suggest that a major function of PICK1 is to bind and translocate activated PKC α to mitochondria (Wang et al., 2003). A PDZ domain mutant of PICK1 is unable to mediate mitochondrial translocation, suggesting an intact PDZ domain is necessary for this PKC α translocation to mitochondria (Wang et al., 2003). Absence of the PDZ binding motif of PKC α impairs its translocation to the mitochondria, although it does not affect the translocation of PICK1 (Wang et al., 2003). Mitochondria-mediated apoptotic pathway is regulated by two groups of proteins, anti-apoptotic proteins, such as B-cell lymphoma-2 (Bcl-2) and pro-apoptotic proteins, such as Bax. Upon activation of apoptotic signal, Bax dimerises with Bcl-2 in outer mitochondria and triggers apoptosis by releasing of cytochrome C in cytosol (Pawlowski and Kraft, 2000). Reports suggest that via phosphorylation of the anti-apoptotic protein Bcl-2 (B-cell CLL/lymphoma 2) present in the outer membrane of the mitochondria, PKC α confers resistance against apoptosis (Nguyen et al., 1993; Ruvolo et al., 1998; Jiffar et al., 2004). PICK1 over-expression increases the phosphorylation of Bcl-2 protein, which confers stabilisation of mitochondrial membrane potential and resistance to dimerisation of pro-

A)

Domain structure of PICK1



B)

PICK1 protein

MFADLDYDIEEDKLGIP^{TP}PGKVTLQKDAQNLIGISIGGGAQYCPCLYIV
QVFDNTPAALDGTVAAGDEITGVNGRSIKGKTKVEVAKMIQEVKGEVTIH
YNKLQADPKQGM^{SLD}IVLKKVKHRLVENMSSGTADALGLSRAILCNDGLV
KRLEELERTAE^{LY}KGMTEHTKNLLRAFYEL^{SQ}THRAFGDVF^{SV}IGVRE^{PQ}
PAASEAFVKFADAHRSIEKFGIRLLKTIK^{PML}TDLN^{TY}LNKAI^{PD}TRL^{TI}
KKYLDVKFEYLSYCLKVKEMDDEEYSCIALGEPLYRVSTGNYEYRLILRC
RQEARARFSQMRKDVLEKME^{LLD}QKHVQDIVFQLQRLVSTMSKY^{YND}CYA
VLRDADVFPIEV^{DLA}HTT^{LAY}GLN^{QEE}FTDGE^{EEEEEEED}TAAGE^{PS}RDTR
GAAGPLDKGGSWCDS






 N-terminal acidic region
 PDZ domain
 α -helical linker region
 BAR domain
 C-terminal acid region

Figure 1.8: Structure and protein sequence of PICK1

A) PICK1 is a PDZ domain containing protein that interacts with several PDZ motif containing proteins. A small acidic region precedes the PDZ domain. The largest domain in PICK1 protein is the BAR domain (144-357), which plays a role in PICK1 dimerisation. The PDZ domain and the BAR domain are linked by a small stretch of α -helical region. The ct of PICK1 contains a long acidic region (AR). B) The protein sequence of PICK1 is shown with different domains.

The CK-1 enzyme can also phosphorylate parkin at multiple sites (S101, S127 and S378) both *in vitro* and *in vivo* (Rubio de la Torre et al., 2009). Here also, phosphorylated parkin shows a tendency to form inclusion bodies (Rubio de la Torre et al., 2009). Analysis of PD brain samples reveal increased levels of phosphorylated parkin (phospho-S101) in Lewy bodies (Rubio de la Torre et al., 2009). The above findings indicate that phosphorylation of parkin has a role to play in the formation of parkin inclusion bodies.

10. PICK1 as a PDZ domain protein

10.1 Introduction to PICK1

PICK1 (Protein Interacting C Kinase) is a synaptic protein of 416 amino acids, which scaffolds and interacts with more than 60 proteins including ion channels, transporters and receptors (Dev et al., 1999). Although the expression of PICK1 is highest in the CNS, PICK1 is ubiquitously present in a number of tissues (Staudinger et al., 1995). Subcellularly, PICK1 is localised in perinuclear regions, RER and Golgi complex (Staudinger et al., 1995).

Structurally, PICK1 is made up of 2 domains (**Figure 1.8**),

- 1. PDZ domain:** The PDZ (PSD95/DlgA/ZO-1) domain of PICK1 is located at the N-terminus of PICK1 immediately after a small stretch of acidic residues. Through the PDZ domain, PICK1 interacts with several PDZ motif containing proteins.
- 2. BAR domain:** The BAR (Bin-Amphiphysin-Rvs) domain is located ct to the PDZ domain after an α -helical linker region of 40 residues. The BAR domain is the largest domain of PICK1 that also corresponds to a coiled-coil domain. The ct of the BAR domain contains a long stretch of acidic residues.

Functionally, these two domains allow PICK1 to dimerise and act as a scaffolding protein. The major function of PICK1 is to regulate the trafficking and phosphorylation of interacting proteins by recruiting protein kinase C- α (PKC α) (Staudinger et al., 1995). PKC α is a member of the serine/threonine kinases PKC family, which plays a role in various physiological processes, including differentiation, proliferation, motility, inflammation and apoptosis (Nakashima, 2002). Generally, PDZ domains can be classified into three classes according to the type of PDZ motifs they bind (Sheng, 2001). Class I PDZ domains bind specifically to the tripeptide sequence (S/T)-X- ϕ (where ϕ and X denote a hydrophobic amino acid and any amino acid respectively), class II PDZ domains bind the ct PDZ motif sequence ϕ -X- ϕ and class III PDZ domains bind D-E-X- ϕ PDZ motifs (Songyang et al.,

MIVFVRFNSSHGFPVEVSDTSTIFQLKEVVAKRQGV PADQLRVI FAKEL ← UBL domain
 RNDWTVQNCDDL DQQSIVHIVQRPWRK GQEMNATGGDDPRNAAGGCERE PQ
SLTRVDLSSSVLP GDSVGLAVILHTD SSRKDS SPPAGS SPAGRSIYNS FYVYC ← Central domain
 KGPCQRVQPGKLRVQCSTCRQATL TLTQGPSCWDDVLI PNRMSGECQSPH
 CPGTSAEFFFKCGAHPTSDKETPVALHLIATNSRNITCITCTDVRSPVLV ← RING 1
 FQCNSRHVICLD CFHLYCVTRLNDRQFVHDPQLGYSLPCVAGCPN SLIKE
 LHHFRILGEEQYNRYQQYGAEECVLQMGVLCPRPGCGAGLLPEPDQRKV ← IBR
 TCEGGNGLGCGFAFCRECKEAYHEGEC SAVFEASGTTTQAYRVDERRAAEQ
 ARWEAASKETIKKTKPCPRCHVPVEKNGGCMHMKCPQPQCRLEWCWNCG ← RING 2
 CEWNRVCMGDHW FDV ← PDZ motif

CK-1: S101, S127, S378

PINK1: T175

Cdk5: S131

Unknown kinase: S136

Figure 1.7: Phosphorylation sites of parkin and responsible kinases.

Several kinases are reported to phosphorylate parkin e.g., caesin kinase 1 (CK-1) phosphorylates S101, S127 and S378; PTEN-induced putative kinase 1 (PINK1) phosphorylates T175 and cyclin-dependent kinase 5 (Cdk5) phosphorylates S131. The S136 residue is also phosphorylated by unknown kinases. The kinases and the amino acids they phosphorylate are indicated in the same colour.

and non-neuronal cells (Huynh et al., 2000; Lazaro-Dieiguez et al., 2008). Oxidative stress and mitochondrial complex I inhibition has been reported to increase actin-parkin interaction in dopaminergic cell lines (SN4741) showing the importance of actin dynamics in neurodegeneration and PD (Kim and Son, 2010).

9. Post-translational modification in parkin

Parkin undergoes various post-translational modifications including nitrosylation and phosphorylation. In nitrosylation, modification of a protein occurs by the addition of a nitrosyl group mediated by nitric oxide producing enzymes. S-nitrosylation, is the addition of a S-nitrosothiols group to the cysteine residue of a protein. Parkin undergoes S-nitrosylation at three cysteine residues present in the IBR domain (Chung et al., 2004). Nitrosylation of parkin is mediated by nNOS and inducible nitric oxide synthase (iNOS), both of which inhibit the E3 ligase activity of parkin (Chung et al., 2004). Mice treated with MPTP show increased amounts of S-nitrosylated parkin in brain (Chung et al., 2005). Post-mortem PD brain samples also show high amounts of S-nitrosylated proteins, indicating high levels of nitrosative stress in PD patients (Chung et al., 2004). Taken together, these data suggest that parkin nitrosylation increases protein aggregation, which may play a major role in the pathophysiology of PD.

In phosphorylation, a phosphate (PO_4^{3-}) group is added to a protein, which is another post-translational process that regulates parkin activity. Several phosphorylation sites have been identified in parkin (**Figure 1.7**), where phosphorylation has been shown to regulate E3 ligase activity and solubility of parkin. The first report of parkin phosphorylation identified five serine phosphorylated sites (S101, S131, S136, S296 and S378), which are phosphorylated *in vitro* by protein kinases including casein kinase-1 (CK-1), protein kinase A (PKA) and protein kinase C (PKC) (Yamamoto et al., 2005). In addition to serine residues, threonine residues of parkin are also phosphorylated. The phosphorylation of parkin is found to reduce under ER stress (Yamamoto et al., 2005). Subsequent studies reveal the involvement of cyclin-dependent kinase 5 (Cdk5) in the *in vivo* and *in vitro* phosphorylation of serine 131 of parkin (Avraham, 2007). This phosphorylation leads to the reduction of parkin's E3 ligase activity, both in the auto-ubiquitination and in the ubiquitination of major substrates, including synphilin-1 and p38 (Avraham, 2007). Mutated S131A parkin is found to form inclusion bodies with synphilin-1/ α -synuclein, indicating a link between phosphorylation and ubiquitination (Avraham, 2007).

ubiquitinates polyglutamine proteins through an HSP70 interaction, thus likely functions in a similar manner as CHIP in degrading proteins via binding to CHIP and/or Hsp70 (Tsai et al., 2003). In agreement with the idea that parkin functions with CHIP, it has been shown that HSP70 degrades PAEL-R in concert with parkin and CHIP. Specifically, unfolded PAEL-R translocates to the cytosol and binds HSP70, initiating an up-regulation of CHIP (Takahashi and Imai, 2003). CHIP then initiates the dissociation of HSP70 from PAEL-R and aids in the binding of parkin as well as the ubiquitination of PAEL-R (Takahashi and Imai, 2003).

8.4 Parkin scaffolding proteins

8.4.1 PDZ domains (CASK and PICK1)

CASK is a member of the membrane-associated guanylate kinase (MAGUK) protein family, which contains a protein-protein interaction PDZ domain. CASK is also known as CAMGUK protein 2 (CMG 2), Ca²⁺/calmodulin-dependent serine protein kinase 3, membrane-associated guanylate kinase 2 and is the homolog of Lin-2 in *C.elegans*. In mammalian cells, CASK forms a tripartite protein complex with Veli and Mint proteins that interacts with a receptor tyrosine kinase, LET-23 (Butz et al., 1998). The PDZ domain of CASK interacts with the ct of neuexin, the receptor for α -latrotoxin (black widow spider venom) (Hata et al., 1996) as well as syndecan (a cell surface heparan sulfate proteoglycan) (Hsueh et al., 1998). Similarly, the last 3 amino acids of ct-parkin associate with the PDZ domain of CASK in cortical neurons, post-synaptic densities and lipid rafts (Fallon et al., 2002). The interaction between CASK and parkin results in the polyubiquitination of CASK leading to its proteasomal-mediated degradation. In addition to the PDZ motif of parkin interacting with the PDZ domain of CASK, the PDZ motif of parkin also interacts with the PDZ domain of PICK1 (Joch et al., 2007). PICK1 (protein interacting C kinase 1) is a scaffolding protein that interacts with various proteins. PICK1 and the parkin-PICK1 interaction are explained in detail in section 10.

8.4.2 Actin

Actin is highly conserved ubiquitous major cytoskeletal protein responsible for composing microfilaments, which is known to participate in many important cellular functions including cell signalling, apoptosis, vesicle and organelle movement and structure organization (Kim and Son, 2010). ROS is found to disrupt actin dynamics which may lead to apoptosis in *Saccharomyces cerevisiae* (Gourlay and Ayscough, 2005; Franklin-Tong and Gourlay, 2008). Parkin specifically interacts with actin and regulates actin remodeling, colocalizing with actin filament and interacting with LIM kinase-1 (actin binding kinase) in both neuronal

8.3 E3 ligase partners of parkin

8.3.1 Cdc4 α

Cdc4 (also known as hSel10, Archipelago, Fbw7 and Fbw7) is an F-Box/WD repeat protein of 707 amino acids long and is an integral part of Skp1, Cul1, F-box containing complex (SCF) E3 complex. The SCF complex contains Skp1 (S-phase kinase-associated protein 1), Cul1 (cullin 1), Rbx1/Roc1 (RING-box protein 1) and an F-box containing protein, such as Cdc4. There are multiple F-box containing proteins, which have specificity towards a particular set of substrate proteins through unique protein–protein interactions. A variety of RING finger containing proteins are integrated in this multiprotein ubiquitin ligase complex (Joazeiro and Weissman, 2000). Parkin can also act in concert with other proteins to form a multiprotein ubiquitin ligase complex, including SCF, which ubiquitinates several proteins. Cdc4 has three isoforms due to alternative splicing in mammals, Cdc4 α , Cdc4 β and Cdc4 γ (Spruck et al., 2002), which are located in nucleoplasm, cytoplasm and nucleolus, respectively (Welcker and Clurman, 2004). SCF^{Cdc4 α} ubiquitinates a variety of substrates, such as cyclin E, peroxisome proliferator-activated receptor gamma coactivator-1 α (PGC-1 α), presenilin, c-Myc, c-Jun, Notch and sterol regulatory element binding proteins (SREBP) (Hubbard et al., 1997; Gupta-Rossi et al., 2001; Koepp et al., 2001; Moberg et al., 2001; Oberg et al., 2001; Strohmaier et al., 2001; Nateri et al., 2004; Welcker and Clurman, 2004; Yada et al., 2004; Sundqvist et al., 2005). Parkin specifically interacts with Cdc4 α (Koepp et al., 2001; Moberg et al., 2001; Strohmaier et al., 2001; Wu et al., 2001). Deletion constructs of parkin have revealed that both the RING fingers, situated on the carboxyl terminus of parkin, interact specifically with the F-Box of Cdc4 α . A second interaction site is found within the Ubl domain of parkin and the WD repeat domain of Cdc4 α (Staropoli et al., 2003). This complex ubiquitinates target proteins with the help of the E2 UbcH7 enzyme (Staropoli et al., 2003). It is also reported that E3 enzyme activity of parkin is enhanced by the over-expression of Cdc4 α (Staripoli et al., 2003). In addition, along with co-expression of Cdc4 α , over-expression of UbcH7 is needed to enhance parkin-mediated ubiquitination (Staripoli et al., 2003). Thus, parkin functions in concert with Cdc4 α and UbcH7.

8.3.2 Heat shock protein 70 (HSP70) and CHIP

Parkin is associated with heat shock protein 70 (HSP70) and the E3 carboxy terminus of HSC70-interacting protein (CHIP). Originally reported as Hsc/HSP70 binding protein, CHIP functions as an E3 ligase to ubiquitinate and degrade its interacting proteins (Murata et al., 2001). Ubiquitination by CHIP and recognition of abnormal proteins by HSP70 is important for degradation of a number of proteins (Imai and Takashashi, 2004). Parkin also

suggest that the parkin Ubl domain interacts with both UIMs of S5a. The lysine (K48) residue of the Ubl domain in parkin is a crucial amino acid in recognition of S5a subunit (Safadi and Shaw, 2010).

8.2.9 Endocytic protein Eps15

Epidermal growth factor receptor substrate 15 (Eps15), encoded by EPS15 gene in human, is an adapter protein involved in epidermal growth factor (EGF) receptor (EGFR) endocytosis and trafficking (Fallon et al., 2006). Upon EGF stimulation, the Ubl domain of parkin interacts with Eps15 and facilitates the monoubiquitination of this protein (Fallon et al., 2006). The binding of the Ubl domain of parkin to Eps15 is essential for ubiquitination of Eps15 (Fallon et al., 2006) such that in null-parkin cells, acceleration of EGFR endocytosis and degradation is observed (Fallon et al., 2006). Furthermore, reduction of EGFR signalling via the phosphoinositide 3-kinase {PI(3)K}-Akt pathway in parkin knockout (parkin-KO) mice suggests that parkin may interfere in the association of Eps15 and ubiquitinated EGFR, resulting in delayed EGFR internalisation and degradation and promotion of PI(3)-Akt signalling (Fallon et al., 2006).

8.2.10 Non-receptor tyrosine kinase c-Abl

Non-receptor tyrosine kinases or non-specific protein-tyrosine kinases are a large family of kinase enzymes responsible for the ATP-dependent phosphorylation of tyrosine residues. One of the members of tyrosine kinase family, c-Abl (a homolog of transforming element of the Abelson murine leukemia virus), present in the nucleus and cytoplasm, is predominantly activated by cellular stress (Hantschel et al., 2004). The c-Abl protein is involved in neuronal plasticity, neurite outgrowth and neurogenesis in brain and also has role to play in tumorigenesis (Reddy et al., 1983; Moresco and Koleske, 2003). Aberrant activation of c-Abl kinase was found in neurological disorders, including AD and Niemann-Pick type-2 disease (Alvarez et al., 2004 and 2008). Stress-induced activation of c-Abl by dopaminergic neurotoxins, such as 1-methyl-4-phenylpyridinium (MPP⁺) and MPTP causes phosphorylation of tyrosine residue (Y143) of parkin (Ko et al., 2010). In addition, the SH3 domain of c-Abl interacts with the RING finger and IBR domains of parkin (Ko et al., 2010). Phosphorylation of parkin inhibits ubiquitination activity of parkin and causes accumulation of parkin substrates that ultimately leads to neuronal death (Ko et al., 2010). Inhibition of c-Abl expression demonstrated neuroprotective effects in case of stress-induced by neurotoxins (Ko et al., 2010).

ARS complex primarily involved in protein synthesis (Ko et al., 2005). The aminoacyl-tRNA synthase (ARS) complex including the p38 subunit is associated with protein biogenesis in a number of tissues as well as in the brain. Upon over-expression of p38 by adenoviral-mediated transfection, selective neuronal death is observed (Ko et al., 2005). Furthermore, the p38 subunit protein was identified in proteinaceous aggregations of sporadic PD patients as well as the Lewy bodies of idiopathic cases of PD (Ko et al., 2005). The RING finger domain of parkin interacts with the 82-162 amino acids of p38 and mediates its ubiquitination for UPS (Ko et al., 2005), likely controlling the neurotoxic effects of high protein levels of p38.

8.2.8 Proteasomal subunit S5a

Substrate recognition and recruitment of ubiquitinated substrates for the 26S proteasome-dependent protein degradation are two important steps in UPS, where E3 ligases play a central role. The N-terminal Ubl domain of parkin, responsible for substrate recognition for ubiquitination, serves as the bridge between the ubiquitinated protein and the 26S proteasome through specific protein-protein interaction. S5a, also called as Rpn10, is a subunit of 19S regulatory protein that serves as the cap structure for 26S proteasomal subunit. Otherwise conjugated with 26S proteasome, a freely available monomeric form of S5a is also found in cytosol. Most E3 ligases, in poly-ubiquitinated conditions, are recognised by S5a (Uchiki et al., 2009). Upon recognition, the S5a subunit undergoes an E3 ligases-mediated poly-ubiquitination, though the poly-ubiquitination of S5a does not lead to its degradation (Uchiki et al., 2009). S5a has a strong affinity towards poly-ubiquitin chain through its two ubiquitin interacting motifs (UIM) that identify poly-ubiquitinated substrates (Uchiki et al., 2009). The presence of intact UIMs of S5a is important for the ubiquitination process as mutation in both UIMs abolishes the ubiquitination of S5a by various E3 ligases (Uchiki et al., 2009). A variety of E3 ligases including monomeric RING finger containing E3 ligases such as parkin {and others including muscle RING-finger protein-1 (MuRF1), murine double minute 2 (Mdm2) and seven in absentia homolog 2 (Siah2)}, multimeric RING finger containing E3 ligases {adenomatous polyposis coli (APC)}, U-box containing E3 ligases {E3 carboxy terminus of HSC70-interacting protein (CHIP)} and HECT domain E3 ligases {E6 associated protein (E6AP) and neural precursor cell expressed developmentally down-regulated protein 4 (Nedd4)} interact with S5a subunit to ubiquitinate their interacting partners (Murata et al., 2001; Kedar et al., 2004; Kim et al., 2007; Uchiki et al., 2009). During the ubiquitination process of S5a, the presence of Class I ubiquitin conjugating enzymes (E2), such as UbcH5 is essential (Uchiki et al., 2009). The Ubl domain of parkin interacts and ubiquitinates the S5a subunit (Safadi and Shaw, 2010). NMR spectroscopy experiments

1999). By interacting with syntaxin, CDCrel-1 inhibits its exocytosis (Zhang et al., 2000) and neurotransmitter exocytosis (Imai and Takahashi, 2004). Upon over-expression in H1T-T15 cells, CDCrel-1 decreases the release of human growth factor, indicating probable regulatory function of CDCrel-1 in synaptic vesicle events involving syntaxin (Dev et al., 2003a).

8.2.5 PAEL-R

In addition to the pre-synaptic proteins indicated above, the parkin associated endothelial like receptor (PAEL-R), which is a G-protein coupled receptor (GPCR) also associates with parkin (Imai et al., 2001). High expression of PAEL-R is found in dopaminergic neurons and oligodendrocytes. PAEL-R is selectively ubiquitinated and promoted for degradation by parkin (Imai et al., 2001; Yang et al., 2003). The presence of PAEL-R is observed in Lewy bodies of PD patient (Murakami et al., 2004) and insoluble fractions of PAEL-R are also detected in the brains of ARJP patients (Imai et al., 2001). A study has showed that PAEL-R over-expression results in the internalization of PAEL-R and complex formation of a large protein complex (≥ 250 kDa) inducing mitosis (Rezgaoui et al., 2006). In this aggregated form, PAEL-R causes cellular toxicity leading to cell death (Rezgaoui et al., 2006).

8.2.6 PARIS (ZNF746)

A zinc-finger containing protein called PARIS has been found to be associated with parkin. This protein consists of an amino terminal Kruppel-associated box (KRAB) and a carboxyl terminal C2HC/C2H2 Zn type finger (Shin et al., 2011). The PARIS gene is located in chromosome 7q36.1 and encodes a protein of 644 amino acids. The PARIS-parkin interaction was first shown in a yeast two hybrid assay (Zhang et al., 2000) and subsequent co-immunoprecipitation (co-IP) studies revealed the RING1 and RING2 of parkin interacts with the zinc finger domain of PARIS (Shin et al., 2011). This interaction is important for parkin-mediated ubiquitination of PARIS and its degradation through UPS in neurons (Shin et al., 2011), such that when endogenous parkin is knocked-down using shRNA a significant upregulation of PARIS protein levels is detected in SH-SY5Y cells (Shin et al., 2011). This data is supported by protein level analysis of brain samples obtained from ARJP patients, which show a two-fold increase in protein levels of PARIS and a lack of functional parkin protein (Shin et al., 2011). Interestingly, high PARIS expression levels were only found in the nigrostriatal pathway with other brain regions showing similar levels of PARIS.

8.2.7 p38 subunit of aminoacyl-tRNA synthase (ARS) complex

Aminoacyl-tRNA synthetases (ARSs) are essential enzymes that ligate amino acids to tRNAs to make nascent polypeptides. The p38 subunit is a key structural component of the

Parkin's second RING finger domain binds to the ankyrin repeat domain of synphilin-1 and causes ubiquitination of synphilin-1 (Chung et al., 2001). Deposition of synphilin-1 was observed in Lewy bodies and synphilin-1 specifically inhibits the degradation of α -synuclein by the 20S proteasome (Alvarez-Castelao et al., 2010). Mutated parkin is able to bind synphilin, but fails to cause the ubiquitination of synphilin (Chung et al., 2001). Since both protein are pre-synaptic, it is interesting to speculate that α -synuclein and synphilin-1 may work in concert to alter the release of dopamine from dopaminergic neurons, where in PD, such roles are aberrant.

8.2.3 Synaptotagmin XI

Following on from the idea parkin interacts with pre-synaptic proteins (i.e. α -synuclein and synphilin-1) that may play a role in regulating dopamine neurotransmission, parkin does indeed interact with proteins that play a role in synaptic vesicle docking, such as Synaptotagmin XI. Briefly, Synaptotagmin XI plays a role in the docking and fusion of synaptic vesicles to the plasma membrane leading to transmitter release (Glass et al., 2004). It belongs to the family of vesicle proteins, namely synaptotagmins and has a single transmembrane region and two cytoplasmic C2 domains (C2A and C2B) in the ct region followed by a conserved terminus (Glass et al., 2004). Parkin interacts with synaptotagmin XI at the C2A and C2B domains and synaptotagmin XI binds to the RING finger 1 motif of parkin (between the amino acid residues 204 and 293) (Huynh et al., 2003). Reports have shown that parkin ubiquitinates and promotes degradation of synaptotagmin (Huynh et al., 2003). Immunolabelling data has also shown the presence of synaptotagmin in the wild type neurons as well as Lewy bodies in the SNPC of PD patient (Huynh et al., 2003). Synaptotagmin is thought to hamper dopamine release in parkin mutated mice (Imai and Takahashi, 2004).

8.2.4 CDCrel-1

Yet another synaptic vesicle-associated protein, namely CDCrel-1, is associated with parkin. CDCrel-1 or cell division control-related protein-1 (CDCrel-1) is a synaptic vesicle enriched septin GTPase. It was the first reported parkin substrate (Zhang et al., 2000). Dopamine-dependent neurodegeneration is observed in the rodent brain upon over-expression of CDCrel-1 (Dong et al., 2003). Parkin interacts with CDCrel-1 via the RING finger 2 domain (Zhang et al., 2000). CDCrel-1 is ubiquitinated by wild type parkin leading to the degradation of CDCrel-1, but not mutant parkin (Q311stop and T415N) (Zhang et al., 2000). CDCrel-1 also co-localises with parkin in synaptic vesicle (Kubo et al., 2001). In addition, CDCrel-1 interacts with syntaxin, a protein promoting exocytosis via SNARE domain (Beites et al.,

8.1 E2 conjugating enzymes: Ubch7 and Ubch8

Ubch7 and Ubch8 are two E2 conjugating enzymes that interact with the RING domains (in particular RING2) of parkin and play important role in the ubiquitination process of substrate proteins (Imai et al., 2000; Shimura et al., 2000; Zhang et al., 2000). Mutation in parkin, specifically, T240R mutation is found to disrupt the interaction with these E2 enzymes, in the case of ARJP (Imai et al. 2000; Zhang et al. 2000; Shimura et al. 2000; Gu et al. 2003). Although the expression of Ubch7 is low compared to Ubch8 (Kimura et al., 1997; Katsanis and Fisher, 1998), the specific association of parkin-Ubch7 was found to be crucial for the ubiquitination of α -synuclein in the brain (Shimura et al., 2001). In addition to parkin, Ubch7 and Ubch8 also interact with other RING-IBR-RING domain containing E3 ligases, including human homologue of *Drosophila ariadne* (HHARI) and Ubch7 associated protein 1 (H7-AP1) (Moynihan et al., 1999).

8.2 Parkin ubiquitinated proteins

8.2.1 α -synuclein

α -Synuclein is a 140 amino acid, neuronal phosphoprotein that upon mutation causes the dominant form of PD. The α -synuclein protein, encoded by PARK1 gene, is thought to be a pre-synaptic expressed protein that plays a role in learning and memory as well as synaptic plasticity (Iwai et al., 1995). The α -synuclein is found to be the integral part of the fibrillary component of Lewy bodies (Polymeropoulos et al., 1997). Three point mutations (A30P, A53T and E46K) in α -synuclein have been identified, which are found in aggregated forms in Lewy bodies (Forno, 1996; Polymeropoulos et al., 1997; Kruger et al., 1998; Singleton et al., 2003). These mutant forms of α -synuclein escape parkin-mediated proteasomal activity (Petrucci et al., 2002) resulting in the build-up of aggregated α -synuclein in Lewy bodies and subsequent neuronal death. Parkin has also been reported to ubiquitinate an O-glycosylated form of α -synuclein (Shimura et al., 2001) and during parkin mutation, accumulation of this O-glycosylated form of α -synuclein has been observed in the rat brain (Shimura et al., 2001).

8.2.2 Synphilin-1

Synphilin-1 is a protein associated with α -synuclein with unknown function. Synphilin-1, like α -synuclein is a pre-synaptic protein associated with synaptic terminals (Ribeiro et al., 2002). Synphilin-1 contains 919 amino acids with different domains, including ankyrin-like repeats, a coiled-coil domain and a putative ATP/GTP-binding domain (Engelender et al., 1999).

Name	Function	Reference
UbcH7/UbcH8	E2 conjugating enzymes	Imai et al., 2000
α -Synuclein	Involved in synaptic vesicle transport	Kahle et al., 2000
Synphilin-1	Unknown	Chung et al., 2008
Synaptotagmin XI	Docking and fusion of synaptic vesicle to release transmitter	Glass et al., 2004
CDCrel-1	Regulates neurotransmitter exocytosis	Imai and Takahashi, 2000
PAEL-R	G-protein coupled receptor	Corti et al., 2003
PARIS	Transcriptional repressor	Shin et al., 2011
p38	Subunit of aminoacyl-tRNA synthetase	Ko et al., 2005
Proteasomal subunit S5a	Substrate recognition for 26S proteasome	Uchiki et al., 2009
Endocytic protein Eps15	Adapter protein in epidermal growth factor receptor (EGFR)	Fallon et al., 2006
Non-receptor tyrosine kinase c-Abl	Phosphorylation of tyrosine residues	Ko et al., 2010
Cdc4 α	F-box domain of SCF E3 ligase complex	Fallon et al., 2002
HSP70/CHIP	E3 ligase	Murata et al., 2001
PICK1	Scaffolding protein	Joch et al., 2007
CASK	Ca ²⁺ /calmodulin-dependent serine kinase	Fallon et al., 2002
Actin	Cytoskeleton protein	Huynh et al., 2000

Table 1.3: List of proteins associated with parkin

The proteins interacting with parkin and a brief description of their roles are depicted.

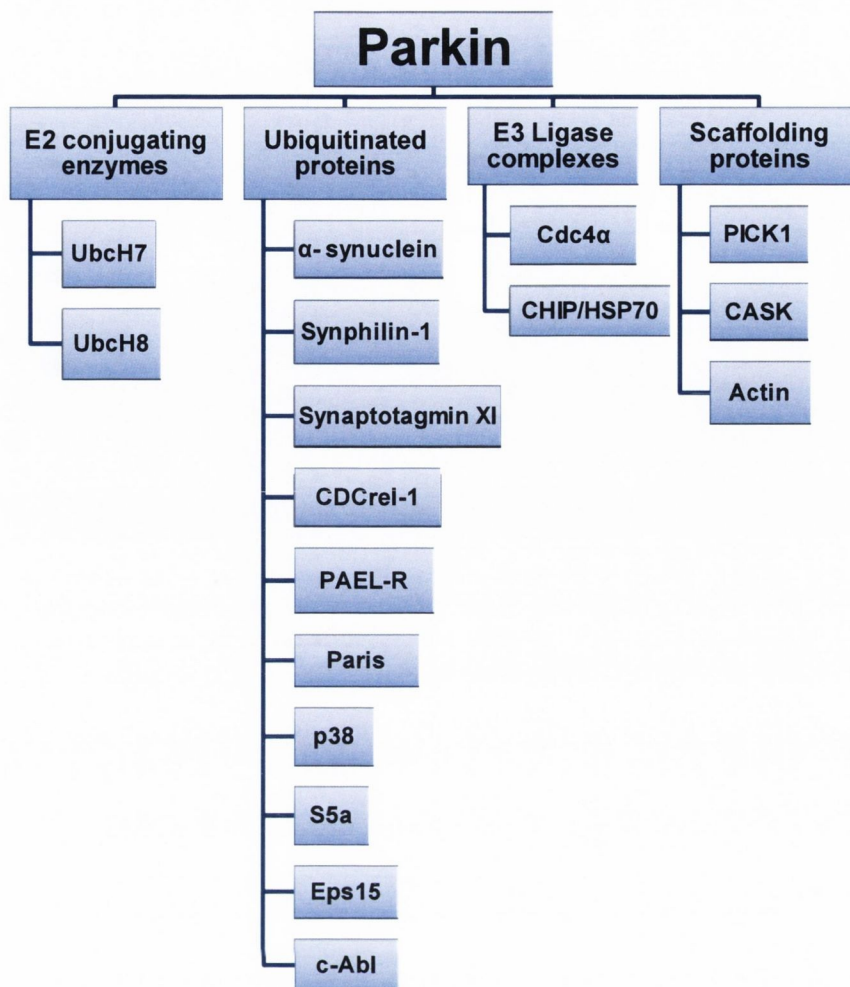


Figure 1.6: Parkin interacting partners

Parkin interacts with several proteins. Parkin interacts with E2 conjugating enzymes, such as Ubch7/Ubch8. Proteins, ubiquitinated by parkin, include α -synuclein, synphilin-1, synaptotagmine XI, CDCrel-1, PAEL-R, Paris, p38, S5a, Eps15 and c-Abl. Parkin also acts in concert with other E3 ligases, including Cdc4 α and CHIP to ubiquitinate a series of additional substrates. Through its PDZ motif, parkin interacts with scaffolding proteins, such as PICK1 and CASK and parkin also interacts with actin.

A)

Domain structure of parkin



B)

Parkin protein- Isoform 1

MIVFVRFNSSHGFPVEVDSDTSI FQLKEVVAKRQGV PADQLRVI FAGKEL
 RNDWTVQNCDDLQQSIVHIVQR PWRK GQEMNATGGDDPRNAAGGCEREPEQ
 SLTRVDLSSSVLPGDSVGLAVILHTDSRKDSPPAGSPAGRSIYNSFYVYC
 KGPCQQRVQPGKLRVQCSTCRQATLTLTQGPSCWDDVLI PNRMSGECQSPH
 CPGTSAEFFFKCGAHPTSDKETPVALHLIATNSRNITCITCTDVRSPVLV
 FQCNSRHVICLDCFHLYCVTRLNDRQFVHDPQLGYSLPCVAGC PNSLIKE
 LHHFRILGEEQYNYQQYGAE ECVLQMGVLCPRPGCGAGLLPE PDQRKV
 TCEGGNGLGCGFAFCRECKEAYHEGEC SAVFEASGTTTQAYRVD ERAAEQ
 ARWEAASKETIKKTKPCPRCHVPVEKNGGCMHMKCPQPQCRLEWCWNCG
 CEWNRVCMGDHWFDV

■ Ubl domain
■ Central domain
■ RING 1
■ IBR
■ RING 2
■ PDZ motif

Figure 1.5: Structure and protein sequence of parkin

A) Structural domains of parkin suggest the presence of an ubiquitin like domain (UBL) at the N-terminus. The two Zn-finger-like RING domains are connected to the UBL domain with a central domain. The two RING fingers are, in turn, linked to each other by a cysteine rich region. The last three amino acids at the ct region constitute a PDZ motif (-FDV) which interacts with PDZ domain containing proteins PICK1 and CASK. B) The protein sequence of parkin shows the different domains and motifs.

Parkin can be structurally divided into four domains/motifs (**Figure 1.5**).

- 1. Ubiquitin Like Domain (Ubl):** The amino terminal residues (1-76) constitute the ubiquitin like domain that has 62% homology with ubiquitin. This domain is believed to be responsible for substrate recognition (Shimura et al., 2000). In addition, the UBL domain also regulates the expression of parkin (Finney et al., 2003).
- 2. Central domain:** Residues 145-232 constitutes the central domain with unknown function.
- 3. RING finger box:** The ct residue 237-449 constitutes a RING box domain, which contains two RING fingers (Kitada et al. 1998; Morett and Bork, 1999). The two RING finger domains are designated as RING1 and RING2 attached to each other by an in-between-region (IBR) domain, which is cysteine rich (Morett and Bork, 1999). The RING fingers are Zn-finger domains, which bind to Zn^{2+} and are believed to interact with other proteins including E2 enzymes (Joazeiro and Weissman, 2000; Borden, 2000). Similar to other Zn-finger containing proteins, known to function as transcription factors, parkin is also believed to play role in the transcriptional regulation (Zheng et al., 2000a).
- 4. PDZ-binding motif:** This motif is situated at the extreme ct of parkin and comprises last the three amino acids (-FDV). The PDS-95/discs large/ZO-1 (PDZ) motif of parkin is a class II PDZ motif, which can interact with various adapter proteins containing PDZ domains (approximately 90 amino acids) (Ponting et al., 1997). Parkin has been shown to interact with the PDZ domain proteins CASK and PICK1 (Fallon et al., 2002).

Via these structural domains and the motifs, parkin interacts with several substrates, most of which are ubiquitinated and degraded. The parkin interacting proteins are explained in following section.

8. Parkin interacting proteins

Parkin has been shown to interact with and ubiquitinate several cellular proteins with distinct functions. They are described in the section below (**Figure 1.6 & Table 1.3**).

4. Stimulation of protein sumoylation in the presence of E3 proteins by simultaneously associating with the UBC9 and the substrate (Geiss-Friedlander et al., 2007; Mukhopadhyay and Dasso, 2007).

The de-sumoylation reaction is carried out by six different SENP enzymes in human cells termed SENP 1 to 6 (Mukhopadhyay and Dasso, 2007; Geiss-Friedlander et al., 2007; Zhao, 2007). Among these six SENPs, the SENP1 and SENP2 are capable of removing all three isoforms of SUMO protein moieties. Other SENPs are specific for SUMO-2 and SUMO-3.

There are many neurodegenerative diseases, where sumoylation plays a role. The diseases, where proteins are abnormally sumoylated, are PD (tau, α -synuclein, DJ-1), HD (Huntingtin), AD (tau and APP), spinocerebellar ataxia type 1 (Ataxin-1) and ALS (SOD1) (Sarge and Paek-Sarge, 2009). In particular, tau has been implicated in the development of both PD and AD. Tau is sumoylated by SUMO-1 at K340 residue. It has been reported that a decrease in sumoylation of tau is observed upon proteasome inhibitor MG102 treatment, which also increases the ubiquitination of tau. The inhibition of tau phosphorylation is also thought to increase tau sumoylation (Sarge and Paek-Sarge, 2009). Of interest, α -synuclein is present in Lewy bodies, the proteinaceous aggregates in the brain of PD patient, is also sumoylated on its K102 residue, preferentially by SUMO-1. Unlike tau, α -synuclein is unaffected by proteasome inhibitor MG132 treatment (Dorval et al., 2006). The function of α -synuclein sumoylation is still unknown. In addition to tau and α -synuclein, DJ-1 is an important protein, which upon mutation causes early onset PD (1-2% prevalence) (Thomas et al., 2007). DJ-1 functions as an anti-oxidant, transcriptional co-activator and molecular chaperone. DJ-1 is also sumoylated on K130 residue. Upon mutation in this residue, a decrease in DJ-1-mediated Ras-dependent transforming and cell-growth-promoting activity is observed (Shinbo et al., 2006). These findings suggest sumoylation may regulate tau, α -synuclein and DJ-1 function that may play a role in neurodegeneration.

7. Parkin as an E3 Ligase

Genetic mutations in the *parkin* gene, which encodes an E3 ligase, are associated with autosomal ARJP. A loss-of-function of mutated parkin results in UPS dysfunction, eventually causing death of dopaminergic neurons. Parkin is the second largest gene in the human genome with a size of 1.5 Mb (the largest gene is *DMD*, size 2.4 Mb, encodes for Dystrophin protein). The genetic location of the gene is 6q25.2-q27. The *parkin* gene has 12 exons, which upon translation, express an approximately 52 kDa protein (465 amino acids) (Kitada et al., 1998; Shimura et al., 1999).

ii) E3 ligases with really-interesting-new-gene (RING) finger domain (Kim et al., 2009) (such as parkin) bind the substrate and the E2 enzyme, but not the ubiquitin molecule, to transfer the ubiquitin to the substrate.

In both cases, the E3 ligase binds the ubiquitin to the substrate via an ϵ -amide bond.

Finally, the tagged substrate is then detected by the 26S proteasome, a large multiprotein complex of 2.5 MDa size, which eventually degrades the substrate in an ATP-dependent manner (Voges et al., 1999).

6.3 Sumoylation

Like ubiquitination, sumoylation is another important post-translational event in which a small protein named SUMO (Small Ubiquitin-like Modifiers) is attached to specific lysine residues in target proteins. The subcellular localisation, protein partnering and transcription factor trans-activation of a target protein can be regulated by sumoylation. SUMO or sentrin proteins are 110 amino acids of which there are three isoforms, e.g., SUMO-1, SUMO-2 and SUMO-3 in vertebrates. In contrast, invertebrates have only one isoform (Kamitani et al., 1998). Different SUMO isoforms (1, 2 and 3) have 50% sequence homology among each other (Muller et al., 2001). NMR spectroscopy data show SUMO-1 and ubiquitin protein share a common three dimensional structure, although only 18% of sequence similarity is found between these two proteins (Bayer et al., 1998).

Sumoylation involves four enzymatic steps,

1. Maturation of the SUMO protein by cleaving its ct to make a carboxyl terminal diglycine motif by a sentrin-specific protease (SENP).
2. Attachment of the mature SUMO protein to a cysteine residue in the SUMO-activating enzyme subunit 2 (SAE2) of the heterodimeric SUMO E1 activating enzyme via formation of a ATP-dependent thioester bond (Johnson et al., 1997a; Desterro et al., 1999; Gong et al., 1999; Okuma et al., 1999).
3. Transfer of the SUMO moiety from E1 enzyme to the SUMO E2 enzyme (UBC9) that ultimately attaches SUMO to the lysine residue of the target protein. The lysine residue is found not always, but most of the time in a consensus sequence Ψ -K-X-E (where Ψ represents hydrophobic amino acids) (Desterro et al., 1997; Johnson et al., 1997b; Rodriguez et al., 2001; Sampson et al., 2001).

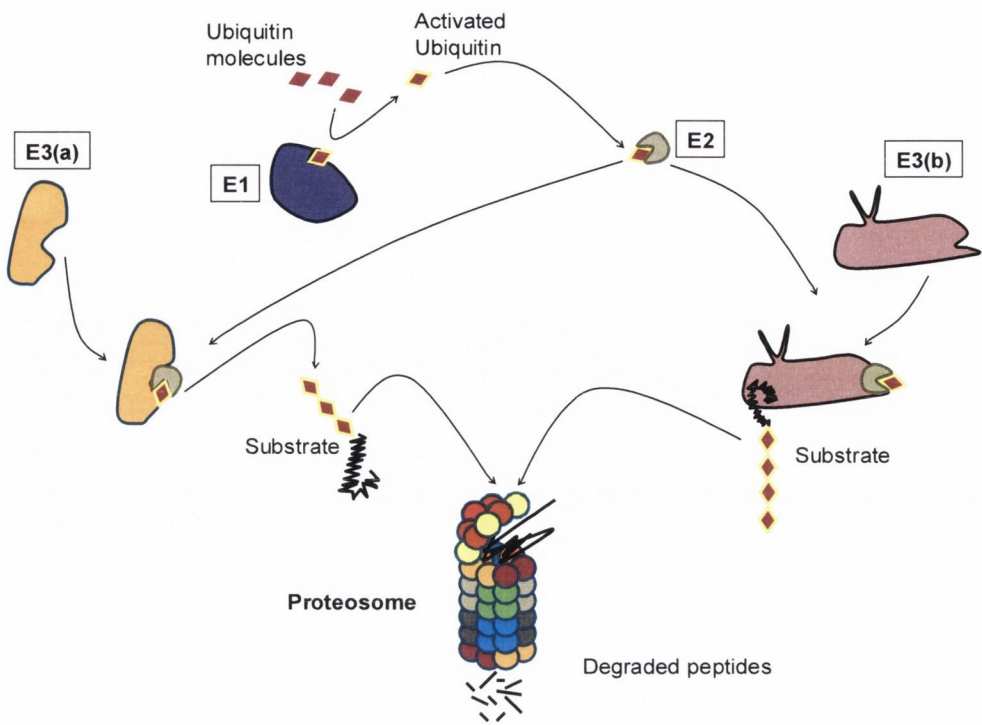


Figure 1.4: Ubiquitin Proteasome System

Unwanted proteins are tagged with ubiquitin by sequential action of three enzymes. E1 and E2 enzymes activate the ubiquitin molecule and help to conjugate the activated ubiquitin with the substrate, respectively. Transfer of the activated ubiquitin molecule to the substrate is mediated by two types of E3 ligase enzyme systems, E3 (a) ligases with HECT domain that directly bind both the ubiquitin molecule and the E2 enzyme to transfer the ubiquitin molecule to the substrate and E3 (b) ligases with RING finger domain that bind the substrate and the E2 enzyme, but not the ubiquitin molecule, to transfer the ubiquitin to the substrate. After successful tagging with ubiquitin, the substrate is poly-ubiquitinated and then processed by 26S proteasome.

Although, in general, Lewy bodies are not detected when parkin is mutated in ARJP (Mori et al., 1998; Hayashi et al., 2000), a patient with a single allele mutation in parkin (with partial E3 ligase activity) was shown to have Lewy bodies (Farrer et al., 2001). Intriguingly, over 90% of Lewy bodies formed in the autosomal dominant PD demonstrated parkin immunoreactivity, suggesting a role of parkin in the formation of Lewy bodies (Dev et al., 2003).

6.2 Ubiquitination

Ubiquitination is an important post-translational modification that plays a wide variety of roles in cellular processes, such as chromatin remodelling, DNA repair, protein trafficking, degradation, signal transduction, peroxisomal biogenesis and viral budding (Di Fiore et al., 2003; Hicke et al., 2003; Haglund and Dikic, 2005). Ubiquitin or ubiquitous immunopoietic polypeptide is an 8.5 kDa protein, which is ubiquitously found in all eukaryotic cells. Ubiquitination involves the covalent attachment of a polyubiquitin chain to a lysine residue of the ubiquitinated protein.

UPS is a three-enzyme pathway eventually resulting in the degradation of unwanted cellular proteins. Unwanted proteins or substrates are molecularly marked or primed with ubiquitin and finally degraded by the UPS (Hershko and Ciechanover, 1998). This three-enzyme system acts chronologically to tag the substrate molecule with single ubiquitin molecules forming a chain of polyubiquitin. The process of tagging a substrate with a polyubiquitin chain is called polyubiquitination, which involves three enzymatic steps (**Figure 1.4**).

- 1) The ATP-dependent ubiquitin activating enzyme (E1) activates the ubiquitin molecules.
- 2) The activated high energy ubiquitin is then accepted by the ubiquitin conjugating enzyme (E2) by forming a thioester bond.
- 3) After activity of the E2 enzyme, the ubiquitin ligase (E3) mediates ligation of activated ubiquitin molecules. Ubiquitin ligases can be divided into two categories according to their mode of action to transfer the ubiquitin molecule to the substrate.
 - i) E3 ligases with homology to E6-AP carboxy terminus (HECT) domain (such as Cdc4) directly bind both ubiquitin molecule and the E2 enzyme to transfer the ubiquitin to the substrate.

Parkinson's study group 2, 1993; Churchyard et al., 1997; Bar-Am et al., 2007). Due to these severe side effects of L-dopa, further drug development efforts are required.

6. Neurodegeneration & protein aggregation

Neurodegeneration is defined as the degradation of neuronal cells in a progressive manner due to apoptosis, autophagy or cytoplasmic cell death, collectively known as programmed cell death (PCD) (Kim et al., 2011). Neurodegeneration is the prevalent cause of many neuropathic diseases, such as PD, AD and HD. There are many causes of neurodegeneration identified, including defects in protein degradation, ROS production, Ca^{2+} dysregulation, mitochondrial dysfunction and excitotoxicity (Schweichel and Merker, 1973; Clarke, 1990). Among all these neurodegenerative processes, protein aggregation has a prominent role in the death of neurons. Particularly, formation of proteinaceous aggregates caused by the deposition of unwanted proteins results in these diseases. Protein aggregation is controlled by various processes, in which ubiquitination and sumoylation are important.

6.1 Lewy bodies: Hallmark of PD

Protein aggregation is a common pathology found in most of the neurodegenerative diseases, including AD, HD and PD. For AD, the formation of plaques composed β -amyloid ($A\beta$) and neurofibrillary tangles composed hyperphosphorylated Tau have been identified to cause neurodegeneration in AD brain (Querfurth and LaFerla, 2010). In the case of HD, protein inclusions of mutated huntingtin protein are a characteristic feature in the brains of HD patients (Temussi et al., 2003). For PD, Lewy bodies are considered as the hallmark feature, which are composed abnormal accumulation of proteins found in the cell bodies of neurons in sporadic as well as autosomal dominant PD (Forno, 1996). In addition, protein aggregates forming smaller inclusions in the neuronal extensions called Lewy neurites are also found in PD (Brundin and Olsson, 2011). These protein inclusions are composed misfolded variant of mutant α -synuclein, constituting the major component along with other proteins including, ubiquitin and UCH-L1 (Lowe et al., 1990; Polymeropoulos et al., 1997; Shults, 2006). Indeed, genome analysis has revealed three point mutations of α -synuclein associated with autosomal dominant PD that appear susceptible to aggregation in Lewy bodies (Venda et al., 2010). Moreover, the level of α -synuclein is found to increase in the aging brain, specifically in the dopaminergic neurons of SNPC (Chu and Kordower, 2007) and the Lewy body density correlates directly with progression of PD (Halliday et al., 2008).

A)

Well-validated loci/genes	Gene	Locus	Risk variants
PARK1/PARK4	α -Synuclein	4q21	Promoter Rep1 5' and 3' variants
PARK8	LRRK2	12q12	G2385R, R1628P (Asians)
Not assigned	MAPT-linked FTDP-17	17q21.1	H1 haplotype (Europeans)
Not assigned	GBA-linked GD	1q21	>300 heterozygous mutations

B)

Putative loci/genes	Gene	Locus	Reference
PARK16	Unknown	1q32	Satake et al., 2009
PARK17	GAK	4p16	Hamza et al., 2010
PARK18	HLA-DRA	6p21.3	Hamza et al., 2010
Not assigned	BST1	4p15	Satake et al., 2009
Not assigned	FGF20	8p22	IPDGC and WTCCC2 2011
Not assigned	ACMSD	2q21	IPDGC and WTCCC2 2011
Not assigned	STK39	2q24	IPDGC and WTCCC2 2011
Not assigned	MCCC1/ LAMP3	3q27	IPDGC and WTCCC2 2011
Not assigned	SYT11	1q22	IPDGC and WTCCC2 2011
Not assigned	CCDC62/ H1P1R	12q24	Saad et al., 2011
Not assigned	STX1B	16p11	IPDGC and WTCCC2 2011
Not assigned	STBD1	4q21	IPDGC and WTCCC2 2011
Not assigned	GPNMB	7p15	IPDGC and WTCCC2 2011

Table 1.2: Novel loci associated with PD

Several new genetic loci linked with PD were discovered by using two genetics approaches, namely, candidate gene approach and GWAS. The tables show a list of identified genetic loci by candidate gene approach (A) and GWAS (B) (Lesage and Brice, 2012).

with PD, identified using candidate gene approach, are shown in **Table 1.2A**. GWAS is one of the most sought after genome search strategies to discover genetic loci influencing disease. In this approach, low penetrance alleles influencing complex diseases can be identified, which may be missed in linkage studies. By using this approach, multiple polymorphic loci have been identified in α -synuclein, MAPT and LRRK2 as risk factors for PD (Satake et al., 2009; Hamza et al., 2010; Saad et al., 2011). In addition to these well known genes, several new loci have been identified by GWAS, listed in **Table 1.2B** (Lesage and Brice, 2012). All these data suggest the importance of a genetic role in PD, although more research is required to validate the exact role of each gene in the onset of PD.

5.4 Current treatments for PD

A major breakthrough occurred in PD therapy when Swedish pharmacologists Arvid Carlsson and Oleh Hornykiewicz discovered dopamine as a neurotransmitter depleted in PD. After this discovery, the precursor of dopamine, levodopa (L-dopa; L-3, 4-dihydroxyphenylalanine) has been widely used as medicine in PD. The conventional treatment regime for PD has been administration of L-dopa with synthetic dopamine agonists to supply dopamine and applying inhibitors of dopamine metabolism. L-dopa is a precursor of dopamine, epinephrine and norepinephrine, collectively called catecholamines. Upon oral ingestion, L-dopa is absorbed in the circulatory system from upper small intestine. Only a small fraction of L-dopa ultimately reaches the brain by crossing the blood brain barrier with the help of active transport (Nutt et al., 1984). In the brain, L-dopa is readily converted to functional dopamine by an enzyme L-amino acid decarboxylase (AAAD).

To increase the efficacy of L-dopa many other compounds have been developed. Carbidopa or benserazide are administered with L-dopa to prevent the conversion of L-dopa to dopamine outside CNS by inhibiting AAAD. To prolong the clearance half-life of L-dopa, compounds, such as entacapone or tolcapone are used to prevent peripheral catechol-O-methyltransferase (COMT) (Tallman et al., 1976). To prolong the breakdown of dopamine converted from L-dopa, several compounds, including selegiline and rasagiline are used inhibiting monoamine oxidase type B (MAO-B) (Collins et al., 1970; Youdim et al., 1972). L-dopa is effective in the recovery of a patient from impairment of speech, dexterity and posture. However, symptoms, such as tremor and imbalance have been observed to remain unchanged (Parkinson's study group 1, 1989). In addition, upon prolonged treatment (a period of 5 years), up to half of patients show severe dyskinesia (uncontrolled movement of muscles) and/or motor fluctuations (Ricaurte et al., 1984; Olanow and Calne, 1992;

Gene	Locus	Mode of inheritance	Function
α -Synuclein (PARK1)	4q21	AD	Pre-synaptic protein, membrane trafficking
Parkin (PARK2)	6q25	AR	E3 ligase
PARK3	2p13	AD	Not known
PARK4	4p15	AD	Not known
UCH-L1 (PARK5)	4p14	AD	Thiol protease
PINK1 (PARK6)	1p35	AR	Serine-threonine kinase
DJ-1 (PARK7)	1p36	AR	Oxidative stress sensor, chaperone
LRRK2 (PARK8)	12q12	AD	Serine-threonine kinase
ATP13A2 (PARK9)	1p36	AR	Lysosomal type 5 P-type ATPase
PARK10	1p32	AD	Not known
GIGYF2 (PARK11)	2q3	AD	Tyrosine kinase regulator
PARK12	Xq21-q25	AD	Not known
HTRA2 (PARK13)	2p12	AD	Serine-threonine protease

Table 1.1: List of gene associated with PD

Autosomal dominant (AD), Autosomal recessive (AR) (Henchcliffe and Beal 2008).

Follow up studies on these genes have, in most cases, been inconclusive (Lesage and Brice, 2012) although a probable association of PD was found with a point mutation in the UCH-L1 gene (I93M) (Leroy et al., 1998). The genes associated with the recessive form of PD include parkin (PARK2, an E3 ligase) (Kitada et al., 1998), Phosphatase and tensin homolog (PTEN)-induced kinase (PINK1/PARK6, a serine-threonine kinase) (Silvestri et al., 2005), DJ-1 (PARK7, an oxidative stress sensor and chaperone) (Bonifati et al., 2003) and the ATP13A2 (PARK9) (Ramirez et al., 2006) (**Table 1.1**).

Autosomal recessive juvenile Parkinsonism (ARJP) has an early age of onset, typically in late 20s and before 40. Almost half of the European families suffering from ARJP carry mutation in the *parkin* gene (Abbas et al., 1999; Kitada et al., 2000; Lucking et al., 2000; Kahle et al., 2000). ARJP is typically caused by loss-of-function of both the alleles of the *parkin* gene (Mizuno et al., 1998). More than 170 mutations associated with ARJP, including large deletions or multiplications of one or more exons, small deletions, small insertions, nonsense mutations and missense mutations have been reported for the *parkin* gene (Nuytemans et al., 2010). Functionally, parkin is an E3 enzyme that targets unwanted proteins to be degraded via the UPS, which may regulate the degradation and removal of more than 30% of proteins made in cell (Schubert et al., 2000). These parkin substrates have vital roles in cellular processes, including signalling, cell cycle, metabolism and immune response (Pagano, 1997, Ben-Neriah, 2002). Thus, the ubiquitin-mediated clearance of many neuronal proteins fails due to the loss-of-function mutations in parkin. These unwanted proteins aggregate in the cell causing toxicity, specifically in cellular compartments, including ER and mitochondria. Cellular toxicity also generates oxidative stress by excess ROS production, ultimately leading to neuronal cell death (Dev et al., 2003).

5.3 GWAS and Linkage studies in PD

Many linkage and genome-wide association studies (GWAS) have identified putative loci in the human genome that increase the susceptibility of PD under the influence of environmental factors (Lesage and Brice, 2012). A candidate gene approach identifying polymorphisms in genes via screening genetic data from a large number of patients has found nucleotide polymorphisms in the promoter region of α -synuclein to be associated with PD (Lesage and Brice, 2012). In addition, the microtubule associated protein tau (MAPT) has been found associated with the H1 haplotype, one of the two most common loci associated with progressive supranuclear palsy, AD and PD (Lesage and Brice, 2012). Two common variants in LRRK2 (G2385R and R1628P) have also been found to be associated with PD (Lesage and Brice, 2012) using linkage studies. The better validated genes linked

10,000 affected patients in Ireland (Healy et al., 2004). The typical clinical features of this disease are shaking muscle (tremor), muscular stiffness (rigidity) and slow movement of limbs (bradykinesia). In extreme cases, patients may become bedridden due to the complete loss of movement. In addition to physical symptoms, PD also gives rise to non-motor symptoms, including sleep disorder, psychosis, depression, dementia and autonomic disturbance. The cause of these clinical symptoms is the excessive loss of nerve cell function in the CNS, more specifically, excessive loss-of-function of dopaminergic neurons in SNPC region of the mid-brain. The eventual loss of dopaminergic neurons leads to reduction of nigrostriatal dopamine level and loss of motor function (Hornykiewicz, 1998; Hornykiewicz and Kish, 1987). Intriguingly, involvement of other non-dopaminergic neurons has been found to be associated with PD, including noradrenergic neurons present in the locus coeruleus, cholinergic neurons in the nucleus basalis of Meynert, and serotonergic neurons in the midline raphe (Forno, 1996).

5.2 Genetic forms of PD

The aetiology of PD is multifactorial and involves interplay between both genetic features and environmental effects. Broadly, PD can be divided into two subtypes, sporadic and genetic. Environmental factors linked to sporadic PD include exposure to toxins and free radicals, which are thought to cause damage via oxidative stress, mitochondrial dysfunction, excitotoxicity, lipid peroxidation, inflammatory changes, dysfunction in UPS and apoptosis. These processes are linked to the formation of ROS, such as superoxides and peroxides (Tanner, 1989; Beal, 2000; Jenner and Olanow, 1996). In contrast to sporadic PD, a relatively small amount of PD patients are identified as familial/genetically inherited. Genetic inheritance is found in 5%-10% of PD patients with linkage to 11 different genes, suggesting most of the patients develop PD sporadically (more than 90%) (Hardy et al., 2006; Klein et al., 2007; Lesage and Brice, 2012).

In familial PD, both autosomal dominant and recessive types of inheritance have been identified. The genes reported, and well accepted, to be responsible for causing dominant form of PD upon mutation are α -synuclein (PARK1) (Polymeropoulos et al., 1997; Kruger et al., 1998) and leucine-rich repeat kinase 2 (LRRK2/PARK8, serine protease) (West et al., 2005). In addition, some other genes are thought to be associated with dominant PD, such as ubiquitin-C terminal hydrolase L1 (UCH-L1/PARK5, thiol protease), growth factor receptor-bound protein 10 (GRB10) interacting glycine-tyrosine-phenylalanine (GYF) protein 2 (GIGYF2/PARK11, tyrosine kinase regulator) (Pankratz et al., 2002), high temperature requirement protein A2 (HTRA2/PARK13, serine-threonine protease) (Moisoi et al., 2009).

depolarization in synaptosomes, three methods are employed including KCl elevation, Na⁺ channel activation and K⁺ channel inhibition (Nicholls, 1993).

1. KCl elevation: In a non-depolarized state, K⁺ resides in a higher concentration in synaptosomes, creating an ionic gradient of K⁺ (inside vs. outside) across the synaptosomal membrane. Elevation of KCl concentration outside the synaptosomes reverses the ionic gradient of K⁺ that ultimately leads to depolarization of the synaptosomal membrane and causes glutamate release (Nicholls, 1993).

2. Na⁺ channel activation: Unlike K⁺, the concentration of Na⁺ is lower in synaptosomes, which creates an ionic gradient of Na⁺ (outside vs. inside) across the synaptosomal membrane. In a non-depolarized state, the Na⁺ channels are momentarily activated and then remain in an inactivated state in the presence of tetrodotoxin, which impairs respiration and lowers Ca²⁺ concentration (Kauppinen et al 1986; Tibbs et al., 1989). The effect of tetrodotoxin can be altered by addition of veratridine which keeps the Na⁺ channels open. As a result, the Na⁺ electrochemical potential across the membrane collapses, resulting synaptosomal depolarization-induced glutamate release (Nicholls, 1993).

3. K⁺ channel inhibition: In this method, the K⁺ channels present on the synaptosomes are targeted. Under the depolarization current, K⁺ channels fire in a transient, rapidly inactivating manner to repolarize the synaptosomal membrane (Bartschat and Blaustein, 1985; Tibbs et al., 1989). Inactivation of K⁺ channels can be prevented by the addition of 4-amino pyridine (4-AP) or dendrotoxin, which simulates an 'epileptic action potential', causing spontaneous repetitive firing of Na⁺ channels (Agoston et al., 1983; Tibbs et al., 1989). Thus, 4-AP simulates an action potential-like event making it a valuable tool to study pre-synaptic regulation (Nicholls, 1993).

5. Parkinson's Disease

5.1 Introduction

Parkinson's disease (PD) is the second most common neurodegenerative disease, which occurs due to genetic mutations, environmental insults or a cumulative effect of both. Approximately, 0.3% of world population suffers from this disease. Roughly, 1-2% of people over the age of 65 and 4% more than 80 years suffer from PD (de Lau, 2006), with almost

ion gradients and neurotransmitter release (Nicholls, 1993).

Synaptosomes consume glucose in both aerobic and anaerobic respiration and also pyruvate during oxidative metabolism (Kauppinen and Nicholls, 1986). High levels of glycolysis driven ATP synthesis can take place in synaptosomes aerobically. Inhibition in the mitochondrial ATP synthesis by anoxia can trigger an anaerobic mode of respiration (Kauppinen and Nicholls, 1986). In an anaerobic mode, the glucose content can be exhausted at a very high rate (10 fold) within synaptosomes in order to maintain normal ATP production (Kauppinen and Nicholls, 1986). In an intact synaptosomal preparation, under low K^+ and Ca^{2+} (0.1-0.2 μM) concentration medium, synaptosomes maintain a plasma membrane potential of -60 to -80 mV (Ashley et al., 1984; Nachshen, 1985; Verhage et al., 1988; Kauppinen et al., 1988).

4.1 Cytosolic and vesicular glutamate release by synaptosomes

Glutamate is found in the cytosol of neurons in high concentration, approximately 10 mM in glutamatergic neurons (Hansson et al., 2000). In synaptosomes, under resting conditions, the extra and intracellular glutamate levels maintain equilibrium by continuous glutamate leakage from the cytosol, balanced by a high-affinity glutamate uptake mechanism (Bradford et al., 1987). The glutamate uptake mechanism takes place through a Na^+ -coupled pump that allows positively charged Na^+ influx along with glutamate uptake, maintaining a thermodynamic equilibrium across the synaptosomal membrane (Nicholls, 1993). Under a depolarising condition, this equilibrium is disturbed and a slow but prolonged leakage of cytosolic glutamate takes place, which is independent of ATP, Ca^{2+} concentration and vesicle-mediated glutamate release from synaptosomes (Nicholls et al., 1987; Nicholls, 1993). Aspartate is also known to release along with glutamate and considered as an indicator of cytosolic neurotransmitter leakage (McMohan et al., 1990). Ca^{2+} -independent cytosolic glutamate release is inhibited by botulinum neurotoxin Type A and B in synaptosomes (Sanchez-Prieto et al., 1987; McMahan et al., 1992). In contrast to cytosolic glutamate leakage, Ca^{2+} has a crucial role to play in synaptic vesicle-mediated neurotransmitter release, where Ca^{2+} is required for the fusion of synaptic vesicles with the pre-synaptic membrane to release neurotransmitters. The details of vesicular glutamate release are described in section 2.1.

4.2 Depolarization of synaptosomes

Due to the absence of a neuronal structure in the synaptosomal preparation, there is no provision to excite a synaptosome by an axon driven action potential. To cause

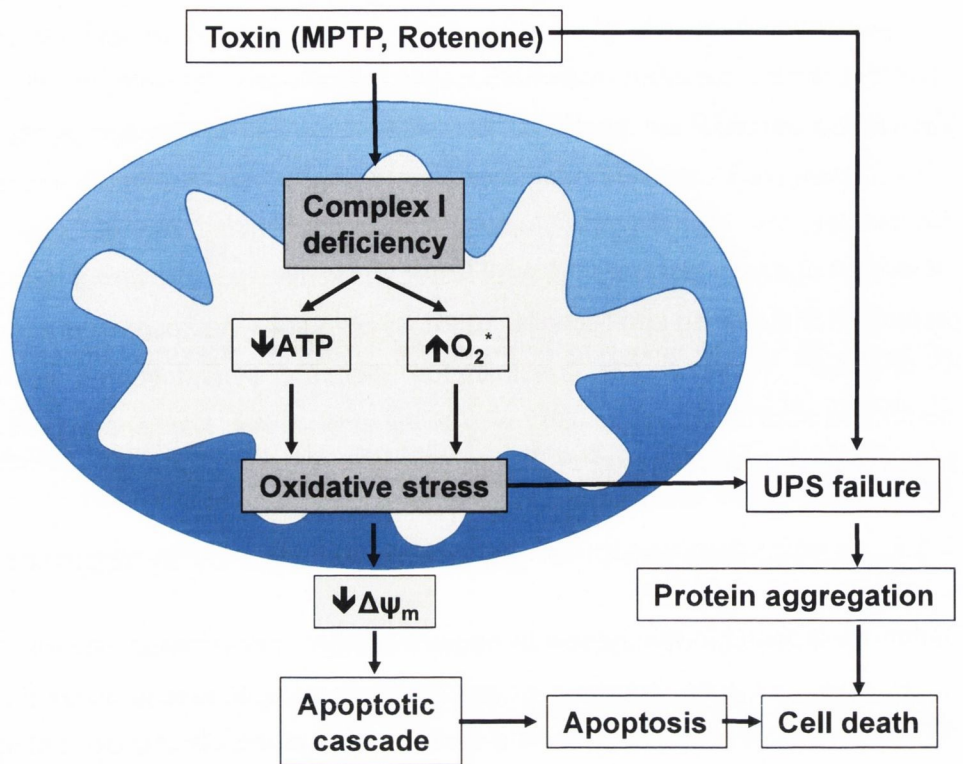


Figure 1.3: Pathways of mitochondrial dysfunction

Mitochondrial dysfunction triggered by toxins, including MPTP and rotenone, hamper complex I activity in the ETC, inducing the production of ROS (O_2^*) and reducing ATP production. Oxidative stress can reduce mitochondrial membrane potential ($\Delta\psi_m$) and causes failure of the UPS. Failure of mitochondria leads to increased protein aggregation, apoptosis and cell death (Schapira, 2008).

(Henchcliffe and Beal, 2008). Normally ROS, produced as a byproduct of oxidative phosphorylation, is converted to water by antioxidant enzymes including superoxide dismutase (SOD), catalase, glutathione peroxidase (Murphy, 2009; Galley, 2011). However, in the case of mitochondrial dysfunction, an overwhelming amount of ROS is produced to an extent where antioxidant enzymes fail to regulate intracellular ROS concentration (Perry et al 1996; Galley, 2011). The lack of removal of peroxides and superoxides leads to oxidative stress-induced damage in lipids, proteins, RNA and DNA in PD patients (Dexter et al., 1989; Zhang et al., 1999).

Oxidative stress and depleted ATP production also hampers the mitochondrial membrane potential. A fall in the mitochondrial membrane potential is thought to be one of the initial indicators of impending apoptosis in neurons (Nicholls and Ward, 2000). Moreover, age-related decreases in the membrane potential of brain mitochondria have been reported by several groups (Joyce et al. 2003; Navarro and Boveris, 2007; Boveris and Navarro, 2008). The depolarization of mitochondria below a threshold level induces apoptosis by releasing mitochondrial Ca^{2+} and death signals, such as Bcl-2-associated X (Bax), cytochrome C and other pro-apoptotic factors, including pro-caspases and caspases into the cytoplasm through mtPTPs (Nicholls and Budd, 2000; Green and Kroemer, 2004). In addition, mitochondrial dysfunction and oxidative stress also play a role in the accumulation of unwanted proteins by hampering the ubiquitin proteasomal system (UPS) pathway, leading to cellular toxicity (Henchcliffe and Beal, 2008). Taken together, mitochondrial dysfunction can be identified by detecting changes in various properties including activity of the ETC cycle complexes, increased production of ROS and change in the mitochondrial membrane potential (**Figure 1.3**).

4. Synaptosomes

Studies using synaptosomal preparations have been important in understanding mitochondrial biology and mechanisms of pre-synaptic glutamate release. In simple terms, synaptosomes are isolated nerve terminals where a typical synaptosome measures around 0.5-1 μm in diameter. Importantly, these synaptosomes contain mitochondria and synaptic vesicles with little or no part of the ER or nucleus (Nicholls, 1993) that makes it ideal for studying mitochondrial functions including activity of ETC, production of ROS, and change in the mitochondrial membrane potential. Isolated synaptosomes can also be used to study synaptic transmission, as all the required machineries for uptake, storage and exocytotic release of neurotransmitters are present. An additional advantage of synaptosomes is that, after extraction, they can be stored on ice for approximately 6 h without loss in ATP levels,

mitochondria thus have a number of vital physiological roles including influencing aerobic ATP production, neurotransmitter release, synaptic transmission, excitability, regulation of organelle dynamics and trafficking, nuclear signalling, regulation of ROS and apoptosis (Duchen, 2004; Nicholls, 2005; Mattson et al., 2008; Starkov, 2010; Chinopoulos and Adam-Vizi, 2010;).

In addition to these Ca^{2+} transporters, the third Ca^{2+} channel present on mitochondria is a voltage and Ca^{2+} -dependent high conductance channel, named a mitochondrial permeability transition pore (mtPTP). The mtPTP was first identified by Hunter and Haworth (1979) and thought to form contact sites between the inner and outer mitochondrial membrane. The composition of mtPTP is still not well established, however, data suggest a putative multi-protein composition including a voltage-dependent anion channel (VDAC), members of the pro and anti-apoptotic protein family, cyclophilin D and the adenine nucleotide (ADP/ATP) translocators (ANTs) (Zoratti and Szabo, 1995; Marzo et al., 1998). In case of Ca^{2+} overload in neuronal mitochondria, the mtPTPs are formed, through which the Ca^{2+} content and pro-apoptotic proteins of mitochondria are released into cytosol (Bernardi et al., 2006). In addition, mtPTPs can also form due to fall of the mitochondrial membrane potential and swelling of the mitochondrial matrix (Bernardi et al., 2006). The induction of mtPTP leading to apoptosis and neurodegeneration is thought to play a role in ischemic brain injury and neurodegenerative diseases including PD, AD and HD (Bezprozvanny, 2009). In addition, the absence of ANT components of mtPTPs, responsible for regulating pore opening, has been found to be susceptible to glutamate-induced excitotoxicity (Lee et al., 2009). Taken together, Ca^{2+} sequestration by mitochondria has an important role to play in the cellular physiology and the loss of mitochondrial Ca^{2+} homeostasis has direct implications in neuronal excitotoxicity and apoptosis.

3.3 Mitochondrial dysfunction

Mitochondrial dysfunction, that is the malfunctioning of the mitochondrial complexes and membrane potential, is often induced by cellular stress and leads to cellular toxicity particularly in neurodegenerative diseases including PD, AD, HD and ALS (Bezprozvanny, 2009; Gibson, 2010; Beal, 2007). Specifically for PD, analysis of tissues derived from the SNPC (Schapira et al., 1990) and frontal cortex areas (Parker et al., 2008) of PD patients revealed mitochondrial dysfunction with hampered complex I respiratory chain and reduced electron transfer efficiency through complex I, which ultimately compromise oxidative phosphorylation (Keeney et al., 2006). This hampered oxidative phosphorylation leads to a reduction in ATP production and Ca^{2+} homeostasis, which triggers ROS production

membrane responsible for creating an electrochemical gradient of protons across the membrane known as proton motive force (Nicholls and Budd, 2000). By using the proton motive force, ATP synthase (EC 3.6.3.14) produces ATP from ADP and a phosphate group. Of note, ATP synthase is also often called complex V. The passage of three protons through complex V into the mitochondrial matrix results in the generation of one ATP molecule.

3.2 Mitochondrial calcium sequestration

Along with ATP production by oxidative phosphorylation, mitochondria have an important role to play in the Ca^{2+} homeostasis, especially in neurons and in Ca^{2+} signalling in other cell types (Berridge, 1998). After endoplasmic reticulum (ER), the mitochondria harbor the highest amount of Ca^{2+} in the neuronal cells. The total Ca^{2+} content of a neuronal cell is found in two states, free Ca^{2+} and protein bound (Pivovarova et al., 2010). The total Ca^{2+} content of a neuron in resting state is 1 mM, in which 99.9% of Ca^{2+} is associated to cytosolic proteins or sequestered inside ER and mitochondria. Therefore, upon receiving a stimulus, a global rise of Ca^{2+} can take place from 100 nM (resting phase) to 1 μM (stimulated phase) in neurons (Meldolesi and Pozzan, 1998; Pozzan and Rizzuto, 2000). In the case of mitochondria, a low amount of total (0.1 mM) and free Ca^{2+} (100 nM) concentration is found in resting neurons (Pozzo-Miller et al., 1997; Babcock and Hille, 1997), which drastically increases after stimulation of the neuron (Pivovarova et al., 1999; Montero et al., 2000). This unique property of Ca^{2+} sequestration makes mitochondria an important player in various processes, including synaptic transmission and Ca^{2+} homeostasis.

Mitochondria have three ion channels present on their outer membrane responsible for influx and efflux of Ca^{2+} . The first of these channels is a group of Ca^{2+} -dependent voltage gated uniporter ion channels, which open in the presence of high concentrations of cytosolic Ca^{2+} to transport excess Ca^{2+} into the mitochondrial matrix (Nicholls and Budd, 2000; Gunter and Sheu, 2009). The second type of Ca^{2+} transporters found to be present on the mitochondrial surface is a group of $\text{Na}^+/\text{Ca}^{2+}$ exchangers, which is responsible for the efflux of Ca^{2+} from mitochondria to the cytosol (Crompton et al., 1978). These two mitochondrial transporters establish together a slow and continuous cycling of Ca^{2+} across the inner membrane driven by the respiratory chain expulsion of H^+ ; and maintain the normal mitochondrial potential (Crompton et al., 1978; Crompton and Heid, 1978). The rate of mitochondrial uptake of Ca^{2+} is always found to be higher than the rate of release into cytosol during the resting phase, so that, after an action potential-evoked Ca^{2+} release into the cytosol, mitochondria sequester Ca^{2+} to return levels to the resting phase (Nicholls, 2005). Sequestered Ca^{2+} present in

Williams, 1956). It specifically hampers the process of electron transfer from iron-sulphur centres of complex I to ubiquinol (Sherer et al., 2003). This blockade reduces the ATP production by interfering with NADP and as a result high amounts of peroxide are produced (Sipos et al., 2003).

B. Complex II: Complex II (Succinate: quinone oxidoreductase, EC 1.3.5.1), catalyses the oxidation of FADH_2 to FAD^+ (flavin adenine dinucleotide), and also functions as a component of the citric acid cycle. Both complex I and complex II can reduce ubiquinol/ubiquinone, donating electrons to complex III. An arginine residue (A297) of complex II acts as a base catalyst for accepting protons during dehydrogenation of succinate (Huang et al., 2006). A plant and fungal toxin, 3-nitropropionic acid can block complex II by irreversibly binding to A297 to form a complex with the side chain of A297 (Huang et al., 2006).

C. Complex III: Complex III (QH₂: cytochrome c oxidoreductase, EC 1.10.2.2), mediates another four protons to pass from the matrix to the intermembrane space. Cytochrome C is reduced by complex III at a redox potential of approximately +250 mV and donates the electrons to complex IV. Antimycin A is a specific inhibitor of the Qi site of complex III that blocks the oxidation of ubiquinol. This inhibition disrupts oxidative phosphorylation by disturbing the proton gradient across the inner membrane. Consequently, the absence of a proton gradient causes unavailability of protons through the ATP synthase complex that ultimately leads to ATP depletion. This inhibition also leads to the production of highly toxic reactive oxygen species (ROS), including peroxides and superoxides (Turrens et al., 2003). In addition, antimycin A induces mitochondrial swelling and mitochondrial depolarization (Sipos et al., 2003).

D. Complex IV: Complex IV (ferrocycytochrome C: oxygen oxidoreductase, EC 1.9.3.1), converts one O_2 molecule to two H_2O molecules from four electrons supplied by reduced cytochrome C (one electron from each cytochrome C molecule). In this process, 4 protons are used from the mitochondrial matrix resulting in a proton electrochemical gradient between matrix and inner membrane space. This electrochemical gradient is used by the ATP synthase to produce ATP. Many molecules, including cyanide, sulfide, azide and carbon monoxide, act as specific inhibitors of the complex IV.

Together these four complexes are called supercomplexes, as they are thought to function together. These supercomplexes are present abundantly in the inner mitochondrial

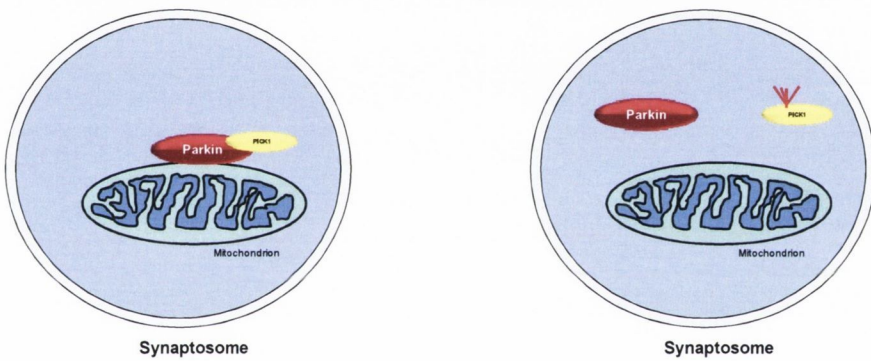
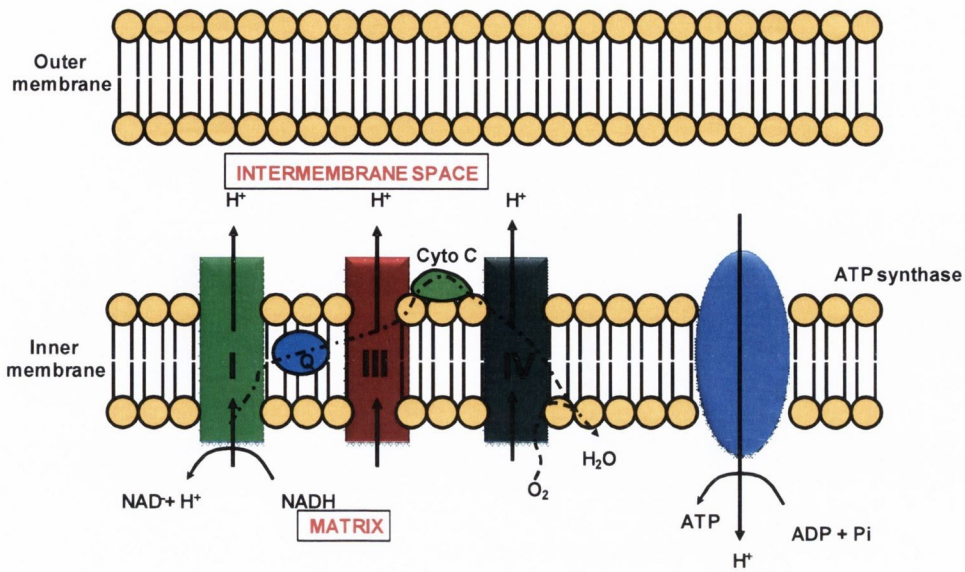


Figure 1.11: Working hypothesis of the project

Studies show that parkin and PICK1 are involved with mitochondrial maintenance. However, the role of parkin-PICK1 in mitochondrial maintenance remains unclear. According to our hypothesis, PICK1 may be involved in the trafficking of parkin to the mitochondrial membrane, thus regulating parkin-mediated mitochondrial effects. We believe that hindrance in parkin-PICK1 interaction may have adverse effect in mitochondrial maintenance.

2. Materials and Methods

Materials and equipment used

The following materials were used: LB media (L3152-1KG, Sigma); MgSO₄ (M2643-500G, Sigma); CaCl₂ (C3306-100G, Sigma); Glycerol (G5516-100ML); Mini-preparation kit (27106, Qiagen); Tryptone (J859-500G, Amresco); Yeast extract (J850-500G, Amresco); NaCl (S3014-500G, Sigma); Ampicillin (A9518, Sigma); Arabinose (A3256-25G, Sigma); IPTG (15502-1G, Sigma); SB buffer (161-0737, Bio-Rad); Triton X-100 (P9284-500ML, Sigma Aldrich); EDTA (A3156-5G, Sigma); GST beads (17-0756-01, GE); BSA (A3156-5G, Sigma); HEPES (H3784-100G); EGTA (E3889-25G, Sigma); Tris (0497-1KG, Amresco); SDS (L4390-25G, Sigma); APS (A3678-25G, Sigma); TEMED (T7024-25ML, Sigma); β-mercaptoethanol (31350-010, Gibco); PVDF membrane (Poly Vinylidene Difluoride Membrane, P2938, Sigma); Sucrose (84097, Fluka); Methanol (34966-2.5lt, Sigma); ε-amino capronic acid (A7824-25G, Sigma); Whatman papers (grade 3, 1003-917, Whatman); Non-fat milk (Marvel); Tween-20 (P7949-500ML); BCIP and NBT (S3771, Promega); EcoRI (10703737001, Roche); BamHI (10220612001, Roche); Pfu buffer and enzyme (15224-017, Invitrogen); dNTP (10226020, Roche); Polyacrylamide (161-0158, Bio-Rad); Phenol/Chloroform/Isoamyl alcohol (P3803-400ML, Sigma); Ethanol (E7023-500ML, Sigma Aldrich); TE (T9285-100ml, Sigma); Agarose (A6013-100G, Sigma); Gel extraction kit (28704, Qiagen); T4 ligase kit (15224-017, Invitrogen); MegaX DH10B T1 Electrocomp cells (C6400-03, Invitrogen); DMEM high-glucose media (L0104-500, Biosera); FCS (F2442-100ML, Sigma); Penicillin/streptomycin (15140-122, Gibco); Calcium phosphate (C7263, Sigma); PBS (20012-019, Gibco); Anti-GST (27-4577-50, GE); Peptides (Peptide 2.0, USA and Genscript, USA) Whatman paper (Schleicher and Schuell); Lipofectamine (18324, Invitrogen); Ficoll (F4375-100G, Sigma); Cytochrome C (C2037, Sigma); Sodium L-ascorbate (A4034, Sigma); Potassium Ferricyanide (P8131, Sigma); KCN (60178, Sigma); NADH (N8129, Sigma); Decyl Q (D7911, Sigma); Rotenone (R8875, Sigma); JC-1 (T3168, Biosciences); Amplex Red (A12222, Biosciences); Horseradish peroxidase P8250, Biosciences); Succinate (S9637, Sigma); Antimycin A (A8674, Sigma); Poly-L lysine (P1399, Sigma Aldrich, UK); Borosilicate glass coverslips 13mm (361-0149, VWR Ireland);

The following equipment was used: Incubator (Binder, Mason Technologies); Shaker (Excella E24 Incubator, New Brunswick Scientific); Spectrophotometer (Biophotometer, Eppendorf); UV transilluminator (Syngene); Powerpack (Biorad); Electroporator (Biorad); 50 ml centrifuge (Hettich Rotina 380R); Heating block (Grant); Tabletop centrifuge (Hermle); Ultracentrifuge (Discovery 100, Sorvell); Platereader Spectramax Gemini XS; PCR machine (Applied Biosys); Water bath (UAB 12 EU Grant); Sonicator (Sonics, Vibra-cell); Glass teflon homogeniser (Fisher).

Animals used in this thesis

Wildtype female Wistar rats (aged 6 weeks and/or weighed 150-200 g) were used in the preparation of synaptosome from rat brain. During the preparation of synaptosomes, they were sacrificed according to the guidelines prescribed by the Animals Act 1986 (Scientific Procedures) Schedule I. These rats were reared and supplied by the Bioresources Unit, School of Biochemistry and Immunology, Trinity College Dublin. For cortical neuronal culture and astrocyte culture, postnatal one day old female Wistar rats were sacrificed humanely (supplied by the Bioresources Unit, Trinity College Dublin).

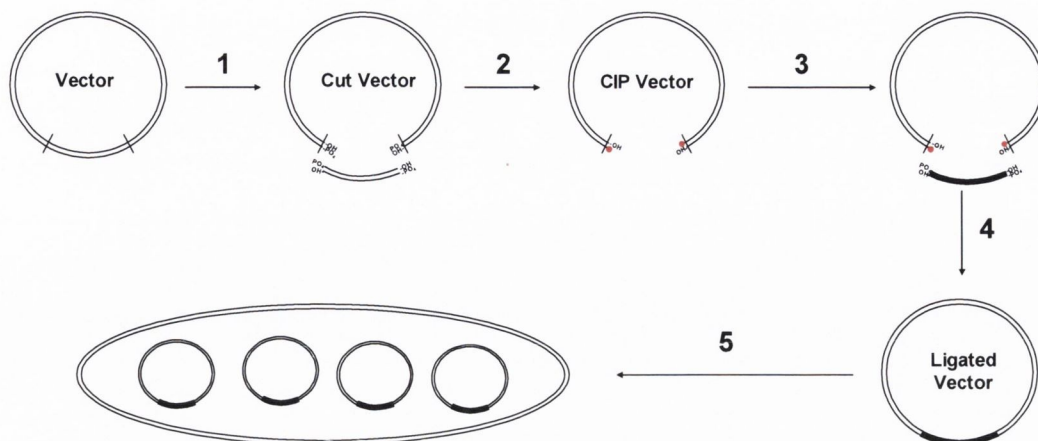
1. Molecular biology methods

1.1 General molecular cloning strategies

Molecular cloning is a useful tool to modify the gene composition of a circular DNA (plasmid) by inserting any gene of interest and express the gene of interest in any system of cells. In this project, various cloning experiments were undertaken to construct plasmids carrying gene of interest for yeast two hybrid assay, mammalian cell transfection and lentiviral-mediated transfection. **Figure 2.1** indicates the basic cloning steps and each step is elaborated below.

1.2 Bacterial competent cell preparation

Luria Bertani (LB) media was prepared for bacterial cell growth. *Escherichia coli* (*E. Coli*) was grown on LB plate overnight at 37°C incubator. A single colony was used to inoculate 5 ml LB medium with continuous shaking at 200 rpm overnight at 37°C in incubator. Thereafter, 2-3 ml of overnight grown bacterial culture was transferred into 100-200 ml of LB and incubated with continuous shaking at 200 rpm for 2-3 h at 37°C to reach an OD⁶⁰⁰ of 0.6-1. The 200 ml sample was divided into 4 cell culture tubes of 50 ml and centrifuged at 3,000 xg for 15 min at 4°C. The bacterial pellet was resuspended thoroughly in ice-cold 20 ml 100 mM MgSO₄ and centrifuged 3,000 xg for 15 min at 4°C. The pellet was again resuspended in ice-cold 2 ml of 100 mM CaCl₂ with 15% glycerol. The bacterial solution was aliquoted by 50 µl in pre-cooled 1.5 ml tubes and snap-chilled in liquid nitrogen. The tubes were finally stored in -80°C until further use.



1. Restriction digestion
2. Dephosphorylation
3. Purification
4. Ligation
5. Transformation

Figure 2.1: Cloning strategy

The cloning steps are shown in roughly 5 steps. (1) Double restriction digestion of vector and the insert by two restriction enzymes to generate sticky ends. (2) Dephosphorylation of vector to remove the flanking phosphate group from the 5' end to save it from self-ligation. (3) Purification of cut vector and cut insert from undigested fraction. (4) Ligation of insert into the vector through compatible flanking sites. (5) Transformation of the ligated vector into competent *E. coli* to increase copy number.

1.3 Heat shock transformation and plasmid DNA extraction from bacteria

Heat shock method of transformation was used to obtain recombinant bacterial colonies. Two *E. coli* strains were used for transformation, DH5 α to yield plasmid DNA and BL21 AI to express recombinant protein. Tubes containing competent cells were thawed on ice for 15-20 min. Next, 1-2 μ g of plasmid DNA was mixed with 50 μ l of competent bacteria and incubated on ice for 15 min. Heat shock was applied for 60-90 sec by placing the tube at 42°C in a water bath/heating block and immediately transferred in ice for 10 min. To recover the cells, 1 ml LB was added to the transformed bacteria and incubated with continuous shaking at 200 rpm for 60-90 min at 37°C. The cells were centrifuged at 3,000 \times g for 2-3 min. The pellet was re-suspended in 200 μ l LB and spread on pre-warmed LB amp or kan agar plates. Plates were kept for incubation at 37°C. Colonies were counted after 8-12 h. A single colony was used to inoculate in 5 ml of LB medium and left overnight with continuous shaking at 200 rpm. The plasmid DNA was extracted from the bacterial culture by using mini-preparation kit, according to manufacturer's recommendation (Qiagen).

1.4 Polymerase Chain Reaction and restriction digestion

The components, used in polymerase chain reaction (PCR) to amplify DNA, were 2 μ g DNA template, 1x Pfu buffer, primers (10 pmol/ μ l), dNTP (200 μ M) and 1 U of high-fidelity Pfu DNA polymerase in a 25 μ l reaction. After the initial denaturation temperature (94°C for 5 min), the PCR reaction cycle was programmed as follows: denaturation (94°C for 30 sec), annealing (66°C for 30 sec) and elongation (72°C for 30 sec). This cycle was repeated 30 times to achieve the desired amplification. Before ending the reaction, the elongation temperature was maintained for 10 min at the end of 30th cycle. The sample is then stored at -20°C until further use. The restriction digestion was performed in a reaction volume of 25 μ l. In this step, 2 μ g of DNA was incubated with 1 U of restriction enzyme and 1x appropriate buffer at 37°C for 1.5 h. The primers used in this project are enlisted in **Table 2.1**.

1.5 Phenol/Chloroform/Isoamyl alcohol (PCI) purification

Phenol/chloroform/isoamyl alcohol was used to purify DNA to remove protein traces. DNA was treated with equal volume of phenol/chloroform/isoamyl alcohol (PCI), vortexed well and centrifuged at 13,000 \times g for 10 min. After centrifugation, the liquid part divided into two layers, including upper aqueous and lower phenolic. The upper aqueous layer with DNA was collected, leaving behind the phenolic layer with the degraded protein fraction. The aqueous

Oligoname	Sequence
Cdc4Frag1_F	5'- TTGAATTCGTGTGGCGGATCAGAGCC -3'
Cdc4Frag3_R	5'- CGGGATCCGTCACCTTCATGTCCACATCAAA -3'
HA-park-AscI_F	5'- CGGCGCGCCATGGCTTACCCAT -3
HA-park-RsrII_R1	5'- CGGTCCGCTACACGTCGAACCA -3
HA-park-Δpdz_R	5'- CGGTCCGCTACCAGTGGTCCC -3'

Table 2.1: List of primers

These primers were used to PCR amplify the deletion constructs of Cdc4α-ct (pGBKT7), HA-Parkin (pLenti-PGK) and HA-ParkinΔpdz (pLenti-PGK).

layer was treated with ice-cold absolute ethanol to precipitate the DNA. The DNA pellet was formed upon centrifugation at 13,000 xg for 15 min at 4°C. The DNA pellet was air dried for 2-3 h and dissolved in 10 µl sterile water.

1.6 DNA gel extraction

To recover small fragments of DNA (below 100 bp), 12% polyacrylamide gel was used. The DNA-PAGE gel was made with 0.8 mg/ml APS and 0.1% TEMED in TBE (40 mM Tris-borate and 1 mM EDTA) buffer. The DNA was separated using constant 70 V for 1 h. After separation, the DNA bands were cut out under UV light. The DNA was recovered from the polyacrylamide using a crush and elute process. The gel pieces containing the DNA were transferred to a small 500 µl Eppendorf tube with a pin-hole made in the bottom. The small Eppendorf tube was placed inside 1.5 ml Eppendorf tube and centrifuged at 13,000 xg for 3 min. Next, 200 µl of TE buffer (10 mM Tris-HCl, pH 8; 1 mM EDTA) was added to the crushed gel in the 1.5 ml Eppendorf tube and vortexed well. The tube was incubated overnight at 37°C to elute the DNA from the gel. After overnight incubation, the tube was vortexed, centrifuged at 13,000 xg for 3 min and 200 µl TE buffer was transferred to a second tube. The process of vortex and centrifugation was repeated after adding another 200 µl of TE to the small tube. At the end, the total 350 µl eluted DNA was purified by phenol/chloroform/isoamyl alcohol. Finally, the DNA pellet was resuspended in 10 µl of TE buffer and stored at -20°C until further use. To recover larger DNA fragments 1-2% agarose gel was used. The gel was run under constant 100 V for 30 min and DNA was extracted using gel extraction kit described by manufacturer (Qiagen).

1.7 Dephosphorylation and ligation

To restrict self-ligation, restriction digested vectors were dephosphorylated, i.e., removal of 5' phosphate group. Restriction digested vector DNA was dephosphorylated by incubating in 1x CIP buffer and 1 U of phosphatase enzyme at 37°C for 1 h. After dephosphorylation, the vector was separated in 2% agarose gel and rescued using gel extraction kit. Ligation reaction was made by adding restriction digested gene insert and vector in 3:1 ratio. The ligation reaction was performed with T4 ligase kit. To ligate 210 ng of insert with 70 ng of cut vector, 1x ligation buffer and 1 U of T4 DNA ligase (total volume of 20 µl) were used. The ligation mixture was incubated overnight at 16°C. After ligation, 2 µl of ligation mixture was used to transform 20 µl electro-competent cells by electroporation (2 kV, 200 Ω, 25 µF). The transformed cells were incubated in 1 ml of SOC medium for 1.5 h. The bacterial cells were centrifuged and pellet was resuspended in 200 µl LB (with kan or amp). The 200 µl cells were plated in respective kan or amp selective LB agar plates. Colonies, found after over-

night incubation, were inoculated in 5 ml of LB media at continuous shaking at 200 rpm for overnight at 37°C. The plasmid DNA was extracted using mini-preparation kit (Qiagen). Each sample was examined by PCR and restriction digestion to investigate the cloned insert. For further verification of the successful cloning, recombinant plasmids were sent for DNA sequencing in Eurofins MWG Operon.

2. Yeast two hybrid methods

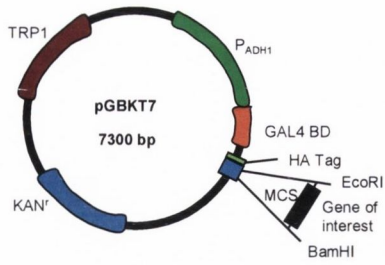
2.1 Competent yeast preparation

Yeast strain *Saccharomyces cerevisiae* AH109 (630444, Clontech) was streaked onto a fresh YPAD-amp plate (1% bacto-yeast extract, 2% peptone, 0.1 mg/ml adenine, 2% agar and supplemented with 2% D-glucose and 50 mg/ml amp) and incubated for 2 days at 30°C. A single colony of 2-3 mm in diameter was re-streaked onto a fresh YPAD-amp plate and incubated for 2 days at 30°C. Thereafter, the single colony was inoculated in 10 ml YPAD media in a 50 ml falcon tube and incubated overnight with shaking at 200 rpm at 30°C. The culture was diluted to an OD⁶⁰⁰ 0.2-0.4 in 50 ml of YPAD media and incubated at 200 rpm shaking for 2-6 h at 30°C in 1 lt baffled flask the until OD⁶⁰⁰ reached 0.8-1. The yeast cells were centrifuged at 1,000 xg for 3 min at 4°C. The pellet was re-suspended in 1 ml TE and centrifuged at 1,000 xg for 3 min. Next, the pellet was re-suspended in 2 ml of LiOAc solution (10mM LiOAc in TE) and then incubated at room temperature for 10 min.

2.2 Yeast transformation

To transform competent yeast, 1 µg plasmid BAIT cDNA pGBKT7 vector (**Figure 2.2A**), 1 µg plasmid FISH cDNA (pGADT7 vector) (**Figure 2.2B**) and 1 mg/ml denatured herring testes carrier sperm DNA were mixed with 100 µl competent AH109. To determine protein interactions as well as efficiency of the transformation, controls were included. Next, 700 µl of PEG solution (100 mM LiOAc; 40% PEG in TE buffer, pH 8) was added and thoroughly mixed to evenly distribute the cells. The samples were then incubated in shaker at 200-250 rpm for 30 min at 30°C. After incubation, 88 µl of dimethyl sulfoxide (DMSO) was added to the tubes and mixed well. Heat shock was administered for 7 min at 42°C in a water bath. The samples were centrifuged for at 1,000 xg for 10 sec and the pellets were re-suspended in 1 ml TE. The samples were again centrifuged at 1,000 xg for 10 sec and re-suspended in 50 µl TE. The transformed AH109 was then spread onto minimal supplement deficient agar base plates {46.7 g drop out (DO) media, pH 5.8} supplemented with 50 mg/ml amp with addition of BAIT supplement (0.74 g DO/-W), FISH supplement (0.69 g DO/-L), BAIT-FISH

A)

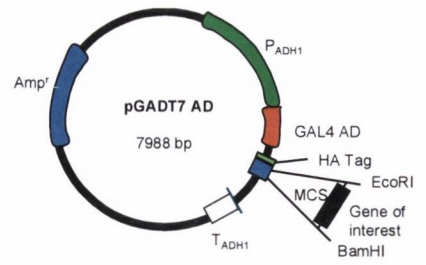


```

CAT ATG GCC ATG GAG GCC AGT GAA TTC CAC CCG GGT GGG CAT CCA TAC GGG ATC CAT
  |   |   |   |   |   |   |   |   |   |   |   |   |   |   |   |   |   |
  KpnI  SbfI  EcoRI  XbaI  XbaI  XbaI  XbaI  XbaI  XbaI  XbaI  XbaI  XbaI  XbaI
                                     |
                                     STOP
05A GCT CBA GCT GCA BATGAATCGTATGATACTGAAAAACCCCAAGTTCACTTC
  |   |   |   |   |   |   |   |   |   |   |   |   |   |   |   |   |
  XbaI  XbaI  XbaI  XbaI  XbaI  XbaI  XbaI  XbaI  XbaI  XbaI  XbaI  XbaI  XbaI
  
```

Mechanistic 7' AD LP Insert Screening Amplifier

B)



```

CAT ATG GCC ATG GAG GCC GAA TTC CCG GGG ATC GGT CCA CCT GCA GCG GCC GCA
  |   |   |   |   |   |   |   |   |   |   |   |   |   |   |   |   |   |
  KpnI  SbfI  EcoRI  XbaI  XbaI  XbaI  XbaI  XbaI  XbaI  XbaI  XbaI  XbaI  XbaI
                                     |
                                     STOP
05A GCT CBA GCT GCA BATGAATCGTATGATACTGAAAAACCCCAAGTTCACTTC
  |   |   |   |   |   |   |   |   |   |   |   |   |   |   |   |   |   |
  XbaI  XbaI  XbaI  XbaI  XbaI  XbaI  XbaI  XbaI  XbaI  XbaI  XbaI  XbaI  XbaI
  
```

T7 Terminator

Figure 2.2: Yeast plasmid vectors

As yeast two hybrid plasmids, A) pGBKT7 BD and B) pGADT7 AD were used, which contain kan and amp resistant genes, respectively.

(0.64 g DO/-W/-L supplement) and INTERACTION supplement (0.6 g DO/-W/-L/-H). The plates were left for 7 days at 30°C and the β -galactosidase assay was used to determine positive BAIT-FISH interaction.

2.3 Interaction plate assay

Interaction between two proteins was evaluated using interaction plate assay. Yeast colonies grown on BAIT/FISH plates were picked up, dissolved in 100 μ l TE buffer and 5 μ l of yeast solution is dropped onto interaction plate. Thereafter, 10 μ l of yeast solution is diluted in 90 μ l of TE and 5 μ l of diluted sample was dropped onto interaction plate. From each yeast plate, 5 colonies were collected and plated onto interaction plate. Plates were then incubated for 24-48 h at 30°C. Growth in both dilutions indicates a positive interaction. Empty vectors, pGBKT7-pGADT7, were used as a negative control and GluR2-PICK1 as positive control in every yeast two hybrid assay.

3. Cellular protein expression methods

3.1 Protein expression in bacterial cell

A single colony of recombinant bacteria was inoculated in 10 ml YTamp media (16 mg/ml tryptone, 10 mg/ml yeast extract, 43 mM NaCl and 50 mg/ml amp) and incubated overnight at 37°C with shaking at 200 rpm. The overnight culture (1 ml) was used to inoculate 100 ml YTamp (prewarmed) in a 500 ml flask and incubated with shaking at 200 rpm for 1-2 h at 37°C until the OD⁶⁰⁰ reached 0.5-0.7. Before induction with 0.2% arabinose or 0.6 mM IPTG (Isopropyl β -D-1-thiogalactopyranoside), 1 ml of non-induced sample was collected as non-induced control to be loaded in a SDS-PAGE (sodium dodecyl sulfate polyacrylamide gel electrophoresis) gel. After addition of arabinose or IPTG, the culture was incubated with shaking at 200 rpm for 4-5 h at 37°C. After every h upon induction, 1 ml of culture was collected to be loaded in a SDS-PAGE. The 1 ml non-induced and induced samples were centrifuged at 12,000 xg for 5 min, resuspended in PBS (3.2 mM Na₂HPO₄; 0.5 mM KH₂PO₄; 1.3 mM KCl; 135 mM NaCl, pH 7.4) buffer, mixed with equal volume of SB buffer, boiled at 100°C for 5 min and loaded in 10% SDS-PAGE to measure the progressive expression profile of the induced protein. At the end of incubation, the rest of the culture was centrifuged at 3,000 xg for 20 min at 4°C. The bacterial pellet was frozen at -20°C and after thawing on ice, resuspended in 5 ml ice-cold PBS (50 μ l PBS/ml bacterial culture). The OD⁶⁰⁰ was determined and was typically 50-60. Next to ensure cell wall lysis of bacteria, 1% Lysozyme was added to the resuspended pellet and incubated at 10 rpm for 1 h at 4°C by

end-over-end agitation. Lysozyme catalyzes hydrolysis of peptidoglycan cell wall of bacteria. The lysate was sonicated on ice in a 15 ml falcon tube to lyse cells (30% amplitude, 10 x 10 sec). After adding 1% Triton X-100 and 0.1 mM EDTA, the bacterial lysate was incubated at 10 rpm for 1 h at 4°C by end-over-end agitation to ensure solubilisation of protein. The bacterial lysate was then centrifuged at 10,000 xg for 15 min at 4°C. Leaving behind the cell debris as pellet, the bacterial sonicate (the supernatant) was aliquoted in Eppendorf tubes and stored at -20°C until required.

3.2 Purification of protein expressed in bacterial cell

To harvest mammalian purified protein, 100 ml bacterial culture of YTamp media was prepared, similar to the procedure described above. The 100 ml culture was divided into two 50 ml sterile tubes and centrifuged at 3,000 xg for 20 min at 4°C to collect the bacterial pellet. Each pellet was resuspended in 10 ml lysis buffer (50 mM Tris-HCl, pH 7.5; 150 mM NaCl; 1 mM EGTA; 1 mM EDTA; 0.5% Triton X-100; 1 unit protease inhibitor cocktail tablet for 10 ml) on ice. The resuspension was lysed by snap freezing in liquid nitrogen. The frozen lysate was thawed under cold water. Sonication was performed (30% amplitude, 8 x 1 min) with regular interval on ice for 1 min. Thereafter, the lysate was centrifuged at 22,000 xg for 1 h at 4°C. The supernatant was collected and mixed with 2 ml binding beads (GST or MBP beads), prewashed with wash buffer (50 mM Tris-HCl, pH 7.5; 150 mM NaCl; 1 mM EGTA; 1 mM EDTA) and resuspended in 50% slurry. Beads were added according to the protein of desire, i.e., maltose binding protein (MBP) beads for MBP tagged proteins and glutathione sepharose transferase (GST) protein beads for GST tagged proteins. The beads were incubated for 2 h at 4°C with end-over-end agitation. Subsequently, the lysate was centrifuged at 1,000 xg for 1 min at 4°C. Beads were collected as pellet and washed with 15 ml wash buffer twice. The bead slurry was transferred into 15 ml tube and centrifuged at 10,000 xg for 1 min at 4°C. The supernatant was discarded carefully. Then, 5 ml of elution buffer (5 mM HEPES, pH 7.6; 0.1% β -mercaptoethanol; 1 mM EDTA; 10% glycerol; 0.1% Triton X-100; 0.1 mM EGTA) was added to resuspend the beads and incubated for 15 min at room temperature. The resuspension was again centrifuged at 10,000 xg for 1 min at 4°C. The supernatant was collected as fraction containing expressed protein. Again, the process was repeated by adding 5 ml elution buffer for collection of the supernatant. Next, 10 ml of supernatant was dialysed for overnight at 4°C using Dialysing kit, following the manufacturer's instructions. At the end, purified proteins were aliquoted in small volume and stored in -20°C till further use.

3.3 Mammalian cell culture and cell transfection

HEK293 cells were grown in DMEM high glucose media with 10% fetal calf serum (FCS) and 1% penicillin/streptomycin in 10 ml culture flasks in a humidified atmosphere of 5% CO₂ at 37°C incubator. Each time, the cell culture was started with 10% confluency and grown until 80%-90% confluency. Generally, the cells were split every 7 days. After every 3 days, the media was changed with pre-warmed fresh media. For cell transfection, 1-2 x 10⁵ cells/ml were grown overnight in 2 ml media in each well of 6-well plates (Nunc) at 37°C. Next day, the media was changed with pre-warmed OPTIMEM media. Lipofectamine based method was used to transfect the cells with 1 µg of mammalian plasmid DNA construct (pCI vector) and 10 µl of Lipofectamine (**Figure 2.3A**). The green fluorescent protein vector (GFP-C2, Clontech) was used as control (**Figure 2.3B**). After 6 h incubation in humidified atmosphere of 5% CO₂ at 37°C, the transfection mixture was replaced with pre-warmed normal DMEM media and the cells were allowed to grow. After overnight incubation in 5% CO₂ at 37°C, the media was changed. After 48 h, the cells were prepared for either affinity chromatography or immunocytochemistry. To perform affinity chromatography, the transfected cells were scrapped in 750 µl PTxE (1 mM EDTA, 1% Triton X-100 in PBS buffer) buffer and sonicated (25% amplitude, 10 x 5 sec). The sonicate was finally centrifuged at 13,000 xg for 15 min at 4°C and stored at -20°C until further use in co-IP assay.

4. Biochemical methods

4.1 Preparation of cell lysate

After the successful transfection, the HEK293 cells were scrapped off using a cell scraper from 6-well plates. The scrapped off HEK293 cells were washed with PTxE buffer and resuspended in PTxE buffer (250 µl per well of 6-well plate). Each sample was sonicated to lyse cells (25% amplitude, 6 x 10 sec). The cell lysate was incubated by end-to-end agitation at 10 rpm for 1 h at 4°C to ensure solubilisation. Then, the cell lysate was centrifuged at 15,000 xg for 5 min at 4°C. The soluble fraction was collected and used for GST pull-down or co-IP studies.

4.2 Preparation of rat brain lysate

The rat brain of approximately 1.50 g was homogenised in 20 volume of ice-cold homogenizing buffer (HB) (0.32 M sucrose; 4 mM HEPES; 1 mM EDTA; 1 mM EGTA, pH 7.4-HCl) in glass teflon homogeniser by gently moving up and down 6-8 times on ice. The

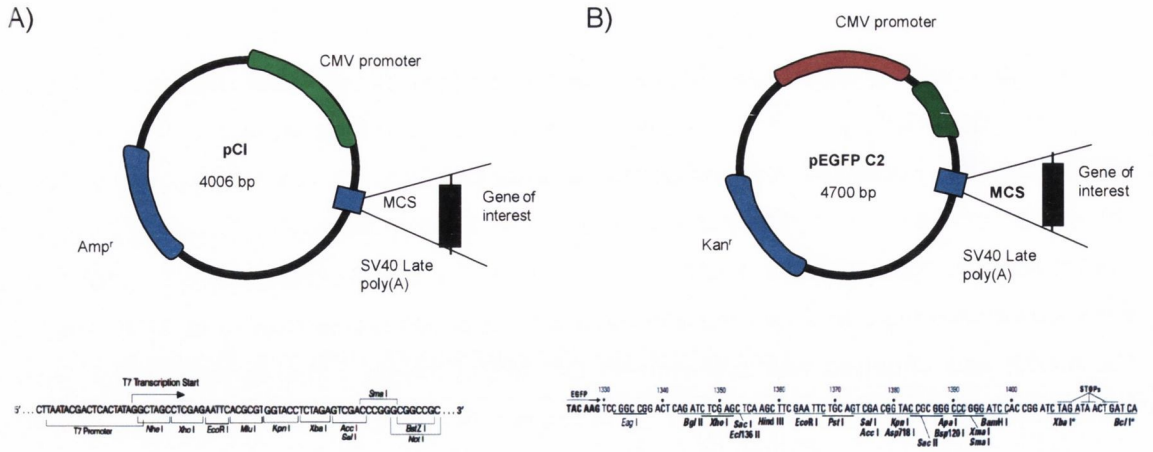


Figure 2.3: Mammalian plasmid vectors

As mammalian cell expressing plasmids, A) pCI and B) pEGFP-C2 were used, which contain amp and kan resistant genes, respectively.

homogenate was centrifuged at 1,000 xg for 10 min at 4°C. The supernatant was aliquoted, 1 ml each in 1.5 ml Eppendorf tubes. The tubes were centrifuged at 13,000 xg for 30 min at 4°C. Each 1 ml pellet was resuspended in 500 µl of PTxE buffer. Each sample was sonicated to lyse cells (25% amplitude, 10 x 5 sec). The cell lysate was rotated at 10 rpm for 1 h at 4°C to ensure solubilisation. The cell lysate was then centrifuged at 15,000 xg for 5 min at 4°C. The soluble fraction was collected and used for co-IP studies.

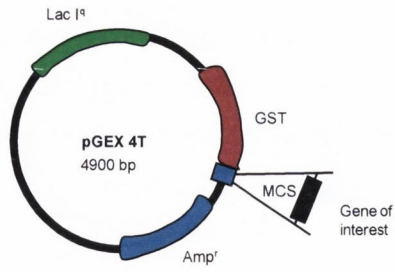
4.3 GST/MBP pull-down assay

Mammalian genes were cloned in GST tagged vector (pGEX 4T) (**Figure 2.4A**) and MBP tagged vector (pMAL C2) (**Figure 2.4B**); and expressed transiently in bacterial cells. GST pull-down was performed with protein extracted from bacterial or mammalian source. Before GST pull-down experiments, the frozen protein samples were thawed on ice. The samples were then sonicated (25% amplitude, 5 x 10 sec) and rotated at 10 rpm for 1 h at 4°C. The sonicate was centrifuged at 13,000 xg for 10 min at 4°C. The GST co-IP experiment was set up as follows: 200-500 µl sonicate, 0.1% BSA and 20 µl of GST beads in a total reaction volume of 1 ml PTxE buffer in 1.5 ml eppendorf tube. In case of MBP tagged proteins, MBP beads were used instead of GST beads. The samples were rotated for 4 h at 4°C. After incubation, beads were settled by short centrifuge at 4,000 xg for 5 sec at room temperature. The beads were washed 4-5 times with PTxE buffer by repeated resuspension and centrifugation. After the washing step, the beads were finally resuspended in 20 µl PTxE buffer and boiled with 2x sample buffer (5% β-mercaptoethanol) for 5 min at 100°C. The boiled samples were centrifuged at 15,000 rpm for 10 min at room temperature. The supernatant was loaded in a 10% protein gel.

4.4 SDS-Poly Acrylamide Gel Electrophoresis and western blotting

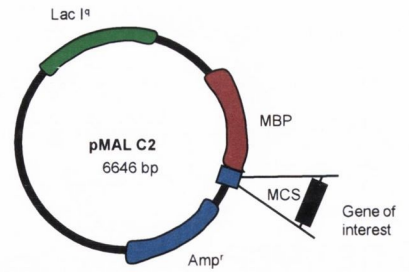
Proteins are separated according to their respective molecular weight in poly acrylamide gels. In our experiments, 10% acrylamide and 4% acrylamide were used as stacking and resolving gel respectively. The resolving gel was made with 10% acrylamide; 0.4 mM Tris-HCl, pH 8.8; 0.1% SDS; 0.05% APS and 0.1% TEMED. The stacking gel was made with 4% acrylamide, 0.37 mM Tris-HCl pH 8.8, 0.1% SDS, 0.05% APS and 0.1% TEMED. The proteins were separated under constant 100 V, when the samples were in stacking gel and constant 150 V, when the samples entered the resolving gel. Separated proteins were identified by the Commassie stain or western blotting. Commassie staining was done by incubating the gel in Commassie Brilliant Blue dye for 1 h. To remove excess stain, the gel was incubated in destaining solution (water: methanol: acetic acid = 5:4:1) for 3 x 20 min. The western blotting was performed using a dry transfer method. The resolved proteins were

A)



Thrombin
 Leu Val Pro Arg Gly Ser Pro Glu Phe Ile Val Thr Asp
 CTG GTT CCG CGT GGA TCC CCG GAA TTC ATC GTG ACT GAC TGA CGA
 BamH I EcoR I Stop codons

B)



Xba I EcoR I BamH I Xba I Sal I Pst I Hind III
 mAE...ATC GAG GGA AGG ATT TCA GAA TTC GGA TCC TCT AGA GTC GAC CTG CAG GCA AGC TTG...lacZα
 Ile glu gly arg

Figure 2.4: Bacterial plasmid vectors

As bacterial expressing plasmids A) pGEX 4T and B) pMAL C2 were used, containing amp resistant gene.

transferred to a PVDF (Poly Vinylidene Difluoride) membrane. The PVDF membrane was cut according to the size of the gel and immersed into methanol for 10 sec. Thereafter, for activation, the membrane was transferred into the solution C (25 mM Tris, 0.02% SDS, 20% methanol and 40 mM ϵ -amino capronic acid) for 1 h. The Whatman papers (grade 3) were cut and two strips each were dipped into solution A (0.3M Tris, 0.02% SDS, 20% methanol), solution B (25 mM Tris, 0.02% SDS, 20% methanol) and solution C. The sandwich for the protein transfer was arranged in the transfer unit in following manner, Anode-2x Whatman papers in solution A-2x Whatman papers in solution B-PDVF membrane -SDS-PAGE gel-2x Whatman papers in solution C-Cathode. The transfer unit was run for 90 min under a constant current of 50 mA. After transfer, the PDVF membrane was blocked by incubating in 5% non-fat milk in PBS-T (0.1% Tween-20 in PBS buffer) buffer for 1 h at room temperature or overnight at 4°C. Then, the blot was incubated with primary antibody overnight at 4°C and washed with PBS-T buffer for 3 x 5 min. Thereafter, the blot was incubated in secondary antibody for 1 h at room temperature. Further, the blot was washed for 3 x 5 min in PBS-T and visualised using alkaline phosphatase (alkphos) buffer (100 mM NaCl; 5 mM MgCl₂; 100 mM Tris-HCl, pH 9.5). For alkphos based visualization, the blot was developed by incubating in BCIP and NBT substrates with alkphos buffer (30 μ l BCIP and 60 μ l NBT in 10 ml of alkphos buffer). In addition, horseradish peroxidase-linked (HRP) secondary antibodies were also used in some experiments. After incubation with secondary antibody and washing steps as described previously, the blot was incubated with chemiluminescent HRP Substrate according to manufacturer's instruction (Millipore). The list of antibodies used in this project is enlisted in **Table 2.2**.

5. Mitochondrial assays

5.1 Isolation of synaptosomes using Ficoll gradients

To isolate synaptosomes from the rat brain, 2 rats were stunned and decapitated. The top of the skull was removed to scoop out the entire brain. The brains were quickly transferred into ice-cold STE (320 mM sucrose; 2 mM EDTA; 10 mM Tris-HCl, pH 7.4) buffer. After removing the excess blood by washing with STE buffer, the brains were chopped properly. The chopped brains were homogenised (12 passes) using the glass Dounce Homogeniser with a tight pestle (0.012). Then, the homogenised brains were then centrifuged at 1,500 xg for 3 min at 4°C to remove the cellular debris. Thereafter, the supernatant was collected and centrifuged at 12,000 xg for 10 min at 4°C. Resultant pellet was the Crude Mitochondrial Pellet (CMP). The CMP was carefully collected leaving behind any trace of blood and then

Name	Raised against	Animal raised in	Conjugate	Cat. No. & Company	Working dilution
Anti-Neurofilament	Neurofilament	Chicken polyclonal	NA	AB5539, Millipore	1/500
β III- Tubulin	β III- Tubulin	Rabbit polyclonal	NA	TP1691, ECMBiosciences	1/500
Anti-Parkin	Parkin	Rabbit-polyclonal	NA	AB6177, Abcam	1/1000
Anti-PICK1	PICK1	Rabbit polyclonal	NA	Sc-11410, Santa Cruz	1/1000
Anti-PRK8	Parkin	Mouse monoclonal	NA	MAB5512, Chemicon	1/1000
Anti-Flag	Flag	Mouse monoclonal	NA	F3165, Sigma	1/10000
Anti-HA	HA	Rabbit	NA	sc-805, Santa Cruz	1/1000
Anti-MBP	MBP	Mouse monoclonal	NA	E8032S, NEB	1/10000
Anti-GFAP	GFAP	Rabbit	N/A	Z0334, DAKO	1/1000
Anti-Mouse IgG	Mouse IgG	Goat	AlkPhos	S3721, Promega	1/500
Anti Rabbit Alexa-633	Rabbit	Goat	Alexa 633	Invitrogen	1/500
Anti-Chicken Dylight-549	Chicken	Donkey	Dylight 549	Jackson ImmunoResearch	1/1000
Anti-Rabbit IgG	Rabbit IgG	Goat	AlkPhos	S3731, Promega	1/500
Anti-mouse HRP	Mouse	Goat	HRP	A8924, Sigma	1/1000
Anti-rabbit HRP	Rabbit	Donkey	HRP	NA934, GE Healthcare	1/5000
Anti-goat HRP	Goat	Rabbit	HRP	A4174, Sigma	1/5000

Table 2.2: List of antibodies used

resuspended into STE buffer. Thereafter, the CMP was loaded carefully over two Ficoll gradients in a ultracentrifuge tube in following manner; 10% (w/v) Ficoll solution, 7.5% (w/v) Ficoll solution and the CMP resuspension, respectively (**Figure 2.5A**). The tubes were then centrifuged in swing-out rotor in a Discovery ultracentrifuge at 104,200 xg for 55 min at 4°C. After ultracentrifugation, the myelin layer was removed formed in the interphase between the isolated medium and 7.5% (w/v) Ficoll layer (**Figure 2.5B**). The synaptosomal fraction was extracted from the interphase between the 7.5% Ficoll layer and the 10% Ficoll layer. The non-synaptic mitochondria formed a pellet at the bottom of the tube. The synaptosomes and pellet were separately resuspended in STE buffer and collected into 1.5 ml Eppendorf tubes. The Eppendorf tubes were centrifuged at 13,000 xg for 10 min at 4°C and the pellets were resuspended in STE buffer. A Bradford protein assay was performed to determine the concentration of protein.

5.2 Determination of protein concentration by Bradford assay

After extraction of synaptosomes, the concentration of synaptosomal protein was quantified by Bradford method (1976). According to this method, Bradford dye was used to rupture membranes of the synaptosomes, so that the protein content could be measured. A range of known concentrations of BSA were made up in triplicates to plot a standard curve against absorbance (OD^{595}), according to the **Table 2.3A**. The synaptosomal protein was diluted (1/100) in STE buffer and 100 μ l was added to 700 μ l of distilled water in triplicates. All the samples were then added with 200 μ l of Bradford dye and mixed thoroughly. After 30 min of incubation, the samples were poured in 1 ml plastic cuvettes and the absorbance is measured at 595 nm by a spectrophotometer.

The synaptosomes are used as medium for studying mitochondrial dynamics due to presence of high number of mitochondria in them (Kilbride et al., 2008). Therefore, synaptosomal preparations were used in different mitochondrial assays and glutamate release to observe the effect of blocking peptides (**Table 2.3**) and compounds. In the following sections, details of the mitochondrial assays and glutamate release are described.

5.3 Measurement of ROS production

ROS, including superoxide (O_2^-) and hydroxyl radicals (OH^\cdot), hydrogen peroxide (H_2O_2) and peroxynitrite ($ONOO^-$) are produced inside the cells as a byproduct of metabolism (True et al., 2000; Meng et al., 2002; Griending et al., 2000). However, high amount of ROS production generates oxidative stress, leading to mitochondria dysfunction and apoptosis (Keeney et al., 2006). H_2O_2 is nonreactive, uncharged, relatively stable and freely diffusible

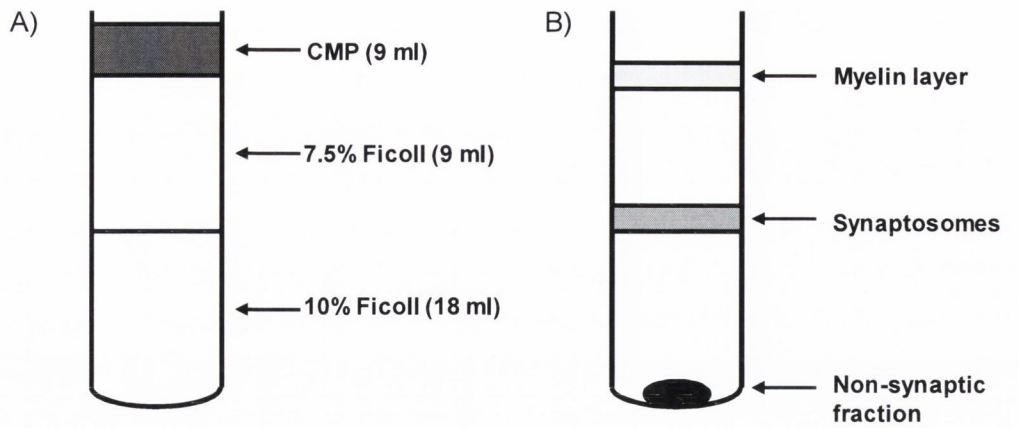


Figure 2.5: Isolation of synaptosomes using Ficoll gradient

a) The gradient of Ficoll is made by delicately layering 9 ml 7.5% (w/v) Ficoll on the top of 18 ml 10% (w/v) Ficoll, ensuring that an interface between the two layers could be seen clearly. The 9 ml of CMP in STE buffer is then layered on top of 7.5% Ficoll layer. b) After ultracentrifugation, myelin protein forms a layer above 7.5% Ficoll, whereas synaptosomes passes through the 7.5% (w/v) layer, forming a layer above 10% Ficoll layer. The non-synaptic fraction was settled as pellet on the bottom of the tube.

A)

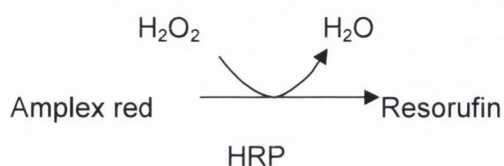
BSA (μg)	0	2	5	10	15	20
H₂O (μl)	800	780	750	700	650	600
BSA (0.1 $\mu\text{g}/\mu\text{l}$) added (μl)	0	20	50	100	150	200
Bradford dye (μl)	200	200	200	200	200	200
Total volume (μl)	1000	1000	1000	1000	1000	1000

B)

Name	Domain	Motif	Peptide sequences	Purity%	Company
MNP201	PICK1	Parkin	VCMGDHWFDV	97.40%	Genescript
MNP201(mut)	PICK1	Parkin	VCMGDHWAAA	91.80%	Genescript
Tat-MNP201	PICK1	Parkin	YGRKKRRQRRRVCMGDHWFDV	95.30%	Genescript
Tat-MNP201(mut)	PICK1	Parkin	YGRKKRRQRRRVCMGDHWAAA	95.50%	Genescript
FITC-MNP201	PICK1	Parkin	YGRKKRRQRRRVCMGDHWFDV	85.90%	Genescript
MNP202	NA	Cdc4 α	LVLDFDVMK	93.75%	Peptide 2.0
MNP202(mut)	NA	Cdc4 α	LVLDFDVAAA	94.78%	Peptide 2.0

**Table 2.3: A) Method of Bradford assay
B) List of peptides**

across adjacent cells or tissues to serve as a mediator of autocrine and paracrine system. H_2O_2 production is an important indicator of mitochondrial dysfunction and cell stress. According to the method of Mohanty et al. (1997), H_2O_2 production was measured by the amplex red assay. In the presence of H_2O_2 , amplex red (10-acetyl-3,7-dihydroxyphenoxazine) converts to resorufin (excitation/emission wavelength = 550/585 nm), a highly fluorescent agent. Horseradish peroxidase catalyses the conversion of amplex red to resorufin, in the presence of H_2O_2 . Production of H_2O_2 is proportional to the conversion of amplex red to resorufin and the amount of resorufin is considered as a quantitative indicator of H_2O_2 production.



Synaptosomes (1 mg/ml) were incubated with 50 μ M amplex red and 2.5 U/ml HRP in Krebs buffer (3 mM KCl; 140 mM NaCl; 10 mM glucose; 2 mM $MgCl_2$; 2 mM $CaCl_2$; 25 mM Tris, pH 7.4); and fluorescence intensity of resorufin was monitored at 37°C for 1-2 h in a Spectramax Gemini XS plate reader. The treatment groups were tested in triplicates for each individual experiment. After generation of the traces, the rate of change in fluorescence was measured over the same linear range for each condition (approximately 15-20 min). The values were converted as a percentage of control and represented in a bar diagram to indicate total peroxide release by the treatment group. Antimycin A induces high amount of peroxide production by selectively blocking complex III (Sipos et al., 2003). Therefore, 1 μ M antimycin A was used as positive control in all the experiments.

5.4 Mitochondrial membrane potential measurement

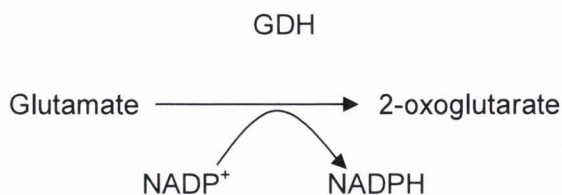
Based on the method of Chinopoulos et al. (1999), the mitochondrial membrane potential was measured using JC-1 (5,5',6,6' tetrachloro-1,1',3,3'-tetra ethylbenzimidazolyl carbocyanine iodide). JC-1 is a cationic, lipophilic carbocyanine dye, which forms J-aggregates inside polarized mitochondria under normal condition, emitting red colour (absorption/emission spectra 585/590 nm upon excitation at 490 nm) (Reers et al., 1991). Under depolarized condition of mitochondria, release of monomeric form JC-1 occurs in cytoplasm, emitting green colour (absorption/emission spectra 510/527 nm upon excitation at 490 nm). The ratio of emission at 590 nm to 535 nm ($JC-1^{590/535}$) is a semi-quantitative measure of *in situ* mitochondrial membrane potential, because the formation of J-aggregate

increases with membrane potential linearly within the range of -30 to -180 mV (Reers et al., 1995). The decrease in 590/535 ratio signifies reduction in mitochondrial membrane potential.

Synaptosomes (4 mg/ml) were incubated in dark with 6 μ M JC-1 and Krebs buffer for 15 min at 37°C. Then, to remove excess JC-1, the sample was centrifuged at 16,000 xg for 5 min. Thereafter, the pellet was resuspended in Krebs buffer in Krebs buffer. The process of centrifugation and resuspension was repeated (3x). Then, the final pellet was resuspended in Krebs buffer and 1 mg/ml of JC-1 treated protein was loaded in 96-well black plate with the treatment groups in triplicates. The fluorescence was measured in a Spectramax Gemini XS plate reader (excitation spectrum of 490 nm and emission spectra of 535 and 590 nm) for 60 min at 37°C. The excitation and emission slits were set at 10 nm. The JC-1^{590/535} was plotted against time representing rate of change in mitochondrial membrane potential with time, as described in Kilbride et al. (2008). To calculate the mitochondrial membrane potential in treated samples, the rate of change in the JC-1^{590/535} was measured over the same linear range for each condition (15-20 min). The values were converted as a percentage of control and represented in a bar diagram indicating the membrane potential of synaptosomal mitochondria.

5.5 Glutamate release assay

Glutamate is a neurotransmitter that has important roles to play in the long term potentiation, learning and memory (Riedel et al., 1996). The release of glutamate from synaptosomes is measured by adapting a continuous fluorimetric method based on Nicholls et al. (1987). Glutamate converts to 2-oxoglutarate using cofactor nicotinamide adenine dinucleotide phosphate (NADP⁺). This reaction is catalysed by the L-glutamate dehydrogenase (GDH) and in the process; NADP⁺ converts to nicotinamide adenine dinucleotide 2'-phosphate (NADPH). The amount of release glutamate is measured by quantifying NADPH (excitation/emission = 340/460 nm) spectrophotometrically.



After extracting fresh synaptosomes, the concentration of synaptosomal protein was measured and aliquoted into 1.5 ml Eppendorf tubes, 1 mg each. Then, each tube was added with 1 ml of TES buffer (250 mM sucrose; 5 mM TES, pH 7.4) and centrifuged at

12,000 xg for 5 min at 4°C. The pellets were stored in ice until used for experiment (15-20 min). During experiment, the pellets were resuspended in 1 ml Kreb's buffer (with and without 2 mM CaCl₂) to obtain a protein concentration of 1 mg/ml. Thereafter, in the 96-well blackplate, 0.5 µg/µl of protein was added with 31.6 U/ml GDH and 1 mM NADP⁺ and the reading was performed in SpectraMax GeminiXS fluorimetric plate reader at 37°C (excitation/emission spectra = 340/460 nm). First, the blank rate fluorescence was recorded as continuous fluorimetric readings for 5 min. Then, treatment group was added to the synaptosomes in triplicates and the baseline fluorescence was monitored for next 5 min. Thereafter, depolarization of synaptosomes were conducted by addition of KCl (final concentration 40 mM) or 4-AP (final concentration 10 mM) and the fluorescence under depolarized condition was recorded for 30 min. Rotenone-mediated inhibition of complex I has been shown to induce glutamate release from synaptosomes (Kilbride et al., 2008). Therefore, 10 µM rotenone was assayed with every glutamate release experiment as positive control. The total glutamate release from non-depolarized and depolarized conditions were calculated over a period of 5 min and 30 min, respectively; and represented as a percentage of control in bar diagrams.

5.6 Respiratory chain complex assay

To determine the activity of respiratory chain complexes, synaptosomal mitochondria were used in the respiratory chain complex assays. To perform these studies, the mitochondrial inner membrane is to be exposed to facilitate the entry of reaction mixture to the respiratory chain complexes. To fracture mitochondria, the synaptosomes were freeze-fractured by quick freeze and thaw cycle in liquid nitrogen and 37°C waterbath (3x), respectively. After freeze-fracture, the synaptosomal samples was used for respiratory chain assays or stored in -80°C for further use.

5.6.1 Complex I assay

Complex I (EC 1.6.99.3, NADH: cytochrome C oxidoreductase) activity was measured by using the method based on Ragan et al. (1987). The activity of complex I was measured by the rate of conversion of NADH to NAD⁺ spectrophotometrically at absorbance 340 nm. To perform the assay, 50 µg of mitochondrial protein was mixed with complex 1 buffer (10 mM MgCl₂; 25 mM potassium phosphate, pH 7.4), 0.2 mM NADH, 2.5 mg BSA and 1 mM KCN (inhibitor of complex IV) in 1 ml of solution. The treatment groups were tested in triplicates and the absorbance of NADH (340 nm) was monitored for 20 min at 37°C in a Cary UV spectrophotometer. CoQ is reduced to ubiquinol during the oxidation of NADH by complex I. To start the reaction, 50 µM

of decylubiquinone (DQ), a CoQ analog, was added after 1-2 min (baseline rate) and the rate of reaction was recorded for 12-13 min. Then, 10 μM of rotenone was added to inhibit complex 1 activity and the reaction was followed for next 5-6 min, as indicated in Ragan et al. (1987). The activity of complex I is a pseudo-first order reaction. The specific activities of the complex I were determined by calculating the linear rate constants of NADH, after addition of DQ (K_{DQ}) and rotenone (K_{ROT}). The rotenone insensitive rate was subtracted from the initial rates to obtain the specific activity of complex I ($K_{\text{DQ}}-K_{\text{ROT}}$) in mitochondria and the values were expressed in $\mu\text{mol min}^{-1} \text{mg}^{-1}$ (Kilbride et al 2008). The data was converted as a percentage of control and represented in bar graph to compare different peptides activity.

5.6.2 Complex IV assay

Complex IV (EC 1.9.3.1, cytochrome c oxidase) assay was based on the method by Wharton and Tzagoloff (1967). The oxidation of reduced cytochrome C by cytochrome C oxidase was measured as a decrease in absorbance at 550 nm at 37°C. The reaction mixture was made of 50 μM reduced cytochrome C and complex IV buffer (10 mM of potassium phosphate buffer, pH 7) to a final volume of 1 ml. The treatment groups were tested in triplicates and the absorbance of cytochrome C (550 nm) was monitored for 2 min (baseline rate) in a Cary UV spectrophotometer. Then, the reaction was initiated by adding 100 μg of freeze-fractured synaptosomal protein and decrease in absorbance was recorded for next 10 min. After a rapid decrease in absorbance, the rate of activity reached a plateau following a first-order rate reaction. The time point of protein addition was named $t = 0$ and the first-order decay rate constant (k) was calculated as from the difference between the natural logarithms of the absorbance at this point and three subsequent time points 1, 2 and 3 min. The mean of the calculated specific activity values was expressed in $k \text{ min}^{-1} \text{mg}^{-1}$. The data was converted as a percentage of control and represented in bar graph to compare the activities of different peptides.

5.6.3 Preparation of reduced cytochrome C

The oxidised cytochrome C (25 mg/ 2.5 ml) was reduced by the addition of a few crystals of ascorbic acid. The deep red colour of cytochrome C changed into bright pink colour. Then, a PD₁₀ gel filtration column was activated by passing through 50 ml of assay buffer (10 mM potassium phosphate buffer, pH 7). The activated column was used to remove the ascorbic acid by passing the solution through 2.5 ml of cytochrome C. The column was eluted by addition of 3 ml assay buffer. The reduced

cytochrome C was collected as darkest band of eluent from the column. The concentration of the reduced cytochrome C was measured on Cary UV spectrophotometer using 10 μ l of 100 mM ferricyanide to oxidise cytochrome C.

5.7 Statistical analysis

The data obtained from the experiments were converted as a percentage of control and expressed in mean \pm SEM (standard error mean) in the result sections. The percentage of control values were used to construct bar diagrams. For statistical analysis, GraphPad Prism 5.03 software was used. To compare two treatment groups, student t-test was used. To compare more than two treatment groups, Dunnett post-hoc test was used under one-way ANOVA. The significance level or p-values depicted in the data were 0.05 (*), 0.01 (**) and 0.001 (***) (p-value).

6. Primary Cell Culture

6.1 Set-up and preparation before primary cell culture

To culture neurons, 6-well plates and coverslipped 24-well plates were used for western blots and imaging, respectively. For culturing on coverslips in 24-well plates, first borosilicate glass coverslips with a diameter of 13 mm were sterilized by immersing in 70% methanol followed by exposure to UV light overnight. Coverslips were then coated with poly-L-lysine (40 μ g/ml) for 1 h at 37°C. Thereafter, to remove excess poly-L-lysine, coverslips were rinsed with cell culture grade water and allowed to air dry in the laminar flow hood before being placed in 24-well plates.

6.2 Brain dissection for primary cultures

Postnatal one day old female Wistar rats (supplied by the Bioresources Unit, Trinity College Dublin) were used for neuronal cultures. The pups were decapitated according to the guidelines prescribed by the Animals Act 1986 (Scientific Procedures) Schedule I. The skull was exposed by cutting the skin from the neck down to the tip of the nose. The brain was exposed by making a sagittal cut along the level of the medial longitudinal fissure and two horizontal cuts along each side of the skull at the level of the ears. The skull was peeled back revealing the cortex, which was rapidly removed with curved forceps.

6.3 Neuronal Culture

Dissected cortices were placed in 20 μ l pre-warmed neuronal culture buffer (116 mM NaCl; 5.4 mM KCl; 26 mM NaHCO₃; 1.3 mM NaHPO₄; 1 mM MgSO₄.7H₂O; 1 mM CaCl₂.2H₂O; 0.5 mM EDTA.2Na.2H₂O; 25 mM glucose, pH = 7.4). Then, the cortices were chopped using a sterile disposable scalpel. The tissue was then transferred into 2.5 ml of 0.15% papain solution and left to incubate at 37°C. The tissue was then carefully transferred into 2 ml of 1% BSA solution. The solution was triturated (15x approximately) with a fine tipped Pasteur pipette, before transferring into another 2 ml of BSA solution to triturate again and this was repeated (3x). Thereafter, the resultant solution was centrifuged at 3,000 xg for 3 min at RT. The supernatant was removed carefully without disturbing the pellet. The pellet was then resuspended with 5 ml pre-warmed supplemented neurobasal-A media (neurobasal-A media, 1 ml B-27, 0.5 ml 200 μ M glutamine). The solution was incubated at room temperature for 5 min so that any connective tissue and any cell clumps can settle to the bottom. The upper layer of the solution was plated, 120 μ l per well for 24-well plates and 500 μ l for 6-well plates. After incubating for 1 h at 37°C with 5% CO₂, the wells were filled with 500 μ l pre-warmed supplemented Neurobasal media. After every third day, 50% of the media was replaced with new media. After maturing the cells for 10-14 days, treatments were carried out with peptides at 37°C for 1 h in 5% CO₂.

6.4 Immunocytochemistry

Treatment on the neuronal cells was done after 10-14 days in 24-well plates. After treatment, the media were taken out and cells were washed with 3 x 1 ml PBS. The cells were fixed by treating with 100% ice-cold methanol at room temperature for 5 min. After fixation, the cells were washed with PBS 2 x 5 min. To permeabilise, the cells were incubated in 0.10% Triton X-100 for 30 min. Later, cells were incubated in blocking solution (5% normal goat serum, 0.5% BSA in PBS) for overnight at 4°C or 1 h at room temperature. Thereafter, the cells were incubated in primary antibodies overnight at 4°C. Then, the cells were washed for 3 x 5 min with PBS. Subsequently, the cells were treated with fluorephore tagged secondary antibodies for 1 h at room temperature (for list of antibodies, see **Table 2.2**). After incubation, the cells were washed with PBS for 3 x 5 min. Thereafter, the coverslips were taken out from the wells and placed inverted onto a glass slide with a drop of 90% glycerol mounting media. The periphery of the coverslips was sealed by applying nail varnish. The cells were then imaged using a Zeiss LSM 510 META confocal laser scanning microscope utilising an Axiovert 200M inverted microscope (Zeiss Ltd, UK). Images were captured and optimized using LSM510 computer program and were acquired at 40x and 63x

magnification. Initially optimal settings for image quality were obtained and thereafter the settings remained unchanged. To calculate mean pixel intensity, the ImageJ software was used.

3. Results: 1
**Validation of parkin-PICK1 interaction and
of the MNP201 parkin peptide**

Abstract

The objective of this project was to investigate the role of parkin-PICK1 interaction in mitochondrial function. The ct-parkin contains a PDZ motif that interacts with the PDZ domain of PICK1 and causes monoubiquitination of PICK1 (Joch et al., 2007). In this chapter, a set of approaches were undertaken to demonstrate an interaction between parkin and PICK1. In addition, the binding of a parkin blocking peptide (MNP201) to PICK1, modelled according to the last 10 amino acids of ct-parkin (VCMGDHW**FDV**), was examined. To show a parkin-PICK1 interaction, in the first approach, a bacterial expressed MBP tagged PICK1 was used to pull-down endogenous parkin from rat brain lysate. In these experiments, due to poor anti-parkin antibody recognition (Abcam), the expression of endogenous parkin was not detected. Then, co-IP experiments were performed using lysates from HEK293 cells transiently transfected with HA-parkin and Flag-PICK1. Due to the absence of the full length HA-parkin expression and poor expression of Flag-PICK1, the results failed to show parkin-PICK1 interaction. Thereafter, pull-down studies were performed using MBP-PICK1 and transiently expressed mutant parkin (Ubl domain deletion). In these experiments the mutant parkin was well expressed although it showed no interaction with PICK1 interaction. These studies also faced technical hurdles, insofar that antibody crossreactive bands were detected in pull-down and CoIP experiments. Thus, as an alternative, fluorescence polarisation assays were used to demonstrate the binding of the MNP201 to PICK1. The data in these experiments showed that MNP201 (VCMGDHW**FDV**), but not a PDZ-motif mutant of MNP201 (VCMGDHW**AAA**), blocked the binding of a DAT-peptide to PICK1 suggesting competitive binding to the PDZ domain of PICK1.

Introduction

ARJP is motor-related neurodegenerative disease that results from death of dopamine producing neurons in the mid-brain. Mutations in parkin, an E3 ligase responsible for inducing degradation of several proteins, are associated with this disease (Kitada et al., 1998). Several mutations in the *parkin* gene have been identified in ARJP patients impairing ubiquitin ligase function of parkin (Bonifati, 2012). A non-functional parkin is unable to ubiquitinate its protein substrates, which are no longer targeted to the proteasome for degradation (Pagano, 1997; Ben-Neriah, 2002). The build up of these parkin substrates results in protein aggregation and causes cell toxicity that ultimately results in cell death. In addition to cellular toxicity induced by unwanted proteins, mitochondrial dysfunction is also identified as a cause for the dopaminergic neurodegeneration in PD (Kosel et al., 1999; Beal et al., 2003). PD patients have been reported to show impaired complex I activity of the ETC cycle that eventually limits oxidative phosphorylation, the key mechanism of ATP synthesis (Schapira et al., 1990; Parker et al., 1989, 2008; Bindoff, 1989). This impairment also leads to ROS production that causes mitochondrial dysfunction and apoptosis (Keeney et al., 2006). Importantly, parkin is believed to play a crucial role in the maintenance of mitochondrial integrity (Abou-Sleiman et al., 2006). Dopaminergic neurodegeneration and malformed mitochondria were identified in the parkin mutant of *Drosophila* (Greene et al., 2003; Whitworth et al., 2005). Many recent reports confirmed a crucial role of parkin in mitochondria, where parkin selectively recruits autophagosomes to depolarized mitochondria causing mitophagy (Narendra et al., 2008; Twig et al., 2008).

One of the interacting partners of parkin is PICK1, which interacts with parkin through a PDZ domain-motif interaction (Joch et al., 2007). Successful pull-down of endogenous PICK1 from mouse synaptosomes using GST constructs of parkin wild type and deletion mutants have been demonstrated (Joch et al 2007). The experiment demonstrated that the parkin-PICK1 interaction was PDZ domain-dependent as the PDZ binding motif deleted parkin constructs were unable to pull-down endogenous PICK1 (Joch et al 2007). Surprisingly, parkin caused mono-ubiquitination of PICK1 but does not induce degradation (Joch et al., 2007). PICK1, originally identified as a PKC α recruiting protein, recruits PKC α to the outer membrane of mitochondria (Wang et al., 2003). PICK1 is also reported to translocate to the mitochondria in National Institute of Health "3-day transfer, inoculum 3 x 10⁵ cells" (NIH3T3) cells in both non-stimulated and serum-stimulated conditions (Wang et al., 2003). Further research revealed that PICK1 recruits PKC α to phosphorylate the Bcl-2 protein of the outer mitochondrial membrane of human promyelocytic leukemia 60 (HL60) cells that confers resistance against Bax-induced apoptosis (Wang et al., 2007). Thus, while there is data

supporting a role for a PKC α -PICK1 interaction in mitochondrial function, the role of the PICK1-parkin interaction in mitochondrial is still unknown.

A working hypothesis in this project is that the parkin-PICK1 interaction is important for recruiting parkin to mitochondria and that this interaction has a role in mitochondrial maintenance. Thus, in this chapter, parkin blocking peptides (MNP201) were designed based on the last 10 amino acids of ct-parkin to block the parkin-PICK1 interaction. The binding of these parkin blocking peptides (MNP201) to PICK1 was then determined. To show a parkin-PICK1 interaction, pull-down and co-IP experiments were also performed. In this chapter, the first aim was to show an interaction between endogenous parkin and bacterial expressed PICK1, using a pull-down approach. To confirm a parkin-PICK1 interaction, co-IP experiments were also performed using transiently expressed parkin and PICK1. In addition, a set of control experiments were conducted, investigating the origin of non-specific bands arising from the antibody cross-reactivity in pull-down and co-IP experiments. In these experiments, the expression of full length parkin was found to be low as previously reported (Finney et al., 2003), thus a mutated version of parkin was also used in the parkin-PICK1 interaction studies. In addition, lentiviral parkin vectors were constructed to over-express full length parkin in neurons to overcome the issue of low parkin expression. Finally, the binding of parkin peptide, MNP201, was investigated in a fluorescence polarisation assay and successfully showed that MNP201 binds to PICK1, likely via its PDZ domain.

Results

3.1 Design of MNP201

The last three amino acids of ct-parkin are found to be crucial for PDZ domain-mediated interaction with PICK1 (Joch et al., 2007). On the basis of these data, peptides were generated based on the last ten amino acids (VCMGDHWFDV) of the ct-parkin, which included the PDZ motif sequence (-FDV). The wild type peptide was named Molecular NeuroPeptide 201 (MNP201). A mutated version of the peptide, to be used as negative control, was also designed {MNP201(mut)}, where the last three essential amino acids were replaced with alanines (VCMGDHWAAA). These MNP201 compounds were ordered from Genscript, USA. The HPLC purity of MNP201 and MNP201(mut) were found to be 97.4% and 85.5% respectively. The list and the HPLC purity profile are shown in **Figure 3.1** were provided by Genscript, USA. Both the MNP201 and MNP201(mut) were dissolved in 50 mM HEPES pH 7.0 solution.

3.2 Pull-down of PICK1 with GST-GluR2-ct

A well established interacting partner of PICK1 is the AMPA receptor subunit GluR2 where the PDZ motif of ct-GluR2 interacts with the PDZ domain of PICK1 (Dev et al., 1999; Xia et al., 1999). To show the interaction between PICK1-GluR2 by pull-down, an experiment with MBP beads was performed using bacterial expressed MBP tagged full length PICK1 (MBP-PICK1) and bacterial expressed GST tagged ct-GluR2 (GST-GluR2-ct), as previously described (Dev et al., 1999). As a negative control, only GST protein and MBP-PICK1 were incubated in similar manner. After the incubation, the samples were washed and separated in a SDS-PAGE gel and western blots were performed using anti-GST and anti-MBP antibodies (**Figure 3.2**). The anti-GST blot revealed presence of GST and GST-GluR2-ct proteins in equal amounts at their respective molecular weights. The anti-MBP blot demonstrated no band of MBP-PICK1 in the GST lane, but a strong MBP-PICK1 band was identified on the GST-GluR2-ct lane. Taken together, in agreement with previous studies (Dev et al., 1999 and 2000), the experiment suggests that PICK1 interacts with the ct-GluR2.

A)

Name	Domain	Motif	Peptide sequences
MNP201	PICK1	PARKIN	VCMGDHWFDV
MNP201(mut)	PICK1	PARKIN	VCMGDHWAAA

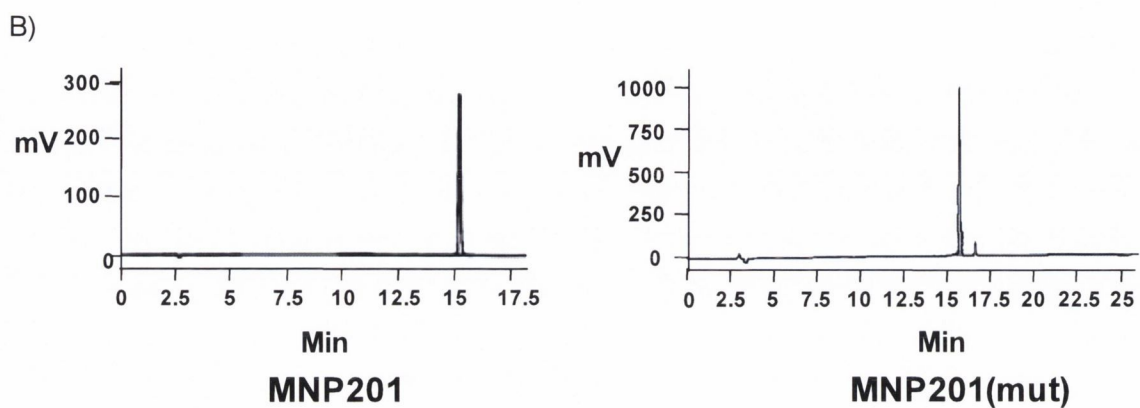


Figure 3.1: Blocking peptides based on the ct of parkin

A) The MNP201 peptides modelled on the ct PDZ motif of parkin are shown in the table. B) The HPLC purity profiles of these peptides measured at 220 nm were found to be 97.4% (MNP201) and 85.5% {MNP201 (mutant)}. The parkin peptides were ordered from Genscript, USA.

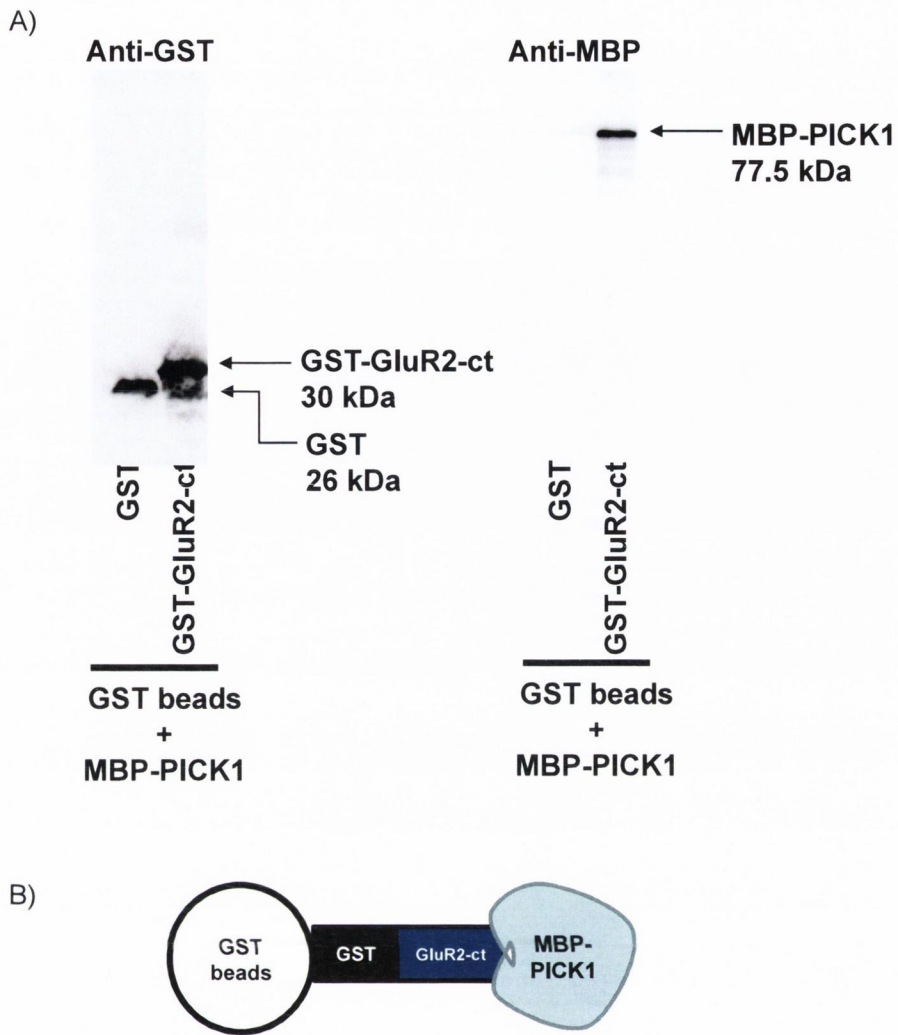


Figure 3.2: GST pull-down experiment showing PICK1-GluR2 interaction

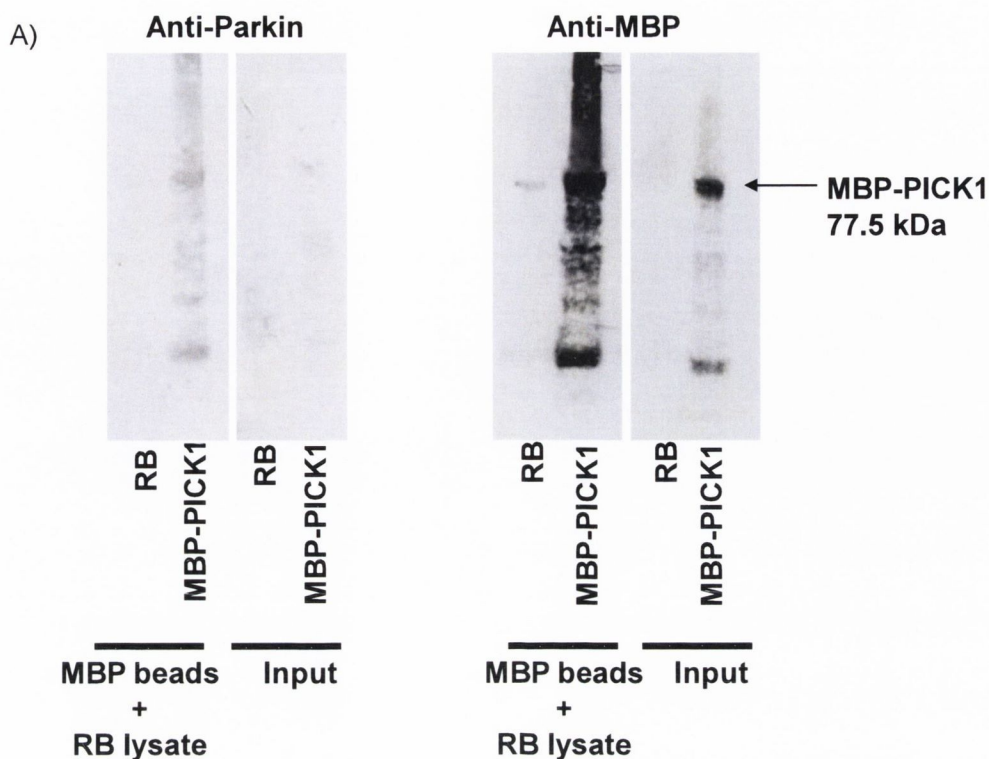
MBP-PICK1 was incubated with GST and GST-GluR2-ct along with GST beads. The samples were boiled in SB buffer, separated in a SDS-PAGE and then western blot was performed with anti-GST and anti-MBP antibody. A) The anti-GST blot showed GST and GST-GluR2-ct bands. In contrast, the MBP-PICK1 band is observed in only the GST-GluR2-ct lane in anti-MBP blot. B) The diagram shows the design of the experiment where GST beads bind with GST tag of GST-GluR2-ct and the associated MBP-PICK1.

3.3 Pull-down of endogenous parkin by MBP-PICK1

To confirm the parkin-PICK1 interaction, MBP pull-down experiments were performed using transformed bacterial lysate expressing MBP-PICK1 and the rat brain lysate as a source of endogenous parkin. MBP-PICK1 was incubated with the rat brain lysate to allow endogenous parkin to interact with MBP-PICK1. The experiments showed that the MBP beads pulled down MBP-PICK1 as determined by western blot using anti-PICK1 antibody. In contrast, no parkin band was detected in the pull-down or in the input fraction as determined by western blot using anti-parkin antibody (**Figure 3.3**). Notably, the absence of a parkin band in the input fraction, suggested that the polyclonal Abcam anti-parkin antibody used in these experiments was not able to detect endogenous parkin. The presence of non-specific bands were also observed in both the anti-parkin and anti-MBP blots, likely due to related binding of the antibodies to the bacterial proteins. In summary, these experiments showed; (1) the Abcam anti-parkin antibody failed to detect endogenous parkin in the rat brain lysate and (2) non-specific bands were detected in the crude bacterial lysate expressing MBP-PICK1 in the anti-parkin and anti-MBP western blots. In the next experiments, transiently transfected HEK293 cells were used to express HA-parkin and Flag-PICK1, and co-IP studies were performed.

3.4 Co-IP experiments using HA-parkin and Flag-PICK1 co-transfected in HEK293 cells

Generally, HEK293 cells are used to transiently over-express proteins of interest. The gene expressing protein of interest is cloned into the mammalian vector and used to transfect HEK293 cells for this purpose. The HA-parkin (pCI) and Flag-PICK1 (pCI) constructs were used to transfect overnight grown HEK293 cells (confluency 60%-80%) by lipofectamine-mediated transfection according to manufacturer's protocol in 6-well plate format. To monitor transfection efficiency, 0.1 µg of pEGFP-C2 was used to transfect a single well of 6-well plate containing HEK293, cells along with the HA-parkin and Flag-PICK1. Transfection was carried out with either HA-parkin (1 µg) and Flag-PICK1 (1 µg) alone or, co-transfecting HA-parkin and Flag-PICK1 (1 µg of each). Transfection efficiency of 30-40% was estimated by pEGFP-C2 expression (excitation/emission spectra = 488/507 nm). After transfection, the cell lysates (500 µl) were prepared from each condition of transfection and incubated with Flag beads. After the western blot analysis, no expression of the HA-parkin was detected by using anti-HA antibody in both input and co-IP fractions of single and double transfection samples (**Figure 3.4**). Low expression of Flag-PICK1 was detected using anti-PICK1 antibody in both single and double transfected samples. In addition, numerous non-specific



B)

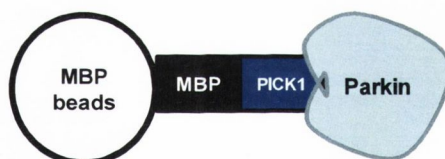


Figure 3.3: MBP pull-down experiment with bacterial expressed MBP-PICK1 and endogenous parkin

Purified bacterial expressed MBP-PICK1 was used to pull down endogenous parkin from rat brain lysate using MBP beads. MBP beads bind the MBP tagged protein (MBP-PICK1) and also the proteins associated with PICK1. In this experiment, rat brain lysate (RB) and MBP-PICK1 were incubated with MBP beads. A) The anti-parkin blot shows no endogenous parkin expression in both pull-down and input fraction except some bands which are likely due to non-specific binding of antibodies to bacterial proteins. The anti-MBP blot shows an MBP-PICK1 (77.50 kDa) in both pull-down blot and 10% input fraction. B) The diagram shows the design of the experiment where MBP beads bind with MBP tag of MBP-PICK1 and associated parkin with MBP-PICK1.

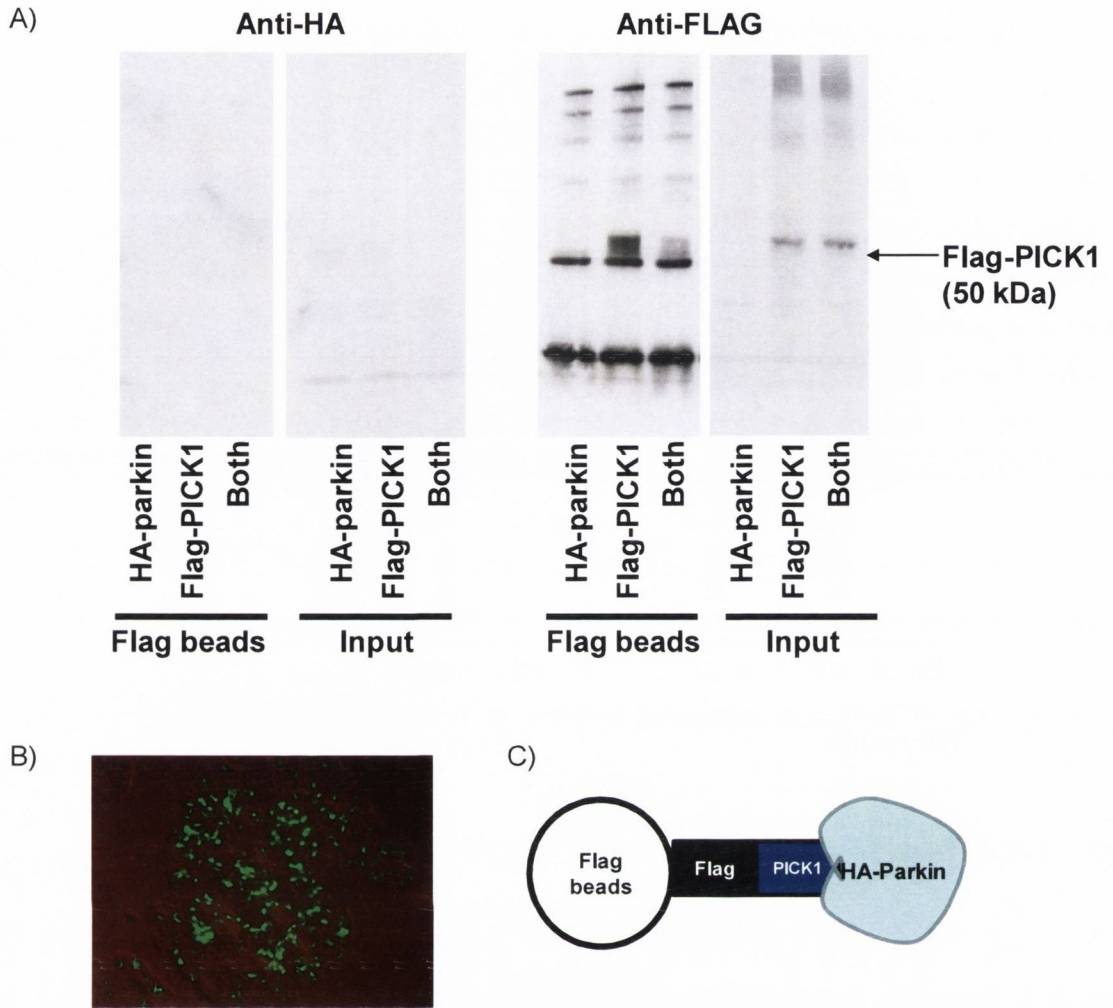


Figure 3.4: Co-IP experiment with transiently transfected HEK293 cells with HA-parkin and Flag-PICK1

HEK293 cells were transiently transfected with HA-parkin and Flag-PICK1 constructs in both single and double transfection format. After making cell lysates, Flag beads were incubated with cell lysates expressing HA-parkin, Flag-PICK1 or both proteins. A) Co-IP blot of anti-HA shows no expression of HA-parkin in both co-IP and input fractions. The anti-Flag blot shows poor expression of Flag-PICK1 (50 kDa) in both co-IP and input fractions. Numerous non-specific bands are visible in the co-IP fraction. B) To estimate the transfection efficiency, the HEK293 cell culture was transfected with pEGFP-C2 vector. The GFP protein fluorescence is visible under 488 nm (transfection efficiency 30-40%). C) The diagram shows the design of the experiment where Flag beads bind with Flag tag of Flag-PICK1 and associated HA-parkin with Flag-PICK1.

bands were detected on the blot incubated with anti-Flag antibody. The absence of HA-parkin expression, suggested that HA-parkin was poorly expressed in these experiments. In summary, these experiments showed; (1) little or no expression of the HA-Parkin, (2) poor expression of the Flag-PICK1 and (3) expression of the non-specific bands probably arising from Flag-beads. In the next experiments, the identification of the non-specific bands (**Figure 3.5**) and use of a parkin Ubl deletion construct for better expression in HEK293 cells (**Figure 3.6**) were investigated.

3.5 Identification of non-specific bands expressed by Flag beads and MBP-beads

The presence of non-specific bands in the anti-Flag blot was further addressed before further use of transiently transfected HEK293 cells to express HA-parkin and Flag-PICK1 in co-IP experiments. Mock experiments with Flag beads and MBP beads were performed to investigate non-specific bands due to antibody cross-reactivity. After incubation and washing the beads, they were directly boiled in SB buffer and loaded into SDS-PAGE gels. The western blots were performed using the alkphos conjugated anti-mouse and anti-rabbit secondary antibodies, separately. Upon development, the Flag bead sample incubated with anti-mouse secondary antibody showed many non-specific bands, indicating mouse antibody cross-reactivity as expected (**Figure 3.5**). This data are in agreement with the non-specific bands found in **Figure 3.4**, where co-IP studies were performed to demonstrate an interaction between parkin and PICK1. In contrast, no non-specific bands were visible in the anti-rabbit antibody incubated blot in Flag bead sample. In addition, the MBP beads did not show bands arising from non-specific reaction in any of the blots. The results suggest that using anti-mouse secondary antibody in the presence of Flag beads will produce non-specific bands that make it difficult to identify a parkin-PICK1 interaction. MBP beads was thus used to determine an interaction between parkin and PICK1.

3.6 Identification of non-specific bands expressed by anti-PRK8 and anti-PICK1 antibody

Due to poor expression of HA-parkin and Flag-PICK1, co-IP of endogenous parkin and PICK1 was performed using rat brain lysate. In previous western blot experiments, the rabbit anti-parkin antibody, used to detect endogenous parkin did not provide strong signal or good specificity (**Figure 3.3**). For this reason, an alternative antibody for parkin, mouse anti-PRK8 was next used for co-IP (Pawlyk et al., 2003). To first evaluate whether the anti-

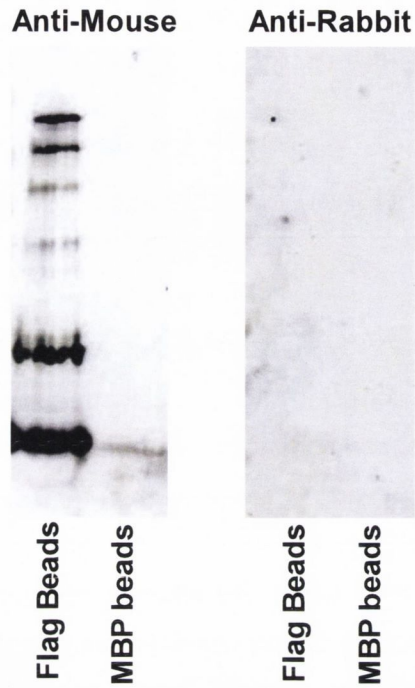


Figure 3.5: Identification of non-specific bands expressed by Flag beads

Flag beads and MBP beads were incubated, washed, boiled in SB buffer and then western blot was performed. The anti-mouse blot shows numerous non-specific bands expressed by Flag beads sample. No bands were visible from MBP beads sample. In the case of the anti-rabbit blot, no non-specific band was visible in either of the samples.

PRK8 antibody itself is capable of producing non-specific bands in the western blots, mouse anti-PRK8 antibody (1 μ l) was incubated with sepharose beads as in a co-IP experiment. As a negative control, sepharose beads alone were incubated. In addition, rabbit anti-PICK1 antibody (1 μ l) and sepharose beads were also incubated. After incubation and washing the beads, they were boiled in SB buffer and loaded onto SDS-PAGE gels. The western blots were performed with mouse anti-PRK8 and rabbit anti-PICK1 antibodies, and then incubated with corresponding alkphos conjugated secondary antibodies, i.e., anti-mouse (BLOT A) and anti-rabbit (BLOT B), respectively (**Figure 3.6A**). The blots were also directly incubated with secondary anti-mouse (BLOT C) and anti-rabbit (BLOT D) antibodies, without primary anti-PRK8 or anti-PICK1 antibodies (**Figure 3.6B**). Upon development of the blots, mouse anti-PRK8 antibody revealed strong non-specific bands in those blots where anti-mouse secondary antibodies were used (BLOT A and BLOT C). The rabbit anti-PICK1 lanes also showed non-specific bands in those blots, where anti-rabbit secondary antibody was used (BLOT B and BLOT D). None of the blots demonstrated any non-specific bands by the negative control (sepharose beads only), confirming that the non-specific bands were due to immunogenic cross-reactivity of mouse anti-PRK8 and rabbit anti-PICK1 antibodies. The data suggest that mouse anti-PRK8 antibody is capable of producing non-specific bands, when incubated with the corresponding anti-mouse secondary antibody. In addition, the rabbit anti-PICK1 antibody shows immunogenic cross-reactivity with the corresponding anti-rabbit secondary antibody. Taken together, these data showed the technical difficulties in conducting co-IP experiments to show a PICK1-parkin interaction. The presence of non-specific bands at similar molecular weights as parkin and PICK1 (approximately 50 kDa) add to these challenges.

3.7 Pull-down of HA-parkin Δ Ub by MBP-PICK1

Full length parkin showed poor expression, when transiently expressed in HEK293 cells (**Figure 3.4**), in agreement with the published data (Finney et al., 2003). Thus, a deletion construct of parkin was used for expression in HEK293 cells. The Ubl domain of parkin is reported to regulate the expression of parkin and deleted Ubl domain construct of parkin is shown to increase its own protein expression (Finney et al., 2003). To obtain a detectable expression of parkin, overnight grown HEK293 cells were transfected with the HA-parkin Δ Ub (1 μ g). To monitor transfection efficiency, 0.1 μ g of EGFP-C2 was used to transfect a single well of 6-well plate containing HEK293 cells along with HA-parkin Δ Ub (estimated transfection efficiency 50-60%). Upon western blot analysis, the expression of HA-parkin Δ Ub was detected by using anti-HA antibody in cell lysate of single transfection samples. Equal amounts of purified MBP and MBP-PICK1 (400 μ g each) were incubated with the cell lysate

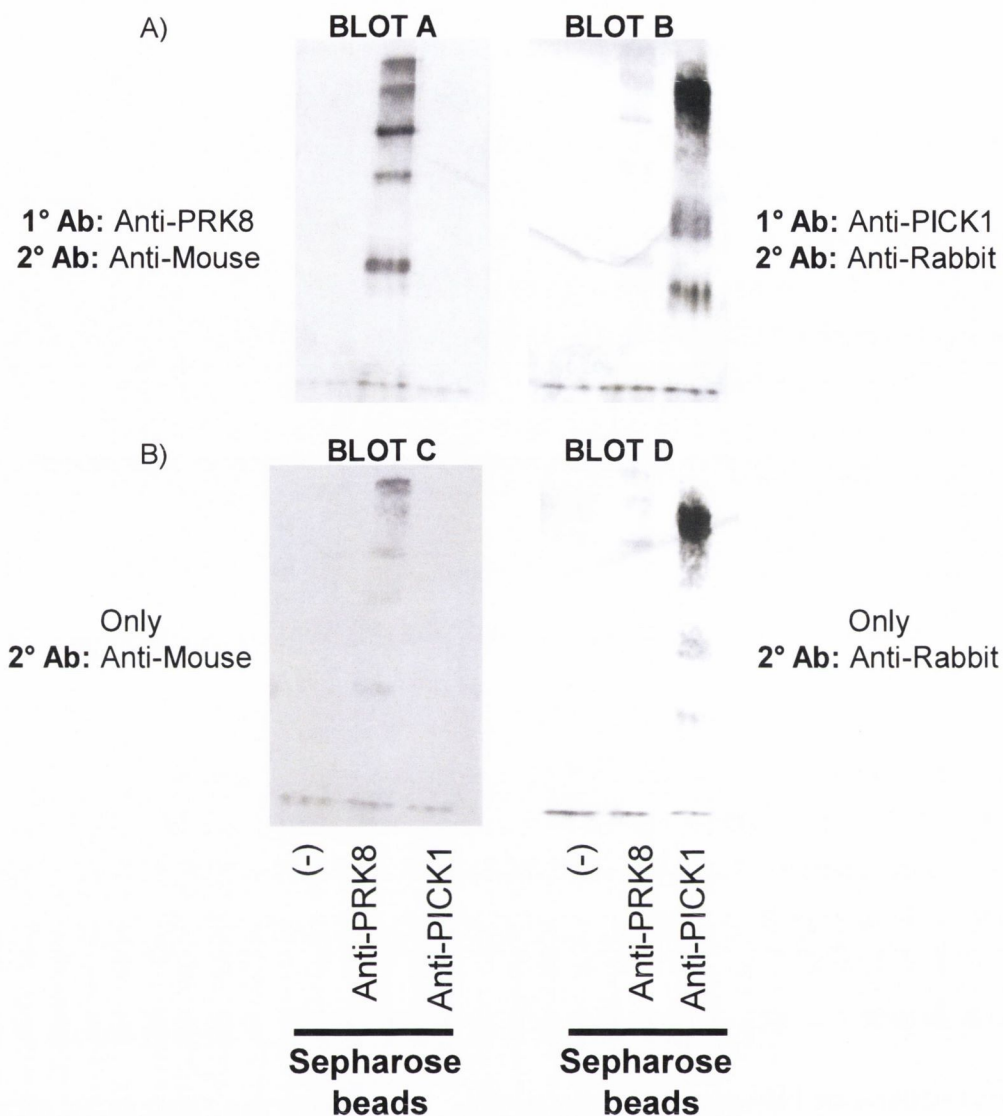


Figure 3.6: Identification of non-specific bands expressed by anti-PRK8 and anti-PICK1 antibodies

Anti-PRK8 and anti-PICK1 antibodies were incubated with sepharose beads along with only sepharose beads, as the negative control (-). Upon incubation and washing, the sepharose beads of each sample were boiled in SB buffer and separated on SDS-PAGE. Thereafter the western blot was performed. A) BLOT A was treated with anti-PRK8 antibody (1° Ab) and anti-mouse antibody (2° Ab). BLOT B was treated with anti-PICK1 antibody (1° Ab) and anti-rabbit antibody (2° Ab). B) BLOT C and D were treated with only anti-mouse and anti-rabbit antibody (2° Ab), respectively.

expressing HA-parkin Δ Ub separately, along with MBP beads. The MBP beads were then boiled in SB buffer and separated in SDS-PAGE. The western blots were performed with anti-HA and anti-MBP antibodies (**Figure 3.7**). The anti-HA blot demonstrated high expression of HA-parkin Δ Ub in input fraction. Likewise, high expression of MBP and MBP-PICK1 expression were found in the anti-MBP blot in both the pull-down and input fractions. The data showed no association between the ubiquitin domain deleted version of parkin (HA-parkin Δ Ub) and PICK1. This lack of parkin-PICK1 interaction may be due to deletion of the Ubl domain of parkin, which may indirectly regulate the interaction of parkin with PICK1.

3.8 Production of lentiviral constructs of HA-parkin and HA-parkin Δ pdz

Previous data showed that the use of transiently expressed HA-parkin demonstrated poor expression of full length HA-parkin (**Figure 3.4**). As an alternative, lentivirus-mediated transfection can be used as efficient way of expressing a protein of interest *in vitro* and *in vivo*. Thus, to overcome expression issues of parkin, a lentiviral construct expressing full length parkin was designed to express this protein in neurons. Having already Flag-PICK1 lentiviral constructs in the laboratory, a HA-parkin lentiviral construct was constructed. The primers were designed to amplify HA-parkin and HA-parkin with mutated PDZ motif (FDV/AAA). Amplified HA-parkin and HA-parkin Δ pdz were separated in 2% agarose gel. After digestion of the PCR products and pLenti-PGK-GFP vector with *Ascl* and *RsrII*, cloning reactions were performed. After transformation, the colonies were screened for correct HA-parkin and HA-parkin Δ pdz constructs. Successful constructs were reconfirmed by commercial sequencing (**Figure 3.8**). The sequencing data confirmed successful cloning of full length HA-parkin and HA-parkin Δ pdz constructs. However, due to the unavailability of lentiviral facility, further work with these HA-parkin and HA-parkin Δ pdz lentiviral constructs was not performed.

3.9 Binding of MNP201 in PDZ domain of MBP-PICK1 in fluorescence polarisation assay

The next approach to determine the binding of MNP201 with PICK1 was by use of a previously described fluorescence polarisation assay (**Figure 3.9A**) (Madsen et al., 2005). In this assay, competitive binding experiments were performed using a fixed concentration (40 nM) of the Oregon Green fluorescently labelled last 13 amino acids of DAT ct (OG-DAT-C13) and fixed concentration of purified PICK1 (0.45 μ M). As the ct PDZ motif

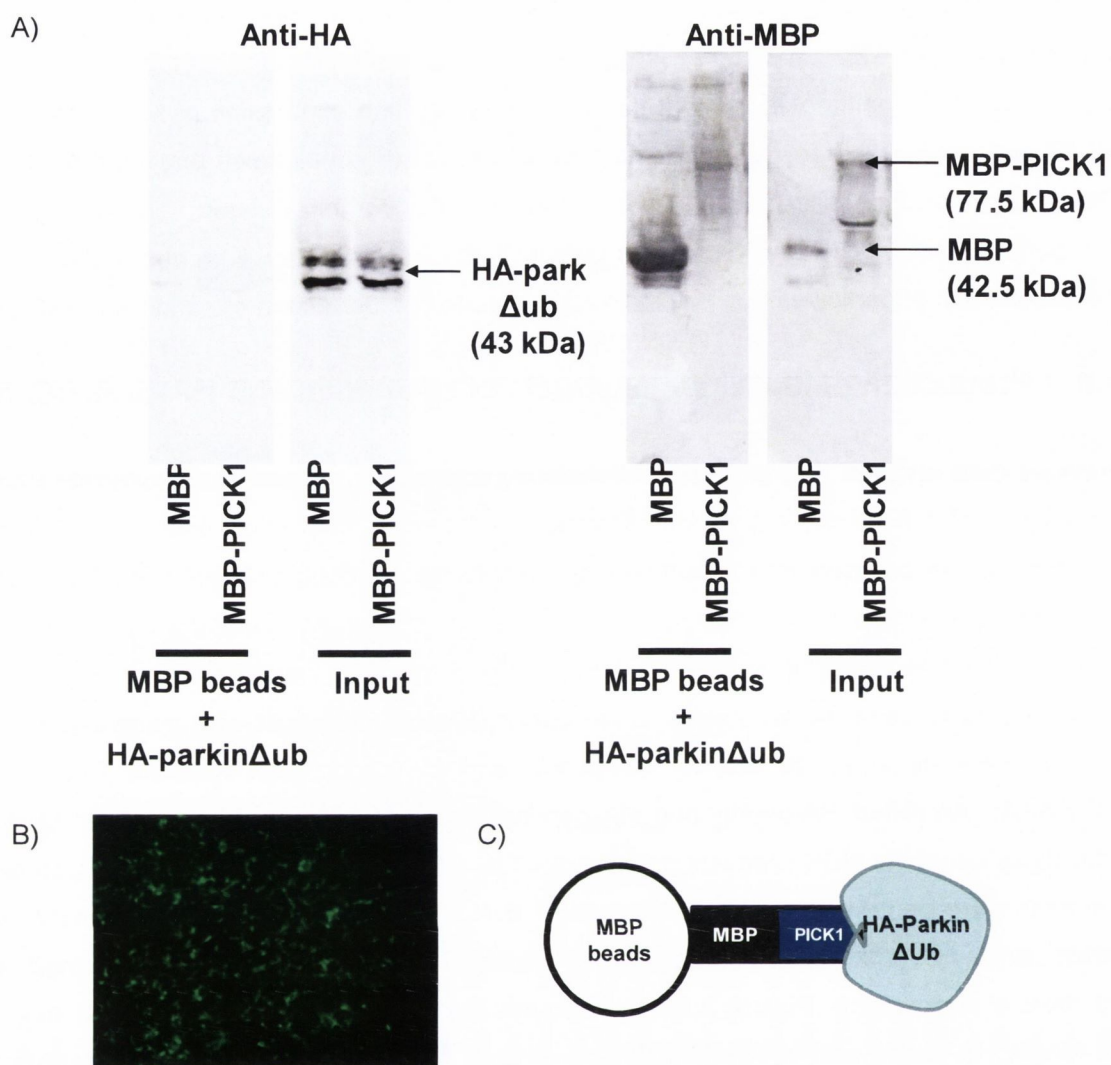


Figure 3.7: MBP pull-down experiment with bacterial expressed MBP-PICK1 and transiently transfected HEK293 cells with HA-parkin Δ Ub

HEK293 cells were transiently transfected with HA-parkin Δ Ub. After making cell lysate, the HA-parkin Δ Ub containing cell lysate and MBP beads were incubated with purified MBP and MBP-PICK1. After separating the samples in SDS-PAGE, western blot was performed. A) The blot of anti-HA shows no band of HA-parkin Δ Ub in pull-down fractions, although input fractions show good expression of HA-parkin Δ Ub (43 kDa). On the other hand, anti-MBP blot shows good expression of MBP and MBP-PICK1 (77.50 kDa) in pull-down and input fractions. B) To estimate the transfection efficiency, HEK293 cell culture was transfected with pEGFP-C2 vector (transfection efficiency 50-60%). The GFP protein fluorescence is visible under 488 nm. C) The diagram shows the design of the experiment where MBP beads bind with MBP tag of MBP-PICK1 and associated HA-parkin Δ Ub with MBP-PICK1.

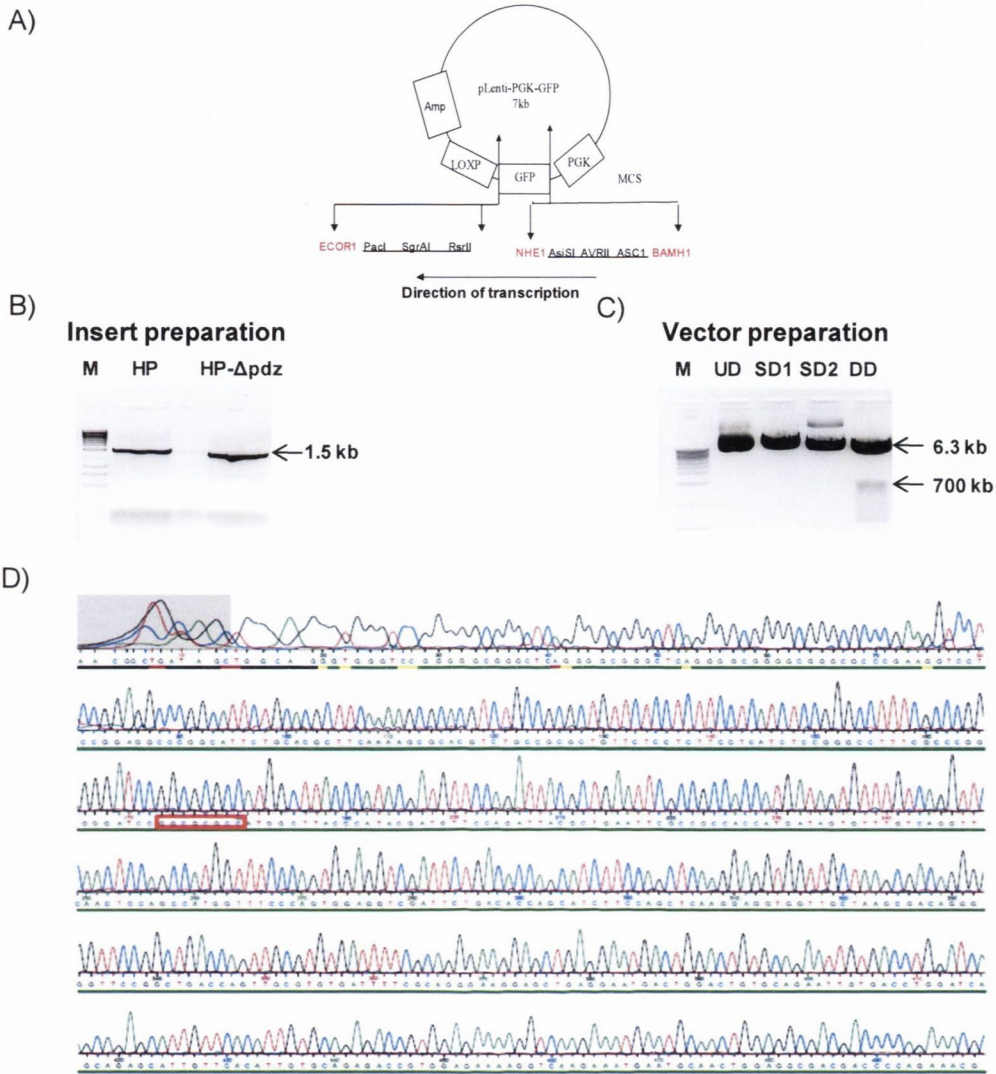


Figure 3.8: Cloning of Lenti-HA-parkin and Lenti-HA-parkinΔpdz

A) The vector map of pLenti-PGK-GFP (7 kb) shows multiple cloning sites flanking along GFP gene. This vector has an ampicillin resistant gene. B) PCR amplified insert of HA-parkin (HP) and HA-parkinΔpdz (HP-Δpdz) were separated in 2% agarose gel along with 1.5 kb DNA marker band (M). C) The vector was digested with Ascl and RsrII in both single and double digestion. After digestion of pLenti-PGK-GFP vector, the undigested (UD), digested with Ascl (SD1), digested with RsrII (SD2) (6.3 kb) and double digested (DD) fractions were separated in 2% agarose gel. Notably, the GFP gene (700 kb) separates out from the double digested vector. D) The chromatogram of HA-parkin in p-Lenti-PGK vector ensures the successful cloning. The red box indicates the recognition site of Ascl and nucleotides following the red box show the initiation codon (ATG) of HA-parkin.

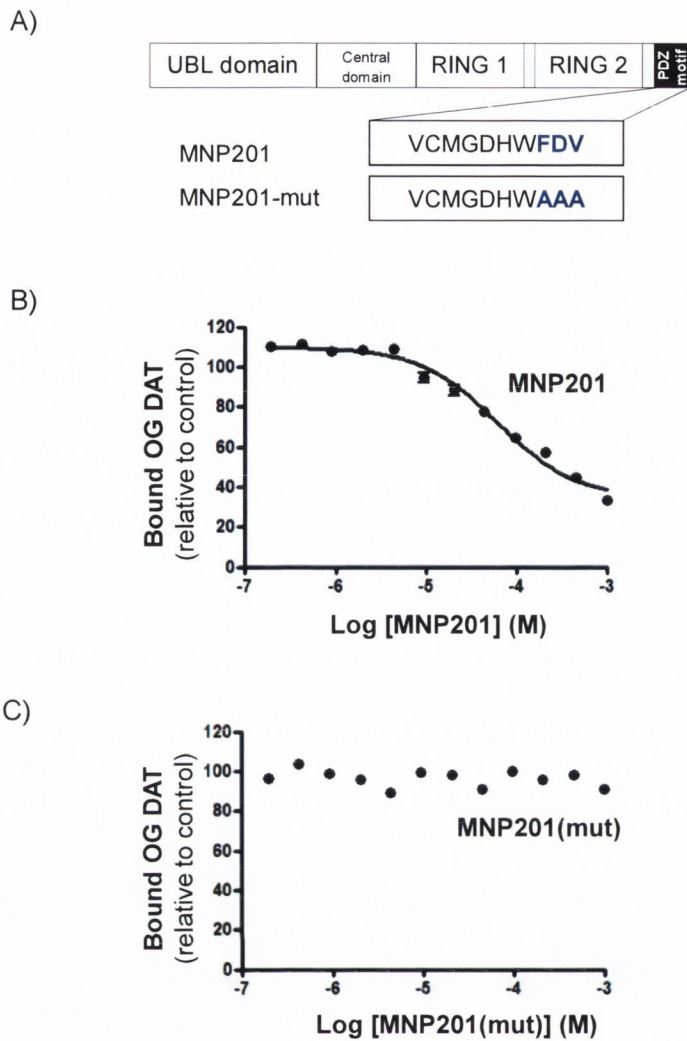


Figure 3.9: Binding of MNP201 in PDZ domain of PICK1

By using fluorescence polarisation assay, the binding of the parkin peptide MNP201 to PICK1 was evaluated. A) MNP201 was modelled according to the ct 10 amino acids of parkin. A mutated version, MNP201(mut), was also designed where the PDZ motif was mutated (FDV/AAA). B) In the graph, the decrease of bound OG DAT signifies that MNP201 competitively replaced OG-DAT-C13 peptide in a dose-dependent manner. C) When MNP201(mut) was introduced in increasing concentrations, no replacement of OG-DAT-C13 peptide was observed.

of DAT interacts with the PDZ domain of PICK1 (Torres et al., 2001), the OG-DAT-C13 binds to the PDZ domain of PICK1 (Madsen et al., 2005; Thorsen et al., 2010). When the MNP201 was titrated, a gradual reduction of Green Oregon fluorescence was observed with the dose-dependent increase of MNP201 (**Figure 3.9B**). The reduction of OG-DAT-C13 fluorescence with the increasing concentration of MNP201 indicated the competitive replacement of OG-DAT-C13 from the PDZ domain of PICK1 by MNP201 in a dose-dependent manner. When the MNP201(mut) was used in the same competition binding assay, no reduction of the OG-DAT-C13 fluorescence was found with the dose-dependent increase of MNP201(mut) (**Figure 3.9C**). Taken together, the data suggest that MNP201 peptide binds the PDZ domain of PICK1 in a dose-dependent manner and last three ct amino acids of MNP201 (FDV) are crucial for interaction with PDZ domain of PICK1. This experiment was performed by our collaborator Prof. Ulrick Gether, Molecular Neuropharmacology Group, Department of Neuroscience and Pharmacology, University of Copenhagen, Denmark.

Discussion

Recent studies have shown an interaction between parkin-PICK1 (Joch et al., 2007). To demonstrate the parkin-PICK1 interaction, a set of biochemical binding assay were undertaken. In addition, the binding of a parkin PDZ motif peptide (MNP201) to PICK1 was also demonstrated. The outcomes and the issues concerning these experiments are summarised below.

- 1) Firstly, to standardise the GST pull-down protocol, the interaction of PICK1-GluR2 was demonstrated (Dev et al., 1999). Using MBP beads incubated with bacterial expressed MBP-PICK1 and GST-GluR2-ct, the association of PICK1-GluR2 was demonstrated by pull-down experiments.
- 2) After standardising the pull-down protocol using the PICK1-GluR2 interaction, a MBP pull-down experiment with bacterial expressed MBP-PICK1 and endogenous parkin was performed. Due to poor specificity of the rabbit anti-parkin antibody, endogenous parkin was not detected.
- 3) Next, co-IP studies were performed using transiently expressed HA-parkin and Flag-PICK1. In these experiments, no expression of full length HA-parkin and poor expression of Flag-PICK1 were observed. In addition, numerous non-specific bands were observed in co-IP experiments. Mock co-IP studies with Flag beads revealed non-specific bands, when blots were incubated with secondary anti-Mouse antibody, indicating antibody cross-reactivity. These studies suggested technical limitations in using the Flag beads to investigate the association of transiently expressed Flag-PICK1 with HA-parkin. Notably, these antibody cross-reactivity studies also showed that MBP beads did not result in non-specific bands when exposed to secondary mouse and rabbit antibodies. The MBP beads were subsequently chosen for future pull-down experiments.
- 4) The co-IP experiments from rat brain lysate also faced technical limitations as the anti-PRK8 and anti-PICK1 antibodies showed antibody cross-reactivity. Thus, the use of MBP pull-down studies with MBP-PICK1 incubated with endogenous parkin or parkin obtained from transiently expressed mammalian cell lines were used to determine parkin-PICK1 interaction.
- 5) To overcome the issue of expression of full length parkin, a parkin mutant (Ubl domain deletion) construct was employed to transiently transfect HEK293 cells. The Ubl deleted parkin is reported to have better expression profile than the full length parkin (Finney et al., 2003). In these experiments, a detectable amount of HA-Parkin Δ Ubl was obtained, as

determined by anti-HA blot. When co-IP experiments were performed using MBP beads with cell lysate expressing HA-Parkin Δ Ub and purified MBP-PICK1, no interaction between parkin and PICK1 was observed. The reason behind this failure could be due to MBP-PICK1 obtained from bacterial system and the lack of the correct post-translational modification needed to interact with parkin and/or due to use of an Ubl deleted parkin, which may limit interaction with PICK1.

- 6) To obtain a mammalian source of parkin, lentiviral HA-parkin and HA-parkin Δ pdz constructs were prepared. A lentiviral Flag-PICK1 construct was already available in our laboratory. These constructs enabled the study of the parkin-PICK1 interaction in both biochemical approaches or by immunocytochemistry studies. However, due to practical issues (i.e., availability of lentiviral culture facility) further work using these constructs was limited.
- 7) The parkin blocking peptide, MNP201, is designed according to the last 10 amino acids of parkin ct. According to the data of Joch et al., 2007, the last three amino acids of parkin ct constituting a PDZ motif are essential for the interaction with PDZ domain of PICK1 (Joch et al., 2007). As MNP201 contains the PDZ motif of parkin, the binding of MNP201 with the PDZ domain of PICK1 would indicate an association between parkin and PICK1. Thus, the final approach taken, was to examine the binding of MNP201 to PICK1 using a fluorescence polarisation assay. Our collaborator Prof. Ulrick Gether, Copenhagen, Denmark, successfully showed that MNP201 (VCMGDHW**FDV**) binds with the PDZ domain of PICK1 in a concentration-dependent manner by replacing Oregon labelled DAT-13 peptide, a known binding partner of the PDZ domain of PICK1. In contrast, the MNP201(mut), i.e., the mutated PDZ motif version of MNP201 (VCMGDHW**AAA**) did not show any specificity towards PICK1. In summary, these data suggest that the MNP201 binds to the PDZ domain of PICK1 through the last three amino acids of MNP201 (-FDV), in agreement with previously published data (Joch et al., 2007). The data also indicate that the last three amino acids of ct-parkin are required for interaction with PICK1.

As a future direction, the biochemical validation of MNP201 in blocking interaction between parkin and PICK1 would be valuable. Parkin is reported to translocate specifically towards depolarized mitochondria to play a role in recruitment of autophagosomes for mitophagy under depolarization stress condition (Narendra et al., 2008). Thus, an alternative approach to show the parkin-PICK1 interaction would be by expressing lentiviral HA-parkin in neurons and determining its translocation and/or association with mitochondria in the presence and absence of lentiviral-mediated Flag-PICK1 expression, and with or without MNP201 treatment of neurons under normal and stressed conditions. Assuming the hypothesis that

PICK1 causes translocation of parkin to the mitochondria, then the overexpression of PICK1 should promote parkin association with the mitochondria while MNP201 would block the parkin-PICK1 interaction and limit parkin translocation towards the depolarized/stressed mitochondria. In the next chapter, the effects of MNP201 on mitochondrial function were examined.

4. Results: 2
Effect of MNP201 on
mitochondrial function

Abstract

Previous studies have shown that the ct PDZ motif of parkin interacts with the PDZ domain of PICK1 (Joch et al., 2007). In the previous chapter, a parkin peptide (MNP201) was designed based on the last 10 residues of ct-parkin containing a PDZ motif. This MNP201 peptide was shown to competitively displace the binding of a fluorescently tagged PDZ motif peptide from the PDZ domain of PICK1. The aim of this current chapter was to investigate the role of the parkin-PICK1 interaction in the mitochondrial function by using MNP201. It was hypothesised that the MNP201 parkin peptide would bind to PICK1 and inhibit its interaction with parkin, which would in turn alter mitochondrial function. Specifically, the effects of the MNP201 peptide was tested on mitochondria based assays including respiratory chain (complex I and IV) activity, ROS production and mitochondrial membrane potential stability. Since PICK1 is known to interact with the AMPA receptor subunit, GluR2; the KA receptor subunit, GluR5 and the metabotropic receptor mGluR7, the effects of MNP201 was also investigated on glutamate release using fresh rat brain synaptosomes. The data showed that MNP201 did not alter any of the mitochondrial parameters investigated nor did it alter glutamate release. The lack of effects of MNP201 was attributed to poor synaptosomal permeability of this peptide, which was further investigated by fusing MNP201 to Trojan peptides in the following results chapter.

Introduction

In recent years, mitochondrial dysfunction has been identified as a key molecular mechanism underlying PD (Beal, 1992; Doble, 1999; Lin and Beal, 2006). Many reports published in the last two years have given important insights about the involvement of parkin in mitochondrial maintenance during stress and selective elimination of malformed mitochondria (Narendra et al., 2008; Twig et al., 2008; Poole et al., 2008, 2010; Geisler et al., 2010; Ziviani et al., 2010). Parkin, otherwise found in the cytosol, has been shown to selectively traffic to engulf depolarized mitochondria to promote autophagy, before the malfunctioned mitochondria can trigger apoptotic signals (Narendra et al., 2008). On the other hand, PICK1, a scaffolding kinase recruiting protein has been shown to resist against Bax-induced apoptosis by recruiting PKC α to phosphorylate the Bcl-2 protein in the outer mitochondrial membrane (Wang et al., 2007). Taken together, these two proteins, directly or indirectly, confer resistance against mitochondrial apoptosis. Intriguingly, parkin and PICK1 interact with each other through a PDZ motif-domain interaction (Joch et al., 2007). Upon interaction, parkin causes monoubiquitination of PICK1, but does not promote degradation of PICK1 (Joch et al., 2007). In addition, parkin indirectly regulates PKC-mediated ASIC2a current via monoubiquitination of PICK1 (Joch et al., 2007). It has also been shown that parkin has no influence in the sub-cellular localisation of PICK1 (Joch et al., 2007). However, no studies to date have investigated whether PICK1 has a role to play in the sub-cellular localisation or trafficking of parkin to mitochondria or in mitochondrial maintenance, especially in neurons. According to our hypothesis, PICK1 may traffic parkin towards mitochondria and thereby regulate mitochondrial function.

The PDZ domain of PICK1 is a multi-protein interacting site through which numerous proteins, including PKC α , GluR2 and parkin interact to influence phosphorylation events and synaptic transmission (Staudinger et al., 1995; Dev et al., 1999; Joch et al., 2007). To investigate the role of PICK1 in neuronal function, many groups have employed the use of blocking peptides, which bind the PDZ domain of PICK1 and inhibit PICK1 interactings. The blocking peptides used have, in general, comprised amino acid stretches of 5-10 residues. These blocking peptides have been based on the extreme ct sequences of PICK1 interacting partners, thus containing the essential PDZ motifs required to interact with the PDZ domain of PICK1. The blocking peptides used have been shown to block PICK1 interactions by competitive inhibition. Many reports have been published demonstrating effects of these blocking peptides in physiological function. For example, GluR2 blocking peptides, based on the PDZ motif of GluR2, block the PICK1-GluR2 interaction and have been shown to block LTD in hippocampal neurons (Daw et al., 2000). Other PDZ domain containing proteins have

also been blocked from interacting with GluR2 using blocking peptides, for example GRIP and syntenin (Li et al., 1999). Similar to these studies, an MNP201 (VCMGDHWFDV) parkin peptide was designed, according to the last ten C-terminal amino acids of parkin (**Figure 3.1**) based on the interaction study by Joch et al. (2007). Data from the previous chapter (Result 1) (**Figure 3.9**) indicated that the parkin blocking peptide (MNP201) competitively inhibits binding of DAT-13 peptide to PICK1, suggesting an interaction of MNP201 with the PDZ domain of PICK1. Here, this peptide was used to investigate the role of the parkin-PICK1 interaction in mitochondrial function and glutamate release.

Mitochondrial function is mainly attributed to fulfilling the energy requirement of the cell, Ca^{2+} homeostasis maintenance and the regulation of apoptosis. In mitochondria, during energy production by the ETC-mediated oxidative phosphorylation, ROS species are formed as byproducts (Henchcliffe and Beal, 2008). Regulation of this ROS production is crucial for proper cell function, where failure to remove ROS results in oxidative stress, causing decreased mitochondrial membrane polarisation and triggering of apoptotic pathways (Galley, 2011; Perry et al 1996). Analysis of SNPC brain samples derived from PD patients has shown extensive reduction in the activity of complex I enzyme (Schapira et al., 1990) and related ROS production. In addition, parkin-KO mice showed respiratory impairment in complex I and IV of ETC (Palacio et al., 2004). Importantly, certain parameters of mitochondria can be monitored, including activity of respiratory enzymes, ROS production and changes in mitochondrial membrane potential to identify mitochondrial dysfunction. According to our hypothesis, if the parkin-PICK1 interaction plays a role in mitochondrial function, changes in mitochondrial parameters in the presence of the parkin blocking peptide (MNP201) should be expected. Therefore, in this chapter, the effects of parkin blocking peptide (MNP201, wildtype and mutant versions) were tested on the activity of respiratory enzymes, ROS production level and change in mitochondrial membrane potential.

The effects of MNP201 on glutamate release were also investigated; there were three reasons for doing so. Firstly, Ca^{2+} sequestration is another important role that mitochondria play to maintain cellular physiology. Mitochondria harbour high amounts of Ca^{2+} in the mitochondrial matrix that remains under a dynamic equilibrium with the cytosol to regulate the cytosolic Ca^{2+} levels (Nicholls and Budd, 2000; Gunter and Sheu, 2009). The regulation of cytosolic Ca^{2+} levels is crucial as Ca^{2+} in the cytosol plays an important role in synaptic transmission and secondary messenger signalling. Particularly, the Ca^{2+} -dependent vesicular release in neurons are sensitive to cytosolic Ca^{2+} influx, which may lead to excitotoxic injury (Choi, 1994). It was hypothesised that if parkin alters mitochondrial function then a change in mitochondrial Ca^{2+} sequestration, cytosolic Ca^{2+} levels and thus glutamate

release would be detected in response to treatment of synaptosomes with MNP201. The second reason for examining the effects of MNP201 on glutamate release was that parkin over-expression diminishes ASIC2a current by monoubiquitination of PICK1 (Joch et al., 2007), which may also play a role in regulating intracellular Ca^{2+} levels and thus alter the release of glutamate. Thirdly, since MNP201 can displace PDZ motifs from interacting with the PDZ domain of PICK1, it could prevent a number of other proteins from interacting with PICK1. In relation to glutamate release, PICK1 interacts with AMPA, kainate and metabotropic receptors, all of which have been found at pre-synaptic sites and alter glutamate release and all of which may be altered by MNP201.

In summary, in this chapter, the effects of MNP201 were demonstrated on various mitochondrial parameters and glutamate release using isolated nerve terminals or synaptosomes. As a negative control, another set of peptides (MNP202) based on the extreme C-terminus of another E3 ligase, Cdc4 α , was used.

Results

4.1 Design and use of MNP202

The MNP201 parkin peptide (**Figure 3.1**) was modelled, according to the last 10 amino acids of parkin's extreme ct. In addition, peptides modelled on the last 10 amino acids of ct of an unrelated E3 ligase, Cdc4 α , was designed. The Cdc4 α protein is a novel F-box containing subunit of SCF E3 ligase complex that acts in concert with parkin to ubiquitinate a series of substrates (Staropoli et al., 2003). Two versions of Cdc4 α peptides, MNP202 (LVLDFDVK) and MNP202(mut) (LVLDFDVAAA) were used. The MNP202 and MNP202(mut) were dissolved in PBS buffer to make a stock solution of 2 mM. These peptides were ordered from Peptide 2.0, USA. The HPLC purity of MNP202 and MNP202(mut) were found to be 93.75% and 94.78% respectively. The list of peptides and their HPLC purity profiles are shown in **Figure 4.1** and were provided by Peptide 2.0, USA.

4.2 The ct of Cdc4 α does not interact with PICK1

As mentioned, Cdc4 α is an F-box containing protein subunit of large SCF E3 ligase complex. As negative control, the MNP202 peptide on the last 10 amino acids of Cdc4 α ct was modelled. Before using the MNP202 peptides, it was necessary to assess a possible interaction between PICK1 and Cdc4 α ct. The last 108 bp of Cdc4 α ct was cloned into a yeast two hybrid vector, pGBKT7, expressing the last 36 amino acids of Cdc4 α ct and named as Cdc4-ct (BAIT). To amplify the extreme ct of Cdc4 α , a pair of primers was generated carrying restriction sites, i.e., EcoRI in the forward primer and BamHI in the reverse primer, so that after restriction digestion, the PCR amplified fragment had flanking overhangs of these restriction sites. After PCR, the insert was digested and purified by PCR purification kit (Qiagen) (**Figure 4.2A**). In parallel, the pGBKT7 digested vector was dephosphorylated using alkaline phosphatase (**Figure 4.2B**). Upon purification, a ligation reaction was performed. The ligated vector was used to transform competent cells and the overnight grown recombinant bacterial cell culture was used to extract the Cdc4-ct construct in pGBKT7. To confirm the cloning, the Cdc4-ct (BAIT) construct was sent for sequencing. The sequencing result confirmed the successful cloning of Cdc4-ct into pGBKT7 (**Figure 4.2C**). Thereafter, a yeast two hybrid experiment using Cdc4-ct (BAIT) and PICK1 (FISH) was performed. A positive control {PICK1 (FISH)-GluR2-ct (BAIT)} and an empty vector negative control {pGAD10 (FISH)-pGBKT7 (BAIT)} were included in all yeast two hybrid experiments. The results showed that the full-length PICK1

A)

Name	Domain	Motif	Peptide sequences
MNP202	n/a	Cdc4	LVLDFDVDMK
MNP202(mut)	n/a	Cdc4	LVLDFDVAAA

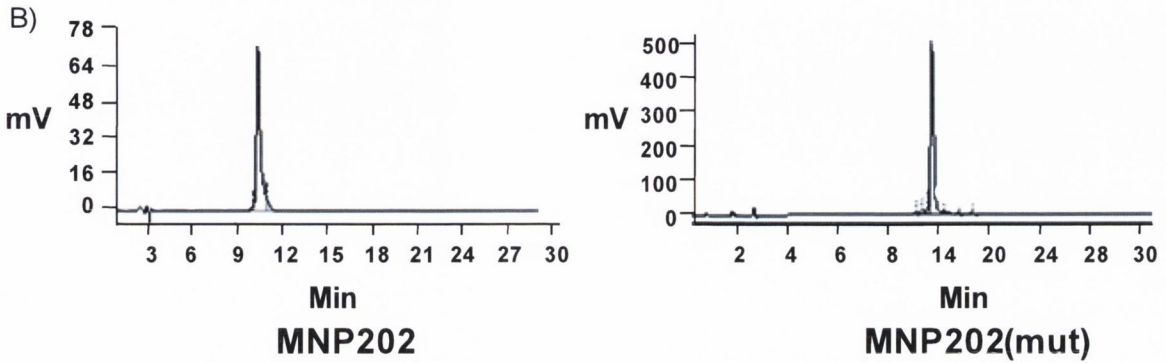


Figure 4.1: List of peptides based on ct of Cdc4 α

A) The MNP202 peptides are modelled on the ct of Cdc4 α (as control) are shown in the table. B) The HPLC purity of these peptides, measured in 220 nm, was found to be 93.75% (MNP202) and 94.78% (MNP202 mutant). The Cdc4 α peptides were ordered from Peptide 2.0, USA.

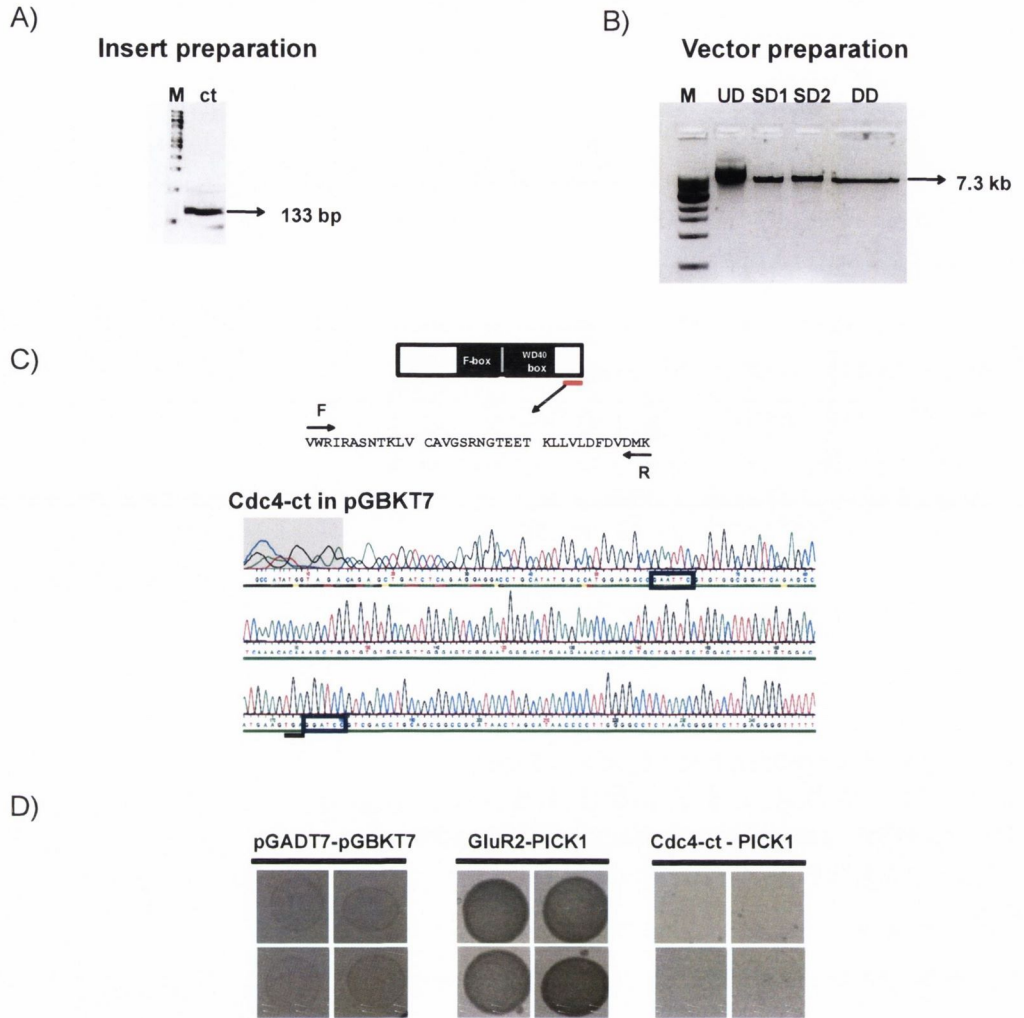


Figure 4.2: Yeast two hybrid assay shows no interaction between Cdc4 α and PICK1

A deletion construct, expressing the last 36 amino acids of Cdc4 α ct, was cloned into the yeast two hybrid vector pGBKT7. A) PCR fragment of 133 bp, encoding the last 36 amino acids of Cdc4 α ct, is shown in 2% agarose gel with DNA marker. B) Digestion of vector DNA was carried out with EcoRI and BamHI. Double digested pGBKT7 (DD) is shown in 2% agarose gel along with marker (M), undigested DNA (UD), EcoRI digested (SD1) and BamHI digested (SD2). C) The chromatogram of successfully cloned construct of Cdc4-ct with the restriction sites (inside the rectangles) EcoRI and BamHI is shown. D) Cdc4-ct (FISH) was tested with PICK1 (BAIT) in yeast two hybrid assay. Representative negative controls (pGBKT7 and pGADT7) and positive (GluR2-ct and PICK1) controls are also shown. Data is representative of three experiments (n=3).

(FISH) did not interact with the Cdc4-ct (BAIT) (**Figure 4.2D**), whereas positive and negative controls indicated growth and no growth of yeast colonies, respectively. The data suggest that PICK1 does not interact with the Cdc4-ct and the MNP202 peptides modelled on Cdc4 α could be used as negative controls in the mitochondrial assays.

4.3 Synaptosomes contain both parkin and PICK1

Following two apparently separate pathways, both parkin and PICK1 have been reported to be associated with mitochondria (Narendra et al., 2008; Wang et al., 2007). Thus, the effects of the parkin blocking peptides and control peptides were investigated on the activities of ETC respiratory chains, including complex I and IV. In addition, the effects of these MNP201 parkin peptides were investigated on production of ROS and mitochondrial membrane potential. Further, the effect of MNP201 on glutamate release assay was tested.

Both parkin and PICK1 are reported to be present in mammalian brain. To demonstrate the expression of parkin and PICK1, rat brain synaptosomes were extracted from mature wistar female rat (150-200 g body weight) brains using Ficoll gradient. Western blot analysis was performed to detect the amount of parkin and PICK1 in synaptic and non-synaptic fractions of rat brain. To identify the levels of parkin and PICK1, anti-PRK8 and anti-PICK1 antibodies were used. The western blots showed presence of parkin and PICK1 in both synaptic and non-synaptic fractions (**Figure 4.3**). The data suggest that synaptosomes derived from rat brain contain relative higher amount of parkin and PICK1 compared to non-synaptic fractions.

4.4 Effect of MNP201 on complex I assay

ETC deficiencies have been implicated in the pathogenesis of PD, where a 35-40% reduction in the activity of complex I has been reported in post-mortem samples obtained from PD patients (Schapira et al., 1989). Complex I utilises NADH as a source of electrons and passes these electrons to complex III via ubiquinone (**Figure 4.4A**). The complex I activity was measured by the rate of conversion of NADH to NAD⁺ spectrophotometrically at absorbance 340 nm, as suggested by previous publications (Telford et al., 2010). Freeze-fractured synaptosomes were treated with 100 μ M of parkin peptides {MNP201 and MNP201(mut)} and control Cdc4 α peptides {MNP202 and MNP202(mut)}; and the absorbance of NADH was observed for 1-2 min. The reaction was then initiated by adding decylquinone and the absorbance of NADH was monitored for a further 12-15 min (**Figure 4.4B**). Finally, rotenone was added to inhibit the complex I activity and the absorbance of

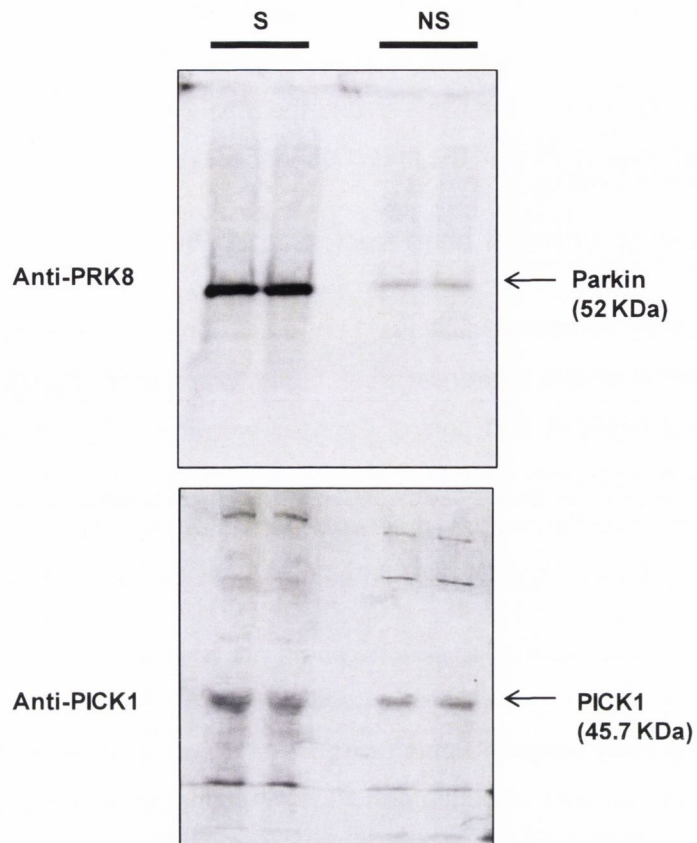


Figure 4.3: Presence of parkin and PICK1 in synaptic and non-synaptic fraction

Western blot analysis of synaptic (S) and non-synaptic (NS) fractions, obtained from rat brain, was performed for parkin using anti-PRK8 antibody and for PICK1 using anti-PICK1 antibody. The data shown is a representative of three experiments (n=3).

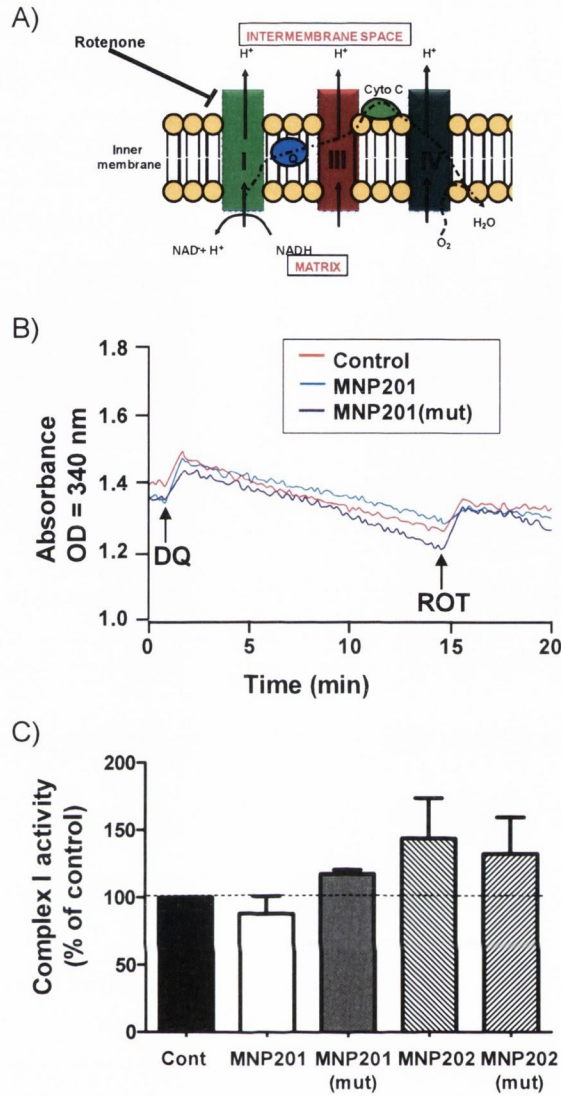


Figure 4.4: Effect of MNP201 in complex I of ETC cycle

Complex I activity is shown in freeze-fractured synaptosomes treated with peptides. A) The schematic diagram depicts that complex I uses NADH as a source of electrons and passes electrons to complex III via ubiquinone. Complex I is inhibited by rotenone. B) The graph represents the raw data of complex I activity by measuring absorbance (340 nm) of depleting NADH in the presence of MNP201 and MNP201(mut) in a time scale of 20 min. Representative traces of complex I activity are shown in the presence of vehicle control (red trace), 100 μ M MNP201 (blue trace) and 100 μ M MNP201(mut) (magenta trace). The first peak (DQ) and second peak (ROT) signify addition of decylquinone (1-2 min) and rotenone (14-15 min), respectively. The complex I activity (pseudo-first order rate constant) was obtained by subtracting the rotenone sensitive rate from the initial rate. C) The bar diagram represent the activity of complex I as a percentage of control (mean \pm SEM) in four separate experiments (n=4) in the presence of vehicle control (Cont), MNP201, MNP201(mut), MNP202 and MNP202(mut).

NADH was monitored for a final 5-6 min. The rate constants were calculated according to the method based on Ragan et al. (1987) and the rotenone insensitive rate was subtracted from the rotenone sensitive value to obtain the activity of complex I. When the values were expressed as a percentage of control and statistically analysed, no significant change in the activity of complex I was observed in MNP201 ($87.51\% \pm 13.00$) treated samples, when compared to MNP201(mut) ($117.29\% \pm 3.20$), MNP202 ($143.82\% \pm 29.71$) and MNP202(mut) ($132.49\% \pm 27.15$) treated samples (**Figure 4.4C**). The data shows that MNP201 has no effect on the activity of complex I of respiratory chain of mitochondria and suggest that parkin-PICK1 interaction does play a role in regulating the activity of the complex I respiratory chain in mitochondria.

4.5 Effect of MNP201 on complex IV assay

Complex IV of ETC has been implicated in AD, where the activity of complex IV was found to be reduced in patients (Chagnon et al., 1995). One study suggested deficiency of complex IV activity in parkin-KO mice (Palacio et al., 2004). Complex IV or cytochrome C oxidase accepts electrons from reduced cytochrome C and converts oxygen to water (**Figure 4.5A**). After investigating the effects of MNP201 on complex I, its effects on complex IV activity in mitochondria was investigated. The complex IV activity was measured by a decrease in the levels of cytochrome C (550 nm) (Telford et al., 2010). The activity of complex IV was determined by calculating the first order rate constant of cytochrome C depletion. In these experiments, parkin and Cdc4 α peptides were incubated with the complex IV reaction mixture and the absorbance of cytochrome C was monitored for 1-2 min. Next, freeze-fractured synaptosomes were added to initiate the reaction and the absorbance of cytochrome C depletion was monitored for subsequent 7-8 min (**Figure 4.5B**). The rate constants of complex IV activity were calculated according to the method of Wharton and Tzagoloff (1967) and expressed as percentage of control. No statistically significant difference in the activity of complex IV was observed in 100 μ M MNP201 ($125.13\% \pm 15.02$) treated samples, when compared to the vehicle control and MNP201(mut) ($135.16\% \pm 24.17$) treated samples (**Figure 4.5C**). In addition, no significant change was observed in complex IV activity with MNP202 ($108.28\% \pm 17.45$) treated samples, when compared to vehicle control and MNP202(mut) ($98.66\% \pm 15.81$) treated samples. The data showed that MNP201 had no effect on the activity of complex IV of respiratory chain in mitochondria and suggested that the PICK1-parkin interaction does not play a role in regulating complex IV activity.

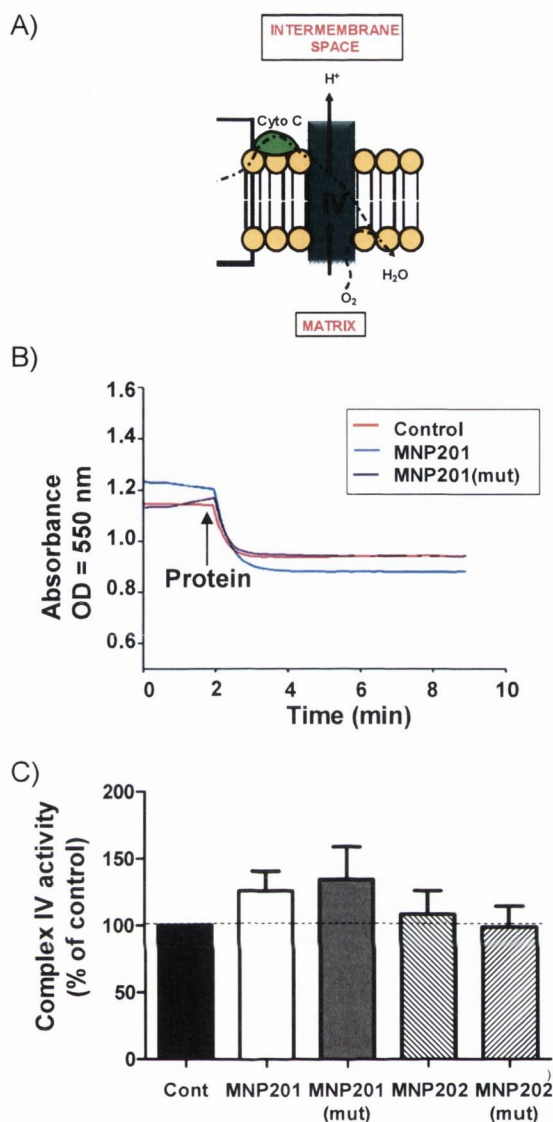


Figure 4.5: Effect of MNP201 in complex IV of ETC cycle

Complex IV activity was measured in freeze-fractured synaptosomes treated with peptides. A) The schematic diagram depicts that complex IV uses the reduced cytochrome C as source of electrons and passes protons out of the matrix to inner membrane space. B) The graph represents the raw data of complex IV activity by measuring absorbance (550 nm) of depleting cytochrome C in the presence of MNP201 and MNP201(mut) in a time scale of 10 min. Representative traces of complex IV activity are shown in the presence of vehicle control (red trace), 100 μ M MNP201 (blue trace) and 100 μ M MNP201(mut) (magenta trace). The peaks in the activity traces are due to addition of freeze-fractured synaptosomal protein (protein) (1-2 min). The complex IV activity was determined by measuring first order decay rate constant of cytochrome C. C) The bar diagram represents the activity of complex IV as a percentage of control (mean \pm SEM) in three separate experiments (n=3) in the presence of vehicle control (Cont), MNP201, MNP201(mut), MNP202 and MNP202(mut).

4.6 Effect of MNP201 on peroxide production

ROS production is a quantitative marker of cellular stress. ROS production plays a role in mitochondrial dysfunction and the pathogenesis of neurodegenerative diseases including PD, AD and HD (Beal, 1998; Kish et al., 1992; Schapira et al., 1990). Conversion of amplex red to resorufin (585 nm) was assayed to measure H₂O₂ production in the presence of controls and MNP201 (**Figure 4.6A**). Freshly prepared synaptosomes treated with peptides were loaded with amplex red and production of resorufin was measured over a 2 h time period. The rate of resorufin production, the quantitative indicator of H₂O₂, was plotted against time (x-axis) and OD⁵⁸⁵ (y-axis) for each treatment group (**Figure 4.6B**). A linear portion of the curve was selected (the same for each treatment group; 15-20 min) and the total H₂O₂ production was calculated. The relative values of peroxide production was expressed as a percentage of control and plotted in a bar graph. No significant difference was observed in peroxide production in synaptosomes treated with 100 μM of MNP201 (84.11% ± 4.05), when compared to the vehicle control and 100 μM MNP201(mut) (95.89% ± 5.31) treated synaptosomes. The unrelated Cdc4α modelled peptides, i.e., MNP202 (88.46% ± 1.30) and MNP202(mut) (79.56% ± 7.38) also showed no significant change, when compared to vehicle control. In contrast, when synaptosomes were incubated with 1 μM of antimycin A, a piscicide (fish toxin) and inhibitor of ubiquinol of ETC (200.73% ± 20.10), a significant 100.73% increase in peroxide production was found, when compared with vehicle control (**Figure 4.6C**), in agreement with previous publications (Sipos et al., 2003). The data showed that MNP201 has no effect on the ROS production in synaptosomal mitochondria.

4.7 Effect of MNP201 on mitochondrial membrane potential

The loss of mitochondrial membrane potential is a hallmark for apoptosis. It is an early event preceding loss of phosphatidylserine from the outer mitochondrial membrane and coinciding with caspase activation (Mantymaa et al., 2000; Korper et al., 2003). Mitochondrial membrane potential was measured by calculating the ratio of red (590 nm, aggregated form) to green (535 nm, monomeric form) of JC-1, as suggested by Chinopoulos et al. (1999) (**Figure 4.7A**). This ratio (JC-1^{590/535}) was found in control synaptosomes as 5.59 on average. The JC-1^{590/535} is a quantitative indicator of mitochondrial membrane potential (Kilbride et al., 2008). Freshly extracted synaptosomes were incubated with JC-1 and then treated with vehicle controls and MNP201. The JC-1^{590/535} ratio (y-axis) was plotted as rate of change in mitochondrial membrane potential over a time period of 1 h (x-axis) (**Figure 4.7B**). A linear portion of the curve was selected (the same for each treatment group; 15-20 min)

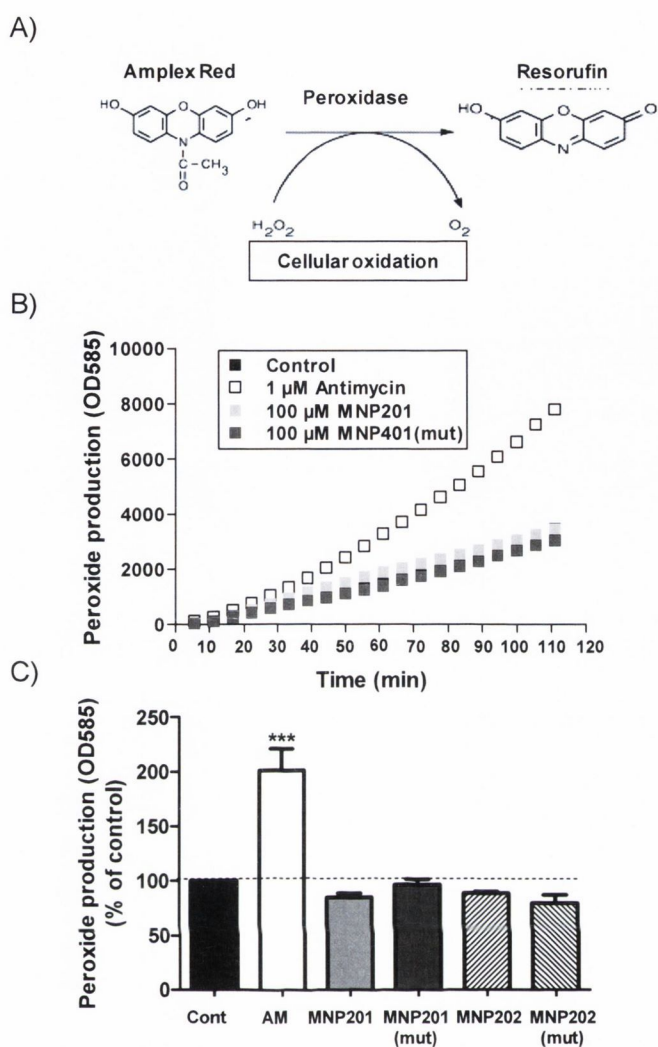


Figure 4.6: Effect of MNP201 on ROS production

Amplex red was used to measure the amount of ROS produced in freshly extracted synaptosomes in the presence and absence of MNP201. A) The principles of the assay is shown, where amplex red is converted to a fluorescent agent resorufin by reacting with ROS, in the presence of peroxidase. The resorufin level (585 nm) thus represents a quantitative indicator of peroxide production. B) The graph demonstrates the rate of peroxide produced in the presence or absence of MNP compounds and antimycin A (as positive control) treated synaptosomes in a time scale of 2 h. Representative traces depicts the rate of ROS production in the presence of vehicle control, 100 μM MNP201 and 100 μM MNP201(mut) along with the positive control 1 μM antimycin A. C) The bar diagram represents the total H_2O_2 production during the linear part of activity (the same for each treatment group; 15-20 min) as a percentage of control (mean \pm SEM) of five separate experiments ($n=5$) in the presence of vehicle control (Cont), antimycin A (AM), MNP201, MNP201(mut), MNP202 and MNP202(mut). The p-value (***) signifies $p<0.001$.

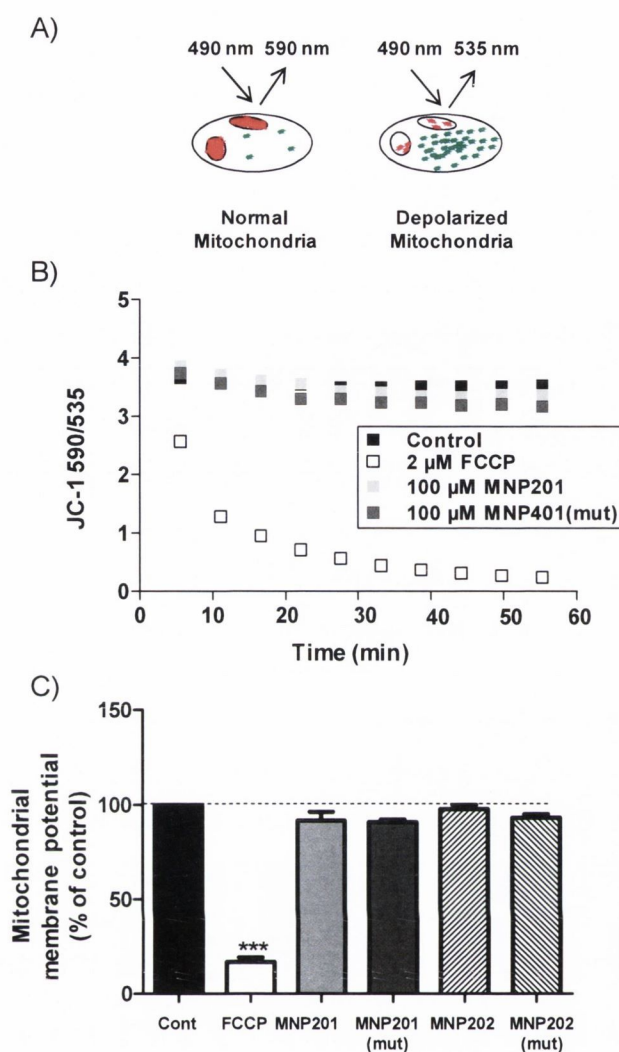


Figure 4.7: Effect of MNP201 on mitochondrial membrane potential

JC-1, changes its emission spectra with the change of mitochondrial membrane potential and was used as a reporter to measure the membrane potential of mitochondria in freshly extracted synaptosomes. A) The principles of the assay are shown, where JC-1 associates with mitochondria in control condition and emits a red (590 nm) colour. In depolarized mitochondria, JC-1 is found in the cytoplasm in a monomeric form emitting a green (535 nm) colour. The JC-1 590/535 ratio thus signifies a quantitative indicator of mitochondrial membrane potential. B) The graph shows the membrane potential in the presence and absence of MNP compounds in a time scale of 1 h. Representative traces depict the rate of change in mitochondrial membrane potential in the presence of vehicle control, 2 μ M FCCP (positive control) 100 μ M MNP201 and 100 μ M MNP201(mut). C) The bar diagram shows the mitochondrial membrane potential during the linear part of the traces (the same for each treatment group; 15-20 min) converted as a percentage of control (mean \pm SEM) in five separate experiments (n=5) in the presence of vehicle control (Cont), FCCP, MNP201, MNP201(mut), MNP202 and MNP202(mut). The p-value (***) signifies $p < 0.001$.

and mitochondrial membrane potential was measured. The relative values of mitochondrial membrane potential was expressed as a percentage of control and plotted in a bar graph. No significant change was observed in mitochondrial membrane potential with 100 μ M MNP peptides ($91.83\% \pm 4.67$), when compared to the vehicle control and negative control, MNP201(mut) ($91.08\% \pm 1.41$) (**Figure 4.7C**). The Cdc4 α E3 ligase modelled peptides, i.e., MNP202 ($97.79\% \pm 2.28$) and MNP202(mut) ($93.34\% \pm 1.91$) also showed no significant effect, when compared to vehicle control. On the other hand, as expected, 2 μ M of carbonylcyanide-p-trifluoromethoxyphenyl hydrazine (FCCP) ($16.97\% \pm 2.35$), a protonophore and uncoupler of mitochondrial oxidative phosphorylation, significantly reduced the membrane potential by 83%, when compared to vehicle control. The data showed that MNP201 has no effect on the mitochondrial membrane potential of synaptosomes.

4.8 Standardisation of glutamate release assay

PICK1 interacts with many glutamate receptors, namely AMPA, KA and metabotropic glutamate receptors that play a role in glutamate release (Barnes et al., 1994; Fujiyama et al., 2004; Hirbec et al., 2003; Herrero et al., 1996). Thus, the effect of 100 μ M MNP201 was investigated on glutamate release using freshly extracted synaptosomes. A continuous fluorimetric technique was employed, where the amount of glutamate was indirectly measured by quantifying the levels of glutamate-induced NADPH production (excitation/emission = 340/460 nm) as described in previous publications (Nicholls et al., 1987; Kilbride et al., 2008). In these experiments, the blank rate of glutamate release was monitored for the first 5 min in the absence and presence of 2 mM CaCl₂. Synaptosomes were then depolarized using 40 mM KCl and 10 mM 4-AP; and the depolarization-induced glutamate release was measured for an additional 30 min (**Figure 4.8A and C**). When the total glutamate release from 40 mM KCl and 10 mM 4-AP-induced synaptosomes were compared, 10 mM 4-AP-induced synaptosomes showed a trend increase rate in glutamate release compared to 40 mM KCl-induced synaptosomes, both in Ca²⁺-independent and dependent conditions (**Figure 4.8B and D**). This data is in agreement with previously published reports indicating increased glutamate release in the presence of 4-AP compared to KCl (Agoston et al. 1983; Muniz et al., 1990). A glutamate standard curve with known concentrations of glutamate was also generated to quantify the amount of glutamate release (**Figure 4.9**).

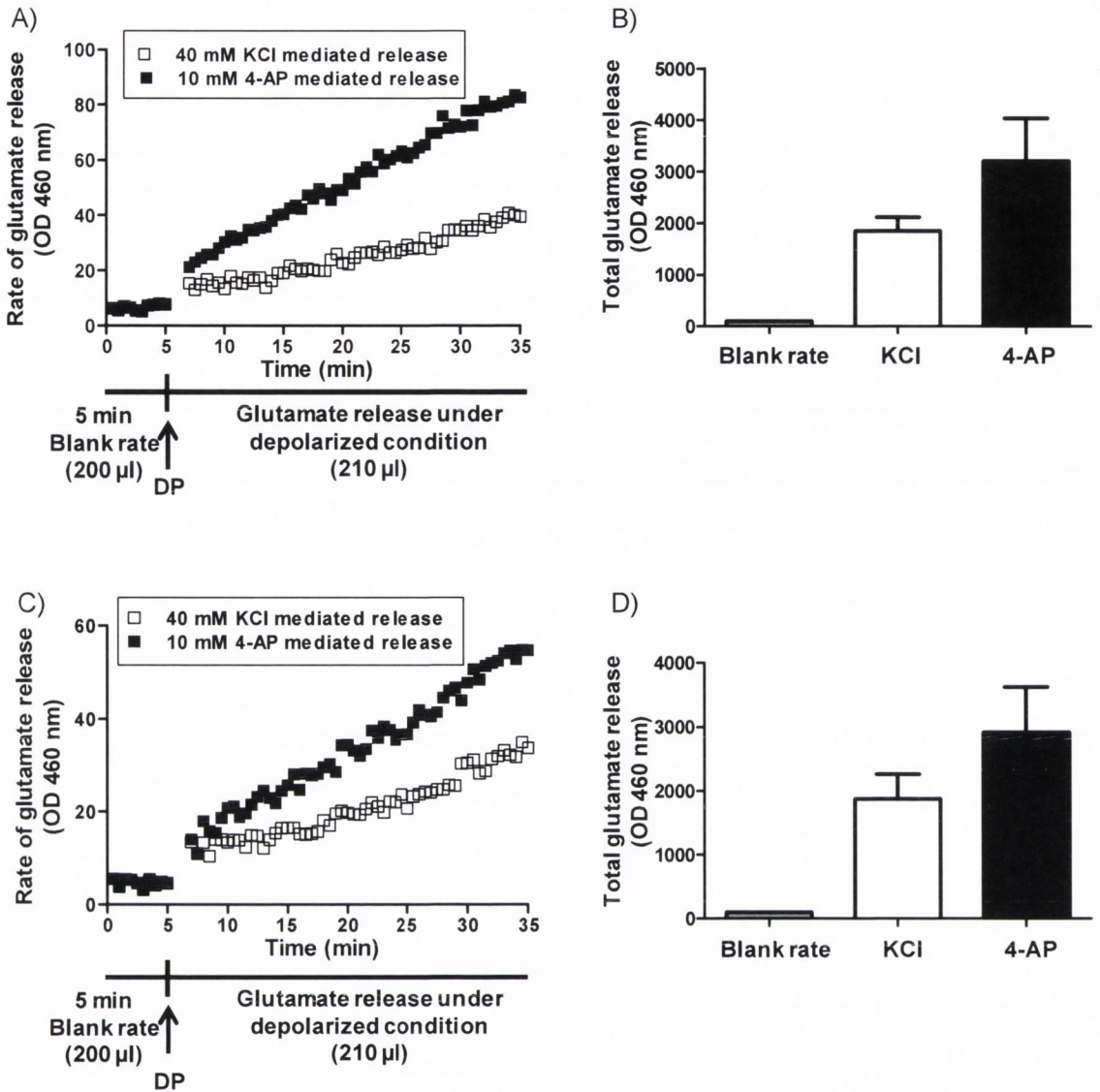


Figure 4.8: KCl and 4-AP-stimulated glutamate release

Glutamate release was performed using continuous fluorimetric method that measured the level of glutamate-dependent generation of NADPH (460 nm). Freshly extracted synaptosomes were incubated with GDH, NADP⁺ and Krebs buffer; and the blank rate was recorded for the first 5 min. Synaptosomes were then depolarized by adding 40 mM KCl and 10 mM 4-AP (DP) and the rate of glutamate release was recorded for a further 30 min. A) The graph indicates representative rates of Ca²⁺-independent glutamate release (OD⁴⁶⁰) in non-depolarized and depolarized synaptosomes with 40 mM KCl and 10 mM 4-AP. B) The bar diagram shows the total glutamate release induced by blank rate, 40 mM KCl and 10 mM 4-AP. C) The graph indicates representative rates of Ca²⁺-dependent glutamate release (OD⁴⁶⁰) in non-depolarized and depolarized synaptosomes with 40 mM KCl and 10 mM 4-AP. D) The bar diagram shows the total glutamate release induced by blank rate, 40 mM KCl and 10 mM 4-AP. The data represented in bar diagrams are mean ± SEM in three separate experiments (n=3).

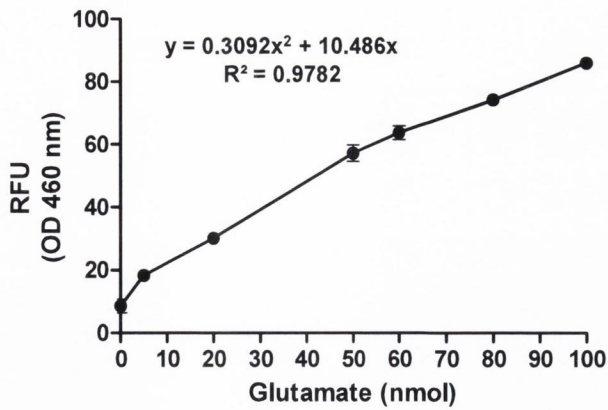


Figure 4.9: Standard curve of glutamate release

Quantification of glutamate release was performed using a continuous fluorimetric assay that quantified the level of converted NADPH (460 nm) in the presence of glutamate. To generate a standard curve for glutamate-induced NADPH production, standard amounts of glutamate were added to the wells of 96-well plate along with glutamate dehydrogenase, NADP⁺ and Krebs buffer (total 200 μ l). Fluorescence was monitored at excitation/emission = 340/460 nm. The mean steady state fluorescence values were plotted against known amounts of glutamate added. The graph represents mean of two separate experiments (n=2).

4.9 Effect of MNP201 on KCl-induced glutamate release without CaCl₂

After performing the standard glutamate release experiments above, the effect of 100 μ M MNP201 was tested in this assay. Complex I inhibition by 10 μ M rotenone has been reported to result in a high rate of glutamate release (Kilbride et al., 2008) and was therefore also used as a positive control. Freshly extracted synaptosomes were incubated with glutamate release media and the blank rates were monitored for the first 5 min. Then, treatment groups, i.e., vehicle control, MNP201 peptides and rotenone were added and the baseline glutamate release was observed from non-depolarized synaptosomes. Total release of glutamate by non-depolarized synaptosomes was measured over a 5 min period. No change in glutamate release was observed compared to vehicle control values in 100 μ M MNP201 ($107.50\% \pm 1.41$) and 100 μ M MNP201(mut) ($100.45\% \pm 2.86$) treated non-depolarized synaptosomes in the absence of CaCl₂. In contrast, samples treated with 10 μ M rotenone ($165.92\% \pm 21.97$) induced a significant 65.92% increase in the glutamate release, when compared to vehicle control (**Figure 4.10A, B**), in agreement with previously published data (Kilbride et al., 2008). Thereafter, the synaptosomes were depolarized with 40 mM KCl in the absence of CaCl₂ and the rate of glutamate release was monitored for a further 30 min. The total release of glutamate by depolarized synaptosomes was measured over this 30 min period. The result suggests no significant change in the rate of glutamate release in 100 μ M MNP201 ($95.65\% \pm 8.00$) treated synaptosomes, when compared to vehicle control and MNP201(mut) ($82.75\% \pm 8.02$) (**Figure 4.10A, C**). In contrast, 10 μ M rotenone (positive control) ($146.35\% \pm 19.12$) showed a significant 46.35% increase in the glutamate release compared to vehicle control, in agreement with previously published data (Kilbride et al., 2008). The data showed that MNP201 has no effect in the Ca²⁺-independent KCl-induced depolarized glutamate release from synaptosomes.

4.10 Effect of MNP201 on KCl-induced glutamate release with CaCl₂

After investigating the rate of glutamate release in the absence of CaCl₂, the same experiment was performed in the presence of 2 mM CaCl₂ under non-depolarized conditions. No statistically significant change was observed in the glutamate release from non-depolarized synaptosomes treated with 100 μ M MNP201 ($102.08\% \pm 2.81$), when compared to vehicle control and MNP201(mut) ($102.53\% \pm 2.03$) in the presence of 2 mM CaCl₂ (**Figure 4.11A, B**). On the other hand, 10 μ M rotenone treated synaptosomes ($160.62\% \pm 15.20$) showed a significant 60.62% increase in glutamate release, in agreement with previously published data (Kilbride et al., 2008). Thereafter, synaptosomes were depolarized using 40 mM KCl and the rate of glutamate release was recorded. No

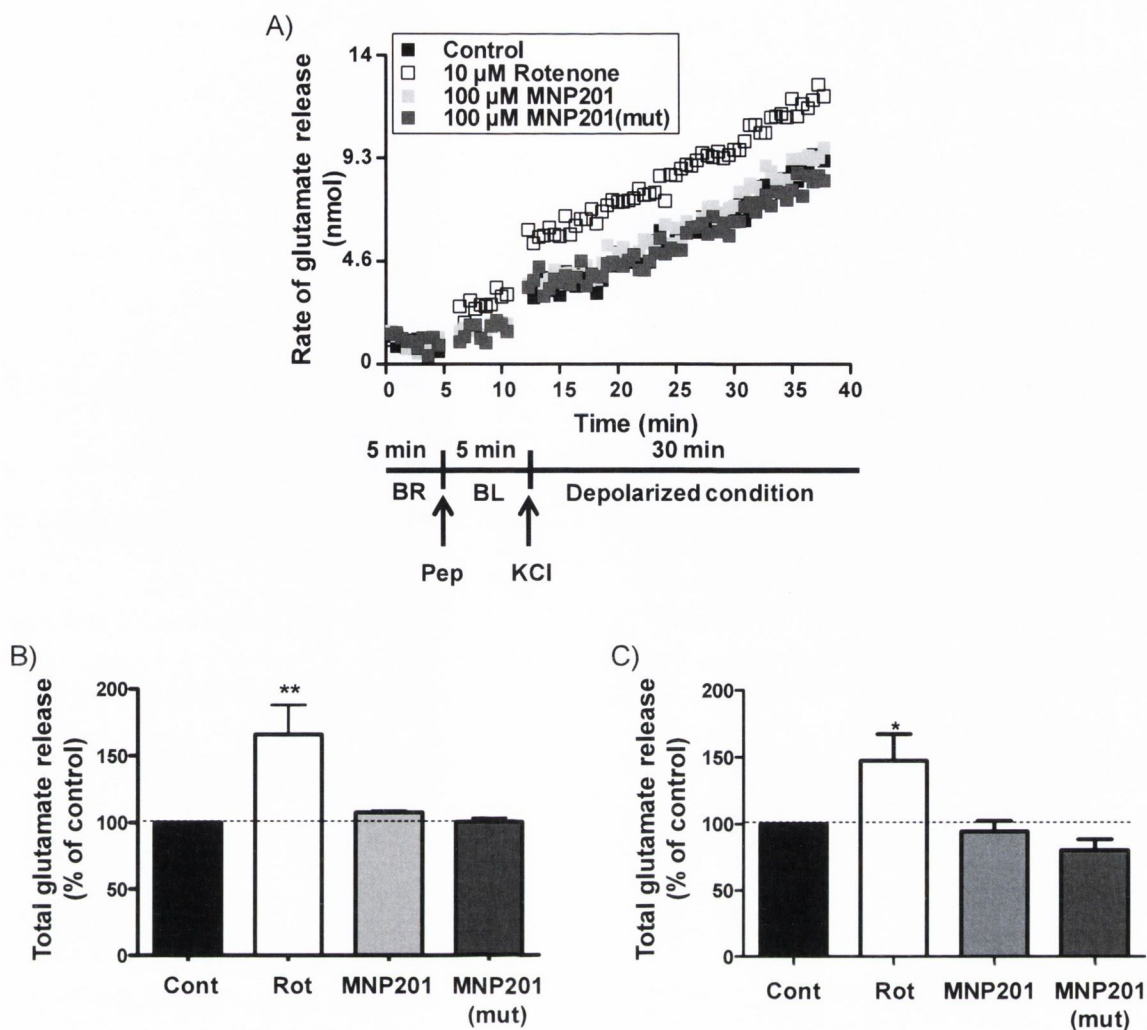


Figure 4.10: Effect of MNP201 on KCl-induced glutamate release in the absence of CaCl_2

The rate of glutamate release was measured by NADPH production at 460 nm. The level of glutamate was determined by generating a standard curve of glutamate-mediated NADPH production (**Figure 4.9**) in the absence of synaptosomes. The blank rate (BR) of glutamate release was recorded for the first 5 min in freshly extracted synaptosomes in the absence of CaCl_2 . Then, synaptosomes were treated with peptides (Pep), i.e. 100 μM MNP201 and 100 μM MNP201(mut) and also 10 μM rotenone; and the rate of glutamate at baseline (BL) was observed from non-depolarized synaptosomes for a further 5 min. Next, depolarization of synaptosomes was initiated by addition of 40 mM KCl and rate of glutamate release was observed for a further 30 min. A) The graph shows representative traces of Ca^{2+} -independent rate of glutamate release (nmol) from synaptosomes treated with vehicle control (Cont), 10 μM rotenone (Rot), 100 μM MNP201 and 100 μM MNP201(mut) in a total time period of 40 min. The bar diagrams show the total glutamate release as a percentage of control (mean \pm SEM) under non-depolarized (B) and depolarized (C) condition in three separate experiments ($n=3$). The p-values (*) and (**) signify $p<0.05$ and $p<0.01$.

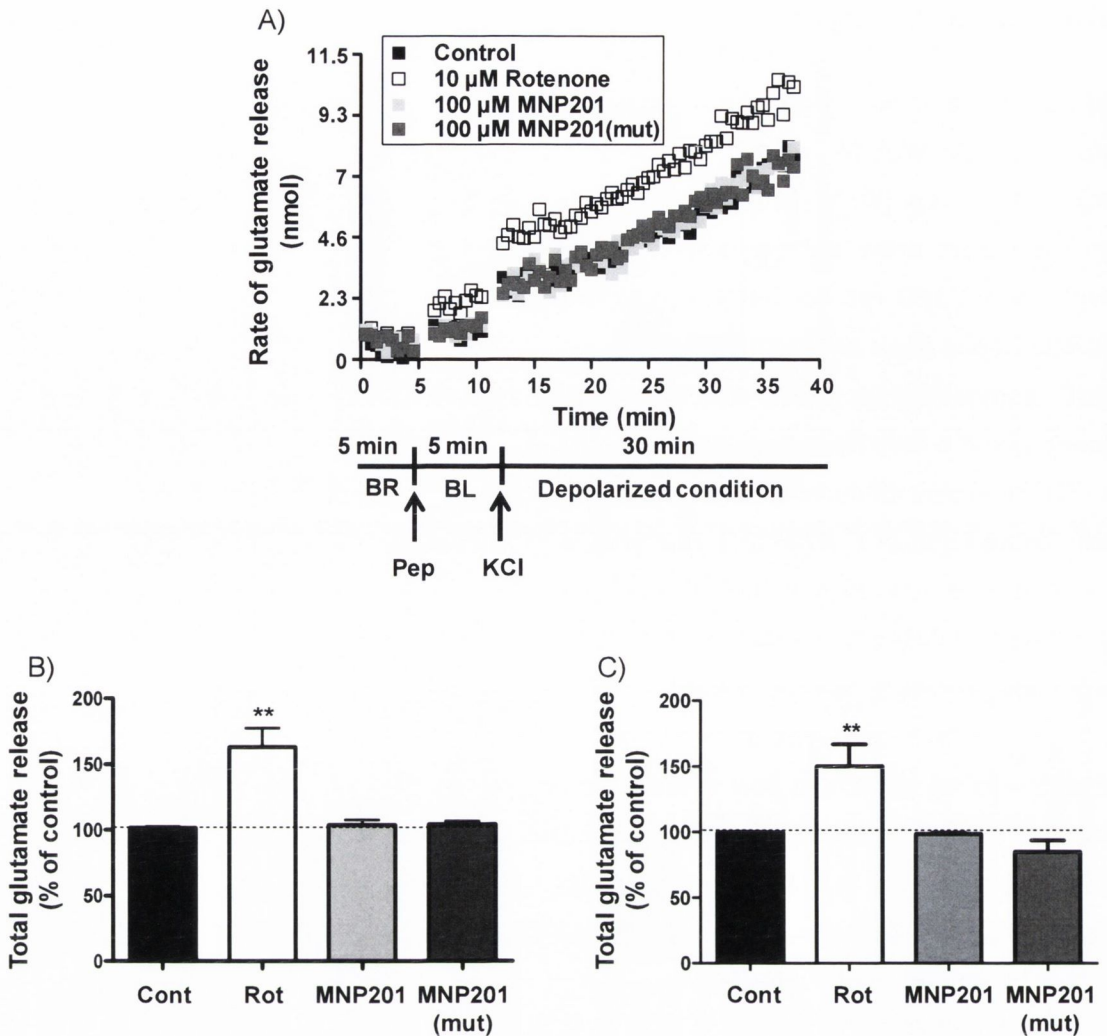


Figure 4.11: Effect of MNP201 on KCl-induced glutamate release in the presence of CaCl_2

The rate of glutamate release was measured by NADPH production at 460 nm. The level of glutamate was determined by generating a standard curve of glutamate-mediated NADPH production (**Figure 4.9**) in the absence of synaptosomes. The blank rate (BR) of glutamate release was recorded for the first 5 min in freshly extracted synaptosomes in the presence of CaCl_2 . Then, synaptosomes were treated with peptides (Pep), i.e. 100 μM MNP201 and 100 μM MNP201(mut) and also 10 μM rotenone; and the rate of glutamate at baseline (BL) was observed from non-depolarized synaptosomes for a further 5 min. Next, depolarization of synaptosomes was initiated by addition of 40 mM KCl and rate of glutamate release was observed for a further 30 min. A) The graph shows representative traces of Ca^{2+} -dependent rate of glutamate release (nmol) from synaptosomes treated with vehicle control (Cont), 10 μM rotenone (Rot), 100 μM MNP201 and 100 μM MNP201(mut) in a total time period of 40 min. The bar diagrams show the total glutamate release as a percentage of control (mean \pm SEM) under non-depolarized (B) and depolarized (C) condition in three separate experiments ($n=3$). The p-value (**) signifies $p<0.01$.

statistically significant change in glutamate release was observed in 100 μM MNP201 ($91.14\% \pm 4.80$) samples compared to vehicle control samples and 100 μM MNP201(mut) ($85.22\% \pm 8.91$) samples (**Figure 4.11A, C**). On the other hand, a significant 38.48% increase in glutamate release was observed, when synaptosomes were treated with 10 μM of rotenone ($138.48\% \pm 14.84$) compared to vehicle control, in agreement with previously published data (Kilbride et al., 2008). In summary, the data showed that MNP201 has no effect in the Ca^{2+} -dependent KCl-induced glutamate release from synaptosomes.

4.11 Effect of MNP201 on 4-AP-induced glutamate release

In addition to investigating the rate of KCl-induced glutamate release, 10 mM 4-AP was used to induce depolarization in synaptosomes. 4-AP induces depolarization of synaptosomes by blocking the voltage-dependent K^+ -channels present on the surface of synaptosomes in a non-selective manner (Nicholls, 1993). Using 10 mM 4-AP, the effect of MNP201 was investigated on freshly prepared synaptosomes in the absence of CaCl_2 . No statistically significant difference in the rate of glutamate release was observed in synaptosomes treated with 100 μM MNP201 ($91.67\% \pm 3.97$), when compared to vehicle control and MNP201(mut) ($74.08\% \pm 2.30$) (**Figure 4.12A, B**). On the other hand, the positive control 10 μM rotenone ($137.25\% \pm 20.20$) induced a significant 37.25% increase in the glutamate release compared to vehicle control, in agreement with previously published data (Kilbride et al., 2008). After investigating the effect of MNP201 in 4-AP-induced synaptosomes in the absence of CaCl_2 , the same experiments in the presence of CaCl_2 was performed. In the presence of 2 mM CaCl_2 and 10 mM 4-AP, no change in the rate of glutamate release was observed in 100 μM MNP201 ($103.50\% \pm 2.96$) treated synaptosomes, when compared to vehicle control and MNP201(mut) ($89.03\% \pm 4.91$) (**Figure 4.13A, B**). The data again showed that 10 μM rotenone ($167.05\% \pm 18.20$) induced a significant 67.05% increase in release of glutamate compared to vehicle control, in agreement with previously published data (Kilbride et al., 2008). Taken together, the data showed that MNP201 has no effect on 4-AP-induced glutamate release from synaptosomes, in the presence or absence of Ca^{2+} .

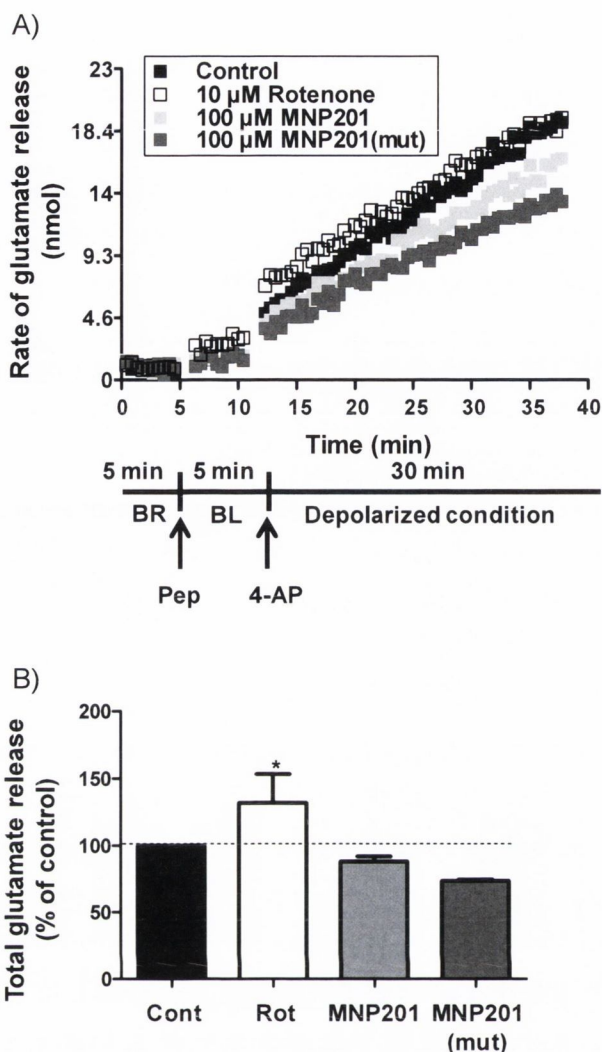


Figure 4.12: Effect of MNP201 on 4-AP-induced glutamate release in the absence of CaCl_2

The rate of glutamate release was measured by NADPH production at 460 nm. The level of glutamate was determined by generating a standard curve of glutamate-mediated NADPH production (Figure 4.9) in the absence of synaptosomes. The blank rate (BR) of glutamate release was recorded for the first 5 min in freshly extracted synaptosomes in the absence of CaCl_2 . Then, synaptosomes were treated with peptides (Pep), i.e. 100 μM MNP201 and 100 μM MNP201(mut) and also 10 μM rotenone; and the rate of glutamate at baseline (BL) was observed from non-depolarized synaptosomes for a further 5 min. Next, depolarization of synaptosomes was initiated by addition of 10 mM 4-AP and rate of glutamate release was observed for a further 30 min. A) The graph indicates representative traces of Ca^{2+} -independent rate of glutamate release (nmol) by vehicle control, 10 μM rotenone, 100 μM MNP201 and 100 μM MNP201(mut) treated synaptosomes in a total time period of 40 min. B) The bar diagram shows the total glutamate release as a percentage of control (mean \pm SEM) in vehicle control (Cont), 10 μM rotenone (Rot), 100 μM MNP201 and 100 μM MNP201(mut) treated synaptosomes under depolarized condition in three separate experiments ($n=3$). The p-value (*) signifies $p<0.05$.

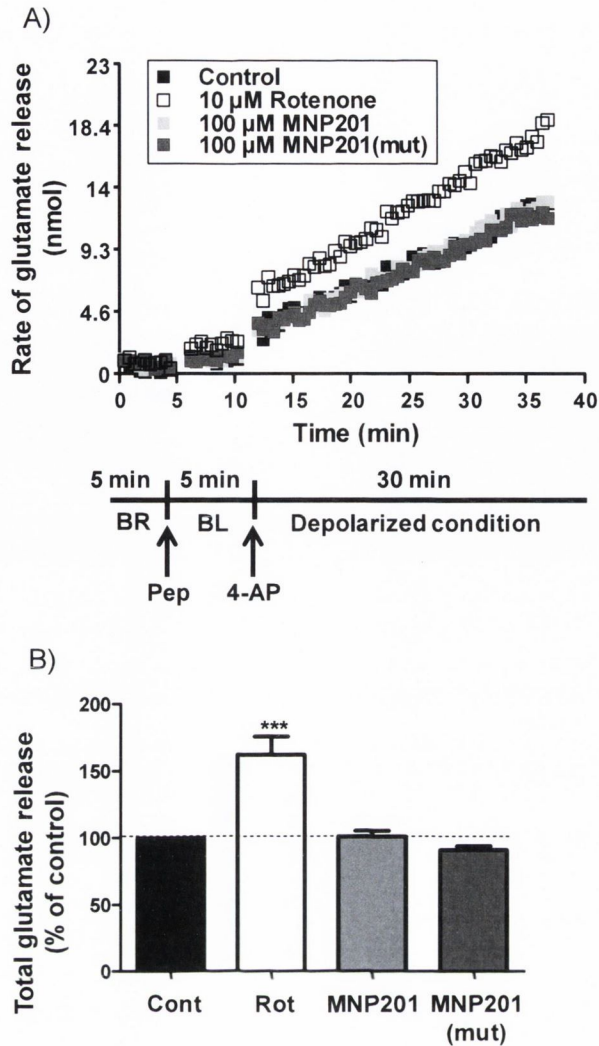


Figure 4.13: Effect of MNP201 on 4-AP-induced glutamate release in the presence of CaCl_2

The rate of glutamate release was measured by NADPH production at 460 nm. The level of glutamate was determined by generating a standard curve of glutamate-mediated NADPH production (**Figure 4.9**) in the absence of synaptosomes. The blank rate (BR) of glutamate release was recorded for the first 5 min in freshly extracted synaptosomes in the presence of CaCl_2 . Then, synaptosomes were treated with peptides (Pep), i.e. 100 μM MNP201 and 100 μM MNP201(mut) and also 10 μM rotenone; and the rate of glutamate at baseline (BL) was observed from non-depolarized synaptosomes for a further 5 min. Next, depolarization of synaptosomes was initiated by addition of 10 mM 4-AP and rate of glutamate release was observed for a further 30 min. A) The graph indicates representative traces of Ca^{2+} -dependent rate of glutamate release (nmol) by vehicle control, 10 μM rotenone, 100 μM MNP201 and 100 μM MNP201(mut) treated synaptosomes in a total time period of 40 min. B) The bar diagram shows the total glutamate release as a percentage of control (mean \pm SEM) in vehicle control (Cont), 10 μM rotenone (Rot), 100 μM MNP201 and 100 μM MNP201(mut) treated synaptosomes under depolarized condition in three separate experiments ($n=3$). The p-value (***) signifies $p<0.001$.

Discussion

1. Summary of results

The purpose of this project was to investigate the role of parkin-PICK1 interaction in mitochondrial function. Previous reports have showed a positive interaction between the PDZ motif of parkin and PDZ domain of PICK1 and that parkin monoubiquitinates PICK1, which inhibits PICK1-induced augmentation of ASIC currents (Joch et al., 2007). Here, the role of parkin-PICK1 interaction was investigated in the maintenance of mitochondrial function. In the first Result 1 chapter, the binding of MNP201 to PICK1 was demonstrated in a fluorescence polarisation assay, by showing that MNP201 dose-dependently inhibited the binding of a DAT peptide to PICK1. In this current chapter, the effect of the MNP201 peptide, modelled on the PDZ motif of parkin, was evaluated on mitochondrial properties, including activity of respiratory chains (complex I and IV), ROS production and change in mitochondrial membrane potential. In addition, the effect of MNP201 was investigated on the rate of glutamate release from synaptosomes. Here, the data generated showed that 100 μ M MNP201 peptide had no effect on mitochondrial properties or glutamate release (please see result summary **Table 4.1**).

2. Design of MNP201 parkin peptide

PDZ motifs are generally three to seven amino acid residues in length and usually reside in the extreme ct of a protein that interacts with the PDZ domain containing proteins (Songyang et al., 1997). A peptide (VCMGDHWF**FDV**) (MNP201) was designed based on the sequence of the last 10 amino acids of the parkin ct, which was predicted to block the interaction between parkin and PICK1. As control, a mutated version of the same peptide MNP201(mut) (VCMGDHW**AAA**), where the PDZ motif of parkin was mutated, was prepared. The effects of 100 μ M MNP201 were observed in mitochondrial assays and glutamate release assay using fresh synaptosomes. In addition to the MNP201(mut), additional peptide controls were also generated. We opted to model peptides based on the protein sequence of Cdc4 α , as this protein interacts with parkin and is also an E3 ligase, similar to parkin (please see Introduction chapter). Specifically, peptides were also modelled on the last 10 amino acids (ct) of Cdc4 α , which was first shown not to directly interact with PICK1. These peptides (MNP202) (LVLD**FDV**DMK wild type and LVLD**FDV**AAA mutant) were thus used as negative controls in the mitochondrial experiments performed. A set of positive controls were also used in these mitochondrial assays and demonstrated effects as expected confirming successful assay setup.

A)

Assay	100 μ M MNP201	100 μ M MNP201(mut)	Measured by
Complex I activity	87.51% \pm 13.00	117.29% \pm 3.20	NADH depletion (OD ³⁴⁰)
Complex IV activity	125.13% \pm 15.02	135.16% \pm 24.17	Cyto C depletion (OD ⁵⁵⁰)
Peroxide production	84.11% \pm 4.05	95.89% \pm 15.31	Resorufin production (OD ⁵⁸⁵)
Membrane potential	91.83% \pm 4.67	91.08% \pm 1.41	JC-1 OD ratio (JC-1 ^{590/535})

B)

Glutamate release	100 μ M MNP201	100 μ M MNP201(mut)	Measured by
Non-depolarized level(-CaCl ₂)	107.50% \pm 1.41	100.45% \pm 2.86	Amount of NADPH production (OD ⁴⁶⁰)
Non-depolarized level (+CaCl ₂)	102.08% \pm 2.81	102.53% \pm 2.03	
- CaCl ₂ , + 50 mM KCl	95.65% \pm 8.00	82.75% \pm 8.02	
+ CaCl ₂ , + 50 mM KCl	91.14% \pm 4.80	85.22% \pm 8.91	
- CaCl ₂ , + 10 mM 4-AP	91.67% \pm 3.97	74.08% \pm 2.30	
+ CaCl ₂ , + 10 mM 4-AP	103.50% \pm 2.96	89.03% \pm 4.91	

Table 4.1: Summary of data obtained using MNP201

A) Mitochondrial function assays and B) glutamate release assay.

The data suggest that MNP201 has no effect on mitochondrial respiratory chain complexes (complex I and IV), mitochondrial membrane potential, ROS production and glutamate release. The values are indicated as percentage of control (Mean \pm SEM).

3. Effects of MNP201 in mitochondrial function

Overall, no significant difference was found in the presence of MNP peptides tested in any of the mitochondrial parameters. Complex I is found to be hampered in PD patients (Schapira et al., 1989). Here, MNP201 showed no significant effect on the activity of complex I in freeze-fractured synaptosomes suggesting that occlusion of the PDZ domain of PICK1 (by MNP201 binding) may not alter function of the complex I respiratory chain. In addition to an altered complex I activity in PD patients, parkin-KO mice show a reduced complex IV activity (Palacio et al., 2004). The data showed that MNP201 did not alter complex IV activity, suggestion that parkin-PICK1 may also not regulate complex IV. In the ROS production assay, the positive control 1 μ M antimycin (a complex III inhibitor) showed 102% increase in ROS production as expected (Sipos et al., 2003). In contrast, no significant change in ROS production between vehicle control, control peptides, MNP201 and MNP201(mut) was observed. This again indicates that parkin-PICK1 may not have a role in the regulation of mitochondria-induced oxidative stress. Lastly, the mitochondrial membrane potential assay showed 83% increase in the membrane potential with 2 μ M FCCP treatment, a mitochondrial uncoupler (Tretter and Adam-Vizi, 2007). Again, however, no change in the mitochondrial membrane potential between vehicle control, control peptides, MNP201 and MNP201(mut) was observed, suggesting that parkin-PICK1 is not involved in maintenance of mitochondrial membrane potential. Given that parkin is known to regulate a number of mitochondrial properties, the lack of effect of MNP201 was surprising. Notably all these studies were performed under controls conditions. However, it is known that under conditions of cell stress parkin is trafficked toward the mitochondria where it is likely involved in mitophagy. Under normal conditions, the role of parkin in regulating mitochondrial function may be somewhat minor and the effects of MNP201 thus limited or not detectable. In contrast, the effects of MNP201 on these mitochondria under conditions of cell stress, where parkin plays a more dominant role, may be observable and thus worthy of further study (please see next chapters).

4. Effects of MNP201 on glutamate release assay

Glutamate-induced excitotoxicity is thought to contribute in preferential dopaminergic cell death in PD (Obeso et al., 2004). Thus, along with mitochondrial properties, the effect of the PDZ motif parkin peptides was also investigated on glutamate release assay. Control experiments were first performed in order to establish the glutamate release assay. In these experiments both 40 mM KCl and 10 mM 4-AP was found to induce depolarization of synaptosomes as expected. In addition, a standard curve of glutamate was also prepared,

which showed that glutamate concentration-dependent increase in the production of NADPH. After these studies, both Ca^{2+} -independent and dependent glutamate release experiments were performed by treating freshly prepared synaptosomes with 100 μM MNP201 in non-depolarised as well as depolarised conditions (triggered by KCl and 4-AP). Previous studies have shown that inhibition of complex I by rotenone induces glutamate release from synaptosomes, depolarized with KCl or 4-AP (Kilbride et al., 2008), thus rotenone was used as a positive control in these experiments. Using 100 μM MNP201, no significant difference in the rate of Ca^{2+} -independent or dependent glutamate release was observed in non-depolarized or in both KCl and 4-AP-induced depolarised synaptosomes, when compared to the vehicle control and MNP201(mut) treated samples. In contrast, rotenone-treated samples showed a significant increase in the rate of glutamate release, in agreement with previous reports. Taken together, the data suggested that MNP201 had no effect on the pre-synaptic release of excitatory glutamate. Similar to the lack of effects of MNP201 on mitochondrial properties, the lack of effects of MNP201 on glutamate release were surprising given that (i) mitochondria play a central role in regulating Ca^{2+} levels, (ii) parkin-PICK1 may regulate Ca^{2+} levels via ASIC-mediated currents, and (iii) PICK1 interacts with a number of glutamate receptors that alter glutamate release. The data thus suggested one or more of the following: (i) the parkin-PICK1 interaction is not important for regulating mitochondrial function; (ii) the effects of parkin-PICK1 on ASIC currents does not alter glutamate release; (iii) PICK1 does not alter glutamate receptor-mediated glutamate release; and/or (iv) MNP201 does not inhibit parkin and/or other proteins from interacting with PICK1 in synaptosomes.

5. Permeability of MNP201

There were two limitations identified in this chapter. Firstly, though MNP201 showed no significant effects on mitochondrial maintenance and glutamate release, the ability of MNP201 to penetrate synaptosomal membranes was not addressed. Generally, oligopeptides upto 6 amino acids long can cross the plasma membrane without any assistance. For longer peptides and proteins, Trojan peptide sequences attached with functional peptides or proteins have been used to pass through bilipid membranes (Nagahara et al., 1998, Ezhevshy et al., 1997). Since MNP201 is a 10 amino acid polypeptide little or no internalisation of MNP201 in synaptosomes may be expected, which may be the cause of its lack of effect. A Trojan peptide, such as Tat, attached to MNP201 may thus aid its membrane permeability and may be worthy to test in mitochondrial and glutamate release assays. In addition to using Trojan peptides, another approach to deliver MNP201 peptides inside synaptosomes, is known as peptide or protein entrapment. In this

approach, peptides or proteins can be entrapped inside synaptosomes while homogenisation of brain tissues and during preparation of synaptosomes. External media can come in contact with the internal compartments of the synaptic terminal for a very short period of time, which is sufficient to transfer non-permeable peptides to the internal compartments of synaptosomes (Pittaluga et al., 2005; Feligioni et al., 2009). Interestingly, using this approach of entrapping peptides, Feligioni et al. (2009) described that sumoylation suppresses KCl-induced glutamate release, but increases KA receptor stimulated glutamate release by entrapping SUMO proteins in synaptosomes (Feligioni et al., 2009). While these entrapment methods are well established the use of large volumes of media (supplemented with peptides) during synaptosomal preparation make them costly. The addition, these entrapment methods do not allow for the addition of peptides at specific timepoints during or within experiments, thus do not allow for temporal control. Thus, here we opted to use a Trojan peptide based internalisation approach to deliver MNP201 into synaptosomes. Specifically, a new version of the MNP201 peptide was engineered, which contained a Tat sequence (YGRKKRRQRRR) fused to the N-terminal of MNP201, named Tat-MNP201. These peptides were tested in neuronal cells and astrocytes to visualise their penetration into the cell. After confirming their penetration, the effect of Tat-MNP201 was tested in mitochondrial and glutamate release assays. These studies are described in the next chapter.

6. Effect of MNP201 in condition of cell stress

The second limitation to the current result chapter is that the effect of MNP201 peptides was tested only in control conditions, and not stressed conditions, in our experimental setup. Previous publications suggest that parkin engulfs depolarized mitochondria under conditions of stress (Narendra et al., 2008). If that is the case, then the parkin-PICK1 interaction may only play a role in regulating mitochondrial function under conditions of mitochondrial depolarization and/or cell stress. In other words, PICK1 may not associate with parkin in control circumstances, which may also account for the lack of effect of MNP201 on mitochondrial properties and glutamate release in the experiments outlined above. To address this issue, in the next chapter the effect of MNP201 was examined under the condition of mitochondrial depolarization stress.

7. Moving to the next chapter

At this stage, our revised hypothesis is that PICK1 plays a crucial role in the trafficking of parkin to depolarized mitochondria, in the condition of cell stress more so than under control

condition. In the next chapter, the effects of a cell-permeable version of MNP201 were examined on mitochondrial function and glutamate release.

5. Results: 3
Effect of Tat-MNP201 on
mitochondrial function

Abstract

In the previous chapter, the effects of wildtype and mutated versions of MNP201 peptides were demonstrated in a set of mitochondrial functional assays and glutamate release using synaptosomes prepared from rat brain tissue. The data suggested no statistically significant effect of MNP201 (100 μ M) in mitochondrial function and glutamate release. However, in the previous experiments the entry of MNP201 into cells, or more specifically across the plasma membrane of synaptosomes, was not determined. To ensure the internalisation of MNP201 through the membrane bilayers of synaptosomes, a Trojan peptide sequence, namely a Tat peptide, was attached onto the N-terminus of MNP201. In this chapter, first, a concentration-dependent internalisation of the Tat-tagged version of MNP201 was demonstrated in neuronal cells and astrocytes. Thereafter, the effects of Tat-MNP201 (and a Tat-MNP201 mutant) on mitochondrial properties, i.e., activity of respiratory complexes, peroxide production and membrane potential in synaptosomes were determined. Further, the effect of this peptide was investigated on glutamate release. No change in the rate of peroxide production and activity of respiratory complexes (complex I and IV) was observed. In addition, the Tat-tagged peptides showed no effect in the rate of glutamate release. Importantly, however, the data demonstrated that Tat-MNP201 (100 μ M) increased the rate of mitochondrial depolarization in control and FCCP-induced stress conditions. Taken together, these studies suggested that the parkin-PICK1 interaction may play a role in the maintenance of mitochondrial membrane potential.

Introduction

In the previous chapter (Result 2), a parkin PDZ motif peptide was designed according to the last 10 amino acids of the ct of parkin (MNP201). The effect of MNP201 and MNP201(mut) was investigated in various mitochondrial properties and the rate of glutamate release was also examined. In these studies, no statistically significant change was observed in synaptosomes treated with MNP201 peptides on any of the mitochondrial properties investigated or in the rate of glutamate release. However, from these studies, it remained unclear whether the lack of the effects of MNP201 was due to its ability to cross synaptosomal and/or mitochondrial membranes. Generally, peptides more than 6 amino acids long do not cross the plasma membrane, unassisted (Scheld et al., 1989) and given that MNP201 is 10 residues in length, it may have not crossed the membrane bilayer of synaptosome in the aforementioned experiments. There are two methods to assist the entry of peptides and proteins into synaptosomes. The first approach involves an 'entrapment' method that includes the peptide/protein into buffers while preparing synaptosomes. In this approach, there is a timepoint where these peptide/proteins can enter 'open' synaptosomes during preparation. While this method is well accepted, it is costly (requiring large amounts of peptides in buffers during synaptosomal preparations) and also does not allow for the addition of peptides at controlled timepoints within the mitochondrial and/or glutamate release experiments to be conducted. Thus, a second approach to transfer peptides into synaptosomes was used and involved the use of Trojan peptides. In this chapter, Specifically, Tat-fused MNP201 peptides were created, which were capable of crossing the plasma membrane.

The ability to create biologically active substances that can internalise live cells crossing the lipid membrane is an important tool in the field of pharmacology and drug development. Many agents have been identified that aid the entry of desired substances, otherwise impermeable to the cell and specific compartments. The identification and application of arginine-rich peptides sequences, including Tat and Antennapedia, capable of crossing the plasma membrane have been proved to be a useful tool of drug delivery (Schwarze et al., 1999; Derossi et al., 1996). Indeed, Tat peptides (YGRKKRRQRRR), derived from transduction domain (PTD) of human immunodeficiency virus (HIV) (Nagahara et al., 1998), are widely used in internalising substances ranging from peptides, proteins, oligonucleotides, liposomes, polymeric particles, phages and adenoviruses (Bonny et al., 2001; Dostmann et al., 2000; Jo et al., 2001; Peitz et al., 2002; Astriab-Fisher et al., 2000; Torchilin et al., 2001; Lewin et al., 2000; Eguchi et al., 2001; Gratton et al., 2003).

Generally, the endocytic system of mammalian cells follows different mechanisms to internalise substances from small soluble ligands to macromolecule (Mercer and Helenius, 2009). The most common mechanism for endocytosis in mammalian cells involves a clathrin-mediated pathway, where external ligands are incorporated into clathrin-coated pits with the help of receptors and adaptor proteins (Conner and Schmid, 2003). The fusion of clathrin-coated vesicles with the early endosomes occurs through a GTPase dynamin mechanism (Mukherjee et al., 1997). Similar to a cathrin-mediated pathway, another well characterised endocytosis mechanism involves a caveolar-mediated pathway, where caveolin-1-coated vesicles (also called as caveolae) are known to mediate endocytosis in a dynamin-dependent manner (Parton and Simons, 2007). Interestingly, formation of lipid rafts, i.e., cholesterol/sphingolipid rich plasma microdomains containing the ligand, has been reported to associate with caveolar-mediated endocytosis (Lajoie and Nabi, 2007). In contrast, micropinocytosis is another lipid raft-mediated endocytic pathway, where entry of lipid rafts inside the cells occurs through a dynamin-independent pathway, involving membrane ruffling, i.e., actin-dependent formation of motile surface around the cell (Cao et al., 2007). Interestingly, the internalisation of Tat peptides takes place through a micropinocytosis mechanism (Kaplan et al., 2004). The Tat peptide is reported to deliver 15 to 120 kDa cargo proteins into different human and murine cell types (Nagahara et al., 1998, Ezhevshy et al., 1997). Many of these Trojan tagged peptides have been expressed *in vivo*, including the brain, by engineering N-terminal Tat fusions (Schwarze et al., 1999). For example, a Tat peptide designed to block the PDZ-based interaction between N-methyl-D-aspartate (NMDA) receptors and post-synaptic density protein 95 (PSD-95), has been used to prevent ischemic brain damage in mice (Aarts et al., 2002).

In addition to Tat, Antennapedia (also called as penetratin) is another example of Trojan peptide. Antennapedia is a 16 residues long polypeptide (RQIKIWFQNRRMKWKK) derived from the homeodomain of *Drosophila* transcription factor, also called Antennapedia. Several reports have described the successful use of this Trojan peptide as a transport vector (Derossi et al., 1998; Pooga et al., 1998; Astriab-Fisher et al., 2000). Unlike the Tat peptide, the Antennapedia sequence enters cells through a non-endocytotic pathway which is independent of receptor and transporter (Derossi et al., 1996; Fisher et al., 2000). Antennapedia, conjugated to as large as 55 bases of hydrophilic oligonucleotides, has been reported to deliver cargo to the cytoplasm and nucleus (Derossi et al., 1996; Prochiantz A, 1996). In this chapter, the Trojan peptide strategy was used by attaching a Tat sequence to the N-terminal to MNP201 in order to enable MNP201 to cross synaptosomal membranes.

While Tat tagged fusions proteins do successfully cross lipid bilayers, certain considerations about using such Tat peptides, which previous reports have indicated, are to be kept in mind. Specifically, studies on mitochondrial properties and glutamate release have reported that the Tat peptide can induce ROS production and mitochondrial membrane depolarization along with the disruption of Ca^{2+} homeostasis and caspase activation in cultured hippocampal neurons (Kruman et al., 1998). High expression of Tat mRNA has also been reported in HIV infected patient's brain and is considered as an important player in causing HIV related dementia (Wesselingh et al., 1993). Importantly, the Tat peptide is also the only viral protein known to be secreted by HIV infected microglia (Tardieu et al., 1992). In addition, the Tat protein is also reported to be released from infected cultured microglia and causes apoptosis by activating non-NMDA glutamate receptors and subsequent Ca^{2+} influx (Cheng et al., 1998). Moreover, a report has suggested induced glutamate release and reduced GABA release in the presence of a Tat peptide from mice synaptosomes (Musante et al., 2009). Although all these reports are based on the effect of full length Tat peptide, (i.e. not the YGRKKRRQRRR shorter Trojan version of Tat) recognition of such possible effects should be noted when using Tat peptide sequences in mitochondrial functional studies and glutamate release assays.

Specifically, to facilitate the entry of MNP201 into the synaptosomes, a Tat sequence was fused to the N-terminal of MNP201 (Tat-MNP201). First, a fluorescein isothiocyanate (FITC) labelled Tat-tagged MNP201 (FITC-Tat-MNP201) was treated with the cortical neurons and astrocytes to investigate the internalisation and intracellular localisation of Tat-tagged MNP201. Then, the effects of the Tat version of MNP201 peptides were tested in mitochondrial properties, including peroxide production and mitochondrial membrane potential. In addition, along with investigating the effect of Tat-MNP201 in mitochondrial membrane potential assay in control conditions, the effect of Tat-MNP201 was also demonstrated under membrane depolarization stress, induced by FCCP (a mitochondrial uncoupler). Finally, the Tat-MNP201 was also tested in the rate of glutamate release. Notably, the effect of these Tat peptides were not examined on complex I and IV assays as these assays are "open cell" enzymatic assays, where no issues regarding membrane permeability was envisaged (Result 2). The outcomes of the experiments are given below.

Results

5.1 Concentration-dependent internalisation of FITC-Tat-MNP201 into neuronal cells

After testing the effects of MNP201, a membrane permeable version of wild type MNP201 was designed by attaching a Trojan peptide, Tat (YGRKKRRQRRR), to the N-terminal of MNP201 (Tat-MNP201). A Tat-MNP201(mut) was also synthesised as control. To monitor the membrane permeability of Tat-MNP201, its entry into cells was visualised by attaching an FITC (excitation/emission spectra = 495 nm/521 nm) fluorophore tag at the N-terminal of Tat-MNP201. These peptides were ordered from Genscript, USA. The HPLC purity of Tat-MNP201, Tat-MNP201(mut) and FITC-Tat-MNP201 were found to be as 97.40%, 85.47%, and 85.90%, respectively. The list of peptides and their purity profile is shown in **Figure 5.1A** and **B** as provided by Genscript, USA. All these Tat versions of MNP201 peptides were dissolved in 50 mM HEPES pH 7 solutions to make 2 mM stock solution. During experiments, 50 mM of HEPES pH 7 was used as vehicle control in equal volume of peptides.

To observe the internalisation of FITC-Tat-MNP201, mature (10-14 days old) cortical neuronal cells were treated with four concentrations of FITC-Tat-MNP201, i.e., 0.1 µg, 1 µg, 10 µg and 100 µg (per ml). The treatment was carried out at 37°C for 1 h in 5% CO₂. After treatment, neurons were fixed and stained with chicken anti-neurofilament (1/1000 dilution) antibody, followed by secondary anti-chicken Dylight-549 (1/1000 dilution) antibody and visualised under 40x objective lens in a confocal microscope. A fluorescent signal of FITC-Tat-MNP201 in neuronal cells was observed in a dose-dependent manner (**Figure 5.2A**). Images (containing 40-50 cells per image) were acquired from each treatment group (6-8 images per treatment group). The mean pixel intensity in the green channel (FITC signal) was quantified by ratio of intensity of green channel with red channel (neurofilament signal). The data was converted to the percentage of mean pixel intensity given by 10 µg/ml of FITC-Tat-MNP201 and represented as a bar graph. A dose-dependent increase of fluorescence was found in treatment groups, i.e., 0.1 µg/ml (19.05% ± 1.71), 1 µg/ml (52.01% ± 4.50), 10 µg/ml (100%) and 100 µg/ml (186.69% ± 41.45), indicating internalisation of FITC-Tat-MNP201 in cortical neurons in a concentration-dependent manner (**Figure 5.2B**). The data suggested that the Tat-tagged MNP201 is able to cross the plasma membrane of cortical neurons.

A)

Name	Domain	Motif	Peptide sequences
Tat-MNP201	PICK1	PARKIN	YGRKKRRQRRRVCMGDHWFDV
Tat-MNP201(mut)	PICK1	PARKIN	YGRKKRRQRRRVCMGDHWAAA
FITC-Tat-MNP201	PICK1	PARKIN	YGRKKRRQRRRVCMGDHWFDV

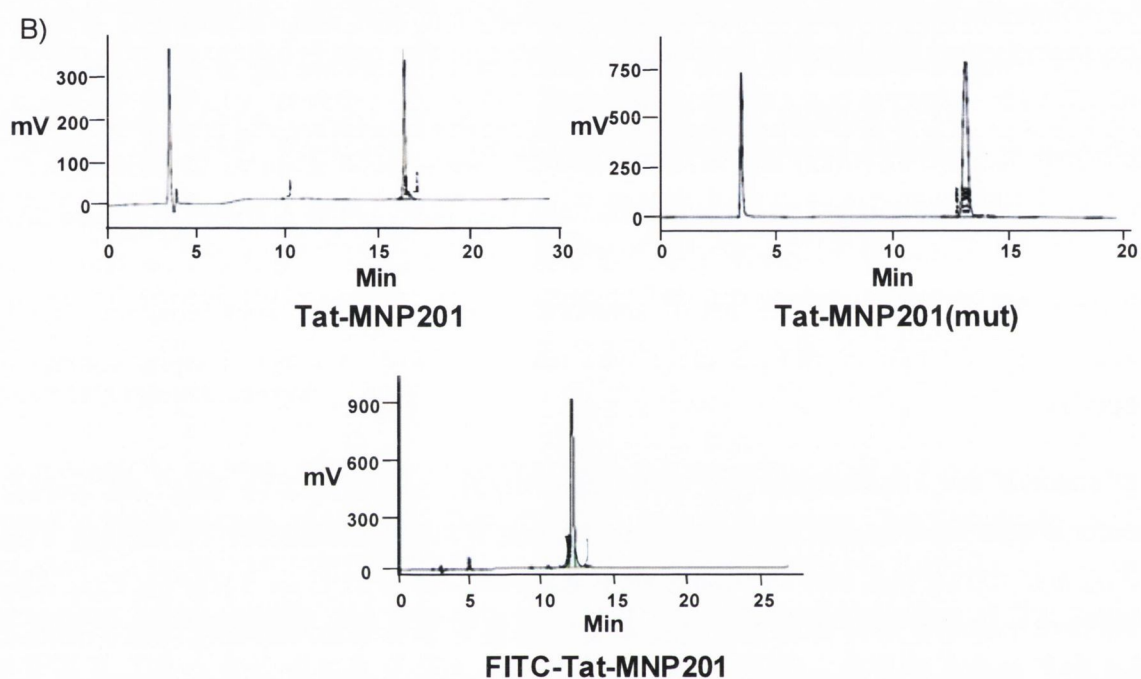


Figure 5.1: List of Tat-tagged MNP201 peptides

The Tat-tagged MNP201 peptides modelled on the PDZ motif of parkin are shown in the table. B) The HPLC purity profiles of these peptides, measured at 220 nm, were found to be 97.40% (Tat-MNP201), 85.47% (Tat-MNP201 mut) and 85.90% (FITC-Tat-MNP201). During HPLC analysis, formic acid treated water (pH 4.00) was used in case of Tat-MNP201 and Tat-MNP201(mut). Therefore, the first peak of these two sample's chromatogram indicates formic acid. The peptides were ordered from Genscript, USA.

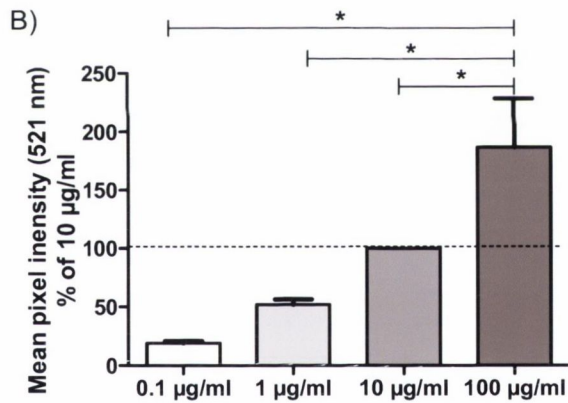
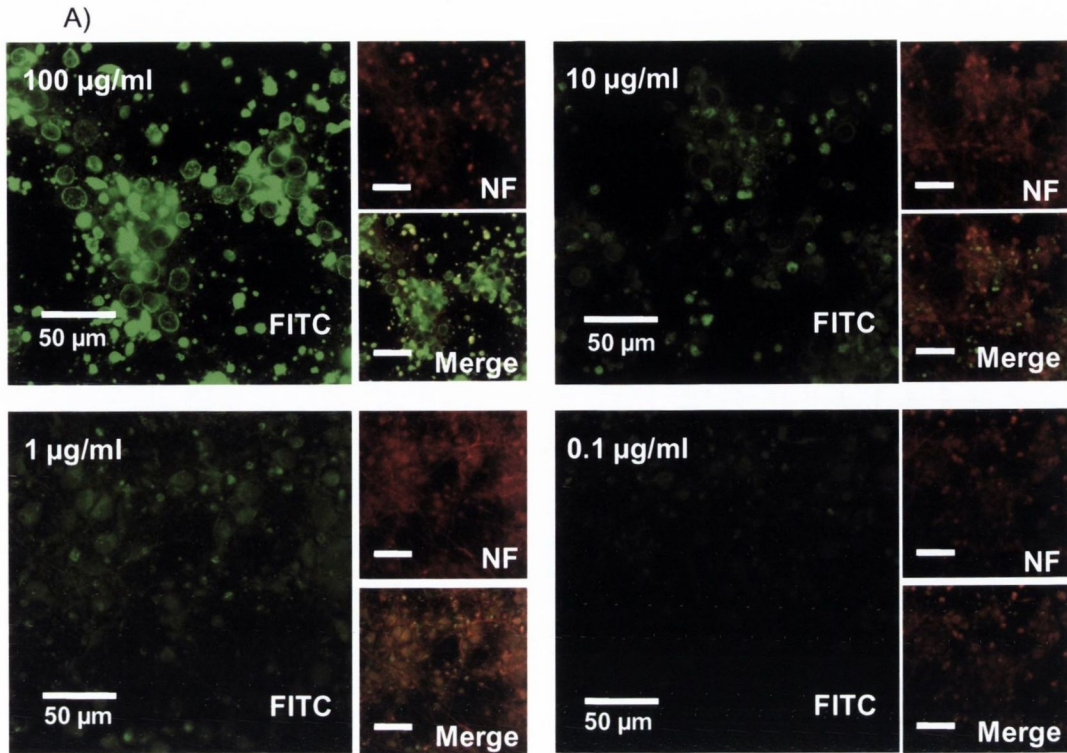


Figure 5.2: Dose-dependent uptake of FITC-Tat-MNP201 into neuronal cells

The FITC-Tat-MNP201 peptide is based on the last 10 amino acids of ct of parkin. A FITC-Tat peptide (FITC-YGRKKRRQRRR) was fused to the N-terminal of MNP201 (VCMGDHWFDV) to facilitate its internalisation into neuronal cells. A) Cortical neuronal cells treated with four concentrations of peptide (0.1 µg, 1 µg, 10 µg and 100 µg per ml) are shown (green channel). Red channel shows anti-neurofilament staining (NF), the green channel shows FITC signal, along with a composite image (Merge). The scale bars depict 50 µm. B) The bar graph depicts % internalisation of FITC-Tat-MNP201 in the cortical neurons treated with 0.1 µg, 1 µg, 10 µg and 100 µg (per ml) of peptide. The fluorescence intensities were calculated using the ratio of green (FITC) and red (NF) intensity obtained from 6-8 confocal images (each containing 40-50 cells) of each treatment group. The values represent a percentage of the mean fluorescence intensity obtained using 100 µg/ml of FITC-Tat-MNP201. The data represents mean ± SEM obtained from three separate experiments (n=3). The p-value (*) signifies p<0.05.

5.2 Concentration-dependent internalisation of FITC-Tat-MNP201 into astrocytes

After demonstrating internalisation of FITC-Tat-MNP201 in mixed cortical neurons, the internalisation of FITC-Tat-MNP201 peptide was also examined on glial cells, namely astrocytes. Similar to the experiments performed with neurons, astrocytes were also treated with 0.1 μg , 1 μg , 10 μg and 100 μg (per ml) of FITC-Tat-MNP201 for 1 h in 5% CO_2 at 37°C. After treatment, the astrocytes were fixed, stained with rabbit anti-GFAP (1/1000 dilution) antibody followed by secondary anti-rabbit Alexa-633 (1/500 dilution) antibody and visualised under 63x objective lens of a confocal microscope. Similar to data found using neurons, in astrocytes a fluorescent signal of FITC-Tat-MNP201 was also observed in a dose-dependent manner with increasing amounts of the peptide (**Figure 5.3A**). Images (containing 20-30 cells per image) were acquired from each treatment group (6-8 images per treatment group). Mean pixel intensity was calculated as a ratio of total intensity in the green channel (FITC) to the total intensity in the red channel (GFAP) and represented as a percentage of the ratio found using 10 $\mu\text{g}/\text{ml}$ FITC-Tat-MNP201, in a bar graph. The data indicated a dose-dependent inclusion of the FITC-Tat-MNP201 peptide in treated astrocytes, which specific values of 0.1 $\mu\text{g}/\text{ml}$ ($6.2\% \pm 5.31$), 1 $\mu\text{g}/\text{ml}$ ($23.51\% \pm 16.75$), 10 $\mu\text{g}/\text{ml}$ (100%) and 100 $\mu\text{g}/\text{ml}$ ($562.29\% \pm 49.19$) (**Figure 5.3B**). Importantly, the close observation of FITC-Tat-MNP201 treated astrocytes showed the FITC-Tat-MNP201 peptide localised in the nucleus as well as processes of astrocytes treated with 100 $\mu\text{g}/\text{ml}$ (**Figure 5.4A and B**) and 10 $\mu\text{g}/\text{ml}$ (**Figure 5.4C and D**). Therefore, the data suggest that the Tat-tagged MNP201 is able to cross the plasma membrane of astrocytes.

5.3 Effect of Tat-MNP201 on peroxide production

ROS production is an essential marker of cell stress. ROS production was measured by quantifying the amount of resorufin (585 nm) converted from amplex red in the presence of ROS. To investigate the effect of Tat-MNP201, freshly prepared synaptosomes were mixed with amplex red and the change in peroxide production was measured over a 1 h time period. A linear portion of the curve was selected (the same for each treatment condition; 15-20 min) and the total H_2O_2 production was calculated. The relative values of peroxide production was expressed as a percentage of control and plotted in a bar graph. No significant changes were observed in peroxide production in 100 μM Tat-MNP201 ($108.84\% \pm 4.79$) treated synaptosomes, when compared to vehicle control and 100 μM Tat-MNP201(mut) treated synaptosomes ($129.76\% \pm 11.68$) (**Figure 5.5A**), similar to the result

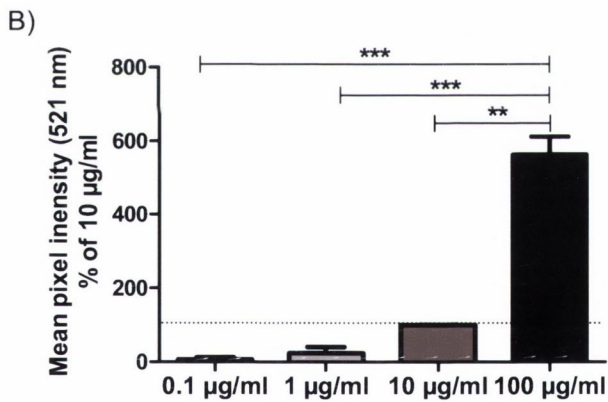
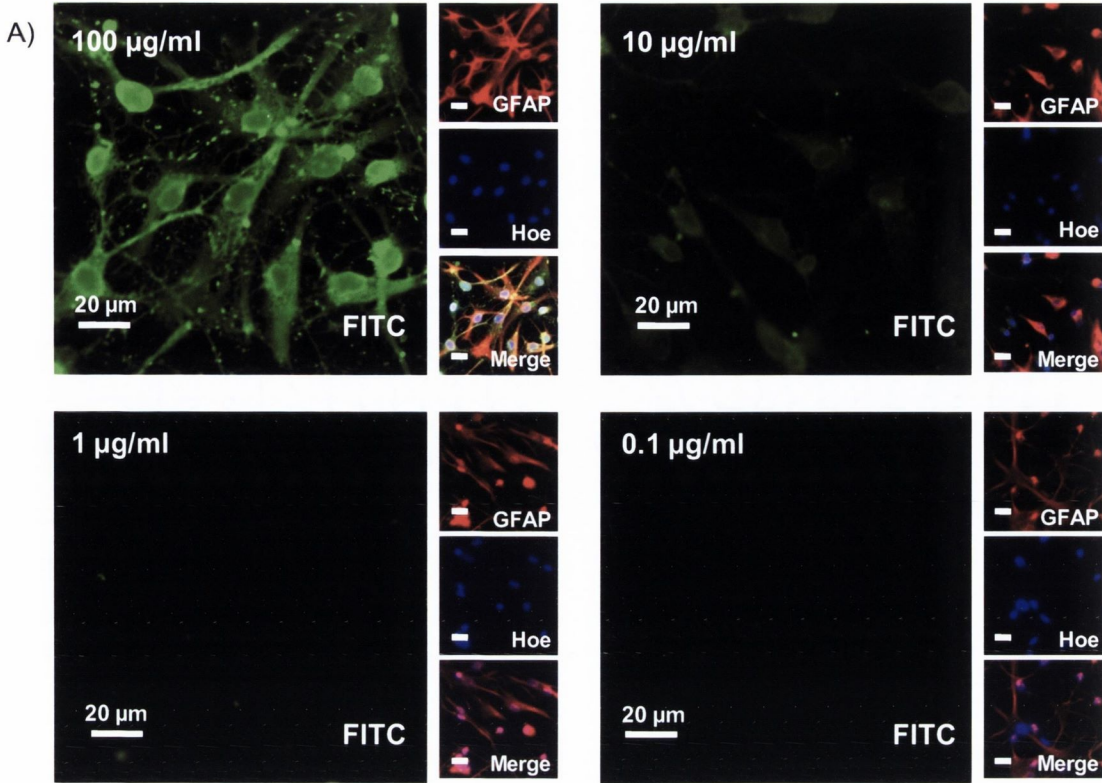


Figure 5.3: Dose-dependent uptake of FITC-Tat-MNP201 into astrocytes

A) Rat brain astrocytes, treated with four concentrations of FITC-Tat-MNP201 peptide (0.1 µg, 1 µg, 10 µg and 100 µg per ml) are shown in green channel (FITC). Red and blue channels show the anti-GFAP (GFAP) and Hoechst (Hoe) staining along with a composite figure of all channels (Merge). The scale bars represent 20 µm. B) The bar graph depicts the mean pixel intensity obtained from astrocytes treated with 0.1 µg, 1 µg, 10 µg and 100 µg per ml of FITC-Tat-MNP201 peptide under 521 nm. The mean pixel intensities were calculated using the ratio of the green channel (FITC) and with the number of GFAP cells (red channel) obtained from 6-8 confocal images (each containing 20-30 cells). The data was represented as a percentage of mean pixel intensity obtained for 10 µg/ml FITC-Tat-MNP201. The data represents mean ± SEM of two separated experiments (n=2). The p-value signifies $p < 0.001$ (***) and $p < 0.01$ (**).

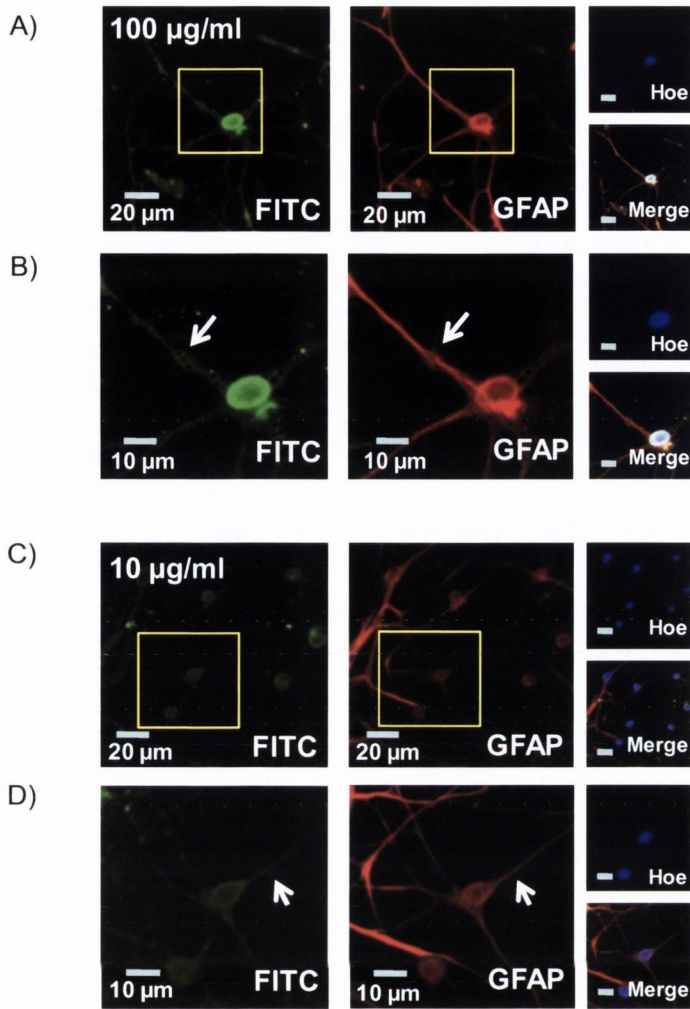


Figure 5.4: Dose-dependent uptake of FITC-Tat-MNP201 into the processes of astrocytes

The internalisation of FITC-Tat-MNP201 in astrocytes occurred in a dose-dependent manner. Astrocytes treated with 100 and 10 µg/ml FITC-Tat-MNP201 are shown in the green channel (FITC). Red and blue channels show anti-GFAP (GFAP) and Hoechst (Hoe) staining along with a composite image of all channels (Merge). The scale bars correspond to the values shown. Yellow boxes represent area of interest which are magnified and depicted in next panels. Area of interests of image (A) and (C) are magnified form image (B) and (D), respectively. White arrows indicate the processes of astrocytes in both green and red channel demonstrating the overlapped regions. The images represent data of two separate experiments (n=2).

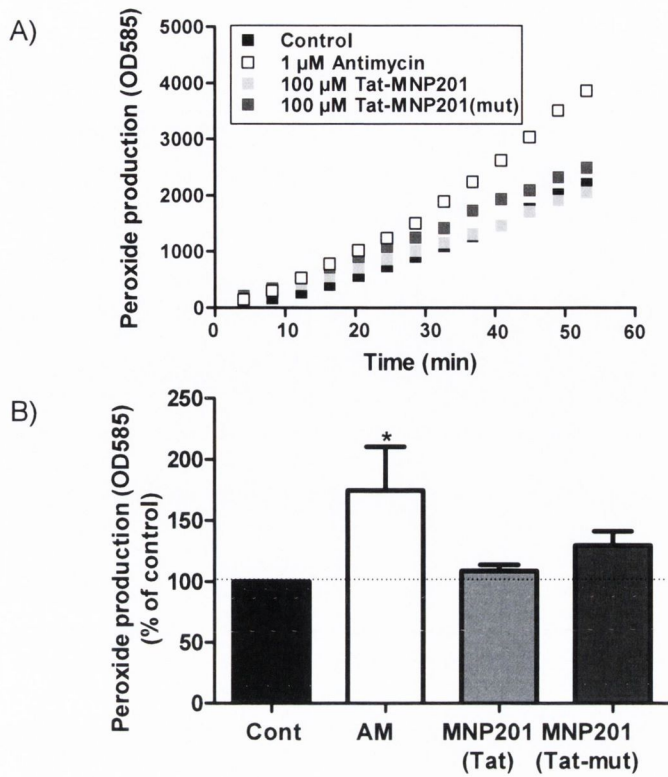


Figure 5.5: Effect of Tat-MNP201 on ROS production

Amplex red measures the amount of ROS produced by fresh synaptosomes in the presence of Tat-MNP201. In this assay, amplex red is converted to a fluorescent agent resorufin by reacting with ROS, in the presence of peroxidase. The resorufin level (585 nm) thus represents a quantitative indicator of peroxide production. A) The graph demonstrates the rate of peroxide produced, in the presence of Tat-MNP compounds and antimycin A (as control) in a time scale of 1 h. Representative traces indicate the rate of ROS production in the presence of vehicle control, 100 μM Tat-MNP201 and 100 μM Tat-MNP201(mut) along with positive control 1 μM antimycin A. B) The bar diagram represents the total H₂O₂ production during the linear part of activity (the same for each treatment condition; 15-20 min) as a percentage of control (mean ± SEM) in five separate experiments (n=5) in the presence of vehicle control (Cont), antimycin A (AM), Tat-MNP201 and Tat-MNP201(mut). The p-value (*) signifies p<0.05.

obtained using the non-tagged Tat version of MNP201. In contrast, when synaptosomes were incubated with 1 μ M of antimycin A, an inhibitor of ubiquinol of ETC ($174.70\% \pm 35.76$), a significant increase of 74.70% peroxide production was found, when compared with vehicle control (**Figure 5.5B**), in agreement with previous publications (Sipos et al., 2003). Thus, the data showed that Tat-MNP201 does not alter peroxide production in synaptosomal mitochondria.

5.4 Effect of Tat-MNP201 on mitochondrial membrane potential

Mitochondrial membrane potential was measured by calculating the ratio of red (590 nm, aggregated form) to green (535 nm, monomeric form) JC-1. The JC-1^{590/535} control value of synaptosomes was found to be 5.59 on average and considered as a quantitative indicator of the mitochondrial membrane potential, as suggested by previous publications (Reers et al., 1991 and 1995). After incubation with JC-1, freshly extracted synaptosomes were treated with vehicle control and Tat-MNP201 peptides. The JC-1^{590/535} was plotted as the rate of change in mitochondrial membrane potential over a time of 1 h (**Figure 5.6A**). A linear portion of the curve was selected (the same for each treatment condition; 15-20 min) and the mitochondrial membrane potential was measured. The relative values of the mitochondrial membrane potential was expressed as a percentage of control and plotted in a bar graph. Unlike MNP201, a statistically significant reduction of 23.74% was observed in mitochondrial membrane potential in synaptosomes treated with 100 μ M Tat-MNP201 ($76.26\% \pm 4.90$), when compared to the vehicle control (**Figure 5.6B**). In addition, 2 μ M FCCP ($18.15\% \pm 0.80$), a protonophore, caused a significant 81.85% reduction in the mitochondrial membrane potential, when compared to vehicle control, in agreement with previously published data (Kilbride et al., 2008). Interestingly, the negative control Tat-MNP201(mut) ($87.61\% \pm 2.06$) treated samples also induced a significant 12.39% increase in mitochondrial depolarization, when compared to vehicle control. However, when Tat-MNP201 and Tat-MNP201(mut) values were compared, a significant 11.35% increase in mitochondrial membrane potential was identified in Tat-MNP201 treated samples compared to Tat-MNP201. Previously, a Tat peptide (N-terminal 72 amino acids) was reported to cause depolarization in mitochondrial membrane potential (Kruman et al., 1998). Thus, the effect demonstrated by Tat-MNP201(mut) in mitochondrial membrane potential was believed to be due to the effect of the Tat peptide. Taken together, the data suggest that Tat-MNP201 increases mitochondrial depolarization by reducing the membrane potential.

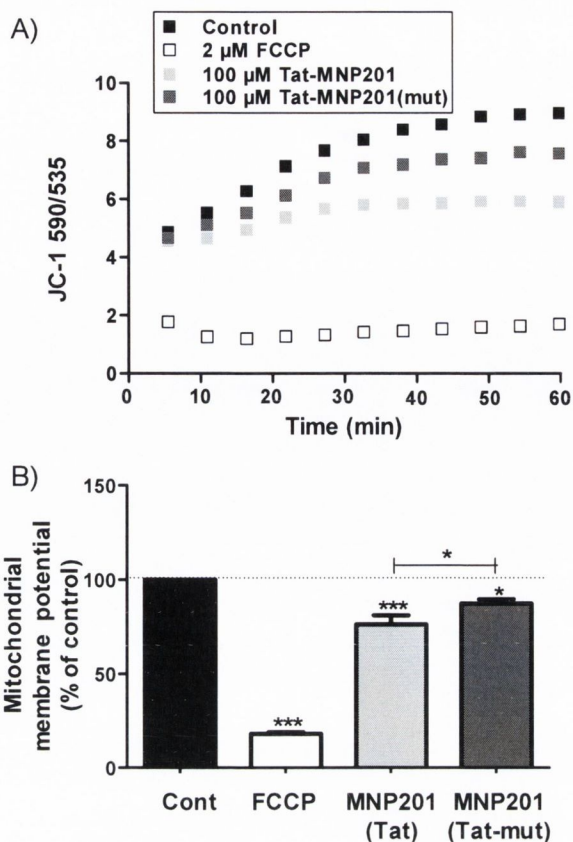


Figure 5.6: Effect of Tat-MNP201 on mitochondrial membrane potential

JC-1 is a known reporter of membrane potential in mitochondria that changes its emission spectra upon a change of mitochondrial membrane potential. In this assay, JC-1 associates with mitochondria under control conditions and emits a red colour (590 nm). In depolarized conditions, JC-1 is found in the cytoplasm in a monomeric form that emits a green colour (535 nm). The JC-1 590/535 ratio thus can be used as a quantitative indicator of the mitochondrial membrane potential. A) The graph represents the rate of change in mitochondrial membrane potential in the presence of Tat-MNP compounds in a time scale of 1 h. Representative traces indicate the rate of change in mitochondrial membrane potential by vehicle control, 2 μ M FCCP (positive control), 100 μ M Tat-MNP201 and 100 μ M Tat-MNP201(mut) treated synaptosomes. B) The bar diagram represents the mitochondrial membrane potential during the linear part of the traces (the same for each treatment condition; 15-20 min) as a percentage of control (mean \pm SEM) in five separate experiments (n=5) by vehicle control (Cont), FCCP, Tat-MNP201 and Tat-MNP201(mut). The p-values (***) and (*) signify $p < 0.001$ and $p < 0.05$, respectively.

5.5 Dose-dependent increase in mitochondrial membrane depolarization with FCCP

According to previous publications, parkin has been reported to engulf depolarized mitochondria and plays a major role in recruiting autophagosomes to depolarized mitochondria (Narendra et al., 2008; Geisler et al., 2010). In particular, parkin has been demonstrated to selectively engulf depolarized mitochondria upon depolarization induced by the protonophore 10 μ M CCCP (Narendra et al., 2008). Another protonophore, FCCP (1 μ M), has been reported to depolarise the mitochondrial membrane potential (Kilbride et al., 2008; Telford et al., 2010). The depolarization effect of FCCP was also demonstrated in this project (**Figure 4.7 and 5.6**). To investigate the effect of Tat-MNP201 under mitochondrial depolarised conditions, synaptosomes were treated with FCCP. Firstly increasing concentrations (from 2 pM to 2 μ M) of FCCP were used to depolarize freshly extracted, JC-1 loaded synaptosomes. This dose-response curve of FCCP inducing mitochondrial depolarization (as measured by JC-1) was prepared to identify the IC_{50} value of FCCP. (**Figure 5.7A**). From the dose-response curve, the half maximal inhibitory concentration (IC_{50}) of FCCP that induced synaptosomal mitochondrial depolarization was determined to be approximately 20 nM (**Figure 5.7B**).

5.6 Tat-MNP201 depolarizes mitochondrial membrane potential in partial stress condition

Next, the effect of Tat-MNP201 was investigated on mitochondrial membrane potential in synaptosomes treated with 20 nM FCCP, where mitochondrial membranes were partially depolarised and stressed. First, JC-1 loaded synaptosomes were treated with vehicle control, 100 μ M Tat-MNP201 and 100 μ M Tat-MNP201(mut); and the mitochondrial membrane potential was monitored for the first 15 min. At the end of these 15 min, all the samples were treated with 20 nM FCCP to induce partial mitochondrial depolarization and the mitochondrial membrane potential was monitored for a further 30 min (**Figure 5.8A**). A linear portion of the curve was selected (the same for each treatment condition; 5-10 min before FCCP treatment and 15-20 min after FCCP treatment) and the values of these mitochondrial membrane potentials were expressed as a percentage of control and plotted in a bar graph. Analysis of non-stressed samples (no FCCP) suggested that there was a statistically significant difference in mitochondrial membrane potential in 100 μ M Tat-MNP201 ($80.51\% \pm 1.93$) treated synaptosomes when compared with vehicle control and 100 μ M Tat-MNP201(mut) ($88.80\% \pm 1.57$) treated synaptosomes (**Figure 5.8B**), in

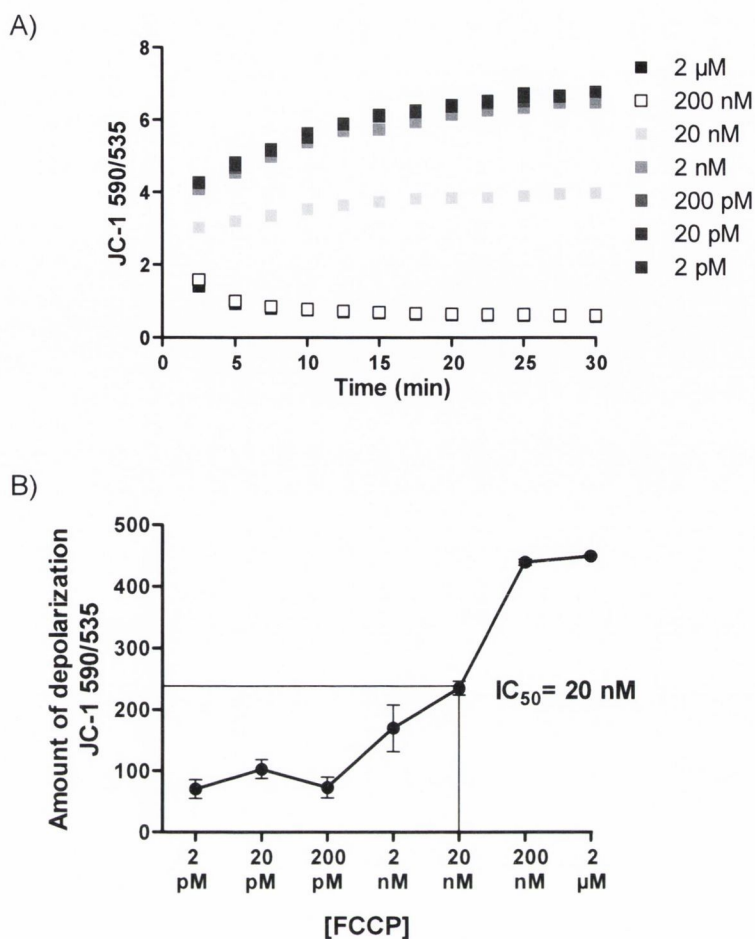


Figure 5.7: FCCP standard curve

FCCP is a protonophore that uncouples mitochondrial membranes and causes mitochondrial depolarization. In a JC-1 based assay, the JC-1 590/535 ratio, calculated by JC-1 aggregate (590 nm) and monomeric form (535 nm), represents a quantitative reporter of mitochondrial membrane potential. A) Serial dilutions of FCCP, concentrations ranging from 2 pM to 2 μM in 10 fold increment, were used to treat JC-1 loaded freshly extracted synaptosomes, and the rate of depolarization was observed for 30 min. B) Total depolarization (n=3), caused by different concentrations (nM) of FCCP, is plotted into a dose-response curve. The IC₅₀ value was found to be approximately 20 nM.

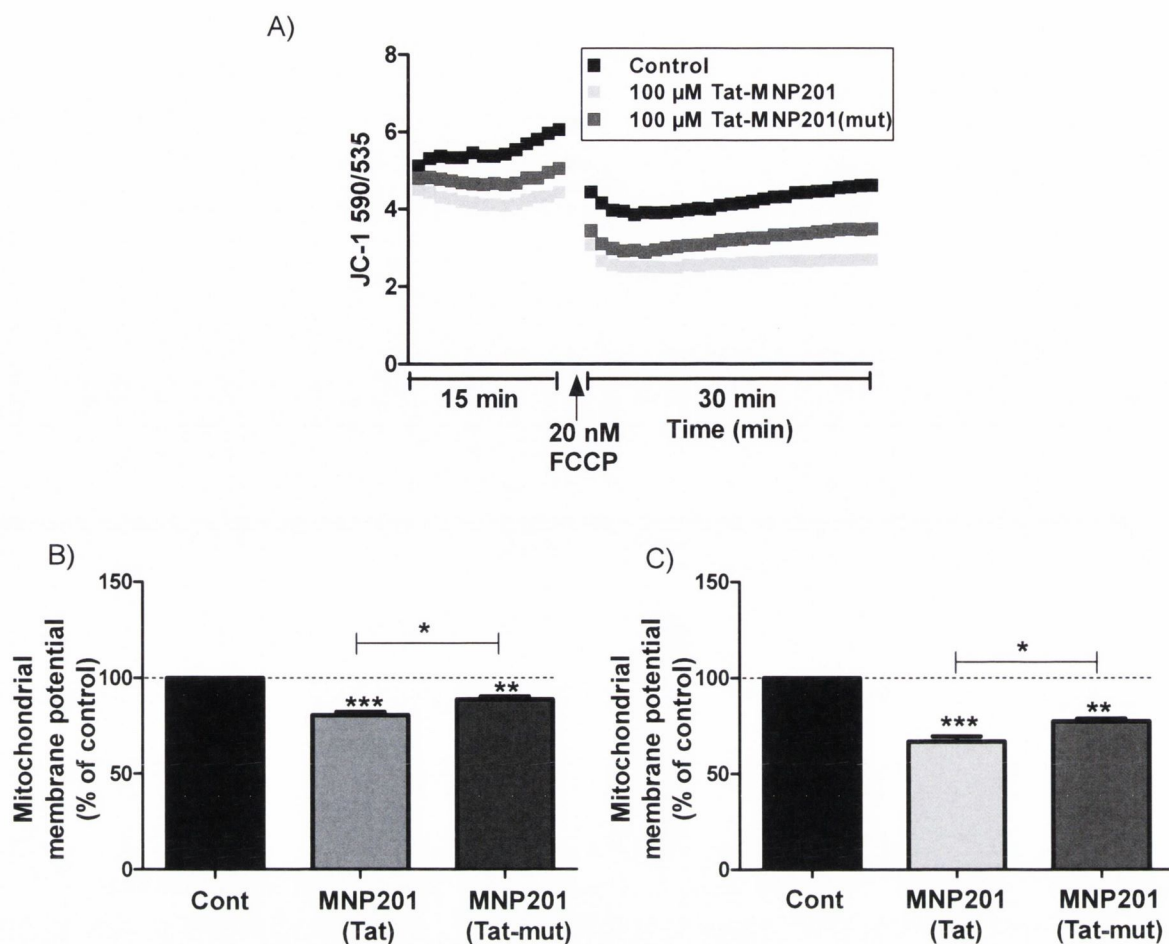


Figure 5.8: Effect of Tat-MNP201 on mitochondrial membrane potential under FCCP-induced partial stress condition

FCCP, a protonophore, induces depolarization of mitochondrial membrane depolarization. A partial mitochondrial depolarization stress was induced by 20 nM FCCP (see **Figure 5.7**). JC-1 treated freshly extracted synaptosomes were treated with vehicle control, 100 μ M Tat-MNP201 and 100 μ M Tat-MNP201(mut); and rate of change in the mitochondrial membrane potential was observed for 15 min. Then, synaptosomes were treated with 20 nM FCCP and the rate of change in mitochondrial membrane potential was observed for a further 30 min. The fluorescence of JC-1 (excitation 490 nm, emission 590 and 535 nm) was recorded from the commencement of the experiment. The JC-1 590/535 ratio represents a quantitative reporter of mitochondrial membrane potential. The fluorescence ratio of JC-1 (590 nm/535 nm) was plotted against time and the representative traces (A) were obtained from synaptosomes treated with vehicle control, 100 μ M Tat-MNP201 and 100 μ M Tat-MNP201(mut). The bar graphs represent the mitochondrial membrane potential during the linear part of the curve (the same for each treatment condition; 5-10 min before FCCP and 15-20 min after FCCP) as a percentage of control (mean \pm SEM) observed in vehicle control (Cont), 100 μ M Tat-MNP201 and 100 μ M Tat-MNP201(mut) treated synaptosomes in three separate experiments ($n=3$) before (B) and after (C) FCCP-induced stress depolarization. The p -values (***), (**) and (*) signify $p<0.001$, $p<0.01$ and $p<0.05$, respectively.

agreement with the data generated in **Figure 5.6**. In addition, when the FCCP-induced stress portion of the graph was analysed, 100 μM Tat- MNP201 ($67.05\% \pm 2.47$) treated samples demonstrated a 32.95% higher amount of mitochondrial depolarization compared to vehicle control treated synaptosomes (**Figure 5.8C**). In addition, 100 μM Tat-MNP201(mut) ($77.45\% \pm 1.53$) treated samples also demonstrated 22.55% increase in mitochondrial membrane depolarization compared to vehicle control. When the value of Tat-MNP201 was compared with Tat-MNP201(mut), an significant increase of 10.4% in mitochondrial depolarization was found in Tat-MNP201 treated synaptosomes compared to Tat-MNP201(mut). The effect of Tat-MNP201(mut) in non-stressed and stressed synaptosomes could be due to the effect of the Tat tag, as described in the previous experiment (**Figure 5.6**). These observations suggest that PICK1-parkin interaction may play a role in the maintenance of mitochondrial membrane potential.

5.7 Effect of Tat-MNP201 on 4-AP-induced glutamate release without CaCl_2

Next, the effect of 100 μM Tat-MNP201 was investigated in glutamate release from freshly extracted synaptosomes obtained from mature female Wistar rat brains. A continuous fluorimetric method based on Nicholls et al. (1987) was used where the amount of NADPH is measured (460 nm) as the quantitative indicator of glutamate release, as indicated in Kilbride et al. (2008). First, freshly extracted synaptosomes were incubated with the glutamate release assay media and the blank rate of glutamate release was monitored for the first 2 min. Then, vehicle control, Tat-MNP201 peptides and rotenone were added and the baseline glutamate release was observed from non-depolarized synaptosomes for the next 5 min. The total release of glutamate in non-depolarized synaptosomes was measured over this 5 min period. No significant difference was observed in Ca^{2+} -independent glutamate release from 100 μM Tat-MNP201 ($98.95\% \pm 2.21$) treated non-depolarized synaptosomes compared to vehicle control and 100 μM Tat-MNP201(mut) ($101.71\% \pm 2.65$) treated samples (**Figure 5.9A, B**). In contrast, the positive control 10 μM rotenone ($126.04\% \pm 4.18$), an inhibitor of complex I, showed a significant 26.04% increase in glutamate release when compared to vehicle control, in agreement with previously published data (Kilbride et al., 2008).

After measuring rate of glutamate release from non-depolarized synaptosomes, the depolarization of synaptosomes was carried out using 4-AP, a non-selective voltage-dependent K^+ -channel blocker, and rate of Ca^{2+} -independent glutamate release was recorded for 10 min. The total release of glutamate from depolarized synaptosomes was

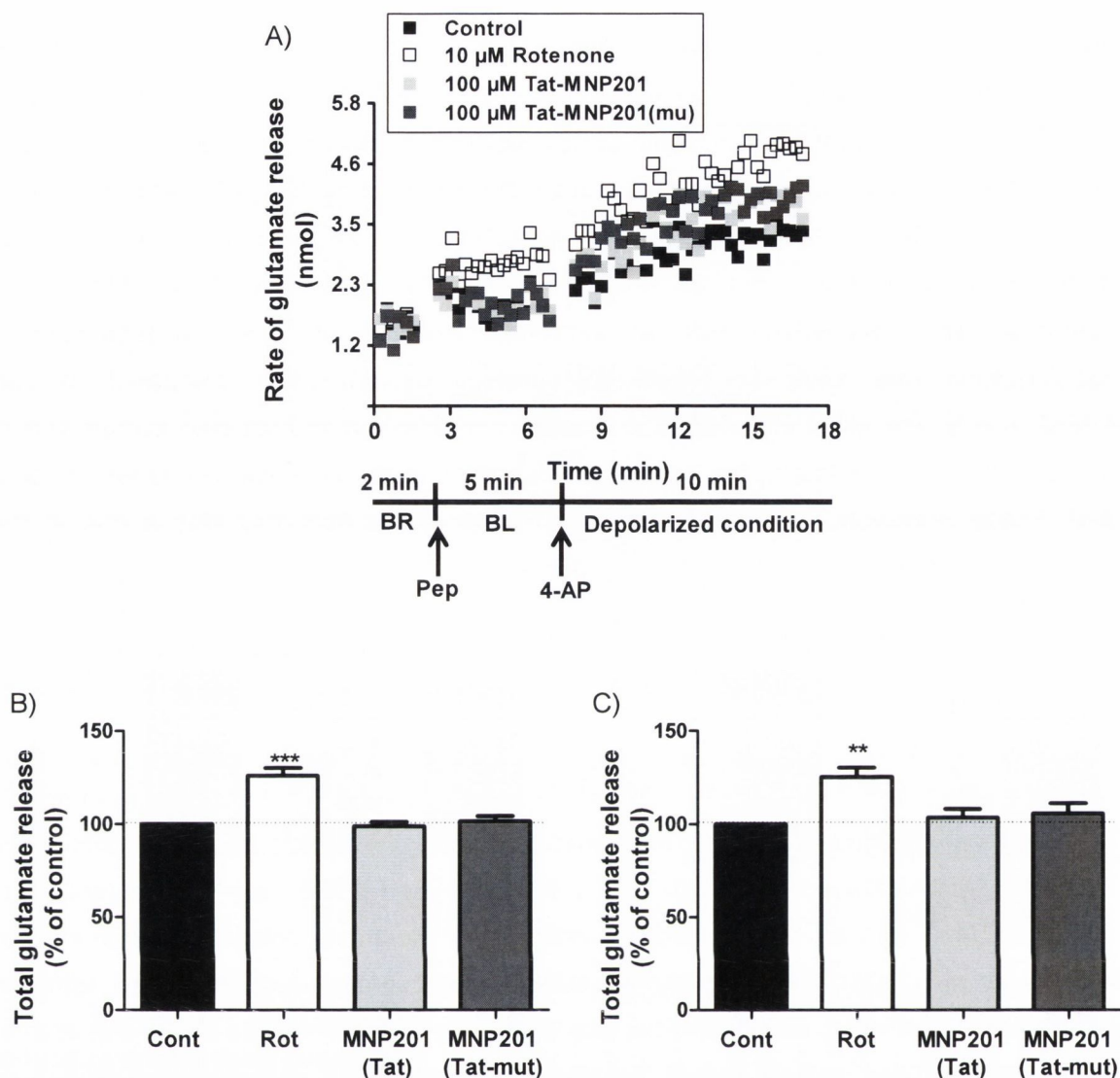


Figure 5.9: Effect of Tat-MNP201 on 4-AP-induced glutamate release without CaCl_2

The rate of glutamate release was measured by NADPH production at 460 nm. The level of glutamate was determined by generating a standard curve of glutamate-mediated NADPH production (Figure 4.9), in the absence of synaptosomes. The blank rate (BR) of glutamate release was recorded for the first 2 min in freshly extracted synaptosomes in the absence of CaCl_2 . Then, synaptosomes were treated with peptides (Pep), i.e., 100 μM Tat-MNP201 and 100 μM Tat-MNP201(mu) and also 10 μM rotenone; and the rate of glutamate release at baseline (BL) was observed from non-depolarized synaptosomes for the next 5 min. Then, depolarization of synaptosomes was initiated by addition of 10 mM 4-AP and the rate of glutamate release was observed for the remaining 10 min. A) The graph indicates the representative traces of Ca^{2+} -independent rate of glutamate release (nmol) from vehicle control, 10 μM rotenone, 100 μM Tat-MNP201 and 100 μM Tat-MNP201(mu) treated synaptosomes in a total time period of 17 min. The bar diagrams show the total glutamate release as a percentage of control (mean \pm SEM) from vehicle control (Cont), 10 μM rotenone (Rot), 100 μM Tat-MNP201 and 100 μM Tat-MNP201(mu) treated synaptosomes under non-depolarized (B) and depolarized (C) conditions in five separate experiments (n=5). The p-values (***) and (**) signify $p < 0.001$ and $p < 0.01$.

measured over this 10 min period. No statistically significant change in the rate of glutamate release was observed in synaptosomes treated with 100 μM Tat-MNP201 ($103.60\% \pm 4.46$) when compared to vehicle control and Tat-MNP201(mut) ($105.86\% \pm 5.29$) (**Figure 5.9A, C**). In contrast, the positive control 10 μM rotenone ($125.24\% \pm 5.05$) induced a significant 25.24% of increase in release of glutamate compared to vehicle control, in agreement with previously published data (Kilbride et al., 2008). Taken together, the data suggest that Tat-MNP201 has no effect in Ca^{2+} -independent 4-AP-induced glutamate release from synaptosomes.

5.8 Effect of Tat-MNP201 on 4-AP-induced glutamate release with CaCl_2

After observing the effect of Tat-MNP201 on Ca^{2+} -independent glutamate release from non-depolarized or 10 mM 4-AP depolarised synaptosomes, the effects of Tat-MNP201 was examined on glutamate release in the presence of 2 mM CaCl_2 . In non-depolarized synaptosomes, 100 μM Tat-MNP201 ($107.27\% \pm 4.49$) showed no statistically significant effect on the Ca^{2+} -dependent rate of glutamate release when compared to vehicle control or 100 μM of Tat-MNP201(mut) ($102.85\% \pm 2.12$) (**Figure 5.10A, B**). On the other hand, the positive control sample 10 μM rotenone ($142.20\% \pm 6.44$) induced a significantly 42.20% higher rate of glutamate release when compared to vehicle control, in agreement with previously published data (Kilbride et al., 2008). After measuring the non-depolarized rates of glutamate release, the synaptosomes were depolarized with 10mM 4-AP. In the presence of 2 mM CaCl_2 and 10 mM 4-AP, again, no change in glutamate release was observed in 100 μM Tat-MNP201 ($110.67\% \pm 2.55$) treated synaptosomes, when compared to vehicle control and Tat-MNP201(mut) ($99.86\% \pm 3.26$) (**Figure 5.10A, C**). In contrast, 10 μM rotenone ($125.10\% \pm 7.95$) induced a significant 25.10% increase of release of glutamate compared to vehicle control, in agreement with previously published data (Kilbride et al., 2008). Taken together, the data showed that Tat-MNP201 has no effect in Ca^{2+} -dependent glutamate release from non-depolarised or 4-AP depolarised synaptosomes.

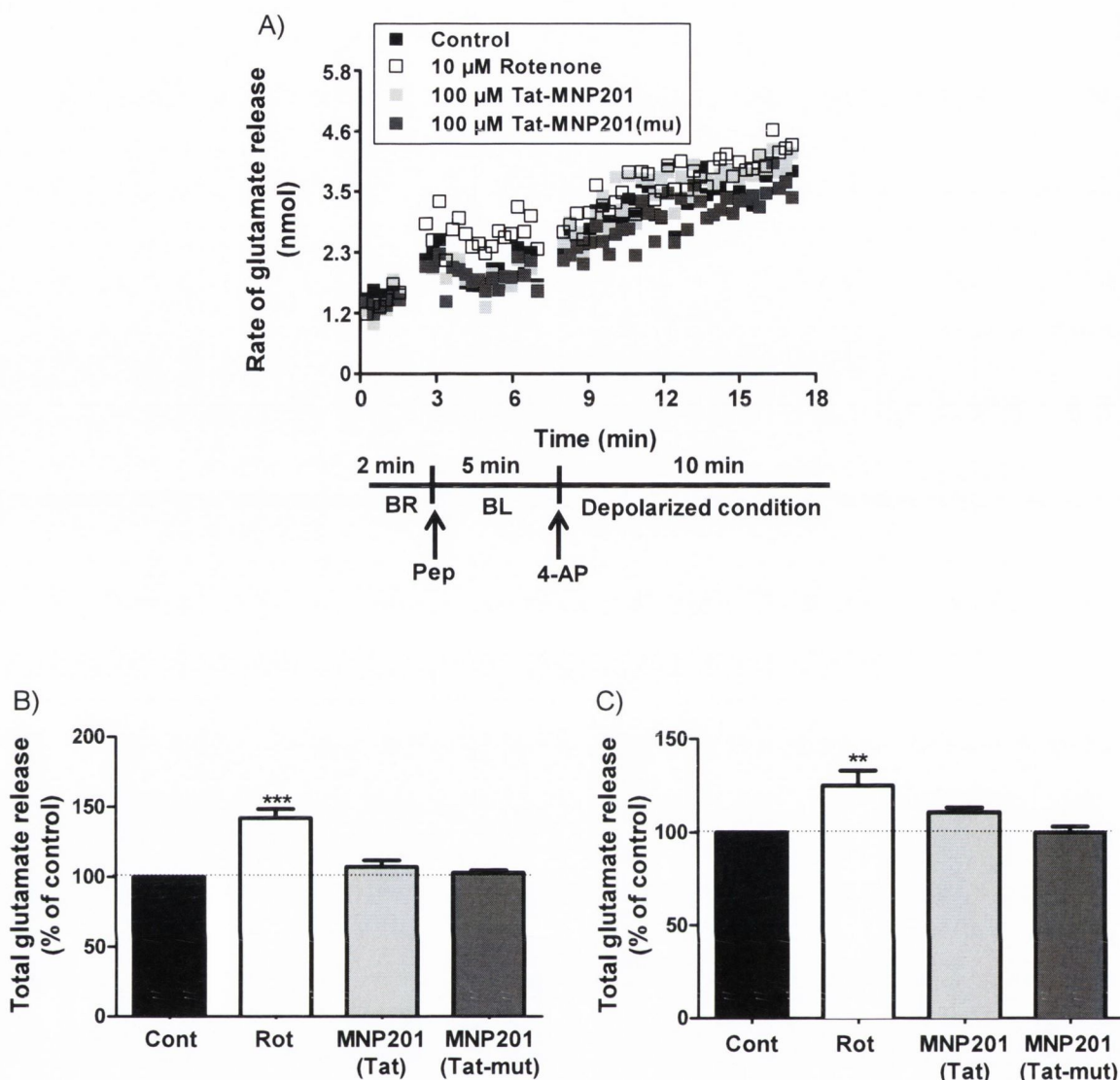


Figure 5.10: Effect of Tat-MNP201 on 4-AP-induced glutamate release with CaCl_2

The rate of glutamate release was measured by NADPH production at 460 nm. The level of glutamate was determined by generating a standard curve of glutamate-mediated NADPH production (Figure 4.9), in the absence of synaptosomes. The blank rate (BR) of glutamate release was recorded for the first 2 min in freshly extracted synaptosomes in the presence of CaCl_2 . Then, synaptosomes were treated with peptides (Pep), i.e., 100 μ M Tat-MNP201 and 100 μ M Tat-MNP201(mut) and also 10 μ M rotenone; and the rate of glutamate at baseline (BL) was observed from non-depolarized synaptosomes for the next 5 min. Then, depolarization of synaptosomes was initiated by addition of 10 mM 4-AP and rate of glutamate release was observed for a further 10 min. A) The graph indicates the representative traces of Ca^{2+} -dependent rate of glutamate release (nmol) in vehicle control, 10 μ M rotenone, 100 μ M Tat-MNP201 and 100 μ M Tat-MNP201(mut) treated synaptosomes in a total time period of 17 min. The bar diagrams show the total glutamate release as a percentage of control (mean \pm SEM) in vehicle control (Cont), 10 μ M rotenone (Rot), 100 μ M Tat-MNP201 and 100 μ M Tat-MNP201(mut) treated synaptosomes under non-depolarized (B) and depolarized (C) conditions in five separate experiments (n=5). The p-values (***) and (**) signify $p < 0.001$ and $p < 0.01$.

Discussion

1. Summary of results

In the previous chapter (Result 2), the effect of 100 μ M MNP201 was investigated on mitochondrial function and glutamate release assays. No statistically significant effect was obtained by using MNP201 on any of the mentioned assays. In this chapter, the N-terminal Tat-sequence tagged MNP201 (Tat-MNP201) was employed to investigate its effects on mitochondrial function and glutamate release assays (Result summary **Table 5.1**). To confirm membrane permeability of the peptide, a fluorescent labelled FITC-Tat-MNP201 peptide was synthesised. Treatment of the cortical neuronal and astrocyte culture showed the successful uptake of FITC-Tat-MNP201, confirming membrane permeability. Thereafter, the effect of Tat-MNP201 was demonstrated in the mitochondrial properties and glutamate release. In summary, the data showed that Tat-MNP201 did not alter glutamate release, however it inhibited mitochondrial membrane potential.

2. Tat-MNP201 reduces mitochondrial membrane potential

The working hypothesis of this project is that parkin-PICK1 interaction plays an important role in mitochondrial function. It has been reported that mitochondrial-induced apoptosis is one of the causes behind the death of dopaminergic neurons in mid brain in PD (Keeney et al., 2006). The two important markers of mitochondrial or cellular stress are (i) peroxide release and (ii) mitochondrial depolarization that play roles in apoptosis. Importantly, oxidative stress is known to cause cellular stress leading to apoptosis (Galley, 2011). Furthermore, collapse of the mitochondrial membrane potential induces the release of cytochrome C into the cytosol, which eventually triggers apoptosis (Ly et al., 2003). The results here indicated that Tat-MNP201 caused a statistically significant reduction in mitochondrial membrane potential, when compared to vehicle control samples in both control and FCCP stressed conditions. Interestingly, Tat-MNP201(mut), the mutated version of the Tat-MNP201 also caused mitochondrial depolarization, although the effects were significantly less than those seen with Tat-MNP201. Published data indicate that the N-terminal 72 amino acids of Tat can increase peroxide production and mitochondrial membrane depolarization along with disruption of Ca^{2+} homeostasis and caspase activation (Kruman et al., 1998). It is possible, therefore, that the Tat sequence in the MNP201 peptides may have some direct effect on mitochondrial membrane potential, although this appears unlikely since the Tat-MNP201 (wild type and mutated) did not induce production of ROS or alter glutamate release.

A)

Assay	100 μ M Tat-MNP201	100 μ M Tat-MNP201(mut)	Measured by
Peroxidase production	108.84% \pm 4.79	129.76% \pm 11.68	Resorufin production (OD ⁵⁸⁵)
Membrane potential	76.26% \pm 4.90	87.61% \pm 2.06	JC-1 OD ratio (JC-1 ^{590/535})
FCCP-induced membrane potential	67.05% \pm 2.47	77.45% \pm 1.53	JC-1 OD ratio (JC-1 ^{590/535})

B)

Glutamate release	100 μ M Tat-MNP201	100 μ M Tat-MNP201(mut)	Measured by
Non-depolarized level (- CaCl ₂)	98.95% \pm 2.21	101.71% \pm 2.65	Amount of NADPH production (OD ⁴⁶⁰)
Non-depolarized level (+ CaCl ₂)	107.27% \pm 4.49	102.85% \pm 2.12	
- CaCl ₂ , + 10 mM 4-AP	103.60% \pm 4.46	105.86% \pm 5.29	
+ CaCl ₂ , + 10 mM 4-AP	110.67% \pm 2.55	99.86% \pm 3.26	

Table 5.1: Summary of data obtained by using Tat-MNP201

Mitochondrial function assays (A) and glutamate release assay (B).

The data suggest that Tat-MNP201 has no effect on ROS production and glutamate release. In contrast, Tat-MNP201 inhibits mitochondrial membrane potential in both control and FCCP stressed conditions. The values are indicated as a percentage of control (mean \pm SEM).

3. Effect of Tat-MNP201 in glutamate release

The glutamate release assay using Tat-MNP201 showed similar results to the non tagged MNP201 version. Specifically, Ca^{2+} -independent and dependent glutamate release experiments were performed by treating freshly prepared synaptosomes with 100 μM Tat-MNP201 in non-depolarized conditions as well as in depolarized conditions (triggered by 4-AP). No significant difference in the rate of Ca^{2+} -independent or dependent glutamate release in Tat-MNP201 treated synaptosomes was observed under non-depolarized and 4-AP-induced depolarized conditions, when compared to the vehicle control and Tat-MNP201(mut) samples. In contrast, rotenone treated samples showed significant increase in the rate of glutamate release. Taken together, the data suggested that Tat-MNP201 has no effect on pre-synaptic release of glutamate from synaptosomes. As indicated in the previous chapter, the lack of effects of Tat-MNP201 on glutamate release was surprising when considering that MNP201 binds to the PDZ domain of PICK1 and thus could competitively block all PDZ motifs interacting with PICK1, in particular pre-synaptic glutamate receptors that control glutamate release. Two possibilities exist that may explain these results: (i) the MNP201 does not block the interaction of PICK1 with GluR2, GluR5 and/or mGluR7 or (ii) PICK1 interaction with GluR2 (AMPA), GluR5 (KA) and/or mGluR7 (metabotropic) does not play a role in glutamate release. Notably, Tat peptides have been reported to increase release of glutamate from human and mouse neocortical nerve endings (Musante et al., 2010). Thus, while the lack of effects of Tat-MNP201 on glutamate release was surprising, these data suggest that the Tat sequence in the Tat-MNP201 and Tat-MNP201(mut) peptides do not cause overt effects on synaptosomal integrity *per se* and therefore support the notion that the Tat-MNP201-induced decrease in mitochondrial membrane depolarization is a significant finding.

4. Parkin-PICK1 role in mitochondrial membrane potential

Several reports have suggested that the trafficking of parkin to depolarized mitochondria plays a role in the induction of mitophagy by recruitment of autophagosomes (Narendra et al., 2009; Narendra et al., 2010; Geisler et al., 2010; Ziviani et al., 2010). These data raise further questions, such as: (i) what is the signalling mechanism that *activates* parkin to translocate towards depolarized mitochondria, (ii) what is the *translocating* mechanism of parkin to depolarized mitochondria and (iii) how does parkin *recognise* depolarized mitochondria? According to our hypothesis, PICK1 may play a role in the trafficking of parkin towards depolarized mitochondria. Indeed, the mitochondrial membrane potential data showed that in the presence of 100 μM Tat-MNP201, a reduction in the mitochondrial

membrane potential was observed in synaptosomes. This data may suggest that Tat-MNP201 alters mitochondrial membrane potential due to the disruption of the parkin-PICK1 interaction, which prevents parkin translocation to mitochondria and leaves mitochondria more susceptible to depolarization (especially during conditions of stress). To further confirm this hypothesis, it would be worthy to examine the effect of Tat-MNP201 on the translocation of parkin to mitochondrial membranes under depolarising conditions using imaging studies.

5. Alternative mechanisms for MNP201 effects on mitochondrial membrane potential

Earlier reports have also suggested that mitochondrial stabilization and cell viability is enhanced when PICK1 recruits activated PKC α to the outer mitochondrial membrane to phosphorylate the anti-apoptotic Bcl-2 protein (Wang et al., 2007). Due to the absence of a mitochondria targeting sequence in PKC α , PICK1 has an important role in the proper targeting of PKC α to mitochondria (Wang et al., 2007). In addition to localisation of PKC α to the mitochondria, PICK1 also modulates the phosphorylation of Bcl-2 proteins. Upon over-expression of PICK1, the phosphorylation of Bcl-2 protein increases in the presence of PKC α (Wang et al., 2007). Phosphorylation of Bcl-2 by PKC α induces anti-apoptotic property by reducing the formation of Bcl2/Bax heterodimers and preventing Bax proteins docking to mitochondrial membranes (Wang et al., 2007). Moreover, PICK1 is also believed to influence the pore forming components, such as the mtPTP to maintain mitochondrial membrane integrity (Halestrap et al., 2003). It is therefore important to note that the effects of Tat-MNP201 on reducing mitochondrial membrane potential may be due to (i) an inhibition of a PKC α -PICK1 interaction, (ii) altering Bcl-2 phosphorylation, and/or (iii) regulation of mtPTP function in addition to (or instead of) blocking a parkin-PICK1 interaction. In addition to these possible alternative mechanisms of MNP201 regulating mitochondrial membrane potential, it is also important to note that PICK1 can form homodimers/oligodimers, which allows it to interact with multiple partners simultaneously, which may also be regulated by MNP201 to alter mitochondrial membrane potential e.g. formation of a parkin-PICK1/PICK1-ASIC complex (Joch et al., 2007). In this context, the over-expression of parkin is reported to induce monoubiquitination of PICK1, which limits PICK1-ASIC interaction and causes a loss of ASIC channel current (Joch et al., 2007). The effect of parkin-mediated PICK1 monoubiquitination on mitochondrial function is still unknown. Thus, it would be interesting to investigate the effect of parkin-mediated monoubiquitination of PICK1 on (i) the role of PKC α -PICK1 on mitochondrial function, (ii) in maintaining mitochondrial integrity and (iii) Bcl-2-dependent apoptosis.

7. Moving to the next chapter

At this stage, the outcome of the experiments propose that the interaction between parkin-PICK1 may play a role in regulating mitochondrial membrane potential under control and cell stress conditions (induced by FCCP). The results show that the Tat-MNP201 compounds reduce mitochondrial membrane potential, with no effects on ROS activity or glutamate release. A number of open questions remain regarding how the Tat-MNP201 peptide alters mitochondrial membrane potential, including does Tat-MNP201 work by (i) inhibiting the parkin-PICK1 interaction?; (ii) limiting PKC α -PICK1 function?; (iii) altering the role of parkin-PICK1-PKC α in mitochondria? and/or (iv) regulating the phosphorylation or ubiquitination of these proteins?

6. Results: 4
Effect of FSC231 on
mitochondrial function

Abstract

In previous two chapters, the effects of PDZ motif peptides modelled on parkin were investigated in mitochondrial function and glutamate release. The two versions of parkin peptides characterised were MNP201 and Tat-MNP201. The MNP201 version, without a cell permeability motif, did not show any effect on mitochondrial function and glutamate release assays. In contrast, Tat-MNP201, a cell permeable version, showed mitochondrial membrane depolarization under control and stress-induced conditions. In this chapter, the compound called FSC231 was used, which is a compound that binding to the PDZ domain of PICK1. FSC231 is an aromatic compound that, as a result of binding the PDZ domain of PICK1, competitively hinders the interaction of PICK1 with the AMPA receptor subunit, GluR2. Due to its small molecular size and lipophilic nature, FSC231 is capable of crossing the plasma membrane unaided (Thorsen et al., 2010). Here, an *in silico* computational modelling analysis was first performed that investigated the docking of FSC231 into the PDZ domain of PICK1 to assess its putative affinity. Then, the effect of FSC231 was investigated on mitochondrial function and glutamate release. Similar to the MNP201 peptides, the data suggested that FSC231 had no effect on the activities of the respiratory chains of ETC (complex I and IV) or on peroxide production. In addition, no effect of FSC231 was observed in the rate of glutamate release. While FSC231 did not alter mitochondrial membrane potential under control conditions, more importantly this compound increased mitochondrial membrane depolarization in treated synaptosomes under FCCP-induced stressed conditions, similar to Tat-MNP201. The data may suggest that PDZ domain interacting proteins of PICK1, such as parkin and/or PKC α , are prevented from interacting with PICK1 in the presence of FSC231 and these interactions play a role in the maintenance of mitochondrial integrity, especially under mitochondrial depolarizing stress conditions.

Introduction

The PDZ domain is composed of 90 amino acids and forms a precise groove responsible for interaction with proteins containing a PDZ motif at their C-terminus. This domain was first discovered in three proteins, i.e., PSD95, Dlg1 and ZO-1 protein (Sheng and Sala, 2001). A PDZ domain is composed of six antiparallel β -strands and two α -helices to form a six-strand β -sandwich surrounded by two α -helices. The interaction groove of a PDZ domain is conformed between the β B strand and α B helix that interacts with the PDZ motif. PDZ domains are divided into three types, i.e., Class I-III (Sheng, 2001). The classes of PDZ domains are defined according to the amino acid composition of tripeptide PDZ motifs they interact with. They are, Class I $\{(S/T)X\phi\}$, Class II $(\phi X\phi)$ and Class III $(D-E-X-\phi)$, where ϕ and X denote an hydrophobic and any amino acid respectively (Sheng, 2001). Intriguingly, the PDZ domain of PICK1 can interact with Class I, Class II and atypical PDZ motifs (Staudinger et al., 1997; Dev et al., 1999; Madsen et al., 2005). Interestingly, this ability of PICK1 to interact with a wide range of PDZ motifs is evolutionarily conserved as indicated by the sequence homology within the PDZ domain of PICK1 across different species.

The identification of interaction “hotspots” within PDZ domains have made them an attractive site for the development of small molecule inhibitors (Berg, 2003; Arkin and Wells, 2004; Fischer and Lane, 2004). Over the past few years several compounds have been shown to block PDZ based interactions. For example, reports have demonstrated that the interaction between the PDZ domain of PSD95 and the PDZ motif of neuronal nNOS can be successfully disrupted with the blocking compounds, including 2-[(1H-benzotriazol-5-ylamino)-methyl]-4,6-dichloro-phenol (IC87201) and 5-(3,5-dichloro-2-hydroxyl-benzylamino)-2-hydrobenzoic acid (ZL006) (Florio et al., 2009; Zhou et al., 2010). The PSD95 protein, containing three distinct PDZ domains, interacts with both NMDA receptors and nNOS; and couples NMDA receptors to nNOS. This NMDA-PSD95-nNOS pathway plays a role in synaptic plasticity, learning and memory (Harkin et al., 1999; Aarts et al., 2002; Florio et al., 2009; Zhou et al., 2010; Doucet et al., 2012). Particularly, IC87201 has been shown to inhibit the interaction between nNOS and PSD95, without disturbing the catalytic activity of nNOS *in vitro* and was able to reduce NMDA-induced thermal hyperalgesia in mice (Florio et al., 2009). In addition, ZL006 has been reported to prevent cerebral ischemic damage in rodents by inhibiting formation of the nNOS-PSD95 complex (Zhou et al., 2010). Both of these compounds successfully demonstrated the potential value of PDZ interactions as drug targets.

As mentioned above, AMPA receptors are ionotropic glutamate receptors responsible for fast excitatory neurotransmission and involved in synaptic formation and stabilisation (Dev et al., 1999). The dynamic membrane trafficking of AMPA receptors plays an important role in the regulation of several forms of synaptic plasticity such as LTP and LTD (Lin and Huganir, 2007). AMPA receptor activation plays an important role in the maintenance of physiological neuronal function, although prolonged activation may lead to neurotoxicity (Choi, 1992). AMPA receptors are composed of four subunits, GluR1-GluR4 (Hollmann and Heinemann, 1994; Bettler and Mulle, 1995). The C-terminus of the GluR2 contains a PDZ motif that interacts with PDZ domain containing proteins, including PICK1 (Dev et al., 1999), GRIP (Dong et al., 1997) and ABP (Srivastava et al., 1998). PICK1 regulates the surface expression and internalisation of GluR2, thus, plays a role in synaptic plasticity. A number of studies have used blocking peptides to inhibit the interaction between PICK1 and GluR2 in order to determine the role of this interaction. More recently, a small molecular weight compound called FSC231, which binds to PICK1, has been used to further evaluate the role of PICK1 in regulating AMPA receptor-mediated synaptic plasticity (Thorsen et al., 2010).

The recent discovery of a PICK1 PDZ domain blocking compound, namely FSC231, has provided a valuable tool to investigate the role of PICK1 and its interacting proteins and demonstrated that PICK1 may be drugable. The FSC231 compound is an aromatic molecule that docks into the PDZ domain of PICK1. The molecular weight of FSC231 is 313 g/mol and the compound is poorly soluble in water. A recent report suggests that 50 μ M FSC231 blocks the interaction between PICK1 and the AMPA receptor subunit, GluR2 (Thorsen et al., 2010). Upon NMDA receptor activation, GluR2 internalisation takes place by a PICK1-mediated transport mechanism (Chung et al., 2000; Daw et al., 2000; Kim et al., 2001). In contrast, the rate of GluR2 internalisation decreases and surface expression of GluR2 increases in the presence of FSC231, even after NMDA receptor activation (Thorsen et al., 2010). In addition, LTD and LTP are significantly reduced in the presence of 50 μ M FSC231 in CA1 hippocampal neurons (Thorsen et al., 2010). It has been shown previously that GluR2 regulates the Ca^{2+} permeability of the AMPA receptor (Liu and Cull-Candy, 2000; Liu et al., 2008), such that Ca^{2+} permeability increases in the absence of wild type GluR2. When PICK1-GluR2 interaction is blocked by using a GluR2 blocking peptide (NVYGIKSVKI), hippocampal and cerebellar LTD are reduced (Xia et al., 2000; Kim et al., 2001). Interestingly, 50 μ M FSC231 shows similar effects in hippocampal neurons (Thorsen et al., 2010). Here, in this chapter, the effect of FSC231 was investigated in the rate of glutamate release.

As described previously, two interacting partners of PICK1, i.e., parkin and PKC α may play a role in the maintenance of mitochondrial function and integrity. The role of PKC α -PICK1 is well described in the published literature (Wang et al., 2003; 2007), while the role of parkin-PICK1 interaction in mitochondrial function is still unknown. Therefore, to investigate the importance of PICK1 and its interacting partners including parkin (and PKC α) in mitochondrial function, the effect of 50 μ M FSC231 was investigated in mitochondrial function including the activity of ETC enzymes (complex I and IV), ROS production and mitochondrial membrane potential. Given that PICK1 regulates AMPA, KA and metabotropic receptor surface expression and that these receptors can regulate pre-synaptic glutamate releases, in addition, the effect of FSC231 was also examined in glutamate release assays.

Results

6.1 Computational data shows docking of FSC231 in PICK1 PDZ domain

FSC231 is reported to bind selectively to PICK1, but not other PDZ domain containing proteins, for example GRIP (Thorsen et al., 2010). Here, the *in silico* binding affinity of FSC231 with PICK1 was analysed. To ascertain the binding affinity of FSC231, Drugscore, a bio-informatic tool was used to model FSC231 in the PDZ domain of PICK1. Drugscore is a computational method, where the strength of a protein-protein interaction is evaluated on the basis of the ligand (PDZ motif) binding into the receptor (PDZ domain) in a conformation that adopts the lowest free energy. In this modelling approach, the higher negative values indicate a higher binding affinity. When the sequence of the PDZ domain of PICK1 was computed with FSC231 by Drugscore computational modelling, a binding score of -66.75 kcal/mol was found (**Figure 6.1**). As a positive control, the GluR2-PICK1 interaction was evaluated in this method and a binding value of -92 kcal/mol was obtained. The result suggests that FSC231 has a strong affinity towards the PDZ domain of PICK1. The *in silico* data was provided by our collaborators Sefika Banu Ozkan (Center for Biological Physics, Arizona State University, USA) and Ozlem Keskin (Center for Computational Biology and Bioinformatics, Koc University, Istanbul, Turkey).

Supplied as white powder, a 5 mM FSC231 stock solution was made in 75% DMSO and 25 mM HEPES pH 7 and used in mitochondrial and glutamate release assays. Therefore, 75% DMSO and 25 mM HEPES pH 7 were used as a DMSO vehicle control in mitochondrial and glutamate release assays. The aliquots of the stock solutions were stored at -20°C until further use.

6.2 Effect of FSC231 in complex I assay

Deficiencies in the respiratory chain of the ETC cause mitochondrial dysfunction and have been identified to play a role in neurodegenerative diseases. The complex I activity was measured by the rate of conversion of NADH to NAD⁺ spectrophotometrically at an absorbance of 340 nm, as suggested by previous publications (Telford et al., 2010). To investigate the role of the parkin-PICK1 interaction, the effect of MNP201 parkin peptide was examined in a complex I assay. The data showed that the MNP201 peptide at a concentration of 100 µM did not have any effect on the rate of complex I activity (**Figure 4.4**). In this chapter, FSC231, a compound that binds the PDZ domain of PICK1 (Thorsen et

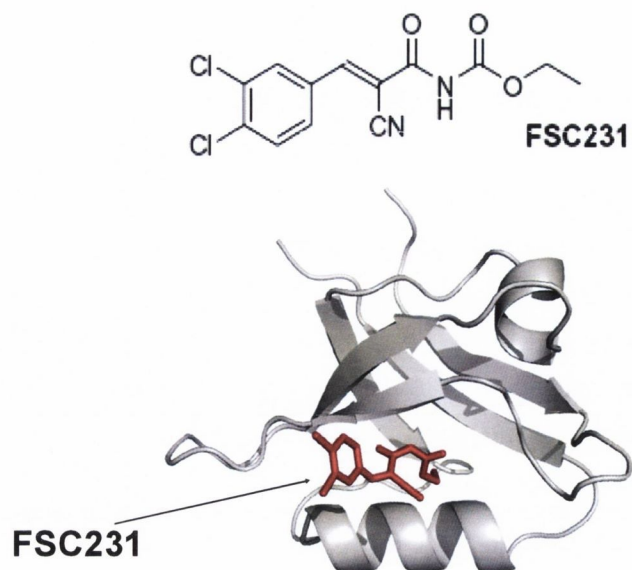


Figure 6.1: FSC231, the blocking compound of PICK1 PDZ domain

FSC231 is a small aromatic compound, which directly binds the PDZ domain of PICK1 causing a competitive block of PDZ-mediated interactions. The binding affinity of FSC231 for the PDZ domain of PICK1 was -66.75 kcal/mol, as measured by the Drugscore computational method.

al., 2010), was used to investigate the effect of PICK1 interacting proteins in the complex I activity. First, freeze-fractured synaptosomes were either treated with DMSO vehicle control or treated with 50 μ M of FSC231 and the absorbance of NADH were monitored for 1-2 min. Next, the reaction was initiated by the addition of decylquinone and the absorbance of NADH was observed for a further 12-15 min (**Figure 6.2A**). To selectively inhibit complex I, rotenone was added and the absorbance of NADH was subsequently monitored for a final 4-5 min. The rate constants of complex I were calculated according to the method based on Ragan et al. (1987) and the rotenone insensitive rate was subtracted from the rotenone sensitive value to obtain the rate of complex I activity. When the values were expressed as a percentage of control, no significant difference in the rate of complex I were observed in 50 μ M FSC231 (93.80% \pm 15.58) treated samples compared to the DMSO vehicle control treated samples (**Figure 6.2B**). The data showed that 50 μ M FSC231 has no effect on the rate of complex I activity and is in agreement with the lack of effects of MNP201 on complex I activity. Thus, the data suggests that PICK1 and its interacting partners do not regulate the activity of mitochondrial complex I.

6.3 Effect of FSC231 in complex IV assay

The aberrant function of complex IV is reported to play a role in the pathophysiology of neurodegenerative diseases. For example, activity of mitochondrial complex IV has been found to be hampered in brain samples of AD patients (Chagnon et al., 1995). Complex IV is the last enzyme complex through which electrons travel to the mitochondria matrix before being utilised by ATP synthase to produce ATP. In the earlier chapter (Result 1), the effect of MNP201 parkin peptide was investigated on complex IV assay to determine the role of the parkin-PICK1 interaction. The data suggested that MNP201 had no effect in complex IV activity (**Figure 4.5**). To further investigate these findings, the effect of FSC231 on complex IV activity was tested. The studies were also performed to investigate the role of PICK1 interacting proteins in the activity of complex IV. The activity of complex IV was measured by monitoring the rate of depletion of cytochrome C (550 nm) by oxidation (Telford et al., 2010), as determined by calculating the first order rate constant of cytochrome C depletion.

First, the DMSO vehicle control and 50 μ M FSC231 was incubated with the complex IV reaction mixture (please see Method) and the absorbance of cytochrome C was monitored for 1-2 min. Next, the reaction was initiated by addition of freeze-fractured synaptosomal protein and the absorbance of cytochrome C depletion was observed for a subsequent 7-8 min (**Figure 6.3A**). The corresponding rate constants of complex IV activity were calculated according to the method of Wharton and Tzagoloff (1967) and expressed as percentage of

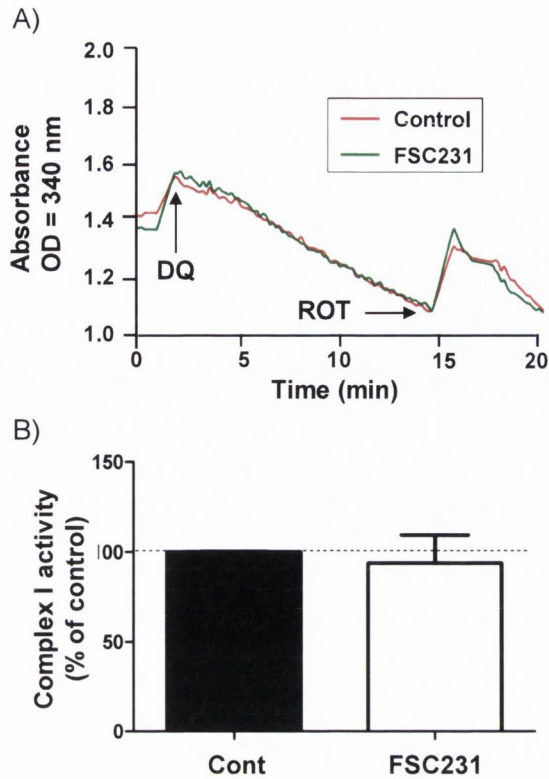


Figure 6.2: Effect of FSC231 on complex I of ETC cycle

Complex I activity is shown in freeze-fractured synaptosomes treated with FSC231. The complex I utilises NADH as a source of electrons and passes electrons to complex III via ubiquinone. Complex I is inhibited by rotenone. A) The graph shows the raw data of complex I activity by measuring absorbance (340 nm) of depleting NADH in the presence or absence of FSC231 over a time scale of 20 min. Representative traces of complex I activity are shown in the presence of DMSO vehicle control (red trace) and 50 μ M FSC231 (green trace). The first peak (DQ) and second peak (ROT) signify addition of decylquinone (1-2 min) and rotenone (14-15 min), respectively. The complex I activity (pseudo-first order rate constant) was obtained by subtracting the rotenone sensitive rate from the initial rate. B) The bar diagram shows the activity of complex I as a percentage of control (mean \pm SEM) in three separate experiments (n=3) in the presence of DMSO vehicle control (Cont), and FSC231.

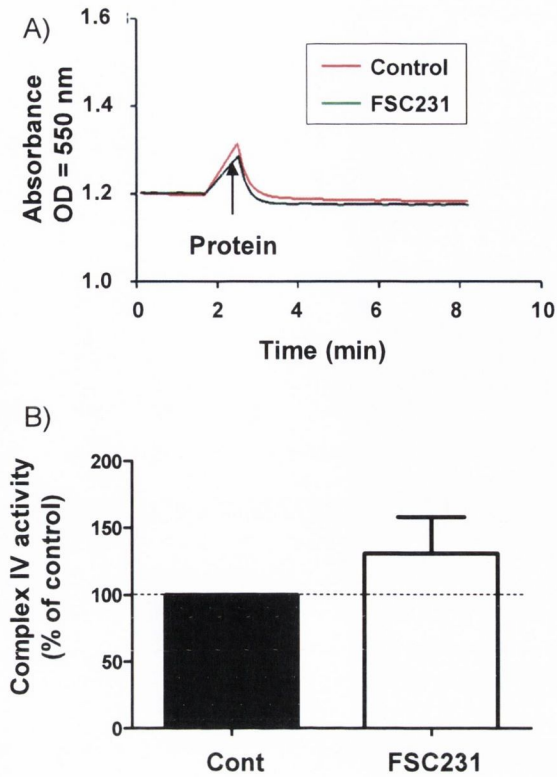


Figure 6.3: Effect of FSC231 on complex IV of ETC cycle

Complex IV activity is shown in freeze-fractured synaptosomes treated with or without FSC231. Complex IV uses complex III as a source of electrons and passes electrons out of the matrix to inner membrane space. A) The graph shows the raw data of complex IV activity of synaptosomal mitochondria by measuring absorbance (550 nm) of depleting cytochrome C in the presence or absence of FSC231 over a time scale of 10 min. Representative traces of complex IV activity are shown in the presence of DMSO vehicle control (red trace) and FSC231 (green trace). The peaks in the activity traces are due to addition of freeze-fractured synaptosomal protein (protein) (1-2 min). The complex IV activity was determined by measuring first order decay rate constant of cytochrome C. B) The bar diagram represents the activity of complex IV as a percentage of control (mean \pm SEM) in three separate experiments (n=3) in the presence of DMSO vehicle control (Cont) and FSC231.

control. In agreement with the results found for MNP201, the data showed no statistically significant difference in complex IV activity in 50 μ M FSC231 ($93.16\% \pm 9.21$) treated synaptosomes, when compared to the DMSO vehicle control (**Figure 6.3B**). The data suggest that PICK1 and its interacting partners do not play a role in regulating complex IV activity in mitochondria.

6.4 Effect of FSC231 on peroxide production

Production of ROS is an indicator of cellular oxidative stress, which plays a key role in apoptotic cell death. The effect of FSC231 was evaluated in ROS production with freshly prepared synaptosomes over a time period of 2 h. An amplex red assay, based on the conversion of amplex red to resorufin in the presence of ROS, was used. The rate of resorufin production, the quantitative indicator of H_2O_2 , in vehicle control and FSC231 treated synaptosomes was plotted against time (x-axis) and OD^{585} (y-axis) (**Figure 6.4A**). A linear portion of the curve was selected (the same for each treatment condition; 15-20 min) and total H_2O_2 production was calculated. The relative values of peroxide production were expressed as a percentage of control and plotted in a bar graph. Analysis of data revealed that 50 μ M FSC231 ($115.08\% \pm 9.98$) treated synaptosomes had no significant effect in the rate of peroxide production in comparison to DMSO vehicle control treated synaptosomes. In contrast, when synaptosomes were treated with 1 μ M of antimycin A ($262.12\% \pm 20.46$), an increase of 162% ROS production was found, when compared with DMSO vehicle control (**Figure 6.4B**), in agreement with previously published data (Sipos et al., 2003). The data suggest that PICK1 does not play a role in the regulation in peroxide production as well as oxidative stress in synaptosomal mitochondria.

6.5 Effect of FSC231 on mitochondrial membrane potential

Mitochondrial membrane potential is an important parameter of mitochondrial function and also a key indicator of cell viability. Mitochondrial membrane potential was measured by calculating the ratio of red (590 nm, aggregated form) to green (535 nm, monomeric form) JC-1, as suggested previously (Chinopoulos et al., 1999). This $JC-1^{590/535}$ ratio is a quantitative indicator of mitochondrial membrane potential. Freshly extracted synaptosomes were first incubated with JC-1 and then treated with DMSO vehicle control and FSC231. The $JC-1^{590/535}$ ratio (y-axis) was measured as the rate of change in mitochondrial membrane potential over a time of 1 h (x-axis) (**Figure 6.5A**). A linear portion of the curve was selected (the same for each treatment condition; 15-20 min) and the mitochondrial membrane potential was measured. The relative values of the mitochondrial membrane potential were expressed as a percentage of control and plotted in a bar graph. No change in the

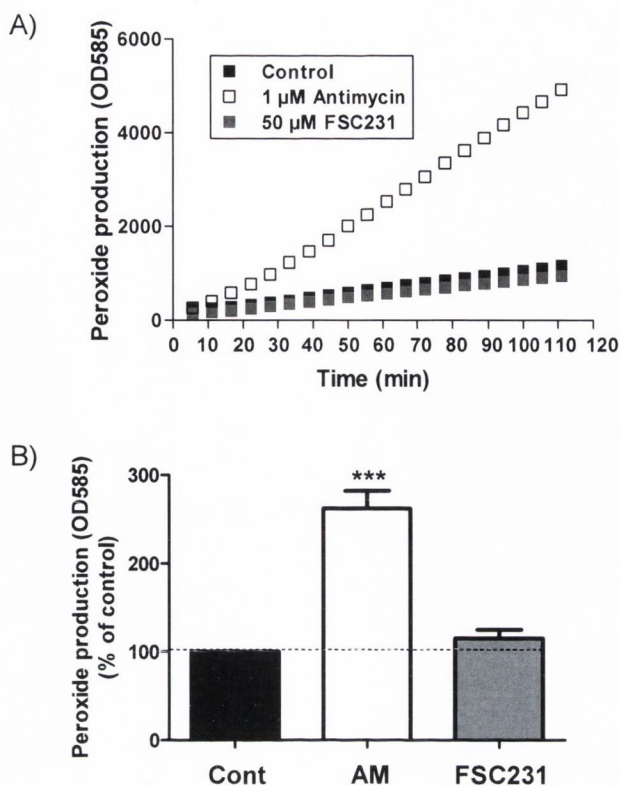


Figure 6.4: Effect of FSC231 on ROS production

ROS production was measured in freshly extracted synaptosomes treated with FSC231 using amplex red. In this assay, ROS production is measured by conversion of amplex red to a fluorescent agent resorufin (585 nm) by reacting with ROS, in the presence of peroxidase. The resorufin level acts as a quantitative indicator of peroxide production. A) The representative traces of the graph show the rate of peroxide produced by DMSO vehicle control, 1 μM antimycin A (positive control) and 50 μM FSC231 in a time scale of 2 h. B) The bar diagram represents the total H₂O₂ production during the linear part of activity (the same for each treatment condition; 15-20 min) as a percentage of control (mean ± SEM) in five separate experiments (n=5) by DMSO vehicle control (Cont), antimycin A (AM) and FSC231. The p-value (***) signifies p<0.001.

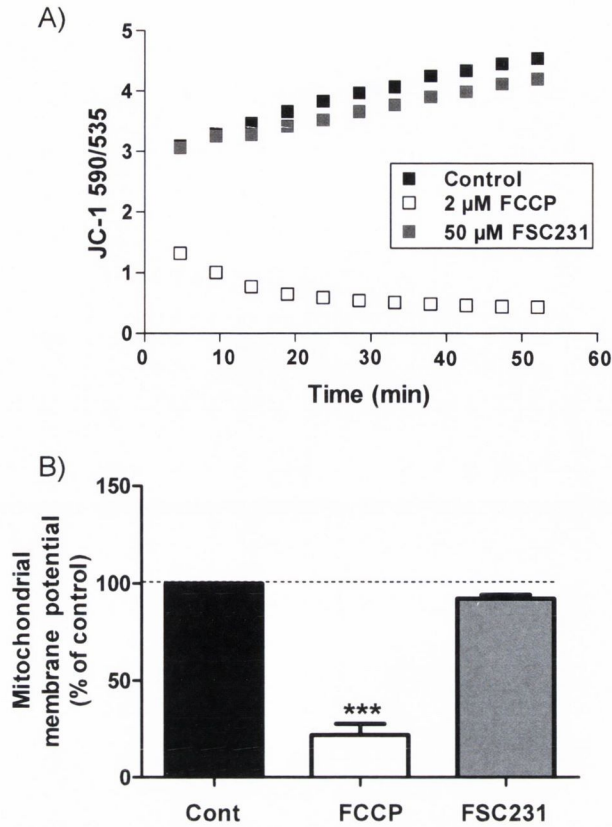


Figure 6.5: Effect of FSC231 on mitochondrial membrane potential

Mitochondrial membrane potential in fresh synaptosomes was measured by monitoring the change in the emission spectra of JC-1. In this assay, JC-1 associates with mitochondria in control conditions and emits a red colour (590 nm). In depolarized conditions, JC-1 is found in the cytoplasm in a monomeric form emitting a green colour (535 nm). The 590/535 ratio signifies a quantitative indicator of mitochondrial membrane potential. A) Representative traces of the graph show the rate of change in mitochondrial membrane potential in the presence of DMSO vehicle control, 2 μM FCCP (positive control) and 50 μM FSC231 in a time scale of 1 h. B) The bar diagram shows the mitochondrial membrane potential during the linear part of the traces (the same for each condition; 15-20 min) as a percentage of control (mean ± SEM) in four separate experiments (n=4) by DMSO vehicle control (Cont), FCCP and FSC231. The p-value (***) signifies p<0.001.

mitochondrial membrane potential was found in 50 μ M FSC231 ($92.33\% \pm 1.83$) treated synaptosomes, when compared to the DMSO vehicle control (**Figure 6.5B**). In contrast, treatment of synaptosomes with 2 μ M of FCCP ($22.11\% \pm 5.64$) reduced the membrane potential by 78%, when compared to DMSO vehicle control. The data suggest that the FCS231 binding to PICK1 does not alter maintenance of the mitochondrial membrane potential under control conditions. This result is somewhat contradictory to the effects of Tat-MNP201, which causes a reduction in mitochondrial membrane potential under control conditions. We suggest the following reasons for this difference: (i) the reduction in mitochondrial membrane potential caused by molecules binding PICK1 (such as MNP201 and FSC231) requires partial stressed conditions and (ii) the Tat tag on MNP201, but not the FSC231, causes mild stress to mitochondria, as evidenced by the effects of Tat-MNP201(mut) on mitochondrial membrane, which is sufficient for Tat-MNP201 to show effects on mitochondrial membrane potential in control and FCCP conditions. If this were the case, then the effects of FSC231 on mitochondrial membrane potential would be apparent under mild stressed FCCP conditions, as is shown in the results below.

6.6 FSC231 depolarizes mitochondrial membrane potential in partial stress condition

Next, the effect of FSC231 was investigated on mitochondrial membrane potential in synaptosomes challenged with 20 nM FCCP, similar to the experiment performed with Tat-MNP201 in Result 3 chapter (**Figure 5.8**). First, JC-1 treated freshly extracted synaptosomes were incubated with DMSO vehicle control and 50 μ M FSC231; and mitochondrial membrane potential was monitored for 15 min. Then, mitochondrial depolarization stress was induced with 20 nM FCCP in all samples to induce partial membrane depolarization (**Figure 5.7**) and the mitochondrial membrane potential was monitored for the next 30 min (**Figure 6.6A**). A linear portion of the curve was selected (the same for each treatment condition; 5-10 min before FCCP treatment and 15-20 min after FCCP treatment) and the mitochondrial membrane potential was measured. The relative values of mitochondrial membrane potential were expressed as a percentage of control and plotted in a bar graph. In non-stressed samples (no FCCP), no statistically significant difference was found in mitochondrial membrane potential between DMSO vehicle control and 50 μ M FSC231 ($100.11\% \pm 1.11$) treated synaptosomes (**Figure 6.6B**), in agreement with previously performed experiments (**Figure 6.5**). More importantly, after inducing stress by 20 nM FCCP, the 50 μ M FSC231 ($67.05\% \pm 7.23$) treated samples showed a 32.95% higher amount of mitochondrial depolarization, when compared to DMSO vehicle control treated synaptosomes (**Figure 6.6C**), similar to the generated data for Tat-MNP201 (**Figure**

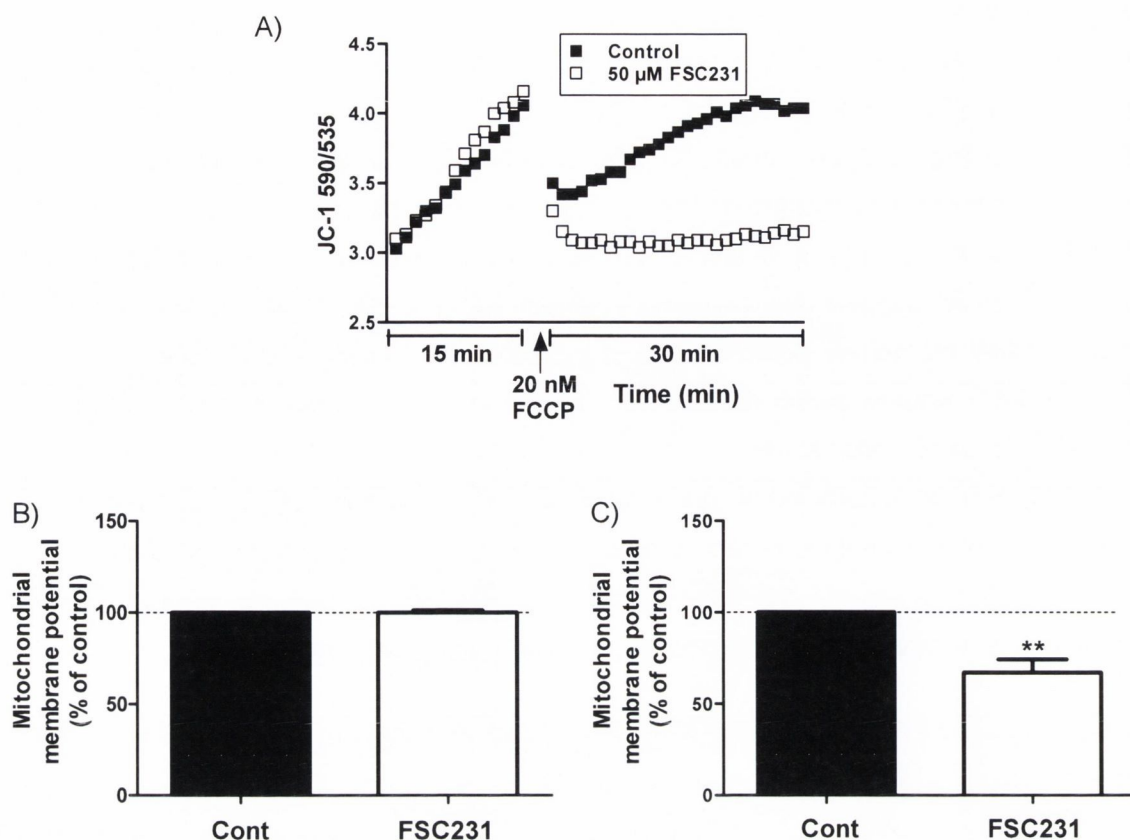


Figure 6.6: Effect of FSC231 on mitochondrial membrane potential under FCCP-induced partial stress condition

FCCP is a protonophore that causes depolarization of mitochondrial membrane potential. To create a condition of partial mitochondrial depolarization stress, 20 nM FCCP was used (see **Figure 5.7**). JC-1 treated freshly extracted synaptosomes were treated with DMSO vehicle control and 50 μM FSC231; and the rate of change in the mitochondrial membrane potential was observed for 15 min. Then, synaptosomes were treated with 20 nM FCCP and the rate of change in the mitochondrial membrane potential was observed for 30 min. The fluorescence of JC-1 (excitation 490 nm, emission 590 nm and 535 nm) was recorded from the commencement of the experiment. JC-1 590/535 ratio signifies a quantitative indicator of mitochondrial membrane potential. The fluorescence ratio of JC-1 (590 nm/535 nm) was plotted against time (A) and the representative traces were obtained from synaptosomes treated with DMSO vehicle control and 50 μM FSC231. The bar graphs represent the mitochondrial membrane potential during the linear part of the traces (the same for each treatment condition; 5-10 min before FCCP and 15-20 min after FCCP) as a percentage of control (mean ± SEM) observed in DMSO vehicle control (Cont) and 50 μM FSC231 treated synaptosomes in three separate experiments (n=3), before (B) and after (C) FCCP-induced stress depolarization. The p-value (**) signifies p<0.01.

5.8C). Furthermore, under FCCP-induced stress conditions, DMSO vehicle control treated synaptosomes treated showed a recovery from the depolarized state of mitochondrial membrane potential at the end of 30 min, whereas FSC231-treated synaptosomes did not show any sign of recovery from 20 nM FCCP treatment. These observations suggest that PICK1 may play a role in the maintenance of mitochondrial membrane potential under depolarizing condition, most likely through its PDZ domain interacting partners.

6.7 Effect of FSC231 in KCl-stimulated glutamate release assay in the absence of CaCl_2

In addition to mitochondrial functional assays, the effect of 50 μM FSC231 on the rate of glutamate release was also investigated using freshly extracted synaptosomes from rat brain tissue. A continuous fluorimetric method was used, where the amount of glutamate was measured by quantifying the amount of NADPH produced (excitation/emission = 340/460 nm), as described in previous publications (Nicholls et al., 1987; Kilbride et al., 2008). Freshly extracted synaptosomes were incubated with the glutamate release assay media (please see Methods) and the blank rate of glutamate release was monitored for the first 5 min. Then, DMSO vehicle control and FSC231 were added; and the baseline glutamate release was measured from non-depolarized synaptosomes for the next 5 min. Similar to the MNP201 glutamate release experiments, 10 μM rotenone was used as positive control. The total release of glutamate from non-depolarized synaptosomes was measured over a 5 min period. No significant difference in the rate of Ca^{2+} -independent glutamate release was observed in 50 μM FSC231 ($125.48\% \pm 10.88$) treated synaptosomes, when compared to DMSO vehicle control treated non-depolarized synaptosomes (**Figure 6.7A and B**). In contrast, the positive control 10 μM rotenone ($166.59\% \pm 17.41$) induced a significant 66.59% increase in the Ca^{2+} -independent non-depolarized rate of glutamate release, in agreement with previously published reports (Kilbride et al., 2008). Next, the depolarization of synaptosomes was carried out with 40 mM KCl and the Ca^{2+} -independent rate of glutamate release was monitored for 30 min. The total release of glutamate from depolarized synaptosomes was measured over this 30 min period. No significant change in Ca^{2+} -independent, KCl-stimulated rate of glutamate release was observed in 50 μM FSC231 ($117.43\% \pm 1.67$) treated synaptosomes, when compared to DMSO vehicle control synaptosomes (**Figure 6.7A and C**). In contrast, the positive control, 10 μM rotenone ($135.64\% \pm 13.41$), demonstrated a trend increase of 35.64% in glutamate release compared to DMSO vehicle control. Taken together, the data suggest 50 μM FSC231 has no effect on Ca^{2+} -independent KCl-induced rate of glutamate release from rat synaptosomes.

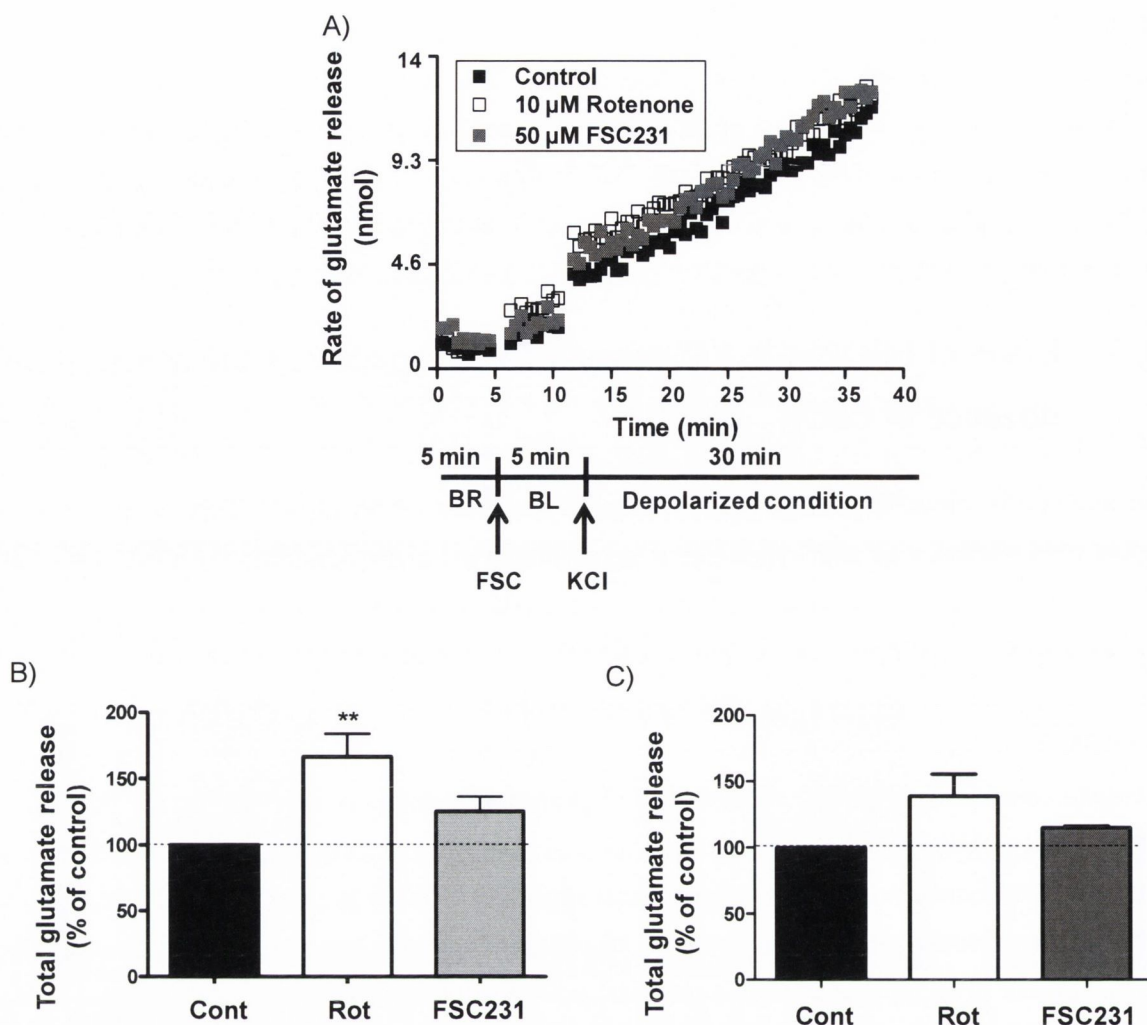


Figure 6.7: Effect of FSC231 on KCl-induced glutamate release in the absence of CaCl_2
 The rate of glutamate release was measured by NADPH production at 460 nm. The level of glutamate was determined by generating a standard curve of glutamate-mediated NADPH production (Figure 4.9), in the absence of synaptosomes. The blank rate (BR) of glutamate release was recorded for 5 min in freshly extracted synaptosomes in the absence of CaCl_2 . Then, synaptosomes were treated with 10 μM rotenone and 50 μM FSC231 (FSC); and the rate of glutamate at baseline (BL) was observed from non-depolarized synaptosomes for 5 min. Depolarization of synaptosomes was subsequently initiated by addition of 40 mM KCl and rate of glutamate release was observed for the next 30 min. A) The graph indicates representative traces of Ca^{2+} -independent rate of glutamate release (nmol) by DMSO vehicle control (Cont), 10 μM rotenone (Rot) and 50 μM FSC231 treated synaptosomes in a total time period of 40 min. The bar diagrams show the total glutamate release as a percentage of control (mean \pm SEM) in DMSO vehicle control (Cont), 10 μM rotenone (Rot) and 50 μM FSC231 treated synaptosomes under non-depolarized (B) and depolarized (C) conditions in three separate experiments ($n=3$). The p-value (**) signifies <0.01 .

6.8 Effect of FSC231 in KCl-stimulated glutamate release assay in the presence of CaCl₂

After evaluation of Ca²⁺-independent glutamate release, the effect of FSC231 on Ca²⁺-dependent glutamate release was examined. Similar to the previously described experiment, the effect of 50 μM FSC231 was evaluated on glutamate release in the presence of 2 mM CaCl₂. When non-depolarized synaptosomes were treated with FSC231, no statistically significant difference was observed in the rate of Ca²⁺-dependent glutamate release from 50 μM FSC231 (157.37% ± 21.57) treated synaptosomes, when compared to DMSO vehicle control (**Figure 6.8A and B**). Again, the positive control 10 μM rotenone (190.50% ± 23.91) treated synaptosomes caused a significant 90.50% increase in Ca²⁺-dependent glutamate release, when compared to DMSO vehicle control, in agreement with previously published data (Kilbride et al., 2008). Thereafter, depolarization of synaptosomes was carried out using 40 mM KCl, and the rate of glutamate release was recorded. No change in the Ca²⁺-dependent, KCl-induced rate of glutamate release was observed in 50 μM FSC231 (114.99% ± 1.07) treated samples, when compared with DMSO vehicle control (**Figure 6.8A and C**). In contrast, synaptosomes treated with 10 μM rotenone (140.19% ± 15.42) demonstrated a trend increase of 40.19% in Ca²⁺-dependent, KCl-induced glutamate release, when compared to DMSO vehicle control, in agreement with previously published data (Kilbride et al., 2008). Taken together, the data suggest 50 μM FSC231 has no effect on Ca²⁺-dependent KCl-induced rate of glutamate release from rat synaptosomes.

6.9 Effect of FSC231 in 4-AP-stimulated glutamate release

After observing KCl-induced glutamate release, the effect of FSC231 in glutamate release was evaluated in 4-AP-induced depolarized synaptosomes. The compound 4-AP is a non-selective blocker of voltage-dependent K⁺-channel, present on the surface of synaptosomes (Nicholls 1993). Depolarization of synaptosomes was carried out by adding 10 mM 4-AP and Ca²⁺-independent glutamate release was monitored for 30 min in the presence of 50 μM FSC231. No statistically significant difference in 10 mM 4-AP-induced glutamate release was observed in 50 μM FSC231 (120.89% ± 10.26) treated synaptosomes, when compared to DMSO vehicle control (**Figure 6.9A and B**). In contrast, the positive control 10 μM rotenone (161.54% ± 37.28) treated synaptosomes demonstrated a trend increase of 61.54% in glutamate level, when compared to DMSO vehicle control synaptosomes, in agreement with previously published data (Kilbride et al., 2008). The data suggest that 50 μM FSC231 has no effect in the rate of Ca²⁺-independent 4-AP-stimulated glutamate release from rat synaptosomes. The same experiment was performed in the presence of 2 mM CaCl₂.

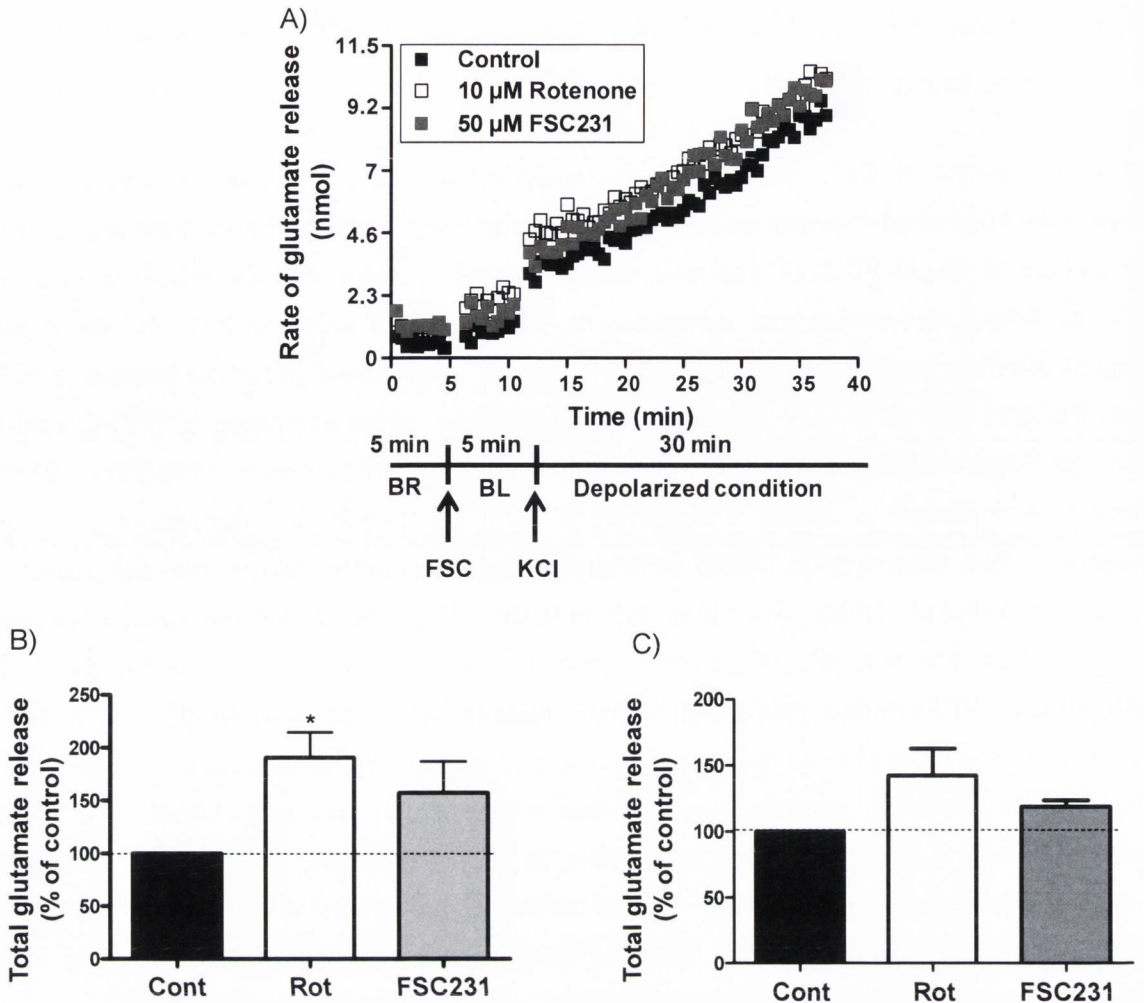


Figure 6.8: Effect of FSC231 on KCl-induced glutamate release in the presence of CaCl_2

The rate of glutamate release was measured by NADPH production at 460 nm. The level of glutamate was determined by generating a standard curve of glutamate-mediated NADPH production (Figure 4.9), in the absence of synaptosomes. The blank rate (BR) of glutamate release was recorded for 5 min in freshly extracted synaptosomes in the presence of CaCl_2 . Then, synaptosomes were treated with 10 μM rotenone and 50 μM FSC231 (FSC); and the rate of glutamate at baseline (BL) was observed from non-depolarized synaptosomes for 5 min. Then, depolarization of synaptosomes was initiated by addition of 40 mM KCl and rate of glutamate release was observed for next 30 min. A) The graph indicates representative traces of Ca^{2+} -dependent rate of glutamate release (nmol) by DMSO vehicle control (Cont), 10 μM rotenone (Rot) and 50 μM FSC231 treated synaptosomes in a total time period of 40 min. The bar diagrams show the total glutamate release as a percentage of control (mean \pm SEM) under non-depolarized (B) and depolarized (C) conditions in three separate experiments (n=3). The p-value (*) signifies $p < 0.05$.

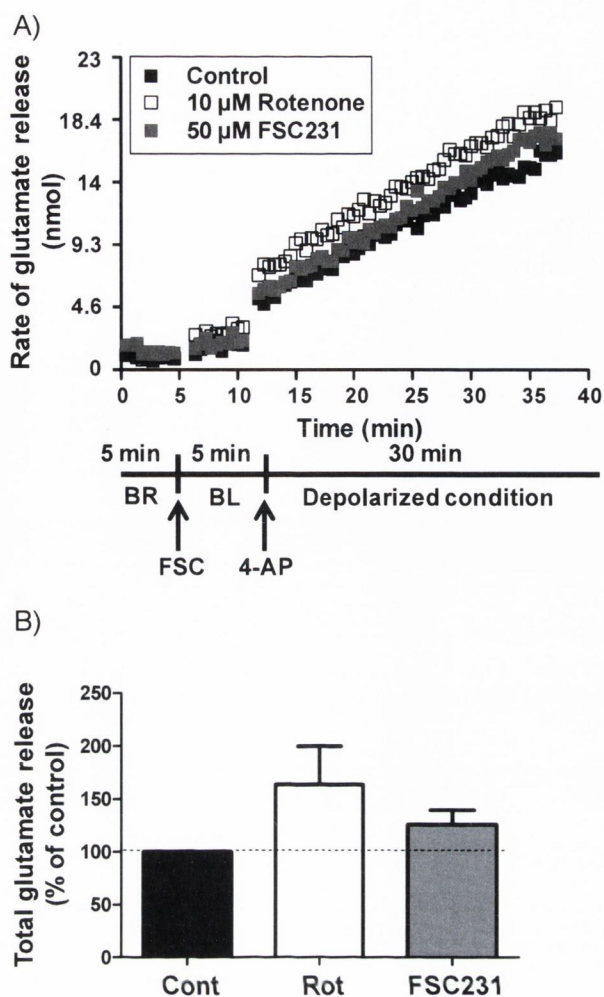


Figure 6.9: Effect of FSC231 on 4-AP-induced glutamate release in the absence of CaCl_2

The rate of glutamate release was measured by NADPH production at 460 nm. The level of glutamate was determined by generating a standard curve of glutamate-mediated NADPH production (**Figure 4.9**), in the absence of synaptosomes. The blank rate (BR) of glutamate release was recorded for 5 min in freshly extracted synaptosomes in the absence of CaCl_2 . Then, synaptosomes were treated with 10 μ M rotenone and 50 μ M FSC231 (FSC); and the rate of glutamate at baseline (BL) was measured from non-depolarized synaptosomes for 5 min. Then, depolarization of synaptosomes was initiated by addition of 10 mM 4-AP and rate of glutamate release was observed for the next 30 min. A) The graph indicates representative traces of Ca^{2+} -independent rate of glutamate release (nmol) by DMSO vehicle control, 10 μ M rotenone and 50 μ M FSC231 treated synaptosomes in a total time period of 40 min. B) The bar diagram shows the total glutamate release as a percentage of control (mean \pm SEM) in DMSO vehicle control (Cont), 10 μ M rotenone (Rot) and 50 μ M FSC231 treated synaptosomes under depolarized condition in three separate experiments (n=3).

Synaptosomes were depolarized using 10 mM 4-AP to observe the effect of 50 μ M FSC231 in Ca^{2+} -dependent glutamate release. Similar to previous results, no significant change in the rate of Ca^{2+} -dependent, 4-AP-induced glutamate release was observed in synaptosomes treated with 50 μ M FSC231 ($120.61\% \pm 9.47$) compared to DMSO vehicle control (**Figure 6.10A and B**). In contrast, the positive control 10 μ M of rotenone ($160.54\% \pm 28.56$) induced a trend increase of 60.54% in glutamate level, when compared to DMSO vehicle control. Taken together, the data suggest that 50 μ M FSC231 has no effect on the rate of Ca^{2+} -dependent, 4-AP-stimulated synaptosomal glutamate release. Overall, the data suggest that 50 μ M FSC231 has no effect in the rate of Ca^{2+} -dependent 4-AP-stimulated glutamate release from rat synaptosomes.

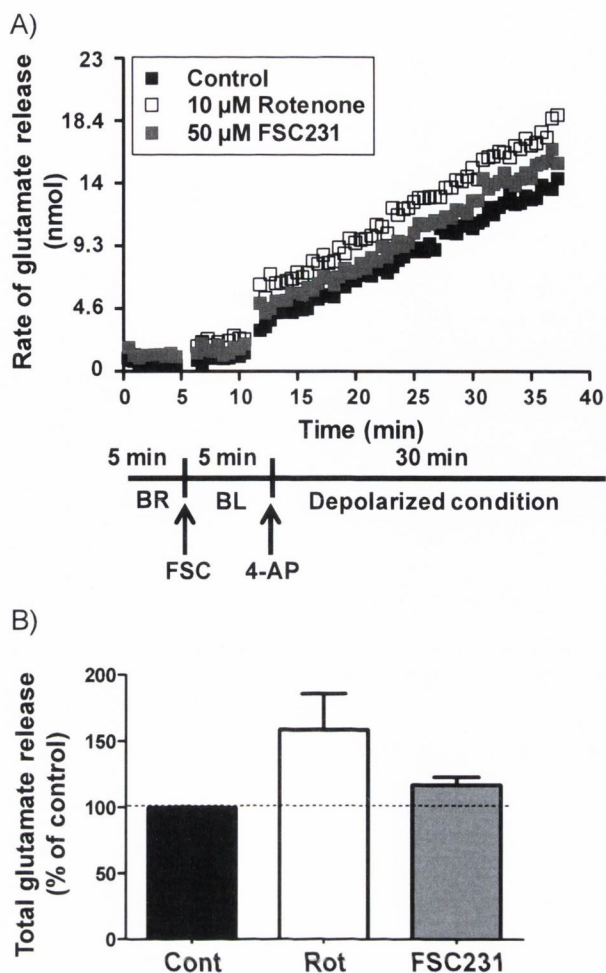


Figure 6.10: Effect of FSC231 on 4-AP-induced glutamate release in the presence of CaCl_2

The rate of glutamate release was measured by NADPH production at 460 nm. The level of glutamate was determined by generating a standard curve of glutamate-mediated NADPH production (**Figure 4.9**), in the absence of synaptosomes. The blank rate (BR) of glutamate release was recorded for 5 min in freshly extracted synaptosomes in the presence of CaCl_2 . Then, synaptosomes were treated with 10 μM rotenone and 50 μM FSC231 (FSC); and the rate of glutamate at baseline (BL) was observed from non-depolarized synaptosomes for 5 min. Then, depolarization of synaptosomes was initiated by addition of 10 mM 4-AP and rate of glutamate release was observed for the next 30 min. A) The graph indicates representative traces of Ca^{2+} -dependent rate of glutamate release (nmol) by DMSO vehicle control, 10 μM rotenone and 50 μM FSC231 treated synaptosomes in a total time period of 40 min. B) The bar diagram shows the total glutamate release as a percentage of control (mean \pm SEM) in DMSO vehicle control (Cont), 10 μM rotenone (Rot) and 50 μM FSC231 treated synaptosomes under depolarized condition in three separate experiments ($n=3$).

Discussion

1. Inhibition of PICK1 by FSC231 induces mitochondrial depolarization

The purpose of this project was to evaluate the importance of PICK1 and the proteins that interact with PICK1 via PDZ domain in mitochondrial function and glutamate release (please see summary **Table 1.1**). In this chapter, a PDZ domain binding compound FSC231 was tested on mitochondrial function and glutamate release. This compound binds the PDZ domain of PICK1 and likely bars most of the PICK1 interacting proteins docking into its PDZ domain.

Previous work in this thesis identified a reduction of mitochondrial membrane potential in the presence of 100 μM Tat-MNP201, a peptide modelled on the PDZ motif of parkin. Similar to the MNP201 and Tat-MNP201 study, the effect of FSC231 was evaluated on the activity of respiratory chain; complex I and IV. In PD patients, 30-40% of reduction in activity of respiratory chain complex I was found (Schapira et al., 1989). FSC231 showed no significant effect on the activity of complex I and IV. In the ROS production assay, 10 μM antimycin increased the rate in ROS release level as expected (Sipos et al., 2003), whereas 50 μM FSC231 had no significant effect, when compared to vehicle control. When tested in the mitochondrial depolarization assay, FCCP-induced an increase in depolarization of mitochondrial membrane as expected (Tretter and Adam-Vizi, 2007). However, no change in mitochondrial membrane potential was observed in 50 μM FSC231 treated samples when compared to the vehicle control. Importantly, when synaptosomes was treated with the partial mitochondrial stress agent, FCCP (20 nM), the FSC231 treated synaptosomes showed a greater extent of mitochondrial depolarization compared to controls. We propose that in the presence of FSC231, the PDZ domain of PICK1 is unable to interact with and traffic proteins responsible for maintaining mitochondrial function, namely parkin and PKC α . It is also believed that the trafficking of these mitochondrial interacting proteins is crucial, when mitochondria are under stress.

2. PICK1 plays no role in glutamate release

As discussed earlier, AMPA receptor plays a role in fast excitatory neurotransmission (Dev et al., 1999). Intriguingly, PICK1 regulates the AMPA receptor excitability by regulating the surface expression of the AMPA receptor subunit GluR2 in hippocampal neurons (Hanley and Henley, 2005; Lin and Huganir, 2007). In the presence of FSC231, upon NMDA receptor

A)

Assay	50 μ M FSC231	Measured by
Complex I activity	93.80% \pm 15.58	NADH depletion (OD ³⁴⁰)
Complex IV activity	93.16% \pm 9.21	Cyto C depletion (OD ⁵⁵⁰)
Peroxide production	115.08% \pm 9.98	Resorufin production (OD ⁵⁸⁵)
Membrane potential	92.33% \pm 1.83	JC-1 OD ratio (JC-1 ^{590/535})
FCCP-induced membrane potential	67.05% \pm 7.23	JC-1 OD ratio (JC-1 ^{590/535})

B)

Glutamate release	50 μ M FSC231	Measured by
Non-depolarized level (- CaCl ₂)	125.48% \pm 10.88	Amount of NADPH production (OD ⁴⁶⁰)
Non-depolarized level (+ CaCl ₂)	157.37% \pm 21.57	
- CaCl ₂ , + 50 mM KCl	117.43% \pm 1.67	
+ CaCl ₂ , + 50 mM KCl	114.99% \pm 1.07	
- CaCl ₂ , + 10 mM 4-AP	120.89% \pm 10.26	
+ CaCl ₂ , + 10 mM 4-AP	120.61% \pm 9.47	

Table 6.1: Summary of data obtained by using FSC231

Mitochondrial function assays (A) and glutamate release assay (B). The data suggest that FSC231 has no effect on mitochondrial respiratory chain complexes (complex I and IV), ROS production, mitochondrial membrane potential and glutamate release. In contrast, FSC231 effects the mitochondrial membrane potential under stress condition. The values are indicated as a percentage of control (Mean \pm SEM).

activation, accelerated recycling of GluR2 to the plasma membrane of hippocampal neurons was observed instead of internalisation through a PICK1-dependent trafficking (Thorsen et al., 2010). Moreover, LTD and LTP were significantly reduced in the presence of 50 μ M FSC231 in CA1 hippocampal neurons (Thorsen et al., 2010). Importantly, in addition to the interaction with AMPA receptor subunits (GluR2), PICK1 also interacts with KA subunits (GluR5) and metabotropic glutamate receptors (mGluR7). Also worthy of note, is that AMPA, KA and mGluR7 pre-synaptic autoreceptors have all been shown to regulate glutamate release. Therefore, to determine if PICK1 plays a role in glutamate release either via effects on pre-synaptic glutamate receptors or via regulating mitochondrial function, the effect of FSC231 in glutamate release was studied using fresh rat brain synaptosomes. Similar to MNP201 and Tat-MNP201, Ca^{2+} -independent and dependent glutamate release experiments were performed by treating 50 μ M FSC231 with freshly prepared synaptosomes under non-depolarizing condition as well as in depolarizing condition (triggered by 40 mM KCl and 10 mM 4-AP). As a control, the data demonstrated an increased Ca^{2+} -independent and dependent rate of glutamate release from 10 μ M rotenone treated synaptosomes under non-depolarizing and depolarizing conditions. This data is in agreement with previous studies, where a high amount of glutamate release was demonstrated by rotenone-induced complex I inhibition (Kilbride et al., 2008), indicating a successful glutamate assay setup. However, using 50 μ M of FSC231 no significant difference was observed in glutamate release, when compared to control sample. Taken together, the lack of effects of FSC231 on glutamate release suggests that PICK1 does not regulate the rate of glutamate release from synaptosomes.

3. The role of parkin-PICK1 and PKC α -PICK1 in mitochondria

Several proteins interact with PICK1 through the PDZ domain. Among these proteins, only parkin and PKC α have been reported to have mitochondrial “protective functions”. Briefly, PICK1 interacts with and recruits PKC α to the outer mitochondrial membrane to confer mitochondrial resistance to Bax-induced apoptosis by phosphorylating Bcl-2 protein (Wang et al., 2007). In addition, parkin selectively engulfs and promotes autophagy of depolarized mitochondria (Narendra et al., 2008) where PICK1 may play a role. FSC231 docks into the PDZ domain of PICK1 and likely competitively hinders interaction with many proteins, most likely in a competitive and non-selective manner. To date, FSC231 has been shown to block interaction of PICK1 with GluR2 and DAT (Thorsen et al., 2010). Thus, the FSC231 is also expected to block the interaction of parkin-PICK1 and/or PKC α -PICK1, both having known mitochondrial function. If FSC231 is capable of blocking both parkin-PICK1 and PKC α -PICK1 interaction, then two possible deleterious effects on mitochondrial function are

expected. Firstly, under FCCP stress condition, the parkin-mediated removal of depolarized mitochondria may be attenuated in the presence of FSC231. Secondly, the blockade of PKC α -PICK1 interaction induced by FSC231 may limit the PKC α -induced anti-apoptotic mechanism. Further studies on FSC231 inhibition of parkin-PICK1 and PKC α -PICK1 are required to confirm this hypothesis through biochemical approaches. In addition, the role of these protein interactions should be evaluated by imaging and localisation studies.

7. Final discussion

7.1 Summary of findings

The data presented in this thesis were aimed to examine the role of PICK1, in particular the parkin-PICK1 interaction, in mitochondrial function. Firstly, biochemical methods were used to demonstrate the binding of the parkin peptide, MNP201, to PICK1. Specifically, it was shown that MNP201 displaced a fluorescently tagged PDZ motif (modelled on the PDZ motif sequence of DAT) from PICK1 in a concentration (and likely a competitive) manner (Result 1). Next, the effects of the MNP201 parkin peptide were tested in a set of mitochondrial functional assays and on glutamate release. This peptide showed little or no effects on mitochondrial function or on glutamate release, likely due to this peptide's inability to internalise synaptosomes (Result 2). In support of this suggestion, the Tat-MNP201, a membrane permeable version of MNP201 peptide, caused mitochondrial depolarization in synaptosomes in both control and FCCP-induced partial stress conditions (Result 3). Lastly, FSC231, the PDZ domain binding ligand of PICK1, demonstrated an increased rate of mitochondrial depolarization in synaptosomes under FCCP-induced partial stress conditions (Result 4). Taken together, the data indicate that PICK1 may play a role in the maintenance of mitochondrial membrane potential and thus mitochondrial function by trafficking PDZ domain interacting proteins to mitochondria including parkin and/or PKC α .

7.2 The parkin-PICK1 interaction

As indicated above, the primary objective of this project was to investigate the possible functional role of the parkin-PICK1 interaction in mitochondrial maintenance and glutamate release. The work extends the finding of Joch et al. (2007), where the group discovered an interaction between the PDZ motif of parkin and the PDZ domain of PICK1. The mode of interaction between these two proteins was found to be PDZ based, where the PDZ motif of parkin (-FDV) was found to interact with the PDZ domain of PICK1. In this work, the authors showed that the parkin-PICK1 interaction was important for parkin-dependent monoubiquitination of PICK1, which suppressed a PICK1-mediated increase in ASIC2a currents. In addition, this study also showed that the parkin-dependent ubiquitination of PICK1 did not lead to degradation of PICK1, that is, parkin caused monoubiquitination but not polyubiquitination of PICK1. It is interesting that PICK1 has the ability to bind both kinases (PKC α) and ubiquitin ligases (parkin). Given that PICK1 can homodimerise and thus form a scaffold that can bring together two separate proteins for interaction, it is interesting to speculate that PICK1 plays a role in regulating the phosphorylation and/or ubiquitination of its interacting proteins. These post-translational modifications are likely important in the trafficking and/or degradation of PICK1 interacting proteins. Although less is known about parkin-mediated ubiquitination of PICK1 interacting proteins, several studies have reported

that PICK1 plays a role in PKC α -dependent phosphorylation of its interacting proteins, the best studied being the interaction between PICK1 and AMPA receptors (Dev et al., 1999; Xia et al., 1999; Lin and Huganir, 2007).

7.3 Oligopeptides need assistance to internalise through bi-lipid membrane

The parkin PDZ motif containing peptides used in this study (MNP201 and Tat-MNP201) were designed to bind the PDZ domain of PICK1. The data showed that MNP201 had no effect on mitochondrial function and glutamate release, which was possibly due to the membrane impermeable nature of this peptide. In agreement with this notion, it is reported that lipophilic, bio-active peptides under 6 amino acids in length can, in general, cross the plasma membrane unassisted and enter the cell, whereas larger peptides are unable to cross lipid bilayers (Scheld et al., 1997). Peptides, which can also pass through the plasma membrane are those with arginine rich, highly cationic and basic amino acid sequences (Vives, 2003). The MNP201 peptide is 10 amino acids long (VCMGDHWFDV) with a slight acidic nature containing only one basic amino acid (Histidine) and unlikely to cross the synaptosomal membrane unassisted. Thus, a Tat peptide (YGRKKRRQRRR) sequence was fused to the N-terminal of MNP201 (Tat-MNP201) to assist its membrane permeability. The membrane permeability of Tat-MNP201 was demonstrated by its ability to enter cortical neuronal cells and astrocytes in culture. More importantly, while MNP201 did not affect the mitochondrial membrane potential, the Tat-MNP201 induced a significant amount of mitochondrial depolarization. The data suggested that presence of a Trojan Tat sequence in Tat-MNP201 assists the membrane permeability of the peptide and that its ability to bind PICK1 alters mitochondrial function.

7.4 Possible effect of Tat portion of Tat-MNP201

Tat peptides have been reported to induce ROS production, promote mitochondrial depolarization, increase glutamate release, decrease GABA exocytosis, disrupt calcium homeostasis and cause caspase activation (Kruman et al., 1998). The experiments conducted with Tat-MNP201 showed this peptide caused a selective mitochondrial membrane depolarization, with little or no effect on any of the other mitochondrial properties tested or on glutamate release. Thus, the data suggested that the Tat sequence used in this study had no overt effects on synaptosomal or mitochondrial integrity. Specifically, the Tat-MNP201 (100 μ M) significantly increased mitochondrial depolarization in synaptosomes ($p < 0.001$) compared to vehicle control. Surprisingly, however, Tat-MNP201(mut) (100 μ M),

the mutated version of Tat-MNP201, also caused a significant level of mitochondrial depolarization ($p < 0.05$) compared to vehicle control. When the mitochondrial membrane potential values of Tat-MNP201 and Tat-MNP201(mut) were compared, the Tat-MNP201 wildtype version was found to cause a significantly greater ($p < 0.05$) amount of mitochondrial membrane depolarization when compared to the mutant version Tat-MNP201(mut). In addition to testing the effects of these parkin peptides in control conditions, their effects on mitochondrial membrane potential was also examined under mild stressed conditions induced by FCCP. In these conditions, Tat-MNP201 caused a significant ($p < 0.001$) increase in mitochondrial membrane depolarization compared to the control. In this case Tat-MNP201(mut) also showed a significant ($p < 0.05$) increase in mitochondrial membrane depolarization when compared to control values. Importantly, however, Tat-MNP201 caused a significantly larger membrane depolarization ($p < 0.05$) when compared to Tat-MNP201(mut). As indicated above, specific effects of the Tat-MNP201 peptide on mitochondrial membrane potential were observed, with little effects on peroxide production and glutamate release suggesting no overt effects on mitochondrial or synaptosomal integrity. That being said, however, the data above suggests the effects of Tat-MNP201(mut) on mitochondrial membrane depolarization may be due to the presence of Tat peptide, which may be inducing mild stress conditions only observable in mitochondrial membrane potential assays and not in assays investigating peroxide production or glutamate release. While, in this study, we did not use peptide entrapment methods to facilitate the entry of peptides into synaptosomes as they do not allow for the addition of peptides at specific timepoints in an experiment, in this case such peptide entrapment methods would be useful future studies to perform in order to examine the effect of MNP201 without a Tat sequence (Feligioni et al., 2009).

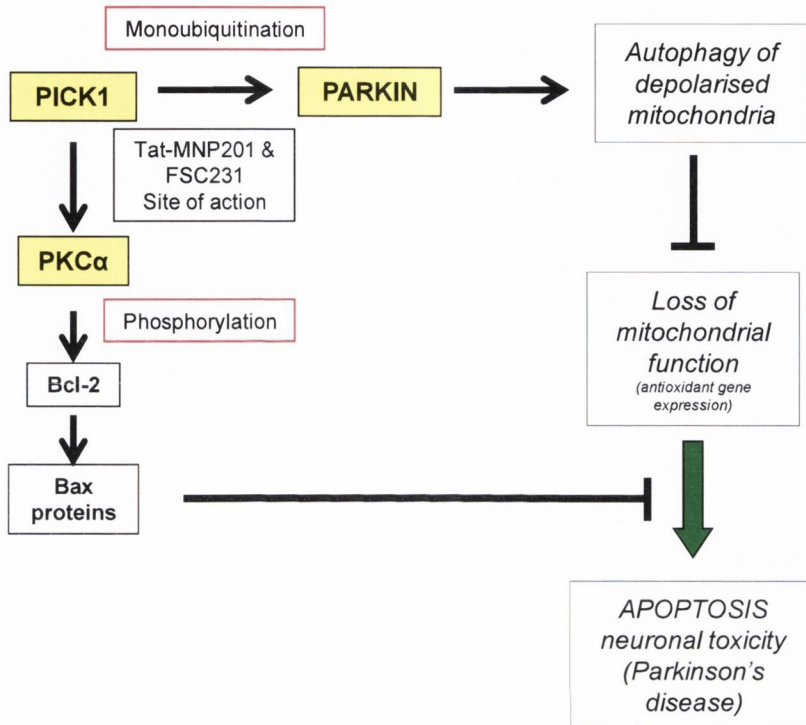
7.5 Proposed model of FSC231 on mitochondrial dysfunction

In the experiments conducted in this thesis, 50 μM FSC231 increased mitochondrial membrane depolarization under mild stress conditions induced by FCCP. The mechanism underlying this FSC231-mediated mitochondrial membrane depolarization likely involves its binding to PICK1. In agreement, it has been shown that FSC231 binds the PDZ domain of PICK1 and competitively blocks the interaction of PDZ motif containing proteins including GluR2 and DAT, which otherwise interact with PICK1 (Joch et al., 2007). Due to this compounds ability to dock within the PDZ domain of PICK1, it likely occludes (in a competitive manner) the binding of many more or all proteins that interact with PICK1. While PICK1 interacts with close to 60 proteins, only two of its interacting proteins, namely parkin and PKC α , have been reported to be directly involved in regulating mitochondrial function. In

particular, parkin regulates mitochondrial function by selectively engulfing and promoting autophagy of depolarized mitochondria (Narendra et al., 2008). On the other hand, PKC α regulates mitochondrial function via a mechanism that involves PICK1-mediated recruitment of PKC α to the mitochondria and the phosphorylation of the Bcl-2 protein in the outer mitochondrial membrane, which confers mitochondrial resistance to Bax-induced apoptosis (Wang et al., 2007). Taken together, we propose that FSC231 causes a reduction in mitochondrial membrane potential due to disruption of the parkin-PICK1 and/or the PKC α -PICK1 interaction(s). If that is the case, then FSC231 may have two possible deleterious effects on mitochondria (**Summary figure**). Firstly, under FCCP stressed conditions, in presence of FSC231, PICK1 will not be able to bind or recruit parkin to mitochondria and thus parkin mediated removal of depolarized mitochondria will not occur. Secondly, due to blockade of PKC α -PICK1 interaction induced by FSC231, the PKC α -induced anti-apoptotic mechanism will be attenuated. Ultimately, due to the absence of parkin- and/or PKC α -dependent mitochondrial maintenance/removal mechanisms, instead dysfunctional mitochondria (i.e. depolarised mitochondria) will ensue, which will induce mitochondria-mediated apoptosis and neurodegeneration.

7.6 Caveat of this study

One obvious caveat of this current work was our inability to prove that the MNP201 peptides and FSC231 do indeed directly block the parkin-PICK1 interaction. During the course of this thesis, several methods were attempted to firstly, confirm the interaction between parkin-PICK1 and then demonstrate effect of the peptides (Result 1). Co-IP and pull-down studies failed to show a direct interaction between parkin and PICK1; and thus the blocking effect of MNP201 peptides on parkin-PICK1 interaction could not be demonstrated. However, the binding of MNP201 peptides to PICK1 was demonstrated by fluorescence polarisation assay, where MNP201 competitively inhibited the interaction of DAT peptide with PICK1. In contrast, MNP201(mut), the mutated PDZ motif version of parkin peptide, did not block the DAT-PICK1 interaction. In addition, given that the Tat-MNP201 peptide showed similar effects on the FSC231 compound, it is hypothesised that both these molecules are acting in a similar manner by binding to the PDZ domain of PICK1. Another possible caveat of this study was the use of synaptosomes extracted from whole rat brain. Most of the work demonstrating regulation of LTP and LTD by PICK1 has been done in hippocampal neurons (Hanley and Henley, 2005; Lin and Haganir, 2007). Therefore, future studies investigating the role of PICK1 in mitochondria prepared from specific brain areas including the hippocampus, rather than the whole brain, may be worthwhile.



Summary figure: Involvement of parkin-PICK1 to regulate mitochondrial function and apoptosis

PICK1 may play key role in mitochondrial function and neuronal survival by interacting with both parkin and PKC α . PICK1 regulates the trafficking of parkin and PKC α and that the parkin-PICK1-PKC α triple protein complex plays in mitochondrial maintenance. This pathway is blocked in the presence of MNP201 and FAC231.

7.7 Future direction

From the data generated in this project, Tat-MNP201 and FSC231, both induced depolarization of mitochondrial membrane potential in control and FCCP-induced stress conditions. Further work and follow-up studies are proposed below:

As indicated above,

- First, it would be worthy to examine the ability of MNP201 and FSC231 to block parkin-PICK1 and/or PKC α -PICK1 interaction in additional biochemical approaches.
- Second, peptide entrapment methods to facilitate the entry of peptides into synaptosomes would be useful future studies to perform in order to examine the effect of MNP201 without a Tat sequence.
- Third, future studies investigating the role of PICK1 in mitochondria prepared from specific brain areas including the hippocampus, rather than the whole brain, may be worthwhile.

In addition,

- Fourth, using immunostaining and cell imaging, future work investigating the role of PICK1 in trafficking parkin and PKC α to mitochondria, under conditions of mitochondrial stress and mitochondrial depolarization in the presence of Tat-MNP201 and FSC231 would be valuable.
- Fifth, parkin trafficking can be also evaluated in neurons derived from PICK1-KO mice (Gardner et al., 2005) under mitochondrial depolarization stress. In this case, impairment of parkin-mediated mitophagy and/or PKC α -mediated phosphorylation of the Bcl-2 would be expected. If the effects of MNP201 and FSC231 on mitochondrial membrane depolarization are mediated via binding to PICK1, the effects of these compounds should also be lost in mitochondria prepared from PICK1-KO animals.
- Sixth, if MNP201 and FSC231 do impair mitochondrial function under conditions of stress, their effects on triggering apoptosis and on neuronal viability should be demonstrated. This particular study is important for understanding the mechanism-of-action, for not only MNP201 or FSC231, but also other peptides that have been reported to bind PICK1 and cause effect on synaptic function.
- Lastly, their exist bias in the area which suggests that peptides that dock to the PDZ domain of PICK1 (such as GluR2 peptide, MNP201, FSC231) are selective in the interactions that they inhibit. This however is unlikely to be the case. Thus, the identification of the PICK1 interacting proteins, which are blocked by previously

reported GluR2 peptides, the MNP201 peptide and the FSC231 compound may provide us a more complete picture in understanding the role of PICK1 in mitochondrial function, neuronal survival and synaptic plasticity.

7.8 Closing comments

The family of PDZ domain containing proteins have been recently noted as novel drug targets for development of new therapies. The work here, however, suggests that PICK1 binding compounds are unlikely to make good drugs due to their effects on mitochondrial function. Further work will be required to develop drugs that selectively block one protein interacting with PICK1 over another. If efforts can develop, for example, a drug that regulates GluR2 (but not parkin) from interacting with PICK1, then such molecules could be useful in regulating synaptic plasticity and help in the development of cognition enhancers. In the case of using PICK1 as a target for Parkinson's disease this, however, appears unlikely given its role in mitochondrial function.

8. References

- Aarts M, Liu Y, Liu L, Besshoh S, Arundine M, Gurd JW, Wang YT, Salter MW, Tymianski M. (2002) Treatment of ischemic brain damage by perturbing NMDA receptor-PSD-95 protein interactions. *Science*. 298:846-50.
- Aarts MM, Tymianski M. (2003) Novel treatment of excitotoxicity: targeted disruption of intracellular signalling from glutamate receptors. *Biochem Pharmacol*. 66:877-86.
- Abbas N, Lucking CB, Ricard S, Durr A, Bonifati V, De Michele G, Bouley S, Vaughan JR, Gasser T, Marconi R, Broussolle E, Brefel-Courbon C, Harhangi BS, Oostra BA, Fabrizio E, Bohme GA, Pradier L, Wood NW, Filla A, Meo G, Deneffe P, Agid Y, Brice A (1999) French Parkinson's Disease Genetics Study Group and the European Consortium on Genetic Susceptibility in Parkinson's Disease. A wide variety of mutations in the parkin gene are responsible for autosomal recessive parkinsonism in Europe. *Human Molecular Genetics*. 8:567– 574.
- Abou-Sleiman PM, Muqit MM, Wood NW. (2006) Expanding insights of mitochondrial dysfunction in Parkinson's disease. *Nat Rev Neurosci*. 7:207-19.
- Agoston D, Hargittai P, Nagy A. (1983) Effects of a 4-aminopyridine in calcium movements and changes of membrane potential in pinched-off nerve terminals from rat cerebral cortex. *J Neurochem*. 41:745-51.
- Alvarez AR, Klein A, Castro J, Cancino GI, Amigo J, Mosqueira M, Vargas LM, Yévenes LF, Bronfman FC, Zanlungo S. (2008) Imatinib therapy blocks cerebellar apoptosis and improves neurological symptoms in a mouse model of Niemann-Pick type C disease. *FASEB J*. 22:3617-27.
- Alvarez AR, Sandoval PC, Leal NR, Castro PU, Kosik KS. (2004) Activation of the neuronal c-Abl tyrosine kinase by amyloid-beta-peptide and reactive oxygen species. *Neurobiol Dis*. 17:326-36.
- Alvarez-Castelao B, Castaño JG. (2010) Synphilin-1 inhibits alpha-synuclein degradation by the proteasome. *Cell Mol Life Sci*. 68:2643-54.
- Amara SG, Kuhar MJ. (1993) Neurotransmitter transporters: recent progress. *Annu Rev Neurosci*. 16:73-93.
- Arkin MR, Wells JA (2004) Small-molecule inhibitors of protein-protein interactions: progressing towards the dream. *Nat Rev Drug Discov*. 3:301–317.
- Artavanis-Tsakonas S, Rand MD, Lake RJ. (1999) Notch signaling: cell fate control and signal integration in development. *Science*. 284:770-6.
- Ashley RH, Brammer MJ, Marchbanks R. (1984) Measurement of intrasynaptosomal free calcium by using the fluorescent indicator quin-2. *Biochem J*. 219:149-58.
- Astriab-Fisher A, Sergueev DS, Fisher M, Shaw BR, Juliano RL. (2000) Antisense inhibition of P-glycoprotein expression using peptide-oligonucleotide conjugates. *Biochem.Pharmacol*. 60: 83–90.
- Avraham E, Rott R, Liani E, Szargel R, Engelender S. (2007) Phosphorylation of Parkin by the cyclin-dependent kinase 5 at the linker region modulates its ubiquitin-ligase activity and aggregation. *J Biol Chem*. 282:12842-50.
- Avraham E, Szargel R, Eyal A, Rott R, Engelender S. (2005) Glycogen synthase kinase 3beta modulates synphilin-1 ubiquitylation and cellular inclusion formation by SIAH: implications for proteasomal function and Lewy body formation. *J Biol Chem*. 280, 42877-86.
- Babcock DF & Hille B (1998) Mitochondrial oversight of cellular Ca²⁺ signaling. *Curr Opin Neurobiol* 8, 398–404.
- Bar-Am O, Amit T, Youdim MB. (2007) Aminoindan and hydroxyaminoindan, metabolites of rasagiline and lisdostigil, respectively, exert neuroprotective properties *in vitro*. *J Neurochem*. 103:500–508.

- Barnard E. (1992) Will the real NMDA receptor please stand up? *Trends Pharmacol Sci.* 13:11-2.
- Barnes JM, Dev KK, Henley JM. (1994) Cyclothiazide unmasks AMPA-evoked stimulation of [3H]-L-glutamate release from rat hippocampal synaptosomes. *Br J Pharmacol.* 113:339-41.
- Baron A, Deval E, Salinas M, Lingueglia E, Voilley N, Lazdunski M. (2002) Protein kinase C stimulates the acid-sensing ion channel ASIC2a via the PDZ domain-containing protein PICK1. *J Biol Chem.* 277:50463-8.
- Bartschat DK, Blaustein MP. (1985) Calcium-activated potassium channels in isolated presynaptic nerve terminals from rat brain. *J Physiol.* 361:441-57.
- Bayer P, Arndt A, Metzger S, Mahajan R, Melchior F, Jaenicke R, Becker J. (1998) Structure determination of the small ubiquitin-related modifier SUMO-1. *J. Mol. Biol.* 280:275–286.
- Beal MF, Shults CW. (2003) Effects of Coenzyme Q10 in Huntington's disease and early Parkinson's disease. *Biofactors.* 18:153-61.
- Beal MF. (1992) Mechanisms of excitotoxicity in neurologic diseases. *FASEB J.* 6:3338-44.
- Beal MF. (1998) Excitotoxicity and nitric oxide in Parkinson's disease pathogenesis. *Ann Neurol.* 44:S110-4.
- Beal MF. (2000) Oxidative metabolism. *Ann N Y Acad Sci.* 924:164-9.
- Beal MF. (2007) Mitochondria and neurodegeneration. *Novartis Found Symp.* 287:183-92.
- Beites CL, Xie H, Bowser R, Trimble WS. (1999) The septin CDCrel-1 binds syntaxin and inhibits exocytosis. *Nat Neurosci.* 2: 434-9.
- Ben-Neriah Y (2002) Regulatory functions of ubiquitination in the immune system. *Nature Immunology.* 3:20–26.
- Berg T. (2003) Modulation of protein-protein interactions with small organic molecules. *Angew Chem Int Ed Engl.* 42:2462-81.
- Bergman H, Wichmann T, Karmon B, DeLong MR. (1994) The primate subthalamic nucleus. II. Neuronal activity in the MPTP model of parkinsonism. *J. Neurophysiol.* 72: 507–520.
- Bernardi P, Krauskopf A, Basso E, Petronilli V, Blachly-Dyson E, Di Lisa F & Forte MA. (2006) The mitochondrial permeability transition from *in vitro* artifact to disease target. *FEBS J* 273: 2077–2099.
- Berridge MJ. (1998) Neuronal calcium signaling. *Neuron* 21: 13–26.
- Bettler B, Mulle C. (1995) Review: neurotransmitter receptors. II. AMPA and kainate receptors. *Neuropharmacology.* 34:123-39.
- Bezard E, Boraud T, Bioulac B, Gross CE. (1997) Presymptomatic revelation of experimental parkinsonism. *Neuroreport.* 8:435-8.
- Bezprozvanny I. (2009) Calcium signaling and neurodegenerative diseases. *Trends Mol Med* 15: 89–100.
- Bindoff LA, Birch-Machin M, Cartledge NE, Parker WD Jr, Turnbull DM. (1989) Mitochondrial function in Parkinson's disease. *Lancet.* 2:49.
- Blazer LL, Neubig RR. (2009) Small molecule protein-protein interaction inhibitors as CNS therapeutic agents: Current progress and future hurdles. *Neuropsychopharmacology.* 34:126–141.
- Bleakman D, Lodge D. (1998) Neuropharmacology of AMPA and kainate receptors. *Neuropharmacology.* 37:1187-204.

- Bleazard W, McCaffery JM, King EJ, Bale S, Mozdy A, Tieu Q, Nunnari J, Shaw JM. (1999) The dynamin-related GTPase Dnm1 regulates mitochondrial fission in yeast. *Nat Cell Biol.* 1:298-304.
- Bliss TV and Collingridge GL. (1993) A synaptic model of memory: long-term potentiation in the hippocampus. *Nature.* 361:31-9.
- Block MR, Glick BS, Wilcox CA, Wieland FT, Rothman JE. (1988) Purification of an N-ethylmaleimidesensitive protein catalyzing vesicular transport. *Proc Natl Acad Sci USA.* 85:7852–7856.
- Bonifati V, Rizzu P, Squitieri F, Krieger E, Vanacore N, van Swieten JC, Brice A, van Duijn CM, Oostra B, Meco G, Heutink P. (2003) DJ-1(PARK7), a novel gene for autosomal recessive, early onset parkinsonism. *Neurol Sci.* 24:159-60.
- Bonifati V. (2012) Autosomal recessive parkinsonism. *Parkinsonism Relat Disord.* 18 Suppl 1:S4-6.
- Bonny C, Oberson A, Negri S, Sauser C, Schorderet DF (2001) Cell-permeable peptide inhibitors of JNK: novel blockers of beta-cell death. *Diabetes.* 50: 77–82.
- Borden KL. (2000) RING domains: master builders of molecular scaffolds? *Journal of Molecular Biology.* 295, 1103–1112.
- Bortolotto ZA, Clarke VR, Delany CM, Parry MC, Smolders I, Vignes M, Ho KH, Miu P, Brinton BT, Fantaske R, Ogden A, Gates M, Ornstein PL, Lodge D, Bleakman D, Collingridge GL. (1999) Kainate receptors are involved in synaptic plasticity. *Nature.* 402:297-301.
- Boudin H, Craig AM (2001) Molecular determinants for PICK1 synaptic aggregation and mGluR7a receptor co-clustering: role of the PDZ, coiled-coil, and acidic domains. *J Biol Chem.* 276:30270–30276.
- Boudin H, Doan A, Xia J, Shigemoto R, Huganir RL, Worley P, Craig AM. (2000) Presynaptic clustering of mGluR7a requires the PICK1 PDZ domainbinding site. *Neuron.* 28, 485–497.
- Boveris A, Navarro A. (2008) Brain mitochondrial dysfunction in aging. *IUBMB Life.* 60: 308-314.
- Bradford HF, Young AMJ, and Crowder JM. (1987) Continuous glutamate leakage from brain cells is balanced by compensatory high-affinity reuptake transport. *Neurosci Lett.* 81: 296–302.
- Bradford MM. (1976) A rapid and sensitive method for the quantitation of microgram quantities of protein utilizing the principle of protein-dye binding. *Anal Biochem.* 72:248-54.
- Brundin P, Olsson R. (2011) Can α -synuclein be targeted in novel therapies for Parkinson's disease? *Expert Rev Neurother.* 11:917-9.
- Butz S, Okamoto M, Südhof TC. (1998) A tripartite protein complex with the potential to couple synaptic vesicle exocytosis to cell adhesion in brain. *Cell.* 94:773-82.
- Cao H, Chen J, Awoniyi M, Henley JR, McNiven MA. (2007) Dynamin 2 mediates fluid-phase micropinocytosis in epithelial cells. *J Cell Sci.* 120:4167–4177.
- Carroll J, Fearnley IM, Skehel JM, Shannon RJ, Hirst J, Walker JE. (2006) Bovine complex I is a complex of 45 different subunits. *J. Biol. Chem.* 281:32724–32727.
- Chagnon P, Bétard C, Robitaille Y, Cholette A, Gauvreau D. (1995) Distribution of brain cytochrome oxidase activity in various neurodegenerative diseases. *Neuroreport.* 6:711–715.
- Chan DC. (2006) Mitochondrial fusion and fission in mammals. *Annu Rev Cell Dev Biol.* 22:79-99.
- Chance B, Williams GR. (1956) The respiratory chain and oxidative phosphorylation. *Adv Enzymol Relat Subj Biochem.* 17:65-134.

- Chen PE, Wyllie DJ. (2006) Pharmacological insights obtained from structure-function studies of ionotropic glutamate receptors. *Br J Pharmacol.* 147:839-53.
- Cheng J, Nath A, Knudsen B, Hochman S, Geiger JD, Ma M, Magnuson DS. (1998) Neuronal excitatory properties of human immunodeficiency virus type 1 Tat protein. *Neuroscience.* 82:97-106.
- Chinopoulos C, Adam-Vizi V. (2010) Mitochondrial Ca²⁺ sequestration and precipitation revisited. *FEBS J.* 277:3637–3651.
- Chinopoulos C, Tretter L, Adam-Vizi V. (1999) Depolarization of in situ mitochondria due to hydrogen peroxide-induced oxidative stress in nerve terminals: inhibition of alpha-ketoglutarate dehydrogenase. *J Neurochem.* 73:220-8.
- Chittajallu R, Braithwaite SP, Clarke VR, Henley JM. (1999) Kainate receptors: subunits, synaptic localisation and function. *Trends Pharmacol Sci.* 20:26-35.
- Choi DW. (1992) Excitotoxic cell death. *J. Neurobiol.* 23:1261-1276.
- Choi DW. (1994) Calcium and excitotoxic neuronal injury. *Ann N Y Acad Sci.* 747:162-71.
- Chu Y, Kordower JH. (2007) Age-associated increases of α -synuclein in monkeys and humans are associated with nigrostriatal dopamine depletion: is this the target for Parkinson's disease? *Neurobiol. Dis.* 25:134–149.
- Chung KK, Thomas B, Li X, Pletnikova O, Troncoso JC, Marsh L, Dawson VL, Dawson TM. (2004) S-nitrosylation of parkin regulates ubiquitination and compromises parkin's protective function. *Science.* 304:1328-31.
- Chung KK, Zhang Y, Lim KL, Tanaka Y, Huang H, Gao J, Ross CA, Dawson VL and Dawson TM (2001) Parkin ubiquitinates the alpha-synuclein-interacting protein, synphilin-1: implications for, Lewy-body formation in Parkinson disease. *Nat. Med.* 7:1144–1150.
- Churchyard A, Mathias CJ, Boonkongchuen P, Lees AJ. (1997) Autonomic effects of selegiline: possible cardiovascular toxicity in Parkinson's disease. *J NeurolNeurosurg Psychiatry.* 63:228–234.
- Clark IE, Dodson MW, Jiang C, Cao JH, Huh JR, Seol JH, Yoo SJ, Hay BA, Guo M. (2006) *Drosophila* PINK1 is required for mitochondrial function and interacts genetically with parkin. *Nature.* 441:1162-6.
- Clarke PG. (1990) Developmental cell death: Morphological diversity and multiple mechanisms. *Anat Embryol* 181:195–213.
- Clarkson ED, Edwards-Prasad J, Freed CR, Prasad KN. (1999) Immortalized dopamine neurons: A model to study neurotoxicity and neuroprotection. *Proc Soc Exp Biol Med.* 222:157-63.
- Clary DO, Griff IC, Rothman JE. (1990) SNAPs, a family of NSF attachment proteins involved in intracellular membrane fusion in animals and yeast. *Cell* 61:709–721.
- Collins GG, Sandler M, Williams ED, Youdim MB. (1970) Multiple forms of human brain monoamine oxidase. *Nature.* 225:817–820.
- Colquhoun D, Jonas P, Sakmann B. (1992) Action of brief pulses of glutamate on AMPA/kainate receptors in patches from different neurones of rat hippocampal slices. *J Physiol.* 458:261-87.
- Conn PJ, Pin JP. (1997) Pharmacology and functions of metabotropic glutamate receptors. *Annu. Rev. Pharmacol. Toxicol.* 37:205–237.
- Conner SD, Schmid SL. (2003) Regulated portals of entry into the cell. *Nature.* 422:37–44.
- Contractor A, Swanson G, Heinemann SF. (2001) Kainate receptors are involved in short- and long-term plasticity at mossy fiber synapses in the hippocampus. *Neuron.* 29:209-16.

Copani A, Uberti D, Sortino MA, Bruno V, Nicoletti F, Memo M (2001) Activation of cell-cycle-associated proteins in neuronal death: a mandatory or dispensable path? *Trends Neurosci.* 24:25–31.

Cossarizza, A., Baccarani-Contri, M., Kalashnikova, G., and Franceschi, C. (1993) A new method for the cytofluorimetric analysis of mitochondrial membrane potential using the J-aggregate forming lipophilic cation 5,5',6,6'-tetrachloro-1,1',3,3' tetraethylbenzimidazolylcarbocyanine iodide (JC-1). *Biochem.Biophys. Res. Commun.* 197: 40-45.

Crompton M, Capano M, Carafoli E. (1976) Respiration-dependent efflux of magnesium ions from heart mitochondria. *Biochem J.* 154:735-42.

Crompton M, Heid I. (1978) The cycling of calcium, sodium, and protons across the inner membrane of cardiac mitochondria. *Eur J Biochem.* 91:599-608.

Crompton M, Moser R, Ludi H & Carafoli E. (1978) The interrelations between the transport of sodium and calcium in mitochondria of various mammalian tissues. *Eur J Biochem.* 82:25–31.

Cui L, Jeong H, Borovecki F, Parkhurst CN, Tanese N, Krainc D. (2006) Transcriptional repression of PGC-1 α by mutant huntingtin leads to mitochondrial dysfunction and neurodegeneration. *Cell.*127:59–69.

Darios F, Corti O, Lücking CB, Hampe C, Muriel MP, Abbas N, Gu WJ, Hirsch EC, Rooney T, Ruberg M, Brice A. (2003) Parkin prevents mitochondrial swelling and cytochrome c release in mitochondria-dependent cell death. *Hum Mol Genet.* 12:517-26.

Darstein M, Petralia RS, Swanson GT, Wenthold RJ, Heinemann SF. (2003) Distribution of kainate receptor subunits at hippocampal mossy fiber synapses. *J Neurosci.* 23:8013-9.

Dauer W, Przedborski S. (2003) Parkinson's disease: mechanisms and models. *Neuron.* 39:889-909.

Daw MI, Chittajallu R, Bortolotto ZA, Dev KK, Duprat F, Henley JM, Collingridge GL, Isaac JT. (2000) PDZ proteins interacting with C-terminal GluR2/3 are involved in a PKC-dependent regulation of AMPA receptors at hippocampal synapses. *Neuron.* 28:873-86.

Dawson TM, Dawson VL. (2003) Molecular pathways of neurodegeneration in Parkinson's disease. *Science.* 302:819-22.

de Lau LM, Breteler MM. (2006) Epidemiology of Parkinson's disease. *Lancet Neurol.* 5:525–35.

Deng H, Dodson MW, Huang H, Guo M. (2008) The Parkinson's disease genes pink1 and parkin promote mitochondrial fission and/or inhibit fusion in *Drosophila*. *Proc Natl Acad Sci USA.* 105: 14503–14508.

Derossi D, Calvet S, Trembleau A, Brunissen A, Chassaing G, Prochiantz A. (1996) Cell internalization of the third helix of the Antennapedia homeodomain is receptor-independent. *J Biol Chem.* 271:18188-93.

Derossi D, Chassaing G, Prochiantz A. (1998) Trojan peptides: the penetratin system for intracellular delivery. *Trends Cell Biol.* 8:84-7.

Desterro JM, Rodriguez MS, Kemp GD, Hay RT. (1999) Identification of the enzyme required for activation of the small ubiquitin-like protein SUMO-1. *J. Biol. Chem.* 274:10618–10624.

Desterro JM, Thomson J, Hay RT. (1997) Ubch9 conjugates SUMO but not ubiquitin. *FEBS Lett.* 417:297–300.

Dev KK, Putten H, Sommer B, Rovelli G. (2003) Parkin-associated proteins and Parkinson's disease. *Neuropharmacology* 45:1–13.

- Dev KK, Nakajima Y, Kitano J, Braithwaite SP, Henley JM, Nakanishi S. (2000) PICK1 interacts with and regulates PKC phosphorylation of mGluR7. *J. Neurosci.* 20:7252–7257.
- Dev KK, Nakanishi S, Henley JM. (2001) Regulation of mGluR7 receptors by proteins that interact with the intracellular C-terminus. *Trends Pharmacol Sci.* 22:355-61.
- Dev KK, Nishimune A, Henley JM, Nakanishi S. (1999) The protein kinase C alpha binding protein PICK1 interacts with short but not long form alternative splice variants of AMPA receptor subunits. *Neuropharmacology.* 38:635-44.
- Dexter DT, Carter CJ, Wells FR, Javoy-Agid F, Agid Y, Lees A, Jenner P, Marsden CD. (1989) Basal lipid peroxidation in substantia nigra is increased in Parkinson's disease. *J Neurochem.* 52:381-9.
- Di Fiore PP, Polo S, Hofmann K. (2003) When ubiquitin meets ubiquitin receptors: a signalling connection. *Nat Rev Mol Cell Biol.* 4:491-7.
- Dimitratos SD, Stathakis DG, Nelson CA, Woods DF, Bryant PJ. (1998) The location of human CASK at Xp11.4 identifies this gene as a candidate for X-linked optic atrophy. *Genomics.* 51:308-9.
- Dingledine R, Borges K, Bowie D, Traynelis SF. (1999) The glutamate receptor ion channels. *Pharmacol Rev.* 51:7-61.
- Doble A. (1999) The role of excitotoxicity in neurodegenerative disease: implications for therapy. *Pharmacol Ther.* 81:163-221.
- Dodson MW, Guo M. (2007) Pink1, Parkin, DJ-1 and mitochondrial dysfunction in Parkinson's disease. *Curr Opin Neurobiol.* Jun;17:331-7.
- Dong H, O'Brien RJ, Fung ET, Lanahan AA, Worley PF, Huganir RL. (1997) GRIP: a synaptic PDZ domain-containing protein that interacts with AMPA receptors. *Nature.* 386:279-84.
- Dong Z, Ferger B, Paterna JC, Vogel D, Furler S, Osinde M, Feldon J, Büeler H. (2003) Dopamine-dependent neurodegeneration in rats induced by viral vector-mediated overexpression of the parkin target protein, CDCrel-1. *Proc Natl Acad Sci USA.* 100:12438-43.
- Dorval V, Fraser PE. (2006) Small ubiquitin-like modifier (SUMO) modification of natively unfolded proteins tau and alpha-synuclein. *J Biol Chem.* 281:9919-24.
- Dostmann WR, Taylor MS, Nickl CK, Brayden JE, Frank R, Tegge WJ. (2000). Highly specific, membrane-permeant peptide blockers of cGMP-dependent protein kinase alpha inhibit NO-induced cerebral dilation. *Proc. Natl Acad. Sci.* 97: 14772–14777.
- Doucet MV, Harkin A, Dev KK. (2012) The PSD-95/nNOS complex: New drugs for depression? *Pharmacol Ther.* 133: 218-29.
- Doyle DA, Lee A, Lewis J, Kim E, Sheng M, MacKinnon R. (1996) Crystal structures of a complexed and peptide-free membrane protein-binding domain: molecular basis of peptide recognition by PDZ. *Cell.* 85:1067-76.
- Duchen MR. (2004) Mitochondria in health and disease: perspectives on a new mitochondrial biology. *Mol Aspects Med.* 25: 365–451.
- Duggan A, Garcia-Anoveros J, Corey DP. (2002) The PDZ domain protein PICK1 and the sodium channel BNaC1 interact and localize at mechanosensory terminals of dorsal root ganglion neurons and dendrites of central neurons. *J Biol Chem.* 277: 5203–5208.
- Egebjerg J, Bettler B, Hermans-Borgmeyer I, Heinemann S. (1991) Cloning of a cDNA for a glutamate receptor subunit activated by kainate but not AMPA. *Nature.* 351:745-8.

- Eguchi A, Akuta T, Okuyama H, Senda T, Yokoi H, Inokuchi H, Fujita S, Hayakawa T, Takeda K, Hasegawa M, Nakanishi M. (2001) Protein transduction domain of HIV-1 Tat protein promotes efficient delivery of DNA into mammalian cells. *J. Biol. Chem.* 276: 26204–26210.
- Ekholm SV, Reed SI. (2000) Regulation of G(1) cyclin-dependent kinases in the mammalian cell cycle. *Curr. Opin. Cell Biol.* 12:676–684.
- El Far O, Airas J, Wischmeyer E, Nehring RB, Karschin A, Betz H. (2000) Interaction of the C-terminal tail region of the metabotropic glutamate receptor 7 with the protein kinase C substrate PICK1. *Eur. J. Neurosci.* 12:1-9.
- Elmore SP, Qian T, Grissom SF, Lemasters JJ. (2001) The mitochondrial permeability transition initiates autophagy in rat hepatocytes. *FASEB J.* 15:2286-7.
- Engelender S, Kaminsky Z, Guo X, Sharp AH, Amaravi RK, Kleiderlein JJ, Margolis RL, Troncoso JC, Lanahan AA, Worley PF, Dawson VL, Dawson TM and Ross CA (1999) Synphilin-1 associates with alpha-synuclein and promotes the formation of cytosolic inclusions. *Nat. Genet.* 22:110–114.
- Ezhevsky SA, Nagahara H, Vocero-Akbani AM, Gius DR, Wei MC, Dowdy SF. (1997) Hypophosphorylation of the retinoblastoma protein (pRb) by cyclin D: Cdk4/6 complexes results in active pRb. *Proc Natl Acad Sci.* 94:10699-704.
- Fallon L, Bélanger CM, Corera AT, Kontogianna M, Regan-Klapisz E, Moreau F, Voortman J, Haber M, Rouleau G, Thorarinsdottir T, Brice A, van Bergen En Henegouwen PM, Fon EA. (2006) A regulated interaction with the UIM protein Eps15 implicates parkin in EGF receptor trafficking and PI(3)K-Akt signalling. *Nat Cell Biol.* 8:834-42.
- Fallon L, Moreau F, Croft BG, Labib N, Gu WJ, Fon EA. (2002) Parkin and CASK/LIN-2 associate via a PDZ-mediated interaction and are co-localized in lipid rafts and postsynaptic densities in brain. *J Biol Chem.* 277:486-91.
- Farrer M, Chan P, Chen R, Tan L, Lincoln S, Hernandez D, Forno L, Gwinn-Hardy K, Petrucelli L, Hussey J, Singleton A, Tanner C, Hardy J, Langston JW. (2001) Lewy bodies and parkinsonism in families with parkin mutations. *Annals in Neurology* 50:293–300.
- Feldman RM, Correll CC, Kaplan KB, Deshaies RJ. (1997) A complex of Cdc4p, Skp1p, and Cdc53p/cullin catalyzes ubiquitination of the phosphorylated CDK inhibitor Sic1p. *Cell.* 91:221-230.
- Felgioni M, Nishimune A, Henley JM. (2009) Protein SUMOylation modulates calcium influx and glutamate release from presynaptic terminals. *Eur J Neurosci.* 29:1348-56.
- Finney N, Walther F, Mantel PY, Stauffer D, Rovelli G, Dev KK. (2003) The cellular protein level of parkin is regulated by its ubiquitin-like domain. *J Biol Chem.* 278:16054-8.
- Fischer PM, Lane DP. (2004) Small-molecule inhibitors of the p53 suppressor HDM2: have protein-protein interactions come of age as drug targets? *Trends Pharmacol Sci.* 25:343-6.
- Fischer PM, Zhelev NZ, Wang S, Melville JE, Fähræus R, Lane DP. (2000) Structure-activity relationship of truncated and substituted analogues of the intracellular delivery vector Penetratin. *J Pept Res.* 55:163-72.
- Florio SK, Loh C, Huang SM, Iwamaye AE, Kitto KF, Fowler KW, Treiberg JA, Hayflick JS, Walker JM, Fairbanks CA, Lai Y. (2009) Disruption of nNOS-PSD95 protein-protein interaction inhibits acute thermal hyperalgesia and chronic mechanical allodynia in rodents. *Br J Pharmacol.* 158:494-506.
- Forno LS (1996) Neuropathology of Parkinson's disease. *Journal of Neuropathology and Experimental Neurology* 55:259–272.

- Forsythe ID, Clements JD. (1990) Presynaptic glutamate receptors depress excitatory monosynaptic transmission between mouse hippocampal neurones. *J Physiol.* 429:1-16.
- Franklin-Tong VE, Gourlay CW. (2008) A role for actin in regulating apoptosis/programmed cell death: evidence spanning yeast, plants and animals, *Biochem. J.* 413:389–404.
- Fujiyama F, Kuramoto E, Okamoto K, Hioki H, Furuta T, Zhou L, Nomura S, Kaneko T. (2004) Presynaptic localisation of an AMPA-type glutamate receptor in corticostriatal and thalamostriatal axon terminals. *Eur J Neurosci.* 20:3322-30.
- Galley HF. (2011) Oxidative stress and mitochondrial dysfunction in sepsis. *Br J Anaesth.* 107:57-64.
- Gandhi S, Wood-Kaczmar A, Yao Z, Plun-Favreau H, Deas E, Klupsch K, Downward J, Latchman DS, Tabrizi SJ, Wood NW, Duchen MR, Abramov AY. (2009) PINK1-associated Parkinson's disease is caused by neuronal vulnerability to calcium-induced cell death. *Mol Cell.* 33:627-38.
- Gardner SM, Takamiya K, Xia J, Suh JG, Johnson R, Yu S, Huganir RL (2005) Calcium-permeable AMPA receptor plasticity is mediated by subunitspecific interactions with PICK1 and NSF. *Neuron* 45:903–915.
- Geisler S, Holmström KM, Skujat D, Fiesel FC, Rothfuss OC, Kahle PJ, Springer W. (2010) PINK1/Parkin-mediated mitophagy is dependent on VDAC1 and p62/SQSTM1. *Nat Cell Biol.* 12:119-31.
- Geiss-Friedlander R, Melchior F. (2007) Concepts in sumoylation: a decade on. *Nat. Rev. Mol. Cell Biol.* 8:947–956.
- Gereau RW 4th, Conn PJ. (1995) Multiple presynaptic metabotropic glutamate receptors modulate excitatory and inhibitory synaptic transmission in hippocampal area CA1. *J Neurosci.* 15:6879-89.
- Gibson GE, Starkov A, Blass JP, Ratan RR & Beal MF. (2010) Cause and consequence: mitochondrial dysfunction initiates and propagates neuronal dysfunction, neuronal death and behavioural abnormalities in age-associated neurodegenerative diseases. *Biochim Biophys Acta* 1802:122–134.
- Giros B, Caron MG. (1993) Molecular characterization of the dopamine transporter. *Trends Pharmacol Sci.* 14:43-9.
- Giros B, el Mestikawy S, Bertrand L, Caron MG. (1991) Cloning and functional characterization of a cocaine-sensitive dopamine transporter. *FEBS Lett.* 295:149-54.
- Giros B, Jaber M, Jones SR, Wightman RM, Caron MG. (1996) Hyperlocomotion and indifference to cocaine and amphetamine in mice lacking the dopamine transporter. *Nature.* 379:606-12.
- Glass AS, Huynh DP, Franck T, Voitalla D, Müller T, Pulst SM, Berg D, Krüger R, Riess O. (2004) Screening for mutations in synaptotagmin XI in Parkinson's disease. *J Neural Transm Suppl.* 68:21-8.
- Gong L, Li B, Millas S, Yeh ET. (1999) Molecular cloning and characterization of human AOS1 and UBA2, components of the sentrin-activating enzyme complex. *FEBS Lett.* 448:185–189.
- Goodnight JA, Mischak H, Kolch W, Mushinski JF. (1995) Immunocytochemical localisation of eight protein kinase C isozymes overexpressed in NIH 3T3 fibroblasts. Isoform-specific association with microfilaments, Golgi, endoplasmic reticulum, and nuclear and cell membranes. *J Biol Chem.* 270:9991-10001.
- Gourlay CW, Ayscough KR. (2005) The actin cytoskeleton: a key regulator of apoptosis and ageing? *Nat. Rev. Mol. Cell Biol.* 6:583–589.

- Gratton JP, Yu J, Griffith JW, Babbitt RW, Scotland RS, Hickey R, Giordano FJ, Sessa WC. (2003) Cell-permeable peptides improve cellular uptake and therapeutic gene delivery of replication-deficient viruses in cells and *in vivo*. *Nat. Med.* 9: 357–363.
- Green DR, Kroemer G. (2004) The pathophysiology of mitochondrial cell death. *Science.* 305:626-9.
- Greenamyre JT, Sherer TB, Betarbet R, Panov AV. (2001) Complex I and Parkinson's disease. *IUBMB Life.* 52:135-41.
- Greene JC, Whitworth AJ, Kuo I, Andrews LA, Feany MB, Pallanck LJ. (2003) Mitochondrial pathology and apoptotic muscle degeneration in *Drosophila parkin* mutants. *Proc Natl Acad Sci USA.* 100:4078-83.
- Griendling KK, Ushio-Fukai M. (2000) Reactive oxygen species as mediators of angiotensin II signaling. *Regul. Pept.* 91:21–27.
- Gu WJ, Corti O, Araujo F, Hampe C, Jacquier S, Lücking CB, Abbas N, Duyckaerts C, Rooney T, Pradier L, Ruberg M, Brice A. (2003) The C289G and C418R missense mutations cause rapid sequestration of human Parkin into insoluble aggregates. *Neurobiol Dis.* 14:357–364.
- Gunter TE, Sheu SS. (2009) Characteristics and possible functions of mitochondrial Ca²⁺ transport mechanisms. *Biochim Biophys Acta* 1787:1291–1308.
- Gunter TE, Gunter KK, Sheu SS, Gavin CE. (1994) Mitochondrial calcium transport: physiological and pathological relevance. *Am J Physiol.* 267:C313-39.
- Gupta-Rossi N, Le Bail O, Gonen H, Brou C, Logeat F, Six E, Ciechanover A, Israël A. (2001) Functional interaction between SEL-10, an F-box protein, and the nuclear form of activated Notch1 receptor. *J Biol Chem.* 276:34371-8.
- Haglund K and Dikic I. (2005) Ubiquitylation and cell signaling. *EMBO J.* 24:3353-9.
- Halestrap AP, McStay GP, Clarke SJ (2002) The permeability transition pore complex: another view. *Biochimie.* 84:153–166.
- Halliday G, Hely M, Reid W, Morris J. (2008) The progression of pathology in longitudinally followed patients with Parkinson's disease. *Acta Neuropathol.* 115:409-15.
- Hamza TH, Zabetian CP, Tenesa A, Laederach A, Montimurro J, Yearout D, Kay DM, Doheny KF, Paschall J, Pugh E, Kusel VI, Collura R, Roberts J, Griffith A, Samii A, Scott WK, Nutt J, Factor SA, Payami H. (2010) Common genetic variation in the HLA region is associated with late-onset sporadic Parkinson's disease. *Nat Genet.* 42:781-5.
- Hansson E, Muyderman H, Leonova J, Allansson L, Sinclair J, Blomstrand F, Thorlin T, Nilsson M, Ronnback L. (2000) Astroglia and glutamate in physiology and pathology: aspects on glutamate transport, glutamate-induced cell swelling, and gap-junction communication. *Neurochem Int.* 37:317–329.
- Hantschel O, Superti-Furga G. (2004) Regulation of the c-Abl and Bcr-Abl tyrosine kinases. *Nat Rev Mol Cell Biol.* 5:33-44.
- Hardy J, Cai H, Cookson MR, Gwinn-Hardy K, Singleton A. (2006) Genetics of Parkinson's disease and parkinsonism. *Ann Neurol.* 60: 389–398.
- Harkin AJ, Bruce KH, Craft B, Paul IA. (1999) Nitric oxide synthase inhibitors have antidepressant-like properties in mice. 1. Acute treatments are active in the forced swim test. *Eur J Pharmacol.* 372:207-13.
- Harmar AJ, Hills RA, Rosser EM, Jones M, Buneman OP, Dunbar DR, Greenhill SD, Hale VA, Sharman JL, Bonner TI, Catterall WA, Davenport AP, Delagrangé P, Dollery CT, Ford SM, Gutman GA, Laudet V, Neubig RR, Ohlstein EH, Olsen RW, Peters J, Pin JP, Ruffolo RR, Searls

- DB, Wright MW, Spedding M. (2009) IUPHAR-DB: the IUPHAR database of G protein-coupled receptors and ion channels. *Nucleic Acids Res.* 37:D680–685.
- Hashimoto K. (2009) Emerging role of glutamate in the pathophysiology of major depressive disorder. *Brain Res Rev.* 61:105-23.
- Hata Y, Butz S, Südhof TC. (1996) CASK: a novel dlg/PSD95 homolog with an N-terminal calmodulin-dependent protein kinase domain identified by interaction with neurexins. *J Neurosci.* 16: 2488-94.
- Hatefi Y. (1985) The mitochondrial electron transport and oxidative phosphorylation system. *Annu Rev Biochem.* 54:1015-69.
- Haugey N, Nath A and Geiger JD. (1995) HIV-1 regulatory protein tat and tat fragments induce calcium in human brain cells. *Can. J. Inf. Dis.* 6:14.
- Hayashi S, Wakabayashi K, Ishikawa A, Nagai H, Saito M, Maruyama M, Takahashi T, Ozawa T, Tsuji S, Takahashi H. (2000) An autopsy case of autosomal-recessive juvenile parkinsonism with a homozygous exon 4 deletion in the parkin gene. *Mov Disord.* 15:884-8.
- Healy DG, Abou-Sleiman PM, Gibson JM, Ross OA, Jain S, Gandhi S, Gosal D, Muqit MMK, Wood NW, Lynch T. (2004) PINK1 (PARK6) associated Parkinson disease in Ireland. *Neurology* 63:1486-1488.
- Henchcliffe C, Beal MF. (2008) Mitochondrial biology and oxidative stress in Parkinson disease pathogenesis. *Nat Clin Pract Neurol.* 4:600-9.
- Henley JM. (2003) Proteins interactions implicated in AMPA receptor trafficking: a clear destination and an improving route map. *Neurosci Res.* 45:243-54.
- Herrero I, Vázquez E, Miras-Portugal MT, Sánchez-Prieto J. (1996) Decrease in $[Ca^{2+}]_c$ but not in cAMP Mediates L-AP4 inhibition of glutamate release: PKC-mediated suppression of this inhibitory pathway. *Eur J Neurosci.* 8:700-9.
- Hersch SM, Yi H, Heilman CJ, Edwards RH, Levey AI. (1997) Subcellular localization and molecular topology of the dopamine transporter in the striatum and substantia nigra. *J Comp Neurol.* 388:211-27.
- Hershko A, Ciechanover A (1998) The ubiquitin system. *Annual Review of Biochemistry.* 67:425–479.
- Hicke L, Dunn R. (2003) Regulation of membrane protein transport by ubiquitin and ubiquitin-binding proteins. *Annu Rev Cell Dev Biol.* 19:141-72.
- Hinchliffe P, Sazanov LA. (2005) Organization of iron-sulfur clusters in respiratory complex I. *Science.* 309:771-4.
- Hirbec H, Francis JC, Lauri SE, Braithwaite SP, Coussen F, Mülle C, Dev KK, Coutinho V, Meyer G, Isaac JT, Collingridge GL, Henley JM. (2003) Rapid and differential regulation of AMPA and kainate receptors at hippocampal mossy fibre synapses by PICK1 and GRIP. *Neuron.* 37:625-38.
- Hocevar BA, Fields AP. (1991) Selective translocation of beta II-protein kinase C to the nucleus of human promyelocytic (HL60) leukemia cells. *J Biol Chem.* 266:28-33.
- Hofhaus G, Weiss H, Leonard K. (1991) Electron microscopic analysis of the peripheral and membrane parts of mitochondrial NADH dehydrogenase (complex I). *J Mol Biol.* 221:1027-43.
- Hollenbeck PJ, Saxton WM. (2005) The axonal transport of mitochondria. *J Cell Sci.* 118:5411-9.
- Hollmann M, Heinemann S. (1994) Cloned glutamate receptors. *Annu Rev Neurosci.* 17:31-108.
- Hornykiewicz O. (1998) Biochemical aspects of Parkinson's disease. *Neurology* 51:2-9.

- Hornykiewicz O, Kish SJ. (1987) Biochemical pathophysiology of Parkinson's disease. *Adv Neurol.* 45:19-34.
- Hruska-Hageman AM, Wemmie JA, Price MP, Welsh MJ. (2002) Interaction of the synaptic protein PICK1 (protein interacting with C kinase 1) with the non-voltage gated sodium channels BNC1 (brain Na⁺ channel 1) and ASIC (acid-sensing ion channel). *Biochem J.* 361:443-50.
- Hsueh YP, Yang FC, Kharazia V, Naisbitt S, Cohen AR, Weinberg RJ, Sheng M. (1998) Direct interaction of CASK/LIN-2 and syndecan heparan sulfate proteoglycan and their overlapping distribution in neuronal synapses. *J Cell Biol.* 142: 139-51.
- Hu ZL, Huang C, Fu H, Jin Y, Wu WN, Xiong QJ, Xie N, Long LH, Chen JG, Wang F. (2010) Disruption of PICK1 attenuates the function of ASICs and PKC regulation of ASICs. *Am J Physiol Cell Physiol.* 299:C1355-62.
- Huang LS, Sun G, Cobessi D, Wang AC, Shen JT, Tung EY, Anderson VE, Berry EA. (2006) 3-nitropropionic acid is a suicide inhibitor of mitochondrial respiration that, upon oxidation by complex II, forms a covalent adduct with a catalytic base arginine in the active site of the enzyme. *J Biol Chem.* 281:5965-72.
- Hubbard EJ, Wu G, Kitajewski J, Greenwald I. (1997) sel-10, a negative regulator of lin-12 activity in *Caenorhabditis elegans*, encodes a member of the CDC4 family of proteins. *Genes Dev.* 11:3182-93.
- Hubel DH. (1979) The brain. *Sci. Am.*, 241:44–53.
- Hunter DR, Haworth RA. (1979) The Ca²⁺-induced membrane transition in mitochondria. I. The protective mechanisms. *Arch Biochem Biophys.* 195:453-9.
- Huynh DP, Scoles DR, Ho TH, Del Bigio MR, Pulst SM. (2000) Parkin is associated with actin filaments in neuronal and nonneuronal cells. *Ann Neurol.* 48:737-44.
- Huynh DP, Scoles DR, Nguyen D, Pulst SM. (2003) The autosomal recessive juvenile Parkinson disease gene product, parkin, interacts with and ubiquitinates synaptotagmin XI. *Hum Mol Genet.* 12:2587-97.
- Imai Y, Soda M, Inoue H, Hattori N, Mizuno Y, Takahashi R. (2001) An unfolded putative transmembrane polypeptide, which can lead to endoplasmic reticulum stress, is a substrate of Parkin. *Cell.* 105:891-902.
- Imai Y, Soda M, Takahashi R. (2000) Parkin suppresses unfolded protein stress-induced cell death through its E3 ubiquitin-protein ligase activity. *J Biol Chem.* 275:35661-4.
- Imai Y and Takahashi R. (2004) How do Parkin mutations result in neurodegeneration? *Curr Opin Neurobiol.* 14:384-9.
- IPDGC and WTCCC2. International Parkinson's Disease Genomics Consortium (IPDGC); Wellcome Trust Case Control Consortium 2 (WTCCC2). (2011) A two-stage meta-analysis identifies several new loci for Parkinson's disease. *PLoS Genet.* 7:e1002142.
- Ishikawa K, Nash SR, Nishimune A, Neki A, Kaneko S, Nakanishi S. (1999) Competitive interaction of seven in absentia homolog-1A and Ca²⁺/calmodulin with the cytoplasmic tail of group 1 metabotropic glutamate receptors. *Genes Cells* 4:381–390.
- Iwai A, Masliah E, Yoshimoto M, Ge N, Flanagan L, de Silva HA, Kittel A and Saitoh T. (1995) The precursor protein of non-A beta component of Alzheimer's disease amyloid is a presynaptic protein of the central nervous system. *Neuron*, 14:467–475.
- Jaskolski F, Coussen F, Nagarajan N, Normand E, Rosenmund C, Mulle C. (2004) Subunit composition and alternative splicing regulate membrane delivery of kainate receptors. *J Neurosci.* 24:2506-15.

- Jenner P and Olanow CW. (1996) Oxidative stress and the pathogenesis of Parkinson's disease. *Neurology*. 47:S161-70.
- Jiffar T, Kurinna S, Suck G (2004) PKC alpha mediates chemoresistance in acute lymphoblastic leukemia through effects on Bcl2 phosphorylation. *Leukemia*. 18:505–512.
- Jo D, Nashabi A, Doxsee C, Lin Q, Unutmaz D, Chen J, Ruley HE (2001). Epigenetic regulation of gene structure and function with a cell- permeable Cre recombinase. *Nat. Biotechnol*. 19: 929–933.
- Joazeiro CA, Weissman AM (2000) RING finger proteins: mediators of ubiquitin ligase activity. *Cell*. 102:549–552.
- Joch M, Ase AR, Chen CXQ, MacDonald PA, Kontogianna M, Corera AT, Brice A, Se'gue'la P, Fon E A (2008) Parkin-mediated Monoubiquitination of the PDZ Protein PICK1 Regulates the Activity of Acid-sensing Ion Channels. *Genes Dev*. 22:252-264.
- Johnson ES, Schwienhorst I, Dohmen RJ, Blobel G (1997a) The ubiquitin-like protein Smt3p is activated for conjugation to other proteins by an Aos1p/Uba2p heterodimer. *EMBO J*. 16:5509–5519.
- Johnson ES and Blobel G. (1997b) Ubc9p is the conjugating enzyme for the ubiquitin-like protein Smt3p. *J. Biol. Chem*. 272:26799–26802.
- Jones SR, Gainetdinov RR, Jaber M, Giros B, Wightman RM, Caron MG. (1998) Profound neuronal plasticity in response to inactivation of the dopamine transporter. *Proc Natl Acad Sci USA*. 95:4029-34.
- Kaech SM, Whitfield CW, Kim SK. (1998) The LIN-2/LIN-7/LIN-10 complex mediates basolateral membrane localisation of the *C. elegans* EGF receptor LET-23 in vulval epithelial cells. *Cell*. 94:761-71.
- Kahle PJ, Leimer U, Haass C. (2000) Does failure of parkin mediated ubiquitination cause juvenile parkinsonism? *Trends in Biochemical Science*. 25:524–527.
- Kamitani T, Kito K, Nguyen HP, Fukuda-Kamitani T, Yeh ET. (1998) Characterization of a second member of the sentrin family of ubiquitin-like proteins. *J. Biol. Chem*. 273:11349–11353.
- Kaplan IM, Wadia JS, Dowdy SF. (2005) Cationic TAT peptide transduction domain enters cells by macropinocytosis. *J Control Release*. 102:247-53.
- Katsanis N and Fisher EM. (1998) Identification, expression, and chromosomal localization of ubiquitin conjugating enzyme 7(UBE2G2), a human homologue of the *saccharomyces cerevisiae* UBC7 gene. *Genomics*. 51:128–131.
- Kauppinen RA, McMahon HT, Nicholls DG. (1988) Ca²⁺-dependent and Ca²⁺-independent glutamate release, energy status and cytosolic free Ca²⁺ concentration in isolated nerve terminals following metabolic inhibition: possible relevance to hypoglycaemia and anoxia. *Neuroscience*. 27:175-82.
- Kauppinen RA, Nicholls DG. (1986) Synaptosomal bioenergetics. The role of glycolysis, pyruvate oxidation and responses to hypoglycaemia. *Eur J Biochem*. 158:159-65.
- Kedar V, McDonough H, Arya R, Li HH, Rockman HA, Patterson C. (2004) Muscle-specific RING finger 1 is a bona fide ubiquitin ligase that degrades cardiac troponin I. *Proc Natl Acad Sci USA*. 101:18135-40.
- Keeney PM, Xie J, Capaldi RA, Bennett JP Jr. (2006) Parkinson's disease brain mitochondrial complex I has oxidatively damaged subunits and is functionally impaired and misassembled. *J Neurosci*. 26:5256-64.

- Kettenmann H, Hanisch UK, Noda M, Verkhratsky A. (2011) Physiology of microglia. *Physiol Rev.* 91:461-553.
- Kies MW, Martenson RE, Deibler GE. (1972) Myelin basic proteins. *Adv Exp Med Biol.* 32:201-14.
- Kilbride SM, Telford JE, Tipton KF, Davey GP. (2008) Partial inhibition of complex I activity increases Ca-independent glutamate release rates from depolarized synaptosomes. *J Neurochem.* 106:826-34.
- Kilty JE, Lorang D, Amara SG. (1991) Cloning and expression of a cocaine-sensitive rat dopamine transporter. *Science.* 254:578-9.
- Kim HT, Kim KP, Lledias F, Kisselev AF, Scaglione KM, Skowrya D, Gygi SP, Goldberg AL. (2007) Certain pairs of ubiquitin-conjugating enzymes (E2s) and ubiquitin-protein ligases (E3s) synthesize nondegradable forked ubiquitin chains containing all possible isopeptide linkages. *J Biol Chem.* 282:17375-86.
- Kim K, Lee SG, Kegelman TP, Su ZZ, Das SK, Dash R, Dasgupta S, Barral PM, Hedvat M, Diaz P, Reed JC, Stebbins JL, Pellicchia M, Sarkar D, Fisher PB. (2011) Role of excitatory amino acid transporter-2 (EAAT2) and glutamate in neurodegeneration: opportunities for developing novel therapeutics. *J Cell Physiol.* 226:2484-93.
- Kim S, Zhang S, Choi KH, Reister R, Do C, Baykiz AF, Gershenfeld HK. (2009) An E3 ubiquitin ligase, Really Interesting New Gene (RING) Finger 41, is a candidate gene for anxiety-like behavior and beta-carboline-induced seizures. *Biol Psychiatry.* 65:425-31.
- Kimura M, Hattori T, Matsuda Y, Yoshioka T, Sumi N, Umeda Y, Nakashima S, Okano Y. (1997) cDNA cloning, characterization, and chromosome mapping of UBE2E2 encoding a human ubiquitin-conjugating E2 enzyme. *Cytogenetics and Cellular Genetics* 78:107–111.
- Kish SJ, Bergeron C, Rajput A, Dozic S, Mastrogiacomo F, Chang LJ, Wilson JM, DiStefano LM, Nobrega JN. (1992) Brain cytochrome oxidase in Alzheimer's disease. *J Neurochem.* 57:776-9.
- Kitada T, Asakawa S, Hattori N, Matsumine H, Yamamura Y, Minoshima S, Yokochi M, Mizuno Y, Shimizu N. (1998) Mutations in the parkin gene cause autosomal recessive juvenile parkinsonism. *Nature.* 392:605-8.
- Kitada T, Asakawa S, Minoshima S, Mizuno Y, Shimizu N. (2000) Molecular cloning, gene expression, and identification of a splicing variant of the mouse parkin gene. *Mammal Genome.* 11:417–421.
- Klein C, Lohmann-Hedrich K. (2007) Impact of recent genetic findings in Parkinson's disease. *Curr Opin Neurol.* 20:453–464.
- Knutti D, Kaul A, Kralli A. (2000) A tissue-specific coactivator of steroid receptors, identified in a functional genetic screen. *Mol. Cell. Biol.* 20:2411-2422.
- Ko HS, Lee Y, Shin JH, Karuppagounder SS, Gadad BS, Koleske AJ, Pletnikova O, Troncoso JC, Dawson VL, Dawson TM. (2010) Phosphorylation by the c-Abl protein tyrosine kinase inhibits parkin's ubiquitination and protective function. *Proc Natl Acad Sci.* 107:16691-6.
- Ko HS, von Coelln R, Sriram SR, Kim SW, Chung KK, Pletnikova O, Troncoso J, Johnson B, Saffary R, Goh EL, Song H, Park BJ, Kim MJ, Kim S, Dawson VL, Dawson TM. (2005) Accumulation of the authentic parkin substrate aminoacyl-tRNA synthetase cofactor, p38/JTV-1, leads to catecholaminergic cell death. *J Neurosci.* 25:7968-78.
- Koepp DM, Schaefer LK, Ye X, Keyomarsi K, Chu C, Harper JW, Elledge SJ (2001) Phosphorylation-dependent ubiquitination of cyclin E by the SCFFbw7 ubiquitin ligase. *Science.* 294:173–177.

- Korper S, Nolte F, Rojewski MT, Thiel E, Schrezenmeier H. (2003) The K⁺ channel openers diazoxide and NS1619 induce depolarization of mitochondria and have differential effects on cell Ca²⁺ in CD34⁺ cell line KG-1a. *Exp Hematol.* 31:815-23.
- Kösel S, Hofhaus G, Maassen A, Vieregge P, Graeber MB. (1999) Role of mitochondria in Parkinson disease. *Biol Chem.* 380:865-70.
- Krishtal O. (2003) The ASICs: signaling molecules? Modulators? *Trends Neurosci.* 26:477–483.
- Kruger R, Kuhn W, Muller T, Woitalla D, Graeber M, Kosel S, Przuntek H, Epplen JT, Schols L, Riess O. (1998) Ala30Pro mutation in the gene encoding alpha-synuclein in Parkinson's disease. *Nature Genetics.* 18:106–108.
- Kruman II, Nath A, Mattson MP. (1998) HIV-1 protein Tat induces apoptosis of hippocampal neurons by a mechanism involving caspase activation, calcium overload, and oxidative stress. *Exp Neurol.* 154:276-88.
- Kubo SI, Kitami T, Noda S, Shimura H, Uchiyama Y, Asakawa S, Minoshima S, Shimizu N, Mizuno Y, Hattori N. (2001) Parkin is associated with cellular vesicles. *J Neurochem.* 78:42-54.
- Kumar KN, Tilakaratne N, Johnson PS, Allen AE, Michaelis EK. (1991) Cloning of cDNA for the glutamate-binding subunit of an NMDA receptor complex. *Nature.* 354:70-3.
- Kuroda Y, Mitsui T, Kunishige M, Shono M, Akaike M, Azuma H, Matsumoto T. (2006) Parkin enhances mitochondrial biogenesis in proliferating cells. *Hum Mol Genet.* 15:883-95.
- Kyung-Hee Kim, Jin H. Son. (2010) PINK1 gene knockdown leads to increased binding of parkin with actin filament. *Neuroscience Letters.* 468:272–276.
- Lahav-Baratz S, Sudakin V, Ruderman JV, Hershko A. (1995) Reversible phosphorylation controls the activity of cyclosome-associated cyclin-ubiquitin ligase. *Proc Natl Acad Sci.* 92:9303-7.
- Lajoie P, Nabi IR. (2007) Regulation of raft-dependent endocytosis. *J Cell Mol Med.* 11:644–653.
- Laszlo Tretter and Vera Adam-Vizi (2007) Uncoupling is without an effect on the production of reactive oxygen species by in situ synaptic mitochondria. *Journal of Neurochemistry.* 103:1864–1871.
- Lauri SE, Delany C, J Clarke VR, Bortolotto ZA, Ornstein PL, T R Isaac J, Collingridge GL. (2001) Synaptic activation of a presynaptic kainate receptor facilitates AMPA receptor-mediated synaptic transmission at hippocampal mossy fibre synapses. *Neuropharmacology.* 41:907-15.
- Lazaro-Dieguez F, Aguado C, Mato E, Sanchez-Ruiz Y, Esteban I, Alberch J, Knecht E, Egea G. (2008) Dynamics of an F-actin aggresome generated by the actin-stabilizing toxin jasplakinolide. *J. Cell Sci.* 121:1415–1425.
- Lee J, Schriener SE & Wallace DC. (2009) Adenine nucleotide translocator 1 deficiency increases resistance of mouse brain and neurons to excitotoxic insults. *Biochim Biophys Acta.* 1787:364–370.
- Leegwater-Kim J, Bortan E. (2010) The role of rasagiline in the treatment of Parkinson's disease. *Clin Interv Aging.* 5:149-56.
- Lemasters JJ, Theruvath TP, Zhong Z, Nieminen AL. (2009) Mitochondrial calcium and the permeability transition in cell death. *Biochim Biophys Acta.* 1787:1395-401.
- Leone TC, Lehman JJ, Finck BN, Schaeffer PJ, Wende AR, Boudina S, Courtois M, Wozniak DF, Sambandam N, Bernal- Mizrachi C. (2005) PGC-1alpha deficiency causes multi-system energy metabolic derangements: muscle dysfunction, abnormal weight control and hepatic steatosis. *PLoS Biol.* 3:101.

- Lerma J, Paternain AV, Rodríguez-Moreno A, López-García JC. (2001) Molecular physiology of kainate receptors. *Physiol Rev.* 81:971-98.
- Leroy E, Boyer R, Auburger G, Leube B, Ulm G, Mezey E, Harta G, Brownstein MJ, Jonnalagada S, Chernova T, Dehejia A, Lavedan C, Gasser T, Steinbach PJ, Wilkinson KD, Polymeropoulos MH. (1998) The ubiquitin pathway in Parkinson's disease. *Nature.* 395:451-452.
- Lesage S, Brice A. (2012) Role of Mendelian genes in "sporadic" Parkinson's disease. *Parkinsonism Relat Disord.* 18 Suppl 1:S66-70.
- Lewin M, Carlesso N, Tung CH, Tang XW, Cory D, Scadden DT, Weissleder R. (2000) Tat peptide-derivatized magnetic nanoparticles allow *in vivo* tracking and recovery of progenitor cells. *Nat. Biotechnol.* 18: 410-414.
- Li P, Kerchner GA, Sala C, Wei F, Huettnner JE, Sheng M, Zhuo M. (1999) AMPA receptor-PDZ interactions in facilitation of spinal sensory synapses. *Nat Neurosci.* 11:972-7.
- Lin DT, Haganir RL. (2007) PICK1 and phosphorylation of the glutamate receptor 2 (GluR2) AMPA receptor subunit regulates GluR2 recycling after NMDA receptor-induced internalization. *J Neurosci.* 27:13903-8.
- Lin J, Wu P, Tarr P, St-Pierre J, Zhang J, Mootha VK, Jager S, Vianna C, Reznick R, Manieri M. (2004) Defects in adaptive energy metabolism with hyperactivity in PGC-1alpha mutant mice. *Cell.* 119:121-135.
- Lin MT, Beal MF. (2006) Mitochondrial dysfunction and oxidative stress in neurodegenerative diseases. *Nature.* 443:787-95.
- Lindsay MA. (2002) Peptide-mediated cell delivery: application in protein target validation. *Curr Opin Pharmacol.* 2:587-94.
- Liu DX, Greene LA (2001) Neuronal apoptosis at the G1/S cell cycle checkpoint. *Cell Tissue Res.* 305:217-228.
- Liu SJ, Lachamp P, Liu Y, Savtchouk I, Sun L. (2008) Long-term synaptic plasticity in cerebellar stellate cells. *Cerebellum.* 7:559-62.
- Liu SQ, Cull-Candy SG. (2000) Synaptic activity at calcium-permeable AMPA receptors induces a switch in receptor subtype. *Nature.* 405:454-8.
- Lowe J, McDermott H, Landon M, Mayer RJ, Wilkinson KD. (1990) Ubiquitin carboxyl-terminal hydrolase (PGP 9.5) is selectively present in ubiquitinated inclusion bodies characteristic of human neurodegenerative diseases. *J Pathol.* 161:153-60.
- Lucking CB, Durr A, Bonifati V, Vaughan J, De Michele G, Gasser T, Harhangi BS, Pollak P, Bonnet AM, Nichol D, Mari MD, Marconi R, Broussolle E, Rascol O, Rosier M, Arnould I, Oostra BA, Breteler MMB, Filla A, Meco G, Deneffe P, Wood NW, Agid Y, Brice A. (2000) Association between early-onset Parkinson's disease and mutations in the parkin gene. *New England Journal of Medicine.* 342:1560-1567.
- Lutz AK, Exner N, Fett ME, Schlehe JS, Kloos K, Lämmermann K, Brunner B, Kurz-Drexler A, Vogel F, Reichert AS, Bouman L, Vogt-Weisenhorn D, Wurst W, Tatzelt J, Haass C, Winklhofer KF. (2009) Loss of parkin or PINK1 function increases Drp1-dependent mitochondrial fragmentation. *J Biol Chem.* 284:22938-51.
- Ly JD, Grubb DR, Lawen A (2003) The mitochondrial membrane potential ($\Delta\psi_m$) in apoptosis; an update. *Apoptosis.* 8:115-128.
- Madsen KL, Beuming T, Niv MY, Chang CW, Dev KK, Weinstein H, Gether U. (2005) Molecular determinants for the complex binding specificity of the PDZ domain in PICK1. *J Biol Chem.* 280: 20539-48.

- Mantymaa P, Siitonen T, Guttorm T, Saily M, Kinnula V, Savolainen ER, Koistinen P. (2000) Induction of mitochondrial manganese superoxide dismutase confers resistance to apoptosis in acute myeloblastic leukaemia cells exposed to etoposide. *Br J Haematol.* 108:574-81.
- Marzo I, Brenner C, Zamzami N, Jürgensmeier JM, Susin SA, Vieira HL, Prévost MC, Xie Z, Matsuyama S, Reed JC, Kroemer G. (1998) Bax and adenine nucleotide translocator cooperate in the mitochondrial control of apoptosis. *Science* 281:2027-2031.
- Mattson MP, Gleichmann M & Cheng A (2008) Mitochondria in neuroplasticity and neurological disorders. *Neuron* 60:748-766.
- Mattson MP. (2003) Excitotoxic and excitoprotective mechanisms: abundant targets for the prevention and treatment of neurodegenerative disorders. *Neuromolecular Med.* 3:65-94.
- McBain CJ, Fisahn A. (2001) Interneurons unbound. *Nat Rev Neurosci.* 2:11-23.
- McMahon HT, Foran P, Dolly JO, Verhage M, Wiegant VM, Nicholls DG. (1992) Characterization of the inhibition of glutamate, GABA and [Met-enkephalin exocytosis from synaptosomes caused by tetanus and botulinum neurotoxins. *J. Biol. Chem.* 267:21338-21343.
- McMahon HT, Rosenthal L, Meldolesi J, Nicholls DG (1990) α -Latrotoxin releases both vesicular and cytoplasmic glutamate from isolated nerve terminals. *J. Neurochem.* 55:2039-2047.
- Meldolesi J & Pozzan T (1998) The endoplasmic reticulum Ca^{2+} store: a view from the lumen. *Trends Biochem Sci.* 23:10-14.
- Meng TC, Fukada T, Tonks NK. (2002) Reversible oxidation and inactivation of protein tyrosine phosphatases *in vivo*. *Mol. Cell.* 9:387-399.
- Minakami R, Jinnai N, Sugiyama H. (1997) Phosphorylation and calmodulin binding of the metabotropic glutamate receptor subtype 5 (mGluR5) are antagonistic *in vitro*. *J. Biol. Chem.* 272:20291-20298.
- Mizuno Y, Hattori N, Matsumine H (1998) Neurochemical and neurogenetic correlates of Parkinson's disease. *Journal of Neurochemistry.* 71:893-902.
- Moberg KH, Bell DW, Wahrer DC, Haber DA, Hariharan IK (2001) Archipelago regulates Cyclin E levels in *Drosophila* and is mutated in human cancer cell lines. *Nature.* 413:311-316.
- Mochly-Rosen D. (1995) Localisation of protein kinases by anchoring proteins: a theme in signal transduction. *Science.* 268:247-51.
- Mohanty JG, Jaffe JS, Schulman ES, Raible DG. (1997) A highly sensitive fluorescent micro-assay of H_2O_2 release from activated human leukocytes using a dihydroxyphenoxazine derivative. *J Immunol Methods.* 202:133-41.
- Moiso N, Klupsch K, Fedele V, East P, Sharma S, Renton A, Plun-Favreau H, Edwards RE, Teismann P, Esposti MD, Morrison AD, Wood NW, Downward J, Martins LM. (2009) Mitochondrial dysfunction triggered by loss of HtrA2 results in the activation of a brain-specific transcriptional stress response. *Cell Death Differ.* 16:449-64.
- Monsalve M, Wu Z, Adelmant G, Puigserver P, Fan M, Spiegelman BM (2000) Direct Coupling of Transcription and mRNA Processing through the Thermogenic Coactivator PGC-1. *Mol Cell.* 6:307-316.
- Montero M, Alonso MT, Carnicero E, Cuchillo-Ibanez I, Albillos A, Garcia AG, Garcia-Sancho J & Alvarez J (2000) Chromaffin-cell stimulation triggers fast millimolar mitochondrial Ca^{2+} transients that modulate secretion. *Nat Cell Biol.* 2:57-61.
- Moresco EM, Koleske AJ. (2003) Regulation of neuronal morphogenesis and synaptic function by Abl family kinases. *Curr Opin Neurobiol.* 13:535-44.

- Morett E, Bork P. (1999) A novel transactivation domain in parkin. *Trends Biochem Sci.* 24:229-31.
- Mori H, Kondo T, Yokochi M, Matsumine H, Nakagawa-Hattori Y, Miyake T, Suda K, Mizuno Y. (1998) Pathologic and biochemical studies of juvenile parkinsonism linked to chromosome 6q. *Neurology.* 51:890–892.
- Moriyoshi K, Masu M, Ishii T, Shigemoto R, Mizuno N, Nakanishi S. (1991) Molecular cloning and characterization of the rat NMDA receptor. *Nature.* 354:31-7.
- Mortiboys H, Thomas KJ, Koopman WJ, Klaffke S, Abou-Sleiman P, Olpin S, Wood NW, Willems PH, Smeitink JA, Cookson MR, Bandmann O. (2008) Mitochondrial function and morphology are impaired in parkin-mutant fibroblasts. *Ann Neurol.* 64:555-65.
- Moss SJ, Blackstone CD, Huganir RL. (1993) Phosphorylation of recombinant non-NMDA glutamate receptors on serine and tyrosine residues. *Neurochem Res.* 18:105-10.
- Moynihan TP, Ardley HC, Nuber U, Rose SA, Jones PF, Markham AF, Scheffner M, Robinson PA. (1999) The ubiquitin-conjugating enzymes UbcH7 and UbcH8 interact with RING finger/IBR motif-containing domains of HHARI and H7-AP1. *J Biol Chem.* 274:30963-8.
- Müftüoğlu M, Elibol B, Dalmizrak O, Ercan A, Kulaksiz G, Ogüs H, Dalkara T, Ozer N. (2004) Mitochondrial complex I and IV activities in leukocytes from patients with parkin mutations. *Mov Disord.* 19:544-8.
- Müller S, Hoegel C, Pyrowolakis G, Jentsch S. (2001) SUMO, ubiquitin's mysterious cousin. *Nat Rev Mol Cell Biol.* 2:202-10.
- Mukherjee S, Ghosh RN, Maxfield FR. (1997) Endocytosis. *Physiol Rev.* 77:759–803.
- Mukhopadhyay D, Riezman H. (2007) Proteasome-independent functions of ubiquitin in endocytosis and signaling. *Science.* 315(5809):201-5.
- Mukhopadhyay D, Dasso M. (2007) Modification in reverse: the SUMO proteases. *Trends Biochem. Sci.* 32:286–295.
- Muniz ZM, Tibbs GR, Maschot P, Bougis P, Nicholls DG, Dolly JO. (1990) Homologues of a K⁺ channel blocker α -dendrotoxin: characterization of synaptosomal binding sites and their coupling to elevation of cytosolic free calcium concentration. *Neurochem. Int.* 16:105-112.
- Murakami T, Shoji M, Imai Y, Inoue H, Kawarabayashi T, Matsubara E, Harigaya Y, Sasaki A, Takahashi R, Abe K. (2004) Pael-R is accumulated in Lewy bodies of Parkinson's disease. *Ann Neurol.* 55:439-42.
- Murata S, Minami Y, Minami M, Chiba T, Tanaka K. (2001) CHIP is a chaperone-dependent E3 ligase that ubiquitylates unfolded protein. *EMBO Rep.* 2:1133-8.
- Murphy MP. (2009) How mitochondria produce reactive oxygen species. *Biochem J.* 417:1-13.
- Musante V, Summa M, Neri E, Puliti A, Godowicz TT, Severi P, Battaglia G, Raiteri M, Pittaluga A. (2010) The HIV-1 viral protein Tat increases glutamate and decreases GABA exocytosis from human and mouse neocortical nerve endings. *Cereb Cortex.* 20:1974-84.
- Nachshen DA. (1985) Regulation of cytosolic calcium concentration in presynaptic nerve endings isolated from rat brain. *J Physiol.* 363:87-101.
- Nagahara H, Vocero-Akbani AM, Snyder EL, Ho A, Latham DG, Lissy NA, Becker-Hapak M, Ezhevsky SA, Dowdy SF. (1998) Transduction of full-length Tat fusion proteins into mammalian cells: Tat-p27Kip1 induces cell migration. *Nat Med.* 4:1449-52.

- Nakajima Y, Yamamoto T, Nakayama T, Nakanishi S. (1999) A relationship between protein kinase C phosphorylation and calmodulin binding to the metabotropic glutamate receptor subtype 7. *J. Biol. Chem.* 274:27573–27577.
- Nakanishi N, Shneider NA, Axel R. (1990) A family of glutamate receptor genes: evidence for the formation of heteromultimeric receptors with distinct channel properties. *Neuron.* 5:569-81.
- Nakanishi S. (1994) Metabotropic glutamate receptors: synaptic transmission, modulation and plasticity. *Neuron* 13:1031–1037.
- Nakashima S (2002) Protein kinase C alpha (PKC alpha): regulation and biological function. *J Biochem* 132:669–675.
- Narendra D, Kane LA, Hauser DN, Fearnley IM, Youle RJ. (2010) p62/SQSTM1 is required for Parkin-induced mitochondrial clustering but not mitophagy; VDAC1 is dispensable for both. *Autophagy.* 6:1090-106.
- Narendra D, Tanaka A, Suen DF, Youle RJ.(2008) Parkin is recruited selectively to impaired mitochondria and promotes their autophagy. *J Cell Biol.* 183:795-803.
- Nateri AS, Riera-Sans L, Da Costa C, Behrens A. (2004) The ubiquitin ligase SCFFbw7 antagonizes apoptotic JNK signaling. *Science.* 303:1374-8.
- Nauta WJH & Feirtag M. (1986) *Fundamental Neuroanatomy.* W.H. Freeman, New York, USA, p. 33.
- Navarro A, Boveris A. (2004) Rat brain and liver mitochondria develop oxidative stress and lose enzymatic activities on aging. *Am J Physiol Regul Integr Comp Physiol.* 287:R1244-9.
- Navarro A. and Boveris A. (2007) The mitochondrial energy transduction system and the aging process. *Am J Physiol Cell Physiol.* 292:670-686.
- Newton AC. (1995) Protein kinase C: structure, function, and regulation. *J Biol Chem.* 270:28495-8.
- Nguyen M, Millar DG, Yong VW, Korsmeyer SJ, Shore GC (1993) Targeting of Bcl-2 to the mitochondrial outer membrane by a COOH-terminal signal anchor sequence. *J Biol Chem.* 268:25265–25268.
- Nicholls DG (2005) Mitochondria and calcium signaling. *Cell Calcium* 38:311–317.
- Nicholls DG and Ward MW. (2000) Mitochondrial membrane potential and neuronal glutamate excitotoxicity: mortality and millivolts. *Trends Neurosci* 23:166- 174.
- Nicholls DG, Budd SL. (2000) Mitochondria and neuronal survival. *Physiol Rev.* 80:315-60.
- Nicholls DG, Sihra TS, Sanchez-Prieto J. (1987) Calcium-dependent and -independent release of glutamate from synaptosomes monitored by continuous fluorometry. *J Neurochem.* 49:50-7.
- Nicholls DG. (1993) The glutamatergic nerve terminal. *Eur J Biochem.* 212:613-31.
- Nirenberg MJ, Chan J, Liu Y, Edwards RH, Pickel VM. (1996) Ultrastructural localization of the vesicular monoamine transporter-2 in midbrain dopaminergic neurons: potential sites for somatodendritic storage and release of dopamine. *J Neurosci.* 16:4135-45.
- Nishiyama A, Yang Z, Butt A. (2005) Astrocytes and NG2-glia: what's in a name? *J. Anat.* 207:687–693.
- Nishizuka Y. (1992) Intracellular signaling by hydrolysis of phospholipids and activation of protein kinase C. *Science.* 258:607-14.
- Niswender CM, Conn PJ. (2010) Metabotropic glutamate receptors: physiology, pharmacology, and disease. *Annu Rev Pharmacol Toxicol.* 50:295-322.

- Nutt JG, Fellman JH. (1984) Pharmacokinetics of levodopa. *Clin Neuropharmacol.* 7:35-49.
- Nuytemans K, Theuns J, Cruts M, Van Broeckhoven C. (2010) Genetic etiology of Parkinson disease associated with mutations in the SNCA, PARK2, PINK1, PARK7, and LRRK2 genes: a mutation update. *Hum Mutat.* 31:763-80.
- Oberg C, Li J, Pauley A, Wolf E, Gurney M, Lendahl U. (2001) The Notch intracellular domain is ubiquitinated and negatively regulated by the mammalian Sel-10 homolog. *J Biol Chem.* 276:35847-53.
- Obeso JA, Rodriguez-Oroz MC, Lanciego JL, Rodriguez Diaz M. (2004) How does Parkinson's disease begin? The role of compensatory mechanisms. *Trends Neurosci.* 27:125-7.
- O'Connor V, El Far O, Bofill-Cardona E, Nanoff C, Freissmuth M, Karschin A, Airas JM, Betz H, Boehm S. (1999) Calmodulin dependence of presynaptic metabotropic glutamate receptor signaling. *Science.* 286:1180–1184.
- Okuma T, Honda R, Ichikawa G, Tsumagari N, Yasuda H. (1999) *In vitro* SUMO-1 modification requires two enzymatic steps, E1 and E2. *Biochem. Biophys. Res. Commun.* 254:693–698.
- Olanow CW, Calne D. (1992) Does selegiline monotherapy in Parkinson's disease act by symptomatic or protective mechanisms? *Neurology.* 42:13–26.
- Olson BL, Hock MB, Ekholm-Reed S (2008) SCF^{Cdc4} acts antagonistically to the PGC-1 α transcriptional coactivator by targeting it for ubiquitin-mediated proteolysis. *Genes Dev.* 22:252-264.
- Osen KK, Storm-Mathisen J, Ottersen OP, Dihle B. (1995) Glutamate is concentrated in and released from parallel fiber terminals in the dorsal cochlear nucleus: a quantitative immunocytochemical analysis in guinea pig. *J Comp Neurol.* 357:482-500.
- Ozawa S, Kamiya H, Tsuzuki K. (1998) Glutamate receptors in the mammalian central nervous system. *Prog Neurobiol.* 54:581-618.
- Pacholczyk T, Blakely RD, Amara SG. (1991) Expression cloning of a cocaine- and antidepressant-sensitive human noradrenaline transporter. *Nature.* 350:350-4.
- Pagano M (1997) Cell cycle regulation by the ubiquitin pathway. *FASEB Journal.* 11:1067–1075.
- Palacino JJ, Sagi D, Goldberg MS, Krauss S, Motz C, Wacker M, Klose J, Shen J. (2004) Mitochondrial dysfunction and oxidative damage in parkin-deficient mice. *J Biol Chem.* 279:18614-22.
- Pankratz N, Nichols WC, Uniacke SK, Halter C, Rudolph A, Shults C, Conneally PM, Foroud T; Parkinson Study Group. (2002) Genome screen to identify susceptibility genes for Parkinson disease in a sample without parkin mutations. *Am J Hum Genet.* 71:124-35.
- Park J, Lee G, Chung J (2009) The PINK1-Parkin pathway is involved in the regulation of mitochondrial remodeling process. *Biochem Biophys Res Commun* 378: 518–523.
- Park J, Lee SB, Lee S, Kim Y, Song S, Kim S, Bae E, Kim J, Shong M, Kim JM, Chung J. (2006) Mitochondrial dysfunction in *Drosophila* PINK1 mutants is complemented by parkin. *Nature.* 441:1157-61.
- Parker WD Jr, Parks JK, Swerdlow RH. (2008) Complex I deficiency in Parkinson's disease frontal cortex. *Brain Res.* 1189:215-8.
- Parker WD Jr, Parks JK. (2005) Mitochondrial ND5 mutations in idiopathic Parkinson's disease. *Biochem Biophys Res Commun.* 326(3):667-9.
- Parker WD, Oley CA, Parks JK. (1989) Deficient NADH: coenzyme Q oxidoreductase in Leber's hereditary optic neuropathy. *N Engl J Med.* 320:1331–1333

- Parkinson Study Group 1. (1989) Effect of deprenyl on the progression of disability in early Parkinson's disease. *N Engl J Med.* 321:1364–1371.
- Parkinson Study Group 2. (1993) Effects of tocopherol and deprenyl on the progression of disability in early Parkinson's disease. *N Engl J Med.* 328:176–183.
- Parton RG, Simons K. (2007) The multiple faces of caveolae. *Nat Rev Mol Cell Biol.* 8:185–194.
- Patton EE, Willems AR, Tyers M, (1998) Combinatorial control in ubiquitin-dependent proteolysis: don't Skp the F-box hypothesis. *Trends Genet.* 14:236–243.
- Pawlowski J, Kraft AS. (2000) Bax-induced apoptotic cell death. *Proc Natl Acad Sci U S A.* 97:529-31.
- Pawlyk AC, Giasson BI, Sampathu DM, Perez FA, Lim KL, Dawson VL, Dawson TM, Palmiter RD, Trojanowski JQ, Lee VM. (2003) Novel monoclonal antibodies demonstrate biochemical variation of brain parkin with age. *J Biol Chem.* 278:48120-8.
- Peitz M, Pfannkuche K, Rajewsky K, Edenhofer F. (2002). Ability of the hydrophobic FGF and basic TAT peptides to promote cellular uptake of recombinant Cre recombinase: a tool for efficient genetic engineering of mammalian genomes. *Proc. Natl Acad. Sci. USA.* 99: 4489–4494.
- Perroy, J., Prezeau L., De Waard M., Shigemoto R., Bockaert J., Fagni L. (2000) Selective blockade of P/Q-type calcium channels by the metabotropic glutamate receptor type 7 involves phospholipase C pathway in neurons. *J. Neurosci.* 20:7896–7904.
- Pesah Y, Pham T, Burgess H, Middlebrooks B, Verstreken P, Zhou Y, Harding M, Bellen H, Mardon G. (2004) *Drosophila* parkin mutants have decreased mass and cell size and increased sensitivity to oxygen radical stress. *Development.* 131:2183-94.
- Petrucelli L, O'Farrell C, Lockhart PJ, Baptista M, Kehoe K, Vink L, Choi P, Wolozin B, Farrer M, Hardy J, Cookson MR. (2002) Parkin protects against the toxicity associated with mutant alpha-synuclein: proteasome dysfunction selectively affects catecholaminergic neurons. *Neuron.* 36:1007-19.
- Petrucelli L, O'Farrell C, Lockhart PJ, Baptista M, Kehoe K, Vink L, Choi P, Wolozin B, Farrer M, Hardy J, Cookson MR. (2002) Parkin protects against the toxicity associated with mutant alpha-synuclein: proteasome dysfunction selectively affects catecholaminergic neurons. *Neuron.* 36:1007-19.
- Pickel VM, Chan J. (1999) Ultrastructural localization of the serotonin transporter in limbic and motor compartments of the nucleus accumbens. *J Neurosci.* 19:7356-66.
- Pin, J-P. and Duvoisin, R. (1995) Review: neurotransmitter receptors I. The metabotropic glutamate receptors; structure and functions. *Neuropharmacology.* 34:1-26.
- Pittaluga A, Segantini D, Feligioni M, Raiteri M. (2005) Extracellular protons differentially potentiate the responses of native AMPA receptor subtypes regulating neurotransmitter release. *Br. J. Pharmacol.* 144:293–299.
- Pivovarova NB, Andrews SB. (2010) Calcium-dependent mitochondrial function and dysfunction in neurons. *FEBS J.* 277:3622-36.
- Pivovarova NB, Hongpaisan J, Andrews SB, Friel DD (1999) Depolarization-induced mitochondrial Ca accumulation in sympathetic neurons: spatial and temporal characteristics. *J Neurosci.* 19:6372–6384.
- Polymeropoulos MH, Lavedan C, Leroy E, Ide SE, Dehejia A, Dutra A, Pike B, Root H, Rubenstein J, Boyer R, Stenroos ES, Chandrasekharappa S, thanassiadou A, Papapetropoulos T, Johnson WG, Lazzarini AM, Duvoisin RC, Di Iorio G, Golbe LI, Nussbaum RL (1997) Mutation

in the alpha-synuclein gene identified in families with Parkinson's disease. *Science*. 276:2045–2047.

Ponting CP, Phillips C, Davies KE, Blake DJ. (1997) PDZ domains: targeting signalling molecules to sub-membranous sites. *Bioessays*. 19:469-79.

Pooga M, Soomets U, Hällbrink M, Valkna A, Saar K, Rezaei K, Kahl U, Hao JX, Xu XJ, Wiesenfeld-Hallin Z, Hökfelt T, Bartfai T, Langel U. (1998) Cell penetrating PNA constructs regulate galanin receptor levels and modify pain transmission *in vivo*. *Nat Biotechnol*. 16:857-61.

Poole AC, Thomas RE, Andrews LA, McBride HM, Whitworth AJ, Pallanck LJ. (2008) The PINK1/Parkin pathway regulates mitochondrial morphology. *Proc Natl Acad Sci USA*. 105:1638-43.

Poole AC, Thomas RE, Yu S, Vincow ES, Pallanck L. (2010) The mitochondrial fusion-promoting factor mitofusin is a substrate of the PINK1/parkin pathway. *PLoS One*. 5:e10054.

Pozzan T & Rizzuto R (2000) High tide of calcium in mitochondria. *Nat Cell Biol*. 2:E25–E27.

Pozzo-Miller LD, Pivovarova NB, Leapman RD, Buchanan RA, Reese TS & Andrews SB (1997) Activity-dependent calcium sequestration in dendrites of hippocampal neurons in brain slices. *J Neurosci*. 17:8729–8738.

Prochiantz A. (1996) Getting hydrophilic compounds into cells: lessons from homeopeptides. *Curr Opin Neurobiol*. 6:629-34.

Querfurth HW & LaFerla FM (2010) Alzheimer's disease. *N Engl J Med*. 362:329–344.

Ragan CI, Wilson MT, Darley-Usmar VM and Lowe PN. (1987) Assays of individual mitochondrial enzymes; Complex I Assay, in *Mitochondria, a Practical Approach*. (Darley-Usmar VM, Rickwood D and Wilson MT., eds) Pp. 90. IRL Press, London.

Ramirez A, Heimbach A, Gründemann J, Stiller B, Hampshire D, Cid LP, Goebel I, Mubaidin AF, Wriekat AL, Roeper J, Al-Din A, Hillmer AM, Karsak M, Liss B, Woods CG, Behrens MI, Kubisch C. (2006) Hereditary parkinsonism with dementia is caused by mutations in ATP13A2, encoding a lysosomal type 5 P-type ATPase. *Nat Genet*. 38:1184-91.

Reddy EP, Smith MJ, Srinivasan A. (1983) Nucleotide sequence of Abelson murine leukemia virus genome: structural similarity of its transforming gene product to other onc gene products with tyrosine-specific kinase activity. *Proc Natl Acad Sci USA*. 80:3623-7.

Reers M, Smiley ST, Mottola-Hartshorn C, Chen A, Lin M, Chen LB. (1995) Mitochondrial membrane potential monitored by JC-1 dye. *Methods Enzymol*. 260:406-17.

Reers M, Smith TW, Chen LB. (1991) J-aggregate formation of a carbocyanine as a quantitative fluorescent indicator of membrane potential. *Biochemistry*. 30:4480-6.

Rezgaoui M, Süsens U, Ignatov A, Gelderblom M, Glassmeier G, Franke I, Urny J, Imai Y, Takahashi R, Schaller HC. (2006) The neuropeptide head activator is a high-affinity ligand for the orphan G-protein-coupled receptor GPR37. *J Cell Sci*. 119:542-9.

Ribeiro CS, Carneiro K, Ross CA, Menezes JR, Engelender S(2002) Synphilin-1 is developmentally localised to synaptic terminals, and its association with synaptic vesicles is modulated by alpha-synuclein. *J Biol Chem*. 277:23927–23933.

Ricaurte GA, Seiden LS, Schuster CR. (1984) Further evidence that amphetamines produce long-lasting dopamine neurochemical deficits by destroying dopamine nerve fibers. *Brain Res*. 303:359–364.

Riedel G, Wetzel W, Reymann KG. (1996) Comparing the role of metabotropic glutamate receptors in long-term potentiation and in learning and memory. *Prog Neuropsychopharmacol Biol Psychiatry*. 20:761-89.

- Roche KW, O'Brien RJ, Mammen AL, Bernhardt J, Haganir RL. (1996) Characterization of multiple phosphorylation sites on the AMPA receptor GluR1 subunit. *Neuron*. 16:1179-88.
- Rodriguez MS, Dargemont C, Hay RT. (2001) SUMO-1 conjugation *in vivo* requires both a consensus modification motif and nuclear targeting. *J. Biol. Chem.* 276:12654–12659.
- Rothman JE. (1994) Mechanisms of intracellular protein transport. *Nature*. 372:55-63.
- Rubio de la Torre E, Luzón-Toro B, Forte-Lago I, Minguéz-Castellanos A, Ferrer I, Hilfiker S. (2009) Combined kinase inhibition modulates parkin inactivation. *Hum Mol Genet*. 18:809-23.
- Ruvolo PP, Deng X, Carr BK, May WS. (1998) A functional role for mitochondrial protein kinase C alpha in Bcl2 phosphorylation and suppression of apoptosis. *J Biol Chem* 273:25436–25442.
- Saad M, Lesage S, Saint-Pierre A, Corvol JC, Zelenika D, Lambert JC, Vidailhet M, Mellick GD, Lohmann E, Durif F, Pollak P, Damier P, Tison F, Silburn PA, Tzourio C, Forlani S, Lorient MA, Giroud M, Helmer C, Portet F, Amouyel P, Lathrop M, Elbaz A, Durr A, Martinez M, Brice A (2011) Genome-wide association study confirms BST1 and suggests a locus on 12q24 as the risk loci for Parkinson's disease in the European population. *Hum Mol Genet*. 20:615-27.
- Safadi SS, Shaw GS. (2010) Differential interaction of the E3 ligase parkin with the proteasomal subunit S5a and the endocytic protein Eps15. *J Biol Chem*. 285:1424-34.
- Sampson DA, Wang M, Matunis MJ (2001) The small ubiquitin-like modifier-1 (SUMO-1) consensus sequence mediates Ubc9 binding and is essential for SUMO-1 modification. *J. Biol. Chem.* 276:21664–21669.
- Sanchez-Prieto J, Sihra T S, Evans D, Ashton A, Dolly JO and Nicholls DG. (1987) Botulinum toxin A blocks glutamate exocytosis from guinea-pig cerebral cortical synaptosomes. *Eur. J. Biochem.* 165:675-681.
- Sarge KD, Park-Sarge OK. (2009) Sumoylation and human disease pathogenesis. *Trends Biochem Sci*. 34: 200-205.
- Satake W, Nakabayashi Y, Mizuta I, Hirota Y, Ito C, Kubo M, Kawaguchi T, Tsunoda T, Watanabe M, Takeda A, Tomiyama H, Nakashima K, Hasegawa K, Obata F, Yoshikawa T, Kawakami H, Sakoda S, Yamamoto M, Hattori N, Murata M, Nakamura Y, Toda T. (2009) Genome-wide association study identifies common variants at four loci as genetic risk factors for Parkinson's disease. *Nat Genet*. 41:1303-7.
- Scannevin RH, Haganir RL. (2000) Postsynaptic organization and regulation of excitatory synapses. *Nat Rev Neurosci*. 1:133-41.
- Schapira AH, Cooper JM, Dexter D, Jenner P, Clark JB, Marsden CD. (1989) Mitochondrial complex I deficiency in Parkinson's disease. *Lancet*. 2:49.
- Schapira AH, Mann VM, Cooper JM, Dexter D, Daniel SE, Jenner P, Clark JB, Marsden CD. (1990) Anatomic and disease specificity of NADH CoQ1 reductase (complex I) deficiency in Parkinson's disease. *J Neurochem*. 55:2142-5.
- Schapira AH. (1999) Mitochondria in the aetiology and pathogenesis of Parkinson's disease. *Parkinsonism Relat Disord*. 5:139-43.
- Scheld WM (1989) Drug Delivery to the Central Nervous System: General Principles and Relevance to Therapy for Infections of the Central Nervous System *Rev. Infect. Dis. Supple*. 11:S1669-S1690.
- Schiavo G, Stenbeck G, Rothman JE, Söllner TH. (1997) Binding of the synaptic vesicle v-SNARE, synaptotagmin, to the plasma membrane t-SNARE, SNAP-25, can explain docked vesicles at neurotoxin-treated synapses. *Proc Natl Acad Sci USA*. 94:997-1001.

Schoepp D, Bockaert J, Sladeczek F. (1990) Pharmacological and functional characteristics of metabotropic excitatory amino acid receptors. *Trends Pharmacol Sci.* 11:508-15.

Schubert U, Antón LC, Gibbs J, Norbury CC, Yewdell JW, Bennink JR. (2000) Rapid degradation of a large fraction of newly synthesized proteins by proteasomes. *Nature.* 404:770-4.

Schwarze SR, Ho A, Vocero-Akbani A and Dowdy SF (1999) *In vivo* protein transduction: delivery of a biologically active protein into the mouse. *Science.* 285:1569-72.

Schweichel JU, Merker HJ. (1973) The morphology of various types of cell death in prenatal tissues. *Teratology.* 7:253–266.

Sheng M, Sala C. (2001) PDZ domains and the organization of supramolecular complexes. *Annu Rev Neurosci.* 24:1-29.

Sherer TB, Betarbet R, Testa CM, Seo BB, Richardson JR, Kim JH, Miller GW, Yagi T, Matsuno-Yagi A, Greenamyre JT. (2003) Mechanism of toxicity in rotenone models of Parkinson's disease. *J Neurosci.* 23:10756-64.

Sherer TB, Kim JH, Betarbet R, Greenamyre JT. (2003) Subcutaneous rotenone exposure causes highly selective dopaminergic degeneration and alpha-synuclein aggregation. *Exp Neurol.* 179:9-16.

Shigemoto R, Kulik A, Roberts JD, Ohishi H, Nusser Z, Kaneko T, Somogyi P. (1996) Target-cell-specific concentration of a metabotropic glutamate receptor in the presynaptic active zone. *Nature.* 381:523-5.

Shimura H, Hattori N, Kubo S, Mizuno Y, Asakawa S, Minoshima S, Shimizu N, Iwai K, Chiba T, Tanaka K, Suzuki T. (2000) Familial Parkinson disease gene product, parkin, is a ubiquitin-protein ligase. *Nat Genet.* 25:302-5.

Shimura H, Hattori N, Kubo S, Yoshikawa M, Kitada T, Matsumine H, Asakawa S, Minoshima S, Yamamura Y, Shimizu N, Mizuno Y. (1999) Immunohistochemical and subcellular localization of Parkin protein: absence of protein in autosomal recessive juvenile parkinsonism patients. *Ann Neurol.* 45:668-72.

Shimura H, Schlossmacher MG, Hattori N, Frosch MP, Trockenbacher A, Schneider R, Mizuno Y, Kosik KS, Selkoe DJ. (2001) Ubiquitination of a new form of alpha-synuclein by parkin from human brain: implications for Parkinson's disease. *Science.* 293:263-269.

Shin JH, Ko HS, Kang H, Lee Y, Lee YI, Pletinkova O, Troconso JC, Dawson VL, Dawson TM. (2011) PARIS (ZNF746) repression of PGC-1 α contributes to neurodegeneration in Parkinson's disease. *Cell.* 144:689-702.

Shinbo Y, Niki T, Taira T, Ooe H, Takahashi-Niki K, Maita C, Seino C, Iguchi-Arigo SM, Ariga H. (2006) Proper SUMO-1 conjugation is essential to DJ-1 to exert its full activities. *Cell Death Differ.* 13:96-108.

Shults CW. (2006) Lewy bodies. *Proc. Natl Acad. Sci. USA.* 103:1661–1668.

Silver I, Erecińska M. (1998) Oxygen and ion concentrations in normoxic and hypoxic brain cells. *Adv Exp Med Biol.* 454:7-16.

Silvestri L, Caputo V, Bellacchio E, Atorino L, Dallapiccola B, Valente EM, Casari G. (2005) Mitochondrial import and enzymatic activity of PINK1 mutants associated to recessive parkinsonism. *Hum Mol Genet.* 14:3477-92.

Singleton AB, Farrer M, Johnson J, Singleton A, Hague S, Kachergus J, Hulihan M, Peuralinna T, Dutra A, Nussbaum R, Lincoln S, Crawley A, Hanson M, Maraganore D, Adler C, Cookson MR, Muentner M, Baptista M, Miller D, Blancato J, Hardy J, Gwinn-Hardy K. (2003) alpha-Synuclein locus triplication causes Parkinson's disease. *Science.* 302:841.

- Sipos I, Tretter L, Adam-Vizi V. (2003) The production of reactive oxygen species in intact isolated nerve terminals is independent of the mitochondrial membrane potential. *Neurochem Res.* 28:1575-81.
- Skowrya D, Craig K, Tyers M, Elledge SJ, Harper JW (1997) F-boxproteins are components of E3 complexes and act as receptors to recruit phosphorylated substrates for ubiquitination. *Cell.* 91:209-219.
- Skowrya D, Koepp DM, Kamura T, Conrad MN, Conaway RC, Conaway JW, Elledge SJ, Harper JW (1999) Reconstitution of G1 cyclin ubiquitination with complexes containing SCFGrr1 and Rbx1. *Science.* 284:662-665.
- Sladeczek F, Pin JP, Récasens M, Bockaert J, Weiss S. (1985) Glutamate stimulates inositol phosphate formation in striatal neurones. *Nature.* 317:717-9.
- Söllner T. (1995) SNAREs and targeted membrane fusion. *FEBS Lett.* 369:80-3.
- Söllner TH, Whiteheart SW, Brunner M, Erdjument-Bromage H, Geromanos S, Tempst P, Rothman JE. (1993) SNAP receptors implicated in vesicle targeting and fusion. *Nature.* 362:318-324.
- Songyang Z, Fanning AS, Fu C, Xu J, Marfatia SM, Chishti AH, Crompton A, Chan AC, Anderson JM, Cantley LC (1997) Recognition of unique carboxyl-terminal motifs by distinct PDZ domains. *Science.* 275:73-77.
- Soper, B. & Rosenthal, G. (1988) The number of neurons in the brain: how we report what we do not know. *Teach. Psychol.* 15:153-156.
- Soriano FX, Martel MA, Papadia S, Vaslin A, Baxter P, Rickman C, Forder J, Tymianski M, Duncan R, Aarts M, Clarke P, Wyllie DJ, Hardingham GE. (2008) Specific targeting of pro-death NMDA receptor signals with differing reliance on the NR2B PDZ ligand. *J Neurosci.* 28:10696-10710.
- Spitaler M, Wiesenhofer B, Biedermann V. (1999) The involvement of protein kinase C isoenzymes alpha, epsilon and zeta in the sensitivity to antitumor treatment and apoptosis induction. *Anticancer Res.* 19:3969-3976.
- Spruck CH, Strohmaier H, Sangfelt O, Müller HM, Hubalek M, Müller-Holzner E, Marth C, Widschwendter M, Reed SI. (2002) hCDC4 gene mutations in endometrial cancer. *Cancer Res.* 62:4535-9.
- Srivastava S, Osten P, Vilim FS, Khatri L, Inman G, States B, Daly C, DeSouza S, Abagyan R, Valtschanoff JG, Weinberg RJ, Ziff EB. (1998) Novel anchorage of GluR2/3 to the postsynaptic density by the AMPA receptor-binding protein ABP. *Neuron.* 21:581-91.
- Starkov AA (2010) The molecular identity of the mitochondrial Ca²⁺ sequestration system. *FEBS J* 277:3652-3663.
- Staropoli JF, McDermott C, Martinat C, Schulman B, Demireva E, Abeliovich A. (2003) Parkin is a component of an SCF-like ubiquitin ligase complex and protects postmitotic neurons from kainate excitotoxicity. *Neuron.* 37:735-749.
- Staudinger J, Lu J, Olson EN. (1997) Specific interaction of the PDZ domain protein PICK1 with the COOH terminus of protein kinase C-alpha. *J Biol Chem.* 272:32019-24.
- Staudinger J, Zhou J, Burgess R, Elledge SJ, Olson EN. (1995) PICK1: a perinuclear binding protein and substrate for protein kinase C isolated by the yeast two-hybrid system. *J Cell Biol.* 128:263-71.
- Stowell JN, Craig AM. (1999) Axon/dendrite targeting of metabotropic glutamate receptors by their cytoplasmic carboxy-terminal domains. *Neuron.* 22:525-536.

- St-Pierre J, Drori S, Uldry M, Silvaggi JM, Rhee J, Jager S, Handschin C, Heng K, Lin J, Yang W (2006) Suppression of reactive oxygen species and neurodegeneration by the PGC-1 transcriptional coactivators. *Cell*. 127:397–408.
- Strohmaier H, Spruck CH, Kaiser P, Won KA, Sangfelt O, Reed SI (2001) Human F-box protein hCdc4 targets cyclin E for proteolysis and is mutated in a breast cancer cell line. *Nature*. 413:316–322.
- Sugiyama H, Ito I, Hirono C. (1987) A new type of glutamate receptor linked to inositol phospholipid metabolism. *Nature*. 325:531-3.
- Sundqvist A, Bengoechea-Alonso MT, Ye X, Lukiyanchuk V, Jin J, Harper JW, Ericsson J. (2005) Control of lipid metabolism by phosphorylation-dependent degradation of the SREBP family of transcription factors by SCF(Fbw7). *Cell Metab*. 1(6):379-91.
- Takahashi R, Imai Y. (2003) Pael receptor, endoplasmic reticulum stress, and Parkinson's disease. *J Neurol*. 250 Suppl 3:III25-9.
- Tallman JF, Saavedra JM, Axelrod J. (1976) Biosynthesis and metabolism of endogenous tyramine and its normal presence in sympathetic nerves. *J Pharmacol Exp Ther*. 199:216–221
- Tanner CM (1989) The role of environmental toxins in the etiology of Parkinson's disease. *Trends in Neuroscience*. 12:49–54.
- Tao-Cheng JH, Zhou FC. (1999) Differential polarization of serotonin transporters in axons versus soma-dendrites: an immunogold electron microscopy study. *Neuroscience*. 94:821-30.
- Tardieu M, Héry C, Peudenier S, Boespflug O, Montagnier L. (1992) Human immunodeficiency virus type 1-infected monocytic cells can destroy human neural cells after cell-to-cell adhesion. *Ann Neurol*. 32:11-7.
- Taverna FA, Wang LY, MacDonald JF, Hampson DR. (1994) A transmembrane model for an ionotropic glutamate receptor predicted on the basis of the location of asparagine-linked oligosaccharides. *J Biol Chem*. 269:14159-64.
- Telford JE, Kilbride SM, Davey GP. (2010) Decylubiquinone increases mitochondrial function in synaptosomes. *J Biol Chem*. 28:8639-45.
- Temussi PA, Masino L, Pastore A. (2003) From Alzheimer to Huntington: why is a structural understanding so difficult? *EMBO J*. 22:355–361.
- Thomas KJ, McCoy MK, Blackinton J, Beilina A, van der Brug M, Sandebring A, Miller D, Maric D, Cedazo-Minguez A, Cookson MR. (2011) DJ-1 acts in parallel to the PINK1/parkin pathway to control mitochondrial function and autophagy. *Hum Mol Genet*. 20:40-50.
- Thorsen TS, Madsen KL, Rebola N, Rathje M, Anggono V, Bach A, Moreira IS, Stuhr-Hansen N, Dyhring T, Peters D, Beuming T, Haganir R, Weinstein H, Mülle C, Strømgaard K, Rønn LC, Gether U. (2010) Identification of a small-molecule inhibitor of the PICK1 PDZ domain that inhibits hippocampal LTP and LTD. *Proc Natl Acad Sci USA*. 107:413-8.
- Tibbs GR, Barrie AP, Van Mieghem FJ, McMahon HT, Nicholls DG. (1989) Repetitive action potentials in isolated nerve terminals in the presence of 4-aminopyridine: effects on cytosolic free Ca²⁺ and glutamate release. *J Neurochem*. 53:1693-9.
- Tolkovsky AM, Xue L, Fletcher GC, Borutaite V. (2002) Mitochondrial disappearance from cells: a clue to the role of autophagy in programmed cell death and disease? *Biochimie*. 84:233-40.
- Torchilin VP, Rammohan R, Weissig V, Levchenko TS. (2001) TAT peptide on the surface of liposomes affords their efficient intracellular delivery even at low temperature and in the presence of metabolic inhibitors. *Proc. Natl Acad. Sci. USA*. 98:8786–8791.

- Torres GE, Yao WD, Mohn AR, Quan H, Kim KM, Levey AI, Staudinger J, Caron MG. (2001) Functional interaction between monoamine plasma membrane transporters and the synaptic PDZ domain-containing protein PICK1. *Neuron*. 30:121-34.
- Tretter L, Adam-Vizi V. (2004) Generation of reactive oxygen species in the reaction catalyzed by alpha-ketoglutarate dehydrogenase. *J Neurosci*. 24:7771-8.
- True AL, Rahman A, Malik AB. (2000) Activation of NF- κ B induced by H₂O₂ and TNF- α and its effects on ICAM-1 expression in endothelial cells. *Am. J. Physiol. Lung Cell Mol. Physiol*. 279:L302–L311.
- Tsai YC, Fishman PS, Thakor NV, Oylar GA. (2003) Parkin facilitates the elimination of expanded polyglutamine proteins and leads to preservation of proteasome function. *J Biol Chem*. 278:22044-55.
- Turrens JF. (2003) Mitochondrial formation of reactive oxygen species. *J Physiol*. 552:335-44.
- Twig G, Elorza A, Molina AJ, Mohamed H, Wikstrom JD, Walzer G, Stiles L, Haigh SE, Katz S, Las G, Alroy J, Wu M, Py BF, Yuan J, Deeney JT, Corkey BE, Shrihail OS. (2008) Fission and selective fusion govern mitochondrial segregation and elimination by autophagy. *EMBO J*. 27:433-46.
- Uchiki T, Kim HT, Zhai B, Gygi SP, Johnston JA, O'Bryan JP, Goldberg AL. (2009) The ubiquitin-interacting motif protein, S5a, is ubiquitinated by all types of ubiquitin ligases by a mechanism different from typical substrate recognition. *J Biol Chem*. 284:12622-32.
- Valle I, Alvarez-Barrientos A, Arza E, Lamas S, Monsalve M (2005) PGC-1 α regulates the mitochondrial antioxidant defense system in vascular endothelial cells. *Cardiovasc. Res*. 66:562–573.
- Vandenbergh DJ, Persico AM, Uhl GR. (1992) A human dopamine transporter cDNA predicts reduced glycosylation, displays a novel repetitive element and provides racially-dimorphic TaqI RFLPs. *Brain Res Mol Brain Res*. 15:161-6.
- Venda LL, Cragg SJ, Buchman VL, Wade-Martins R. (2010) α -synuclein and dopamine at the crossroads of Parkinson's disease. *Trends Neurosci*. 33:559–568.
- Verhage M, Besselsen E, Lopes Da Silva FH, Ghijsen WE. (1988) Evaluation of the Ca²⁺ concentration in purified nerve terminals: relationship between Ca²⁺ homeostasis and synaptosomal preparation. *J Neurochem*. 51:1667-74.
- Voges D, Zwickl P, Baumeister W. (1999) The 26S proteasome: a molecular machine designed for controlled proteolysis. *Annual Review of Biochemistry*. 68:1015–1068.
- Vonsattel JP, DiFiglia M. (1998) Huntington disease. *J. Neuropathol. Exp. Neurol*. 57:369–384.
- Wang WL, Yeh SF, Chang YI, Hsiao SF, Lian WN, Lin CH, Huang CYF, Lin WJ. (2003) PICK1, an anchoring protein that specifically targets protein kinase C- α to mitochondria selectively upon serum stimulation in NIH 3T3 cells. *J Biol Chem*. 278:37705–37712.
- Wang WL, Yeh SF, Huang EYK, Lu YL, Wang CF, Huang CYF, Lin WJ. (2007) Mitochondrial anchoring of PKC α by PICK1 confers resistance to etoposide-induced apoptosis. *Apoptosis*. 12:1857–1871.
- Welcker M, Clurman BE. (2005) The SV40 large T antigen contains a decoy phosphodegron that mediates its interactions with Fbw7/hCdc4. *J Biol Chem*. 280:7654-8.
- Wells JA, McClendon CL (2007) Reaching for high-hanging fruit in drug discovery at protein-protein interfaces. *Nature*. 450:1001–1009.

- Wesselingh SL, Power C, Glass JD, Tyor WR, McArthur JC, Farber JM, Griffin JW, Griffin DE. (1993) Intracerebral cytokine messenger RNA expression in acquired immunodeficiency syndrome dementia. *Ann Neurol.* 33:576-82.
- West AB, Moore DJ, Biskup S, Bugayenko A, Smith WW, Ross CA, Dawson VL, Dawson TM. (2005). Parkinson's disease-associated mutations in leucine-rich repeat kinase 2 augment kinase activity. *Proc. Natl Acad. Sci. USA.* 102:16842–16847.
- Wharton DC, Tzagoloff A. (1967) *Methods Enzymol.* 10:245-246
- Whitworth AJ, Theodore DA, Greene JC, Benes H, Wes PD, Pallanck LJ. (2005) Increased glutathione S-transferase activity rescues dopaminergic neuron loss in a *Drosophila* model of Parkinson's disease. *Proc Natl Acad Sci USA.* 102:8024-9.
- Williams ME, Wu SC, McKenna WL, Hinck L. (2003) Surface expression of the netrin receptor UNC5H1 is regulated through a protein kinase C-interacting protein/protein kinase-dependent mechanism. *J Neurosci.* 23:11279-88.
- Winklhofer KF, Henn IH, Kay-Jackson PC, Heller U, Tatzelt J. (2003) Inactivation of parkin by oxidative stress and C-terminal truncations: a protective role of molecular chaperones. *J Biol Chem.* 278:47199-208.
- Wo ZG, Oswald RE. (1995) A topological analysis of goldfish kainate receptors predicts three transmembrane segments. *J Biol Chem.* 270:2000-9.
- Wu G, Lyapina S, Das I, Li J, Gurney M, Pauley A, Chui I, Deshaies RJ, Kitajewski J. (2001) SEL-10 is an inhibitor of Notch signaling that targets Notch for ubiquitin-mediated protein degradation. *Mol. Cell. Biol.* 21:7403–7415.
- Xia J, Zhang X, Staudinger J, Huganir RL. (1999) Clustering of AMPA receptors by the synaptic PDZ domain-containing protein PICK1. *Neuron.* 22:179-87.
- Xiong ZG, Chu XP, Simon RP. (2006) Ca²⁺-permeable acid-sensing ion channels and ischemic brain injury. *J Membr Biol.* 209:59–68.
- Xu F, Gainetdinov RR, Wetsel WC, Jones SR, Bohn LM, Miller GW, Wang YM, Caron MG. (2000) Mice lacking the norepinephrine transporter are supersensitive to psychostimulants. *Nat Neurosci.* 3:465-71.
- Yada K, Kashima K, Daa T, Kitano S, Fujiwara S, Yokoyama S. (2004) Expression of CD10 in basal cell carcinoma. *Am J Dermatopathol.* 26:463-71.
- Yamamoto A, Friedlein A, Imai Y, Takahashi R, Kahle PJ, Haass C. (2005) Parkin phosphorylation and modulation of its E3 ubiquitin ligase activity. *J Biol Chem.* 280:3390-9.
- Yang Y, Nishimura I, Imai Y, Takahashi R, Lu B. (2003) Parkin suppresses dopaminergic neuron-selective neurotoxicity induced by Pael-R in *Drosophila*. *Neuron.* 37:911-24.
- Yang Y, Ouyang Y, Yang L, Beal MF, McQuibban A, Vogel H, Lu B. (2008) Pink1 regulates mitochondrial dynamics through interaction with the fission/fusion machinery. *Proc Natl Acad Sci USA.* 105(19):7070-5.
- Yang Y, Gehrke S, Imai Y, Huang Z, Ouyang Y, Wang JW, Yang L, Beal MF, Vogel H, Lu B. (2006). Mitochondrial pathology and muscle and dopaminergic neuron degeneration caused by inactivation of *Drosophila* Pink1 is rescued by Parkin. *Proc. Natl. Acad. Sci. USA.* 103:10793–10798.
- Yedovitzky M, Mochly-Rosen D, Johnson JA, Gray MO, Ron D, Abramovitch E, Cerasi E, Neshler R. (1997) Translocation inhibitors define specificity of protein kinase C isoenzymes in pancreatic beta-cells. *J Biol Chem.* 272:1417-20.

- Youdim MB, Collins GG, Sandler M. (1972) Human brain monoamine oxidase, multiple forms and selective inhibitors. *Nature*.236:225–228.
- Zhang J, Perry G, Smith MA, Robertson D, Olson SJ, Graham DG, Montine TJ. (1999) Parkinson's disease is associated with oxidative damage to cytoplasmic DNA and RNA in substantia nigra neurons. *Am J Pathol*. 154:1423-9.
- Zhang Y, Dawson VL, Dawson TM. (2000) Oxidative stress and genetics in the pathogenesis of Parkinson's disease. *Neurobiol Dis*. 7:240-50.
- Zhang Y, Gao J, Chung KK, Huang H, Dawson VL, Dawson TM. (2000a) Parkin functions as an E2-dependent ubiquitin-protein ligase and promotes the degradation of the synaptic vesicle-associated protein, CDCrel-1. *Proceedings of the National Academy Science of the USA*. 97:13354–13359.
- Zhao J. (2007) Sumoylation regulates diverse biological processes. *Cell Mol Life Sci*. 64:3017-33.
- Zhou C, Huang Y, Shao Y, May J, Prou D, Perier C, Dauer W, Schon EA, Przedborski S. (2008) The kinase domain of mitochondrial PINK1 faces the cytoplasm. *Proc Natl Acad Sci USA*. 105:12022-7.
- Zhou FM, Hablitz JJ. (1999) Activation of serotonin receptors modulates synaptic transmission in rat cerebral cortex. *J Neurophysiol*. 82:2989-99.
- Zhou L, Li F, Xu HB, Luo CX, Wu HY, Zhu MM, Lu W, Ji X, Zhou QG, Zhu DY. (2010) Treatment of cerebral ischemia by disrupting ischemia-induced interaction of nNOS with PSD-95. *Nat Med*. 16:1439-43.
- Ziviani E, Tao RN, Whitworth AJ. (2010) *Drosophila* parkin requires PINK1 for mitochondrial translocation and ubiquitinates mitofusin. *Proc Natl Acad Sci USA*. 107:5018-23.
- Zoratti M, Szabo I. (1995) The mitochondrial permeability transition. *Biochim. Biophys. Acta* 1241:139–176.